USING POLYMER TO MAXIMIZE

CO_2 FLOODING PERFORMANCE IN LIGHT OILS

A Dissertation

by

WEIRONG LI

Submitted to the Office of Graduate and Professional Studies of
Texas A&M University
in partial fulfillment of the requirements for the degree of

DOCTOR OF PHILOSOPHY

Chair of Committee,	David S. Schechter
Committee Members,	Stephen A. Holditch
	Maria A. Barrufet
	Yuefeng Sun
Head of Department,	A. Daniel Hill

December 2014

Major Subject: Petroleum Engineering

ABSTRACT

Carbon dioxide has been used to recover oil for more than 40 years. Currently, about 43% of EOR production in U.S. is from CO_2 flooding. Although CO_2 flooding is a well-established EOR technique, its density and viscosity nature is a challenge for CO_2 projects. Low density (0.5 to 0.8 g/cm^3) causes gas to rise upward in reservoirs and bypass many lower portions of the reservoir. Low viscosity (0.02 to 0.08 cp) leads to poor volumetric sweep efficiency. In heterogeneous reservoirs with high-permeability zones and natural fractures, the condition is even worse.

Two methods related to polymers are studied to improve CO_2 flooding performance. One is adding polymers to water to increase water viscosity during the water-alternating-gas (WAG) process, named polymer-alternating-gas (PAG) flooding. The other one is adding polymers with cosolvent to CO_2, named CO_2 viscosifier, to increase CO_2 viscosity.

To analyze the feasibility of PAG, couples model considering both miscible and polymer flooding processes are built to study the performance of PAG. Polymer adsorption and concentration, reservoir permeability, permeability variation and fluid viscosity are studied. Results show that PAG process could get higher recovery than WAG if not injectivity problem occurs. The Upper Ness formation in Spe10 model is used to study the PAG performance in a reservoir with channels. Oil recovery from PAG with a polymer concentration of 0.20 lb/stb is 6% higher than WAG process in this model.

To analyze the impact of CO_2 flooding in the North Burbank Unit, five sections that best represent the characteristics of the field were selected for reservoir modeling. Based on simulation results, the conventional WAG process increased average oil recovery in the North Burbank Unit by 10-13%, PAG are forecasted to increase average oil recovery 4-7% more than conventional WAG flooding in the North Burbank Unit. Based on assumptions, PAG could get positive NPV when oil price higher than $40/bbl while PAG could also obtain higher NPV than WAG in all these five sections, which indicates that PAG is both technically and economically feasible in the North Burbank unit.

A black-oil pseudo-miscible model is used for study CO_2 viscosifier performance in synthetic model, SPE10 model and Section TR78 in the North Burbank Unit. Results show that higher cumulative oil recovery and better sweep efficiency was observed for viscosified CO_2 case in homogeneous, heterogeneous and channels reservoirs.

DEDICATION

I lovingly dedicate this dissertation to my wife, Zhenzhen Dong, who supported me each step of the way.

I dedicate this dissertation as a gift to my lovely son, Jeffery Li.

To my mother and my father, Xianying Chen and Tiancai Li, for their encouragement and support.

To the rest of my family for always supporting me.

ACKNOWLEDGEMENTS

I would never have been able to finish my dissertation without the guidance of my committee members, help from friends, and support from my family and husband.

I would like to express my deepest gratitude to my advisor, Dr. Schechter, for his advice, encouragement, and support during the course of this research and for his confidence in my ability which played an important role in the completion of this work.

I would like to thank my committee members, Dr. Holditch, Dr. Barrufet and Dr. Sun, for their guidance and support throughout the course of this research.

I would like to thank my wife, Zhenzhen Dong. She was always there cheering me up and stood by me through the good times and bad.

Thanks also go to my friends and colleagues and the department faculty and staff for making my time at Texas A&M University a great experience.

NOMENCLATURE

CCE	Constant composition expansion
CGI	Continuous gas injection
EOR	Enhanced oil recovery
EOS	Equation of state
FAWAG	Foam-assisted water alternating gas
IFT	Interfacial tension
Kv	Vertical permeability
Kh	Horizontal permeability
MMP	Minimum miscibility pressure
NPV	Net present value
PVT	Pressure-volume-temperature
PAG	Polymer-alternating-gas
RRF	Residual resistance factor
SWAG	Simultaneous water and solvent injection
VDP	Dykstra-Parsons permeability variation coefficient
WAG	Water alternating gas
C_t	Net cash inflow during the period
C_o	Initial investment
r	Discount rate
t	Number of time periods

TABLE OF CONTENTS

LIST OF FIGURES

Page

LIST OF TABLES

Page

1. INTRODUCTION AND LITERATURE REVIEW

1.1 Introduction of CO_2 Flooding

During the life of a producing oil field, several production stages are encountered. Initially, oil flows naturally to the surface due to existing reservoir pressure in the primary phase. As reservoir pressure drops, water is typically injected to boost the pressure to displace the oil in the secondary phase. Lastly, a variety of means such as gas injection, chemical flooding, and steam recovery in the final tertiary or enhanced oil recovery (EOR) phase are used to recovery the remaining oil. Depending on the reservoir and fluid specifics, oil recovery estimates for each phase are shown in **Table 1.1.**

Table 1.1—Oil recoveries from different recovery mechanism (Geiger, 2006)

Mechanism	Oil Recovery (%)
Primary	6-15
Secondary	6-30
Tertiary	8-30
Remaining	80-35

Based on Oil & Gas Journal's 2014 EOR/Heavy Oil Survey (Moritis, 1990-2014), oil rate from EOR continues increasing slightly. About 778,048 bbl/day of oil will be produced by EOR methods **(Figure 1.1**). 40% of EOR production is from thermal flooding, and 60% is from gas injection. CO_2 flooding is generally considered as the fastest-growing improved oil recovery (IOR) technique. Miscible CO_2 continues to eclipse steam injection (**Figure 1.2**). Production from US miscible CO_2 flooding is 292,735 b/d versus 284,725 b/d from steam flooding (Moritis, 1990-2014). Production from CO_2 flooding accounts for 38% of US output from EOR. Miscible CO_2 dominates in US EOR project number in 2014 (**Figure 1.3**).

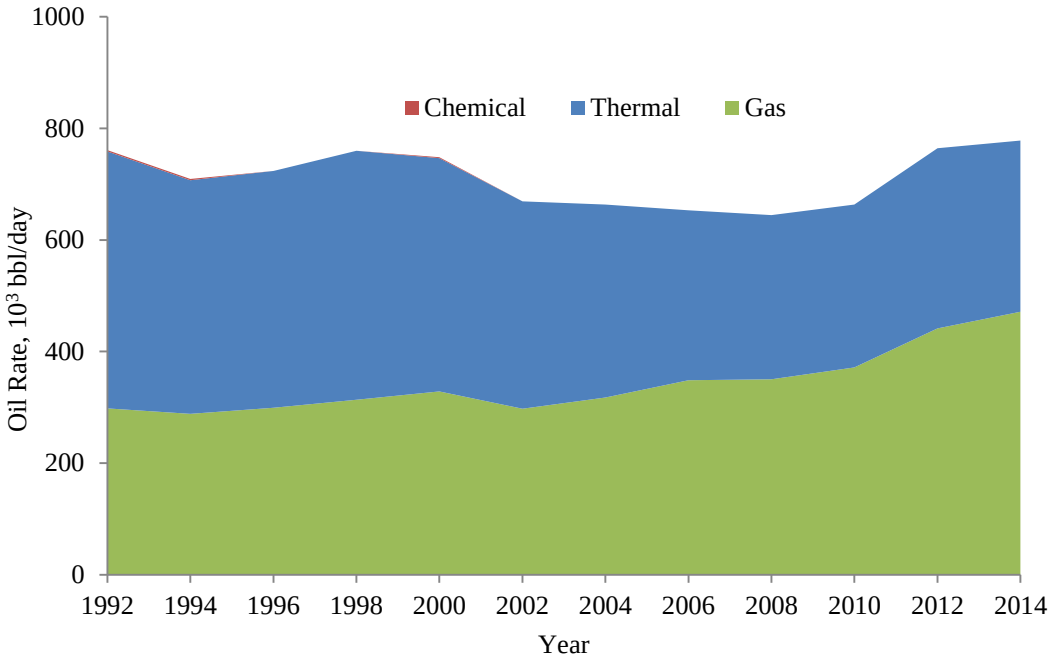

Figure 1.1—US EOR production

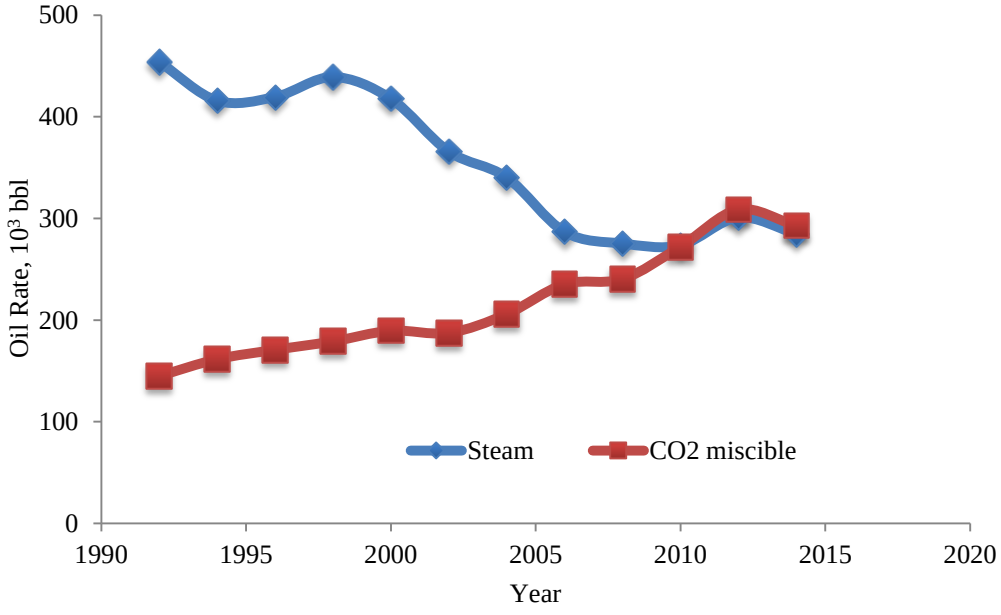

Figure 1.2—US oil production from steam injection and CO_2 miscible injection

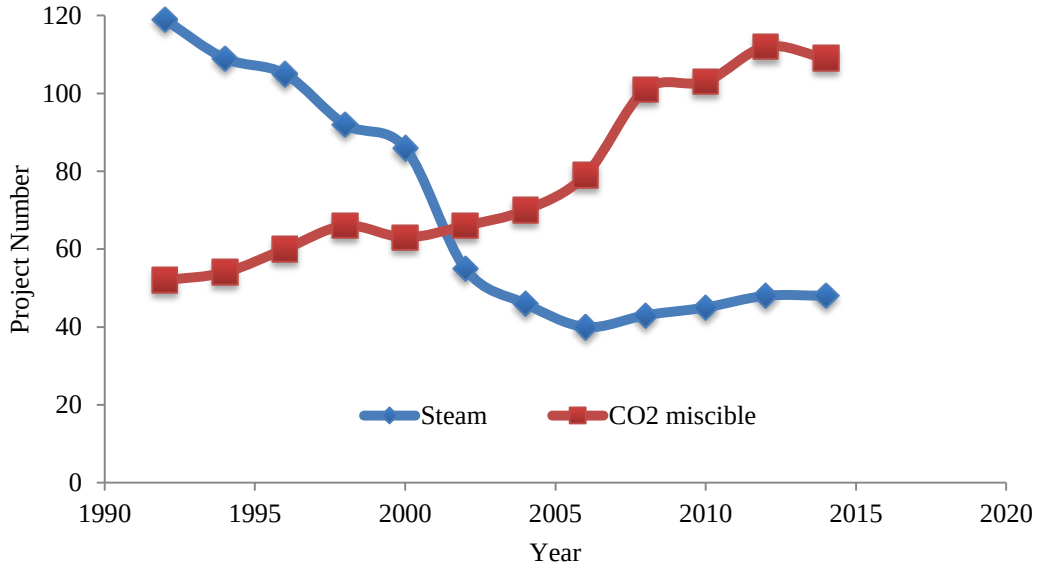

Figure 1.3—Project number of steam flooding and CO_2 miscible flooding

CO_2 flooding is carried out by injecting large quantities of CO_2 into the reservoir. Although CO_2 is not truly miscible with the crude oil, the CO_2 extracts the light-to-intermediate components from the oil. And if the pressure is high enough, CO_2 can develop miscibility to displace the crude oil from the reservoir. The main mechanism includes generation of miscibility, swelling the crude oil, lowering the viscosity of oil, and lowering the interfacial tension between the oil and the CO_2-oil phase in the near miscible regions.

When a reservoir's pressure is depleted through primary and secondary production, CO_2 flooding can be an ideal tertiary recovery method. It is particularly effective in reservoirs deeper than 2,500 ft, where CO_2 will be in a supercritical state, with API oil gravity greater than 22–25°, and remaining oil saturation greater than 30%. **Table 1.2** summarizes the screening criteria for CO_2 miscible flooding (Ronald, 2001).

Table 1.2—Screening criteria for CO_2 miscible process

Oil Gravity, API	>25
Oil Viscosity, cp	<12
Oil Saturation, %	>30
Formation Type	Sandstone or Carbonate
Net Thickness, ft	15-25
Average Permeability	Not critical but should be compatible
Depth, ft	>2000
Temperature, ^oF	Not critical but should be compatible

On the basis of laboratory displacement experiments and field applications, at pressures above the minimum miscibility pressure (MMP) of CO_2 and reservoir oil, a developed miscibility flood could be expected to produce a significant fraction of the remaining oil in the formation. CO_2 flooding can increase oil recovery by 7-15% of original oil in place and can be sustained for 10 to 30 years. The use of CO_2 flooding for EOR is increasing due to the following reasons:

(1) CO_2 fluiding is miscible or partial miscible with many hydrocarbon components at reservoir conditions;

(2) CO_2 has relatively low solubility in water compared to oil;

(3) The US has CO_2 resources near many oil fields;

(4) As a displacement fluid, CO_2 costs are relatively low if the CO_2 is found near an oil field;

(5) Environmental and economic benefits are derived from related CO_2 sequestration and the worldwide potential increases for CO_2 use in IOR.

1.2 Limitation of CO_2 Flooding

Even though most field projects have been shown to be technically and economically successful, CO_2 flooding is associated with poor sweep efficiency, which is due to the relative low viscosity and density of CO_2 compared to that of brine and most crude oils. Low density (0.5 to 0.8 g/cm^3) causes gas to rise upward in reservoirs and bypass many lower portions of the reservoir. Low viscosity (0.02 to 0.08 cp) would lead to poor volumetric sweep efficiency. In heterogeneous reservoirs with high-permeability zones

and natural fractures, the condition is even worse (Zhang et al. 2010). A need for mobility control during CO_2 flooding has led to the study WAG, SWG, cross-linked gel conformance control, CO_2 viscosifier and CO_2 foams.

1.3 Improving Methods for CO_2 Flooding

1.3.1 WAG

Almost all commercial miscible gas injection projects use WAG to control mobility of gas and alleviate fingering problems. Recovery of WAG is better than gas injection alone, And 80% of commercial WAG projects in the US are economic (Christensen *et al*. 1998). However, recent studies show that most of the fields could not reach the excepted recovery factor from the WAG process, especially, for reservoirs with high-permeability zones or there are naturally fractured (Christensen et al. 2001).

1.3.2 Gel

Gel has been used to reduce channeling through fractures or high-permeability zones of reservoirs (Ali and Schechter 2013).

Woods *et al*. (1986) presented one of the earliest successful gel treatments for Lick Creek field in Arkansas. The in-situ polymer gel treatments of wells 27-3 and 4-1 block the inter-well channels successfully and improve areal and vertical sweep efficiency. The oil rate has increased an average of 65 BOPD and total oil increment is estimated to be 25000 bbl as a result of the treatments. This treatment is considered economically and technically successful.

Hild and Wackowski (1999) reported a successful gel treatment at the Rangely Weber Sand Unit in northwestern Colorado. The study of well patterns revealed poor injection performance - poor vertical sweep was evident in the injection profile data, and poor areal sweep was recognized by rapid breakthrough to only one producer in the pattern (early indications of poor sweep was evident in initial CO_2 breakthrough times that were on the order of 10-20 days). The study also indicated that fluid flow in the Rangely field can be dominated by fractures or fracture-like high permeability streaks. Previous efforts

at improving conformance had primarily been limited to near well bore methods such as selective injection equipment, dual injection strings, cement squeezes, straddle packers, solid plugging materials, and small volume polyvinyl alcohol and chromium gels. Although controlling fluids at the wellbore has improved the water and CO_2 flooding performance in the past, the current well age and associated poor wellbore integrity has made their utility very limited. In this treatment, a large volume (10,000 bbl) chromic-acetate acrylamide polymer gel was applied to improve CO_2 flooding performance. The cost of the gel treatment was estimated to be around USD 6 to 8/bbl, and the project return rate was 365%. The polymer gel treatment program at Rangely has produced a wide range of responses: (1) no apparent impact on injection or production; (2) smoothing of production; (3) oil rate increase; (4) reduction in water; (5) reduction in gas; (6) areal sweep improvement; (7) reduction or elimination of oil decline rate, and (8) improved pattern CO_2 retention and utilization.

Karaoguz et al. (2007) and Topguder (2010) reported several field applications of gel in Bati Raman field. Conformance improvement treatments were performed in Bati Raman Field which is a well-known heavy oil field by the CO_2 flooding project. 27,500 bbl of gels were injected into three wells (BR-109, BR-116, BR-124) in 2002. Post-gel oil rate from 19 offset producers was 720 bbl/day compared with pre-gel oil rate of 645 bbl/day. Production rate from the treatments was increased by 75 bbl/day or 12%, which indicated a payout time of 12 months. Four more CO_2 injector wells were treated in 2004. This treatment provided some increase in oil production, however, this increase just was found in a limited area and for a limited time.

Borling (1994) summarized the performance by using gel at the Wertz Field CO_2 tertiary flooding in Wyoming. The Wertz Tensleep is a sandstone reservoir with a gross thickness of about 470 feet and a net pay thickness of about 240 feet. The reservoir has an average porosity of 10%, and permeability of 13 md, and some natural fractures. Natural fractures make injection conformance control with foam very difficult, since foam diversion longevity was reduced considerably when natural fractures were present. Borling (1994) also mentioned that workover would be shut-down for at least 24-hours to allow in-situ crosslinking to occur when more than five parts per million polymer were detected at a producing well with using a simple kaolinite flocculation test. Two types of workover were performed in Wertz Field.

Matrix type workover used from 250,000 to 500,000 molecular weight material with total gel volumes just less than 1000 barrels. Acrylamide-polymer concentration varied from 25,000 to 50,000 ppm and a chromium delayed crosslinking agent was added. Fracture type workover used as high as 8 to 12 million molecular weight material with total gel volumes near 15,000 barrels. Acrylamide-polymer concentration varied from 5,000 to 8,000 ppm and a chromium delayed crosslinking agent was added. The cost of each treatment ranges from $50,000 to 139,000. Incremental oil ranges from 100 to 300 bbl/day. Payouts were usually less than 3 months based on a $12 net oil price and the associated daily pattern operating expenses.

Pipes and Schoeling (2014) summarized the performance by using gel at the SACROC unit CO_2 tertiary flooding in Texas. Poor sweep efficiency is a challenge of miscible CO_2 flooding in SACROC unit. This problem leads to very high gas oil ratio and CO_2 gross utilization as well as large unsweep reservoir volume. The authors pointed out that large amount of gel polymer treatment are the most long-term successful method to plug high permeability channels and conduit and divert injected CO_2 to unsweep reservoir. In the SACROC, usually 20, 000 bbl or more of polymer gel consisting of Chromium crosslinked medium and high molecular weight polyacrylate polymer was injected in each treatment. At the beginning of treatment, gel concentration 5,000 ppm was used, and increased to 12,000 ppm in the later stages. The paper showed that using very high concentration polymer (>30,000 ppm) or even cement in some cases was a one of the keys to a successful gel treatment. For a reservoir with proven conformance problem, polymer gel treatments before CO_2 injection are suggested to reduce early CO_2 breakthrough and prevent lost production due to shut in time from polymer gel breakthrough. Using gel treatment post CO_2 activation, the total project polymer cost is $0.39 per barrel oil to date. Using gel treatment pre CO_2 activation, the total project polymer cost is $1.50 per barrel oil to date and forecasted to decrease to less than $0.38 as the project matures.

Performance of gel treatments in south Swan Hills miscible project was summarized by Wagner et al (1986). Gel was used at nine injectors in an attempt to reduce solvent and water cycling caused by severe channeling. 13 producers had a significant increase in incremental oil, and the total incremental oil production from this project was estimated to be 3,300,000 barrels. Gross revenue of $33 MM (Can.) was

generated by incremental oil and the cost was 1.3 MM (Can.). Thus, these treatments are considered a technical and economic success.

Smith et al. (2006) described the performance of gel treatment in Anton Irish. The polymer gel solution was injected into the five producing wells (wells 251 and 252 in 2003, well 282, 284, and 292 in 2005). The formulation of the gel solution was injecting 6,000 barrels of a high molecular weight (16–18 million) polyacrylamide at a concentration of 0.4wt%, followed by 2,000 barrels of the same polymer at a concentration of 0.6wt%, and chased with 2,000 barrels of foamed cement in 2012. In this manner, gel was generated in reservoir and the treatment was strongest near the wellbore (foamed cement) and was less rigid deep into the reservoir (0.4wt% gel). Oil rate was increased by 490 BOPD from five producing wells. Gas production rate was reduced by 30 MM scf/d. One year later, oil rate was increased by 320 BOPD and gas production rate was only 5 MM scf/d less than the pre-treatment value.

Creel et al. (2001) and Honnert et al. (2006) reported the gel treatments in Slaughter Field, Central Mallet Unit (CMU), Texas. In these treatments, monomers, instead of polymers, were used. Treatments were performed on 20 wells from 2000 to 2005. These treatments were successful in maintaining oil rate while reducing CO_2 injection and production rate. And these treatments were considered an economic success.

Cain (2010) reported the gel treatment in Brookhaven Field. About 1,500–7,000 bbl of polymer solution and organic crosslinker were injected into the formation at polymer concentrations of 0.3–0.9 wt% at a rate of 1 bbl/minute. The wells were shut in after treatment to allow the gel to crosslink. Although injectivity decreased in three of the four injectors, improvements in the injection profile were modest and the effect on oil production was difficult to ascertain. It was concluded that the volumes of gel solution injected into the wells were too small.

In General, gels can treat water coning successfully in reservoir with vertical fracture. However, water coning through matrix reservoir is very difficult to be treated successfully with gels. On the other hand, conventional foams are considered effectively in matrix rock and are not applicable in reservoir fracture channels with aperture widths on the order of greater than 0.5 mm (Terry 2001).

1.3.3 Foam

Bond and Holbrook (1958) first proposed the idea of using foam for mobility control. Since then, CO_2 foam with surfactant has been used as an effective mobility-reducing agent for CO_2 flooding in the oil recovery process. One of the largest full-scale field demonstrations of foam for gas mobility control was the foam-assisted water alternating gas (FAWAG) project in the Snorre field on the Norwegian Continental Shelf from 1997 to 2000 (Blaker et al. 2002). Unfortunately, field experiences showed that conventional foam with surfactant injected in water had some significant limitations, as shown in **Table 1.3** and **1.4** (Enick and Olsen 2012). Enick et al. (2012) concluded the problems of FAWAG: (1) the dilution of CO_2 foam by subsequently injected water; (2) the inability of foam to be effective in formations containing fractures or extremely high-permeability open flow paths; (3) the very short propagation of the CO_2 from the injection well, cold weather ice and hydrate formation, unacceptably large decreases in injectivity associated with coinjection, and other unspecified "operational problems."

1.3.4 CO_2 Viscosifier

Viscosity of CO_2 is very low, ranging from 0.02 to 0.08 cp, which leads to a high mobility ratio for the CO_2 and in turn significantly decreases the sweep efficiency of CO_2. Increasing the viscosity of CO_2 with CO_2 viscosifier is a direct way to improve the sweep efficiency. Polymer and cosolvent are blended and pressurized together with CO_2 so that the fluid viscosity could be greatly increased before CO_2 is injected for oil recovery. A number of studies show that gas viscosifier chemicals can increase CO_2 viscosity by an order of one to two and can control CO_2 mobility (Heller et al. 1985, Terry et al. 1987, McClain et al. 1996, Bae and Irani 1993, DeSimone 1992, DeSimone 1994, Kendall and DeSimone 1997, Ali and Schechter 2013). However, the main barriers of viscosifer includes: (1) the large volume requirement of cosolvent makes pilot-testing costs prohibitive (Enick et al. 2012); (2) copolymers do not dissolve in CO_2 unless pressure far exceeds the minimum miscibility pressure (MMP) (Enick et al. 2012); (3) the environmental impact is negative (Kulkarni and Rao 2005).

Table 1.3—Reservoir parameter for CO_2 foam flooding

Field	Location	Geology	Depth m	Porosity range %	Perm range mD	Net Pay m	Oil viscosity at res. cp
JoffreViking	Canada	Sandstone	1500	13	500	3	1
Wasson	Texas	Dolomite (fractured)	1550	10-20	10	10	1
EVG/SAU	New Mexico	Dolomite (weakly fractured)	610	21.7		7.6	
SACROC	Texas	Limestone carbonate (dual porosity)	2100	8	~19	42	0.4
Wilmington	California	Clastic sands					
Rock Creek	West Virginia	Sandstone	610	21.7	21.5	7.6	3.2
Wertz	Wyoming	Sandstone					
North Ward Estes	Texas	Sandstone	800	18	15	18	1.4
Rangely Weber	Colorado	Sandstone	1782 -2106	11	10		
EMU 31	Texas	Dolomite	1520	1 - 18	0.01 - 28	30	
EMU 68	Texas	Dolomite	1520	1 - 18	0.01 - 28	30	
MCU 19	Utah	Carbonate					
MCU 21	Utah	Carbonate	1750	3-12	0.01 - 1000	15	
SACROC	Texas	Limestone carbonate (dual porosity)	2106	8	~19	42	0.4

Table 1.4—Performance of CO_2 foam

Field	Inc. in Inj P?	Dec injectivity?	Dec in GOR?	Inc. in Oil Prod?	Technical Success?	Economic Success?	References
Joffre Viking	2 MPa	Moderate	No	Difficult to Assess	No	No	Derril, et al., 1993
Wasson		Yes	30%	No?	Yes	No	Henry et al., 1996
EVG/SAU	3.5 Mpa		Yes	Yes	Yes	Yes But low	Heller, et al, 1994
SACROC			No	No	No	No	Smith, 1988
Wilmington	yes	yes			Partial	No	Holm and Garrison, 1988
Rock Creek	Yes	Yes			No	No	Heller, Boone, and Watts, 1985
Wertz					No	No	Borling, 1994
North Ward Estes	2.1	40 - 85%	9 times	15 times	Yes	Yes;	Chou et al. 1992
Rangely Weber	Yes	Yes	Yes	Yes	Yes	Yes	Jonas, Chou and Vasicek, 1990
EMU 31	2.6	Yes	2	31%	Yes	Yes	Hoefner and Evans, 1995
EMU 68	Too high	Too much	No	0	No	No	
MCU 19	Yes			Yes,		No	
MCU 21		Yes		No;	No	No	
SACROC		Yes		Phase 1	Yes	On-going	Sanders, 2010 (a)(b)

1.3.5 Simultaneous Water and Solvent Injection (SWAG)

Caudle and Dyes (1958) carried out the first SWAG study. They found that one way to improve the miscible displacement sweep efficiency was to lower the mobility behind the flooding front by injecting water with miscible gas. This reduced relative permeability to gas and lowered total mobility. Their laboratory study showed that sweep efficiency for a five-spot pattern could be increased to 90% with SWAG. However, only 60% of oil was recovered with CGI. Stone (2004) showed that the water-above-gas process can reach better sweep efficiency than simultaneous coinjection from the same location and can increase injectivity. Sohrabi et al. (2005) studied SWAG residual oil and water/gas injection ratio.

Faisal et al. (2009) suggested that a small slug size instead of coinjection water and gas would increase SWAG injectivity. Aleidan and Mamora (2010) studied how salt concentration affects SWAG/WAG recovery. Like CO_2 viscosifier, most SWAG researches are still in the experimental stage.

1.4 Research Objectives of Research

Early gas breakthrough has been a very common problem in CO_2-related projects, especially when there is a significant presence of heterogeneous elements such as fractures, channels and high permeability streaks within the reservoir. Cross-linked gel conformance control is most successful method to improve gas performance, while large volume gel polymer injection is required to reach successful treatment. Less than half of CO_2 foam is considered both technique and economic successful. CO_2 viscosifier and simultaneous water and gas injection are still in experiment level.

The paper proposed a new combination method, named as polymer-alternating-gas (PAG), to improve the volumetric sweep efficiency of WAG process. The feature of this new method is that polymer is added to water during WAG process to improve mobility ratio, and polymer flooding and immiscible/ miscible CO_2 injection are combined. In a PAG process, we used water to delay gas breakthrough and improve gas performance and used polymer to improve water sweep efficiency. The objective of this study was to analyze the feasibility of PAG in synthetic reservoir, channel reservoir and study the performance of PAG in typical section of the North Burbank Unit. I also studied CO_2 viscosifier performance in these models.

1.5 Structure of the Dissertation

The structure of this dissertation is as follows:

Section 2 introduced the simulator and models used for modeling PAG and CO_2 viscosifier. E100-Eclipse which includes polymer flooding model and pseudo-miscible model was used for PAG simulation and CO_2 viscosifier study.

Section 3 analyzed the sensitivity of polymer adsorption and concentration in PAG process, studied the feasibility of PAG in reservoirs with different permeability, Dykstra-Parsons permeability

variation coefficient (VDP), and type fluids. PAG performance in channel reservoir (SPE10b model) also was studied in the section. This study demonstrated that PAG can significantly improve recovery for immiscible/miscible flooding in homogeneity or heterogeneity of reservoirs.

Section 4 presented a field application for PAG injection. We first introduced the geologic feature, reservoir characteristic and fluid properties in the North Burbank Unit. We also reviewed the production history in this unit, especially, the EOR history. Then we built the reservoir and fluid models for five typical sections. After that we matched production history and optimized the CO_2 flooding injection and production, investigated the oil rate and gas rate performance in continue gas injection and WAG process. Next, we applied the PAG in these sections and compared the performances among PAG, WAG, CGI and polymer flooding. We further optimized the polymer concentration and injection slug patterns in the PAG process. We also evaluated the economics of different EOR methods for each section. In the end, we concluded this section with our discussions and recommendations about the PAG application in the North Burbank Unit.

In section 5, we showed a detailed study of CO_2 viscosifier performance through pseudo-miscible/ solvent model. CO_2 viscosity increased 2-fold, 5-fold, 10-fold, and 20-fold were used in this section. We started from an investigation of CO_2 viscosifier in reservoir models with different permeability and different heterogeneity. It was followed by a detailed comparison of recovery, oil rate, and gas oil ratio for CO_2 viscosifier injection in a channel reservoir model (SPE10 model). Then we also studied the CO_2 viscosifier performance in section TR78, which is a typical section in the North Burbank unit. Both continue gas injection and WAG performance with viscosified CO_2 were studied here. This section was concluded with some discussions and future work proposal.

Section 6 is the general conclusion and discussion about research work. I briefly discussed the potential and limitations of each part of our work, and then I proposed the future work plan to further this work.

2. METHODOLOGY

In this paper, we describe the software used for used for polymer alternating gas and CO_2 viscosifier simulation. In the PAG process, polymer flooding and gas flooding should be modeled at the same time. The commercial software E100, which is a simulator that can model both the Pseudo-miscible / solvent process and polymer flooding, is used for PAG study. Pseudo-miscible /solvent model is used for CO_2 viscosifier simulation.

2.1 Polymer Flooding

A high-molecular-weight and viscosity-enhancing polymer is added to the water of the waterflood in polymer flooding, to decrease the mobility of the flood water and, as a consequence, improve the sweep efficiency of the waterflood. Major aspects of a polymer flood and screening criteria are discussed as follow.

2.1.1Mobility Reduction

Mobility reduction is the primary conformance-improvement benefit of polymer waterflooding. The mobility reduction can be imparted by one of two distinctly different mechanisms. First, the polymer can increase brine viscosity. The second mechanism is the permeability reduction. The resistance factor R_f is used to measure of mobility reduction. R_f is defined as

$$R_f = \frac{\lambda_w}{\lambda_p}$$

where λ_w is the water mobility, and λ_p is the mobility of the polymer solution. When the polymer solution imparts no permeability reduction and for measurements made at ambient temperature,

$$R_f = \mu_{eff}$$

where μ_{eff} is the effective viscosity of the polymer solution as it flows through the reservoir matrix rock. Alternatively, for a single-phase polymer solution flowing through matrix reservoir rock at a given temperature and there is no imparted permeability reduction,

$$R_f = \frac{\mu_{eff}}{\mu_w}$$

where μ_w is the brine viscosity.

2.1.2 Polymer Retention/Adsorption

Polymer retention has profoundly impact on the technical and economic success of a polymer-flooding project. The amount of oil that will be recovered per pound of polymer injected is inversely related to polymer retention. Higher polymer adsorption means higher polymer consumption and lower polymer utilization.

Polymer adsorption/ retention:

- Increases as the permeability decreases
- Increases as the polymer molecular weight increases
- Increases as the clay content in the reservoir rock increases
- Usually decreases as oil wetness increases
- Tends to increase in sand and sandstone reservoirs with decreasing anionic charge and increasing cationic charge of the polymer's pendant groups
- Has been reported to increase at times in the presence of crude oil

Polymer retention should be determined carefully, or at least estimated carefully, before initiating a polymer waterflood. Polymer retention for a given polymer flood is normally best estimated by conducting core flooding experiments in reservoir rock with reservoir fluids at reservoir temperature.

2.1.3 Permeability Reduction

Polymer flow through reservoir matrix rock can lead to permeability reduction. Residual resistance factor R_{rf} is used to measure of the polymer-induced permeability reduction:

$$R_{rf} = \frac{k_b}{k_a}$$

where k_b is brine permeability measured before polymer flooding, and k_a is brine permeability measured after polymer flooding.

2.1.4 Inaccessible Pore Volume

When the flow of polymer molecules through the porous medium is restricted in pores with small openings, only the passage of water or brine is permitted. These small openings not contacted by flowing polymer molecules form what is called inaccessible pore volume (IPV).

The IPV can have beneficial effects on field performance. The rock surface in contact with the polymer solution will be less than the total pore volume, thus decreasing the polymer retention. More importantly, if connate water is present in the smaller pores inaccessible to the polymer, the bank of connate water and polymer-depleted injection water that precedes the polymer bank is reduced by the amount of inaccessible pore volume. One drawback however, is that movable oil located in the smaller pores will not be contacted by the polymer and therefore may not be displaced.

2.1.5 Polymer Degradation

A decrease in the average molecular weight of the polymer can be caused by chemical, biological, mechanical, or thermal degradation. Polymer stability, the inverse of degradation, should be evaluated and quantified under reservoir conditions in terms of a time span relevant to the lifetime of the polymer flood in question.

These factors are all very important when predicting the performance of a polymer flooding, however, the most important benefits are due to the decrease in mobility ratio and the increase in apparent viscosity due to polymer adsorption. The description of polymer flood simulation model can be found in "Eclipse Technical Description" or "CMG IMEX manual".

2.1.6 Screening Criteria for Polymer Flooding

The following screening guidelines can be used to determine where polymer waterflooding is most applicable, in terms of reservoir properties

- Oil viscosity < 150 cp (preferably < 100 and > 10 cp) and API gravity > 15°
- Matrix-rock permeability > 10 md, with no maximum
- Reservoir temperature: low temperatures are best (best at < 176°F; maximum of approximately 210°F)
- Water injectivity should be good with some spare capacity (hydraulic fracturing of injection wells may help)
- Reservoir clay content should be low
- Low salinity of the injection and reservoir brines are preferable

2.2 Pseudo-Miscible/Solvent Model

The objective of miscible displacement is to reduce the residual oil saturation through the complete elimination of the interfacial tension (IFT) between oil and the displacing fluid (solvent). This is achieved if oil and the displacing fluid are miscible, i.e. they mix together in all proportions to form one single-phase. Miscibility can be obtained on 'first contact' or through 'multiple contact'.

Miscible displacement is characterized by unstable frontal advances, in the form of either viscous fingering or gravity tonguing. These instabilities are caused by the highly adverse viscosity ratio and large density difference that generally exist between oil and the displacing solvent.

There are six major aspects of a solvent/Pseudo-miscible flood that need to be rigorously represented in a numerical model. They are:

Miscibility with pressure: In many miscible displacements, the gas is only miscible with the reservoir oil at high pressure. Typically the gas-oil capillary pressure reduces with increasing pressure, and only when it has reduced to zero can the two fluids be considered to be miscible. It is possible to model the

transition between miscibility and immiscibility as a function of pressure by defined the correlation between miscibility and pressure.

Todd and Longstaff mixing parameter: Todd and Longstaff proposed a method of simulating miscible displacement performance without reproducing the fine structure of the flow. Their method involves modifying the physical properties and the flowing characteristic of the miscible fluids in a three-phase black-oil simulator. They introduced a mixing parameter ω, which determines the amount of mixing between the miscible fluids with in a grid block. A value of zero corresponds to the case of a negligible dispersion rate, whereas a value of one corresponds to complete mixing.

Viscosity model: The effective oil and miscible gas viscosities follow the Todd-Longstaff model

Density model: The treatment of effective oil and gas densities is based on the same 1/4-power rule as the effective viscosities. By default the density calculation will use the same mixing parameter as the viscosity. However, a separate mixing parameter may optionally be specified for the effective density calculation.

Relative permeability: The injected gas and reservoir oil are considered to be miscible components of the hydrocarbon (non-wetting) phase. The flow is 2-phase in character and 2-phase relative permeability curves need to be defined for the water and hydrocarbon phases.

Effect of water saturation: A feature of miscible gas injection processes that may also be modeled is the screening effect of high water saturation on the contact between the miscible gas and the oil in-place in each grid cell. The effective residual oil saturation to a miscible gas drive is found to increase with increasing water saturation and correct modeling of the effect is important since it may reduce the efficiency of the miscible displacement.

The description of pseudo-miscible/solvent simulation model can be found in “Eclipse Technical Description” or “CMG IMEX manual”.

2.3 Discussion

When modeling polymer alternating gas by E100-Eclipse, most keywords of polymer flooding and pseudo-miscible/ solvent can be used together, except TLMIXPAR and PLMIXPAR.

PLMIXPAR: This keyword should only be used in runs which use the Polymer Model (keyword POLYMER). This keyword defines the Todd-Longstaff mixing parameter for the viscosity calculation. The value of the mixing parameter for each polymer mixing region should be in the range 0.0 to 1.0 inclusive.

TLMIXPAR: This keyword should only be used in runs which use the miscible flood option or the solvent model. The keyword is obligatory in these runs. First variable is Todd-Longstaff mixing parameter for the viscosity calculation. The value of the mixing parameter for each miscibility region should be in the range 0.0 to 1.0 inclusive. Second variable is Todd-Longstaff mixing parameter for the density calculation. The second data item can be ignored when PLMIXPAR is used in a Polymer flood model.

After test, we found that the second item in TLMIXPAR is not very sensitive in the Pseudo-Miscible/Solvent model, which gave us a confidence to use eclipse to model polymer alternating gas process.

3. PAG SIMULATION IN SYNTHETIC AND SPE 10 MODEL

To analyze the feasibility of PAG, coupled model considering both pseudo-miscible and polymer flooding process were built to study the performance of PAG. This section analyzed the sensitivity of polymer adsorption and concentration in PAG process, studied the feasibility of PAG in reservoirs with different permeability, Dykstra-Parsons permeability variation coefficient, and type fluids. PAG performance in channel reservoir (SPE10 model) also was studied in the section. This study demonstrated that PAG can significantly improve recovery for immiscible/miscible flooding in homogeneity or heterogeneity of reservoir.

3.1 PAG Simulation Based on Synthetic Reservoir

3.1.1 Synthetic Reservoir Model and Fluid Characterization

The reservoir model used in this study consists of 10×10×6 grid blocks. Grid dimensions are 44 ft ×44 ft ×10 ft, resulting in a reservoir 440 ft length, 440 ft width and 60 ft thick. The reservoir is thick enough to see the effect of gravity segregation. The reservoir is located 3,000 ft beneath the surface and has no dip. The reservoir is heterogeneous in vertical direction. **Figure 3.1** shows the synthetic reservoir model. The vertical injection and production wells are diagonally located in the model. In all study cases, the injection rate is fixed at 400,000 ft^3/day for gas injection well and 400 bbl/day for water injection well, and the bottom-hole pressure (BHP) at the production well is fixed at 2100 psi during gas flooding process. **Table 3.1** presents the input reservoir rock and fluid properties used for the simulation study.

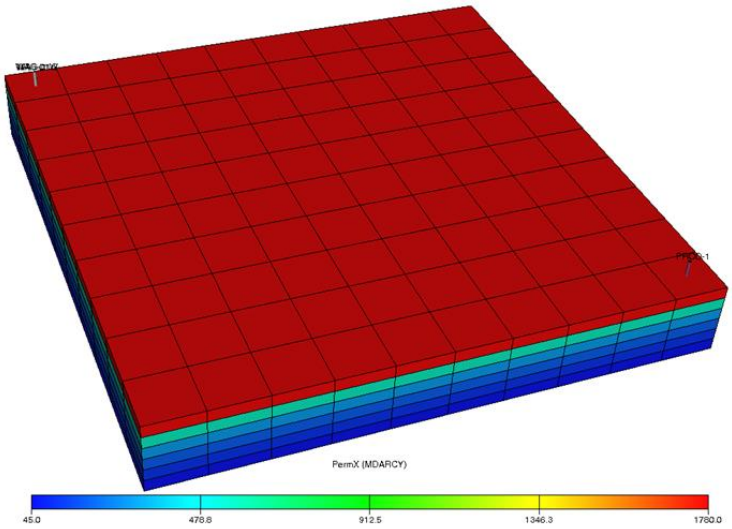

Figure 3.1—3D View of the Synthetic Reservoir Model (Permeability, md）

Table 3.1—Reservoir rock and fluid properties

Reservoir rock		Reservoir fluid	
Parameters	Value	Parameters	Value
Reservoir size, ft	440×440×60	Water density, lb/ft^3	63.0
Number of grid	10×10×6	Water viscosity,cp	0.5
Porosity	0.2	Initial oil saturation	0.2
kv/kh	0.01	Initial water saturation	0.8
Permeability,md	1-2,000	Water Salinity, mg/L	7,000

Relative Permeability Curves. Oil/water and gas/liquid relative permeability curves used for simulation are shown in **Figure 3.2** and **3.3**. Figure 3.2 shows that the oil relative permeability declines as the water saturation increases in the pore volume and restricts the flow of oil. The maximum oil relative permeability is 0.70 at connate water saturation, Swc = 25%. At 70% water (25% residual oil saturation to water, Sor), the oil relative permeability is zero. As water is injected, the water relative permeability increases, reaching a maximum value of 0.7 at 70% water saturation. Figure 3.3 demonstrates that the liquid relative permeability increases as the liquid saturation increases in the pore volume. The maximum liquid relative permeability is 0.70 at connate gas saturation, Sgc = 0.0%. At 55% liquid saturation, the liquid relative permeability is zero. As gas is injected, the gas relative permeability increases, reaching a maximum value of 0.6 at 45% gas saturation.

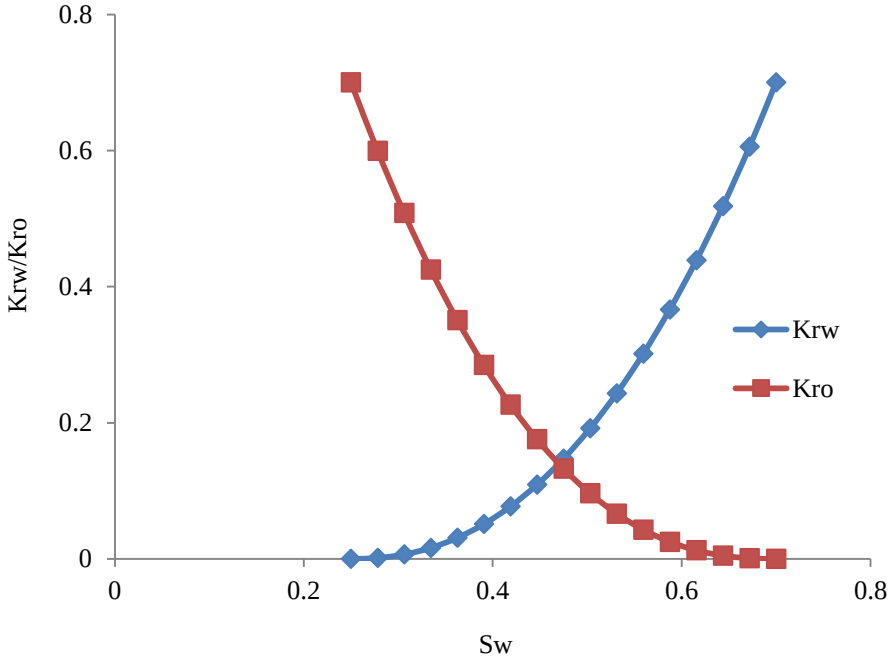

Figure 3.2—Water and oil relative permeability curves

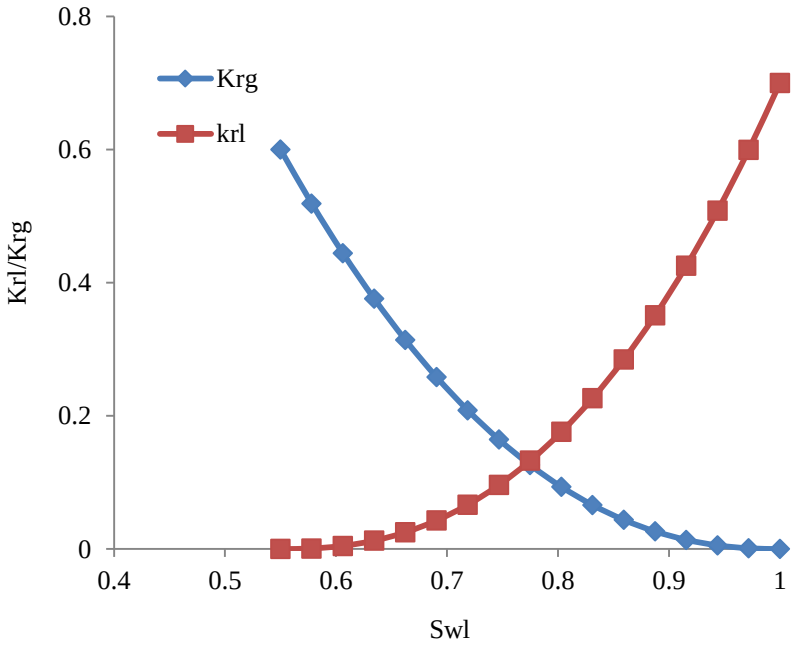

Figure 3.3—Liquid and gas relative permeability curves

Fluid Property. Five oil samples were used to study the feasibility of PAG in miscible and immiscible flooding and different oil viscosity. **Figure 3.4** shows correlation between oil viscosity and pressure. Viscosity of each oil sample at reservoir condition is 0.75, 2.25, 7.5, 22.5, and 45 cp, respectively. **Figure 3.5** shows a correlation between mix parameter ω and pressure for these five samples. Mix parameter ω controls the transition between immiscible and miscible. A value of ω=1 results in a piston-like displacement of oil by the injected gas. If ω=0, the displacement is similar to an immiscible displacement (except for the treatment of relative permeability). Compared with oil sample #2, oil sample #1 has a higher value of mix parameter at the same pressure, which means oil sample #1 has better miscible possibility. The minimum miscible pressure for each oil sample is 1700, 1700, 2500, 2500, and 2500 psi, respectively. In this study, the highest injection pressure at injectors is set to 2,100 psi, which implies that miscible flooding is possible for oil sample #1 and #2 and oil sample #3 to5 would be used for immiscible flooding in the study.

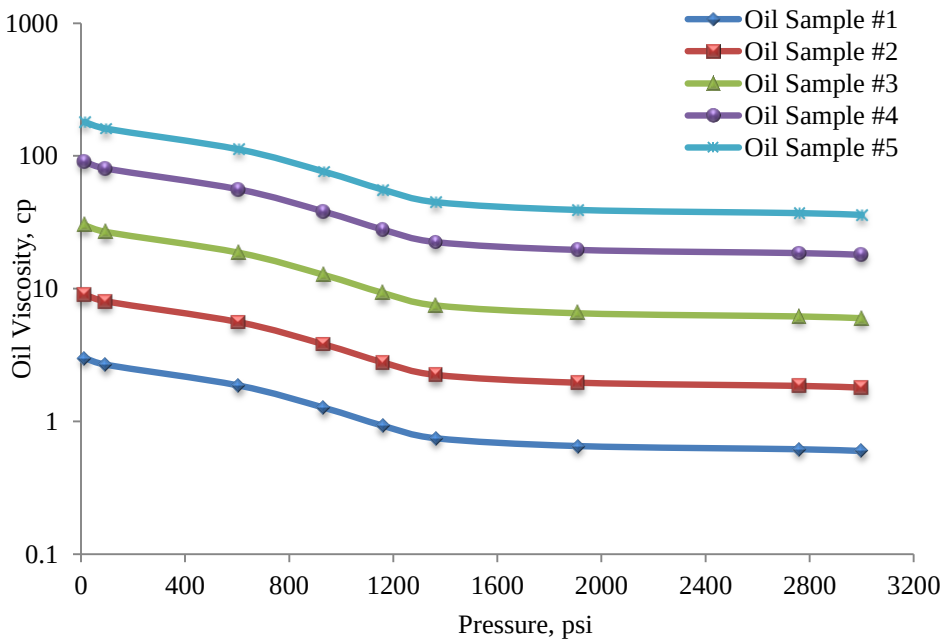

Figure 3.4—Correlation between oil viscosity and pressure

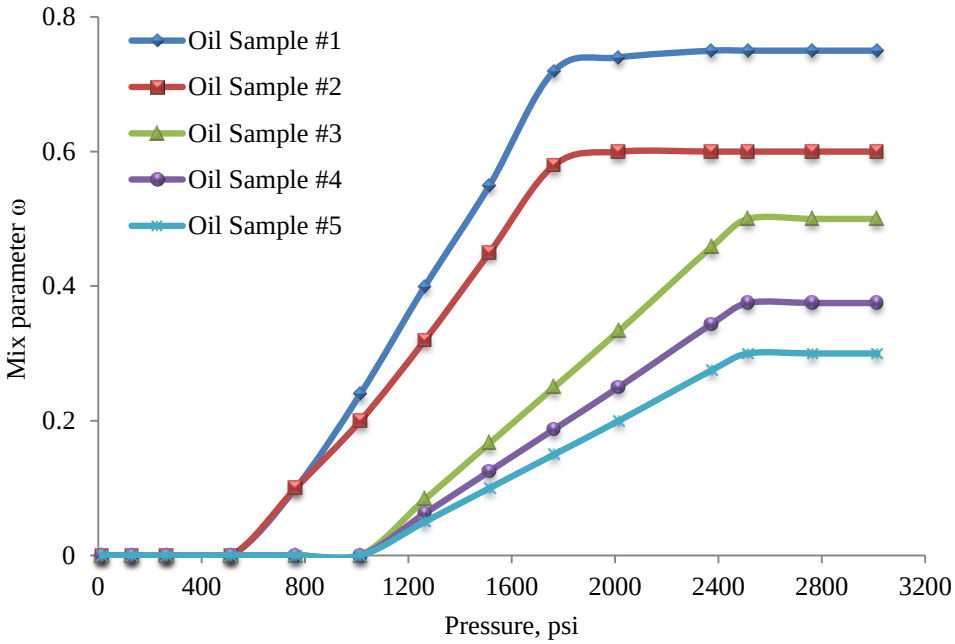

Figure 3.5—Correlation between mix parameter ω and pressure

Parameters for Polymer Flooding. Rock adsorption and polymer viscosity are two important parameters for polymer flooding. As lack of polymer test, polymer viscosity and adsorption were assumed in this simulation. The correlation between polymer viscosity and polymer concentration is shown in **Figure 3.6**. **Figure 3.7** shows three correlations between polymer concentration and polymer adsorption. For Function 1, the maximum adsorption is 10 ug/ (g rock); for Function 2, the maximum adsorption is 50 ug/ (g rock); for Function 3, the maximum adsorption is 200 ug/ (g rock). We also assumed a residual resistance factor (RRF) value of 1.8 at 0.55 lb/stb in this study.

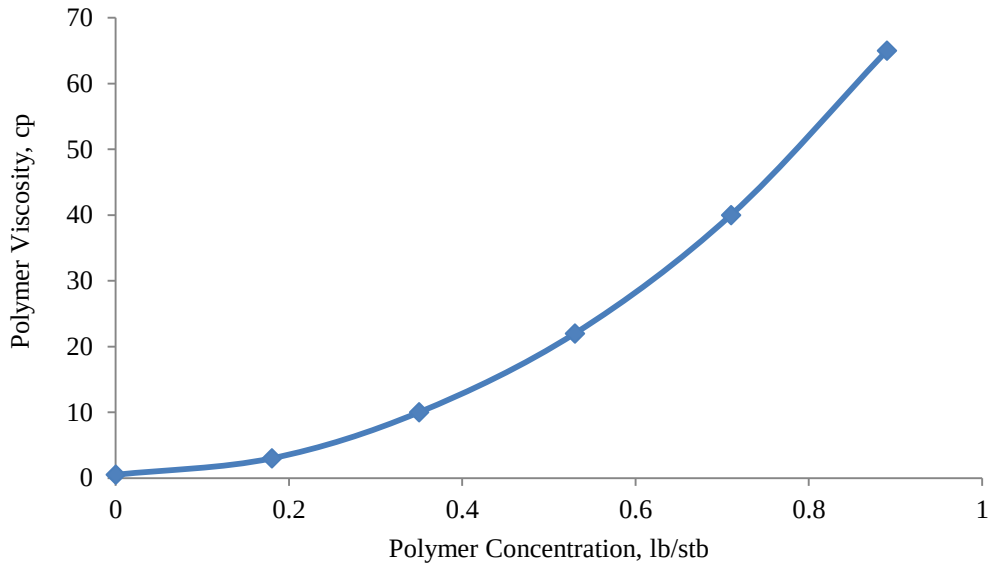

Figure 3.6—Correlation between polymer concentration and polymer viscosity

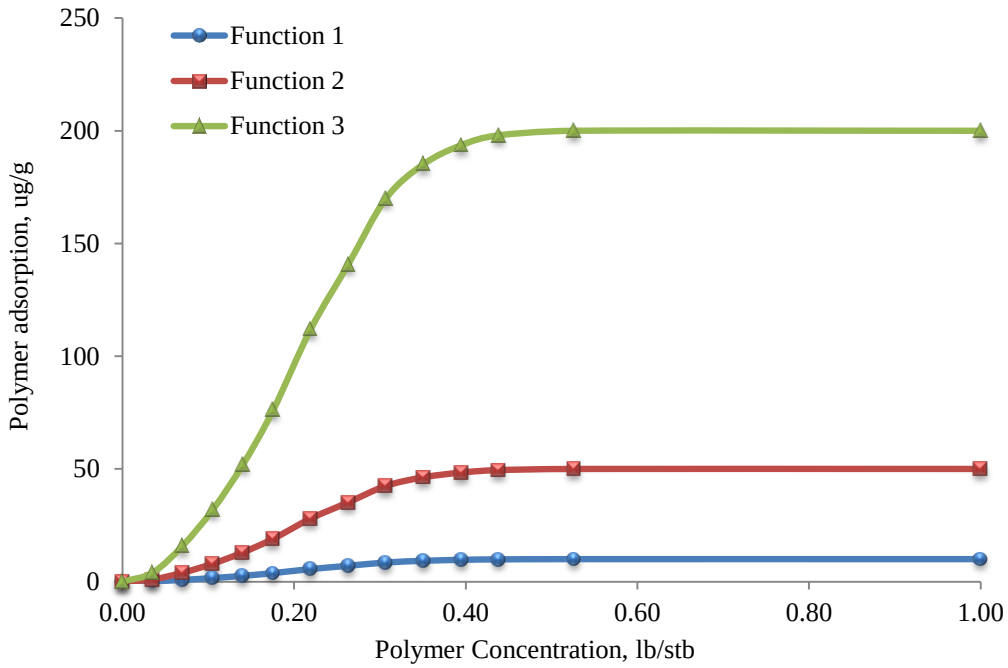

Figure 3.7—Polymer Adsorption Functions

3.1.2 Sensitivity Study of Polymer Parameters

To have a sensible study, we assumed that the simulation model data are based on a water flooded reservoir with water cut 98%. Base case was defined by water alternating gas injection. PAG case was defined by the injection of chemical slug which contains polymer alternating gas injection. The reservoir performance during PAG process was compared with WAG. A sensitivity analysis was performed on critical parameters that affect the process significantly, including polymer adsorption and polymer concentration.

Polymer Adsorption. Three processes with different adsorption functions were analyzed. Results are plotted in **Figure 3.7**. In the PAG process, WAG ratio 1:1 (3:3 months) and fluid injection rate 0.1 pore volume per year (0.05 pore volume of gas and 0.05 pore volume of water) were used and polymer concentration was set to 0.2 lb/stb. **Figure 3.8** and **3.9** indicate that reducing polymer adsorption would significantly increase oil rate and reduce water cut. Higher polymer adsorption would lead to lower oil recovery (**Figure 3.10**). Polymer retention leads to loss of polymer from solution, which causes the mobility control effect to be lost. If both the polymer slug and concentration of injected polymer solution is low, retention may lead to polymer flooding fail. From these three run processes, it can be seen that the smaller polymer adsorption, the higher peak oil rate and higher oil recovery.

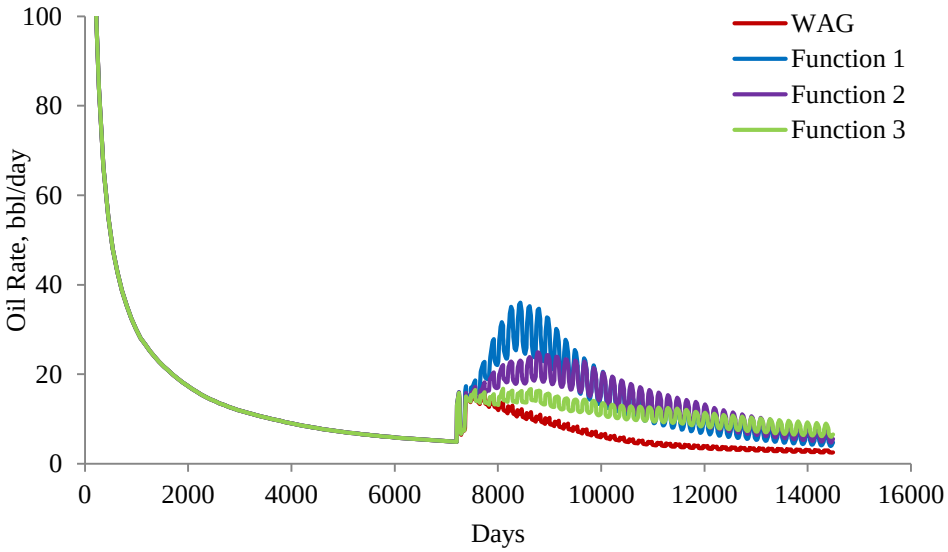

Figure 3.8—Oil production rate with different polymer adsorption function

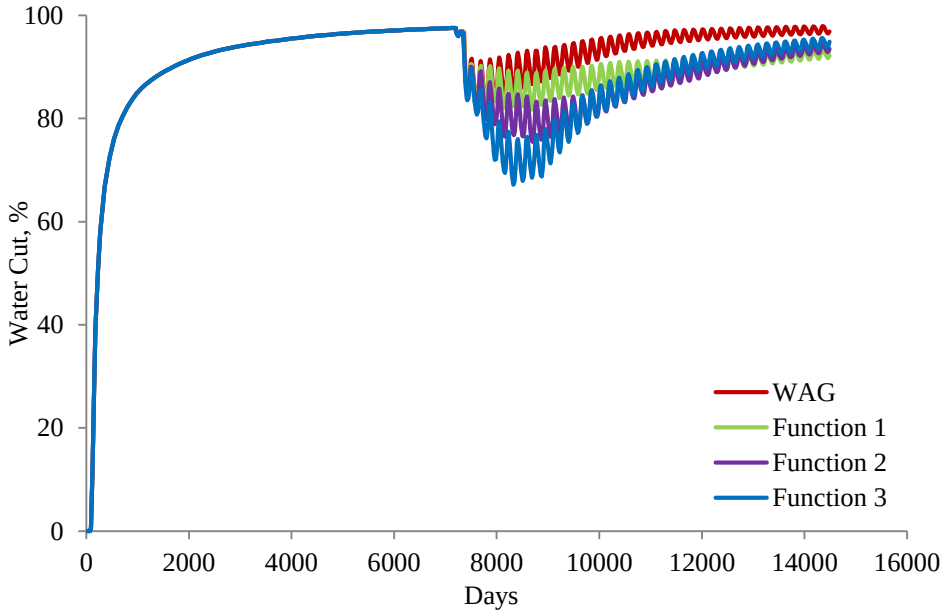

Figure 3.9—Water cut with different polymer adsorption function

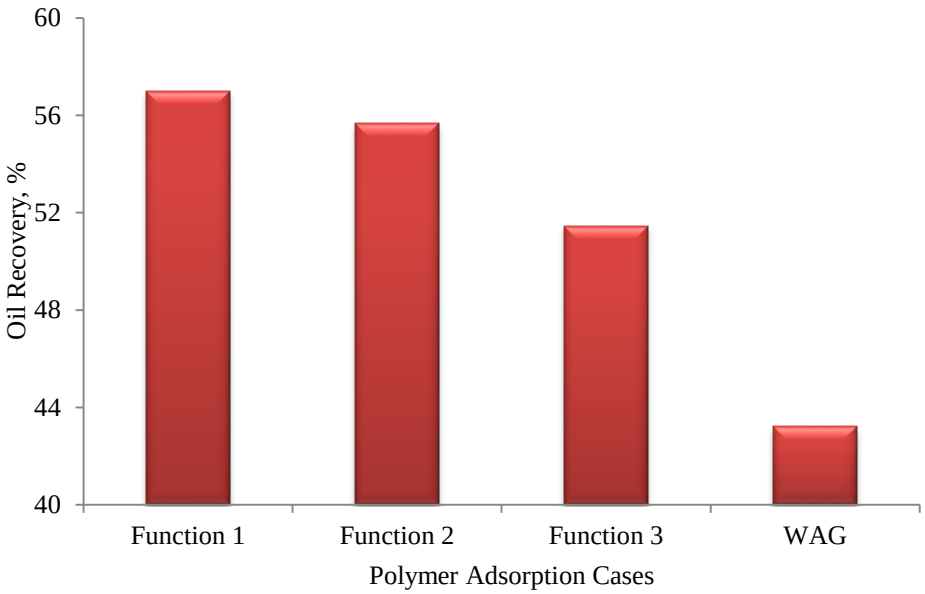

Figure 3.10—Oil recovery under PAG with different polymer adsorption functions

Polymer Concentration. Compared with WAG, one main purpose of PAG process is to control the water viscosity by adding polymer into injected water to lower the water mobility, especially, for high permeability river channel reservoir. The biggest benefit of polymer flooding is from the viscosity increasing of water phase, which improves the water-driving. Higher polymer concentration leads to higher viscosity. **Figures 3.11 to 3.13** show simulation results of WAG and PAG process with different polymer concentrations. The three PAG processes have the same injected polymer slug size. The higher the polymer concentration is, the more oil can be recovered (Figure 3.11). Practically, polymer concentration cannot be increased without upper limit. With polymer concentration increasing, the viscosity will be highly increased. As a result, the injecting pressure will correspondingly increase if the injection rate is kept stable. If the pressure is too high, the reservoir rock will be fractured.

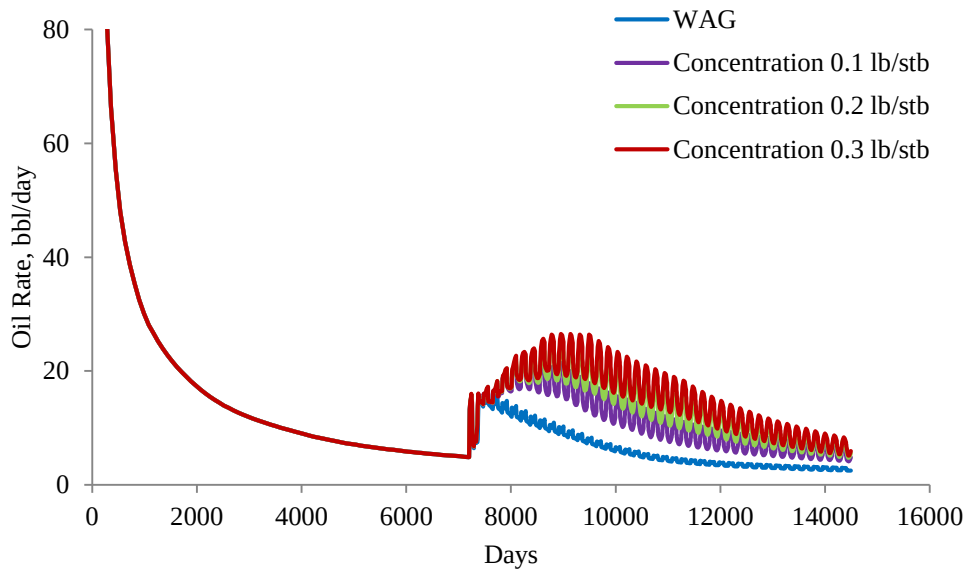

Figure 3.11—Oil production rate with different polymer concentration

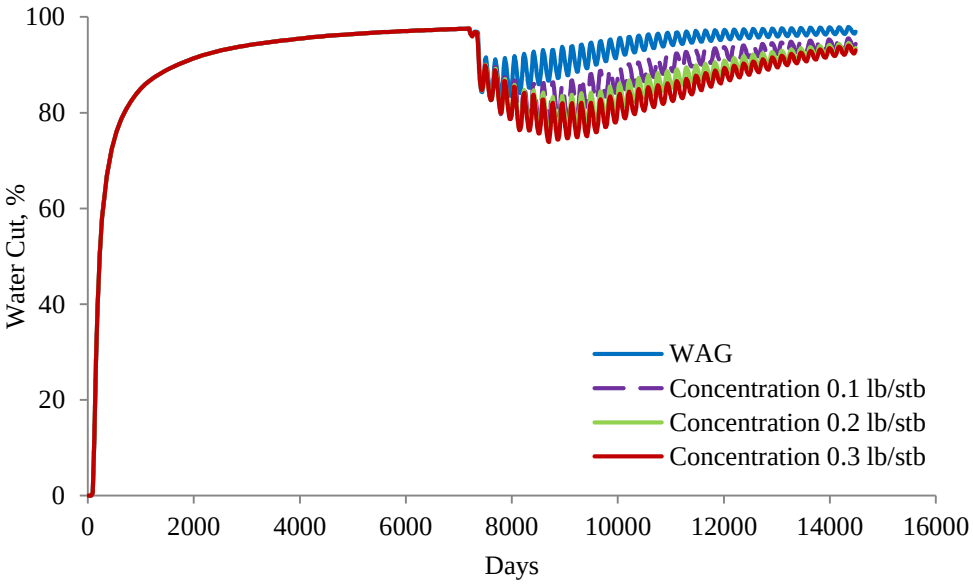

Figure 3.12—Water cut with different polymer concentration

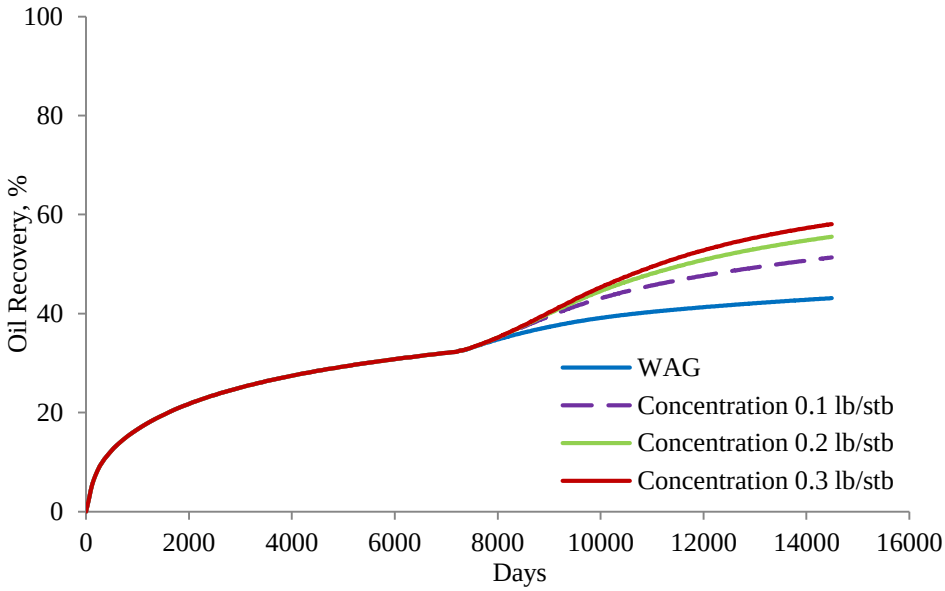

Figure 3.13—Oil recovery under PAG with different polymer concentration

3.1.3 Feasibility Study of PAG in Different Reservoir and Fluid Conditions

To address what type of fluids and reservoirs are the PAG flooding candidates, feasibility study was carried out on different fluid viscosity, reservoir permeability and VDP. Reservoir with permeability 500 md and VDP 0.70 is used for feasibility study in fluid viscosity. Oil sample #2 is used for feasibility study in both homogenous and heterogeneous models.

Fluid Viscosity. Polymer flooding is usually used for reservoir fluid with viscosity range 10-150 cp, while CO_2 flooding prefers light oil with viscosity below 10 cp. A sensitivity study of the reservoir performance due to oil viscosity was conducted on the PAG model by changing the oil viscosity values. Five oil viscosity values (0.75, 2.25, 7.5, 22.5, and 45 cp) were studied. During PAG process, polymer concentration was set to be of 0.20 lb/stb for these five cases. **Figure 3.14** shows that: (1) lower viscosity would lead to higher recovery of waterflooding, WAG and PAG; (2) oil recovery from PAG process is 16-24% higher than that of water flooding; (3) oil recovery from PAG process is 10-13% higher than that of WAG; (4) PAG could significantly increase recovery in both miscible and immiscible flooding.

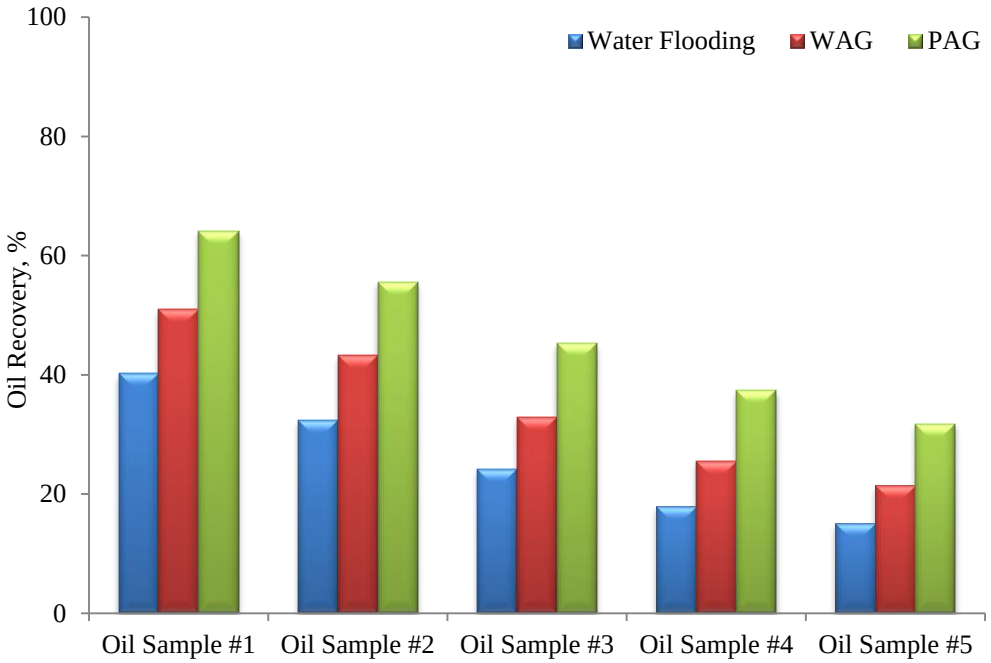

Figure 3.14—Comparison of oil recovery among waterflooding, PAG and WAG for models with oil viscosity

Homogenous Formation. Permeability from 50-1,000 md was studied. **Table 3.2** shows the polymer injection concentrations for formations with different permeability. **Figure 3.15** indicates that: (1) No significant difference in waterflooding recovery when permeability varies from 50 to1,000 md; (2) PAG does not improve recovery when permeability is lower than 500 md in this study. The main reason is WAG could reach very high recovery (more than 60%) for homogenous formation with low permeability, while polymer has injectivity problem in such a low permeability formation; (3) Oil recovery from PAG process is 7-15% higher than that from WAG when permeability is higher than 500 md in homogenous formation.

Table 3.2—Polymer injection concentration

Permeability, md	50	100	200	500	1,000
Polymer concentration, lb/stb	0.05	0.05	0.1	0.2	0.2

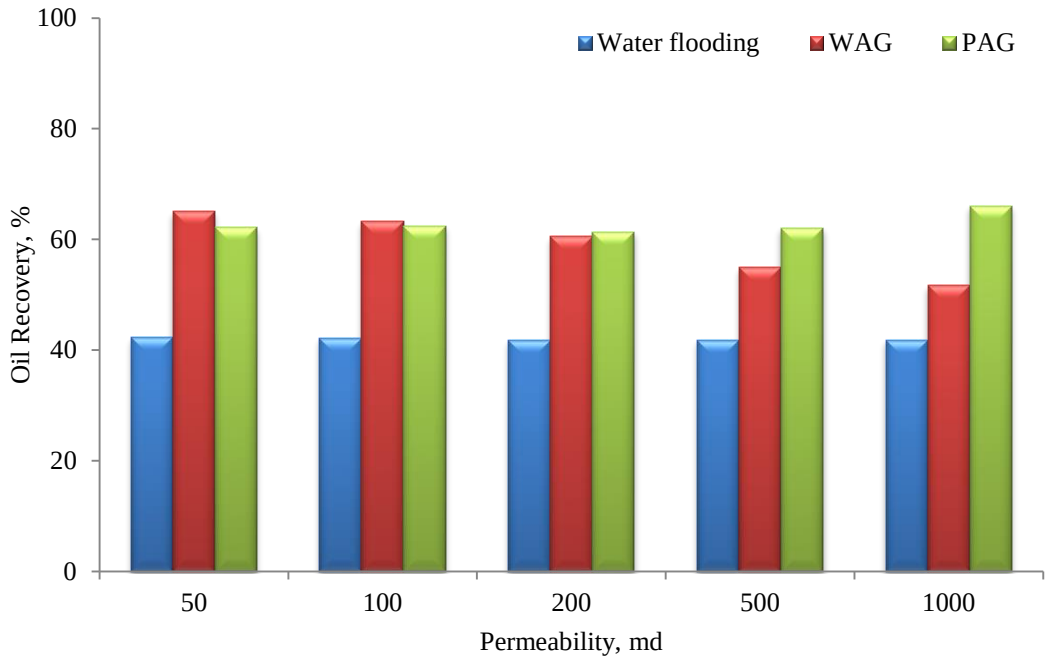

Figure 3.15—Comparison of oil recovery from models with difference permeability

Heterogeneous Formation. Vertical heterogeneity of formation would lead to CO_2 fast breakthrough. In this paper, two groups of heterogeneous models were studied. One group model has average permeability of 100 md, the other one has average permeability of 500 md. VDP values range from 0.5 to0.9 for both group models. Polymer concentration was set to 0.2 lb/stb for all the cases.

Figure 3.16 shows that: (1) lower VDP would lead to higher recovery of waterflooding, WAG and PAG; (2) oil recovery from PAG process is 18-29% higher than that from waterflooding; (3) oil recovery from PAG process is 7-13% higher than that from WAG; (4) Compared with WAG, increment of recovery from PAG decreases with the increasing VDP value. It means that higher polymer concentration is needed for high permeability formation with high VDP value.

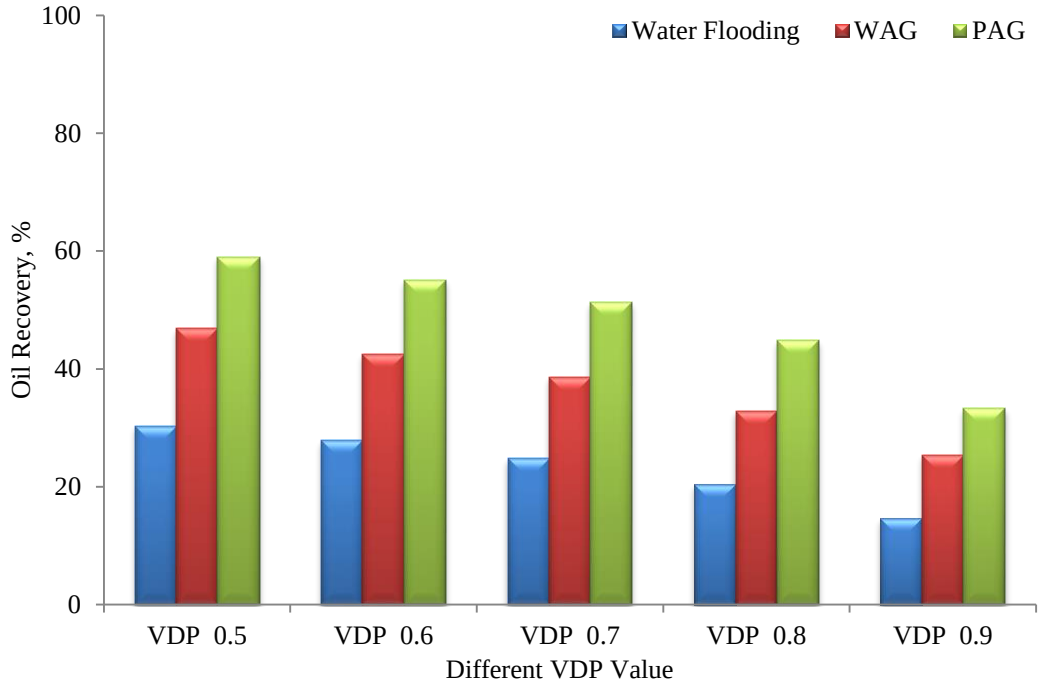

Figure 3.16—Comparison of oil recovery from models with different VDP

Figure 3.17 points out that: (1) lower VDP would lead to higher recovery of waterflooding, WAG and PAG; (2) oil recovery from PAG process is 21 to 25% higher than that from water flooding; (3) oil recovery from PAG process is 3 to 11% higher than that from WAG; (4) Compared with WAG, increment recovery from PAG increases with the increasing VDP value. It means that lower permeability formation with high VDP value is a good candidate for PAG flooding.

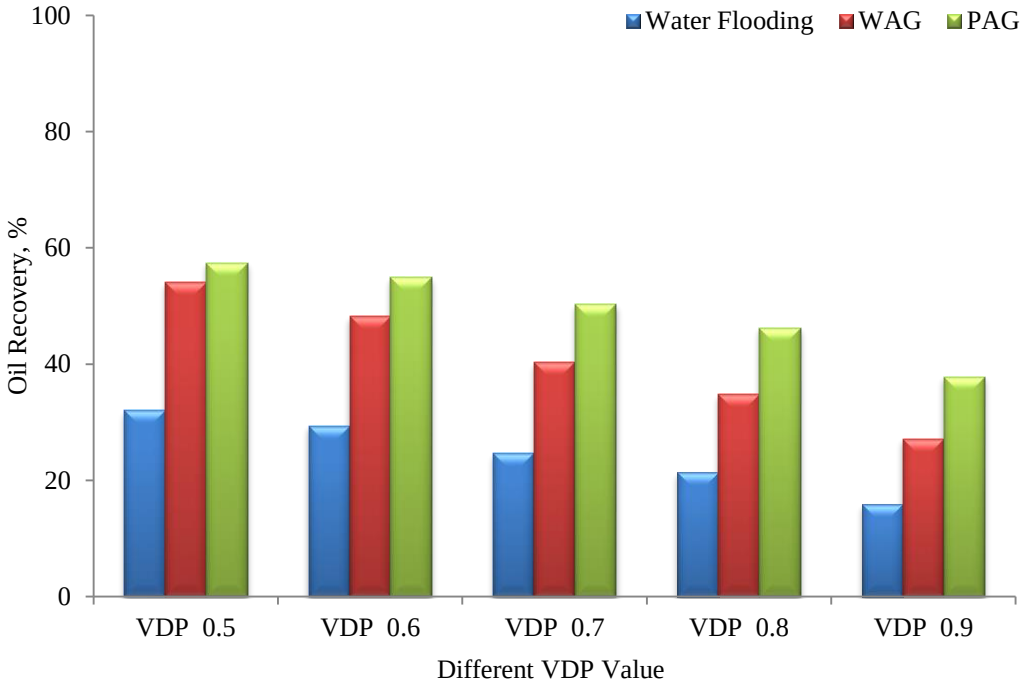

Figure 3.17—Comparison of oil recovery among waterflooding, PAG and WAG for models

Different Permeability Distribution. Vertical heterogeneity of formation would lead to CO_2 fast breakthrough and different permeability distribution has significantly impact on CO_2 performance. Three different permeability distributions, including high permeability at top, at bottom and mi-layer (**Figure 3.18**) were studied to demonstrate the influence.

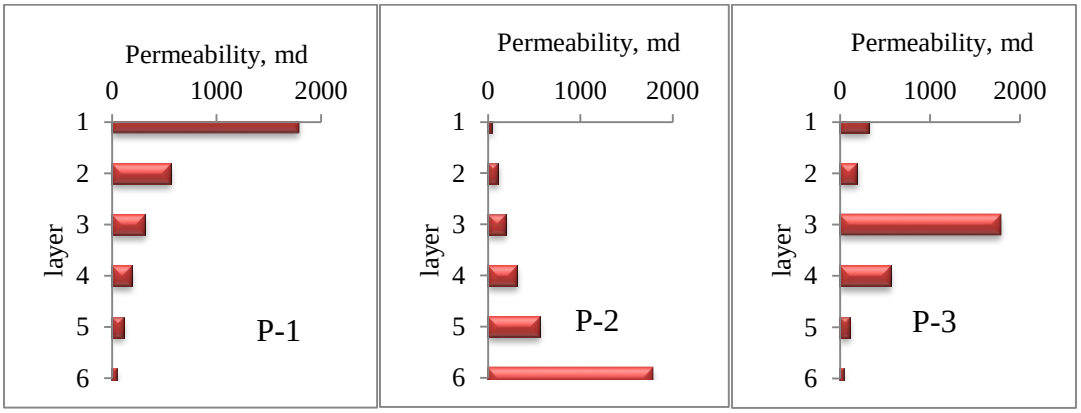

Figure 3.18—Different permeability distributions

P-2 has lowest water flooding recovery, and P-1 has highest water flooding recovery (**Figure 3.19**). It indicates that water flooding prefer the reservoir with high permeability at top dues to water gravity effect. In the Gas flooding process, P-1 has lowest recovery and P-2 has highest. The results show that high permeability at top would lead to poor CO2 performance due to CO2 override. Figure 3.19 also show that similar recovery was obtained in PAG process for different permeability distributions. It indicates that PAG could improve WAG process most significantly in P-1 permeability distribution.

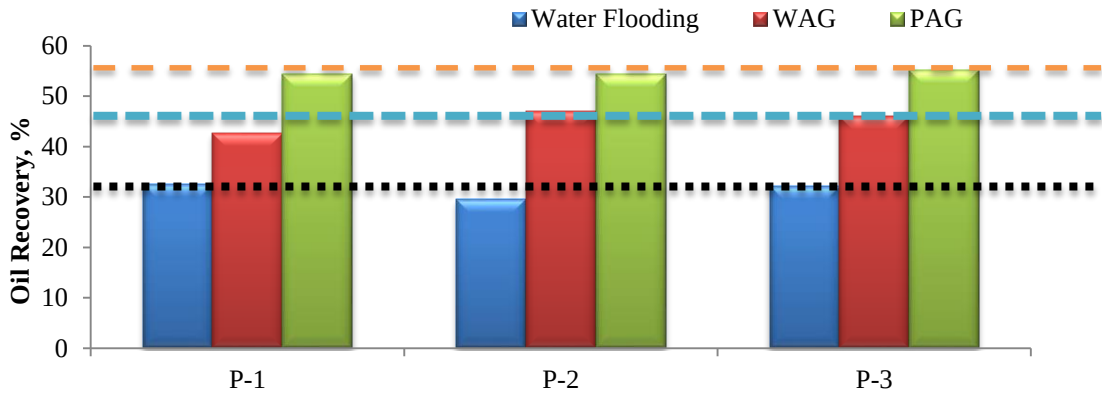

Figure 3.19—Recovery from different permeability distributions

3.1.4 Conclusions of PAG Simulation Based on Synthetic Reservoir

A new EOR method, named PAG, was proposed to improve the efficiency of conventional WAG process. The following conclusions are made for this study:

(1) PAG is very sensitive with polymer adsorption. Lower adsorption would lead to higher recovery.

(2) Increasing polymer concentration would increase oil recovery in PAG process if it does not cause injectivity problem.

(3) Based on recovery from different type of oil, PAG could significantly increase recovery in both miscible and immiscible flooding.

(4) Oil recovery from PAG process is 7 to 15% higher than that of WAG when permeability is higher than 500 md in homogeneity reservoir in this study.

(5) PAG could improve WAG perform in both high and low permeability heterogeneity reservoir with VDP vary from 0.5 to 0.9.

3.2 Reservoir Simulation of PAG in SPE10 model

In the previous synthetic models, we do not consider the channels in the model, which usually would have significantly impact on recovery in the gas flooding project. Here we studied the PAG performance in the SPE10 model, which includes channels in the model.

3.2.1 Reservoir Description

SPE10 model has a simple geometry, with no top structure or faults. At the fine geological model scale, the model is described on a regular cartesian grid. The model dimensions are 1200 × 2200 × 170 (ft). The fine scale cell size is 20 ft × 10 ft × 2 ft. The fine scale model size is 60 × 216 × 85 cells (1.10×10^6 cells). The model consists of part of a Brent sequence. The model was originally generated for use in the PUNQ project. **Figure 3.20** shows the porosity for the whole model. The top part of the model is a Tarbert formation, and is a representation of a prograding near shore environment. It includes 70 ft (37 layers) in the vertical direction. The lower part (Upper Ness) is fluvial. The thickness is about 100 ft (48 layers). **Figure 3.21** shows the porosity of the Upper Ness sequence, with the channels clearly visible. In this study, upper Ness sequence (named SPE10b) is used for study.

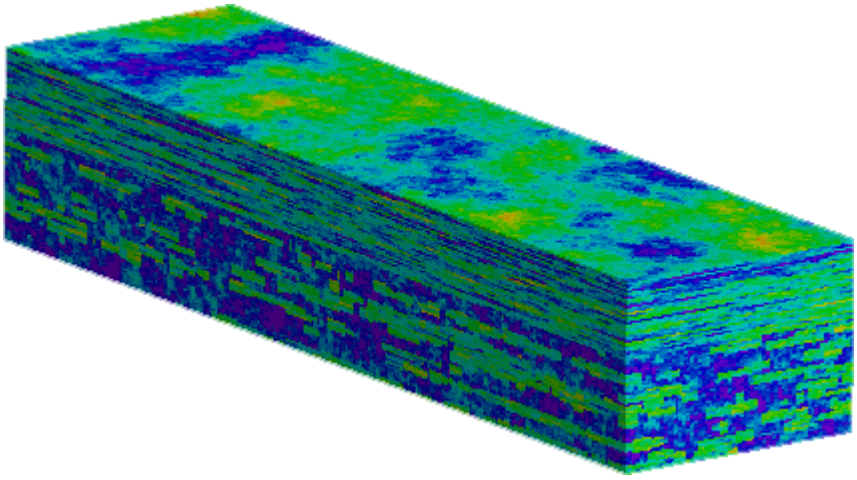

Figure 3.20— SPE10 reservoir model

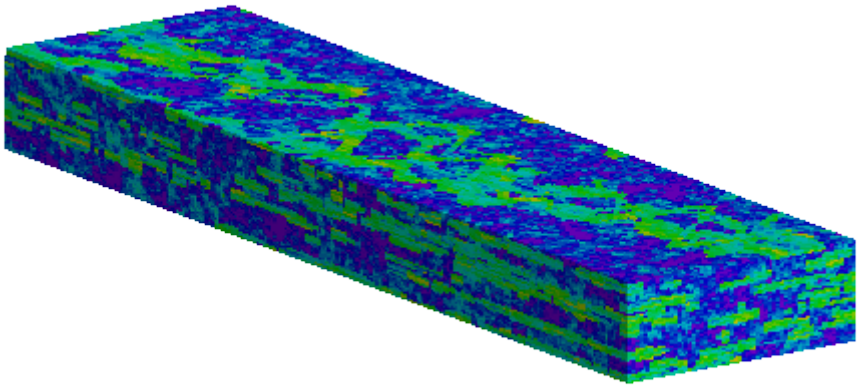

Figure 3.21— SPE10 reservoir model—Upper Ness Sequence

3.2.2 Relative Permeability

Oil/water and gas/liquid relative permeability curves used for simulation are shown in **Figure 3.22** and **3.23**. Fig 3.20 shows that the oil relative permeability declines as the water saturation increases. The maximum oil relative permeability is 1.0 at connate water saturation, Swc = 20%. At 80% water (20% residual oil saturation to water, Sor), the oil relative permeability is zero. As water is injected, the water relative permeability increases, reaching a maximum value of 1.0 at 80% water saturation. Figure 3.21 shows that the interrelation between gas and liquid relative permeability. The maximum liquid relative

permeability is 1.0 at connate gas saturation, Swc = 0.05%. At 85% gas (15% residual liquid saturation to gas), the liquid relative permeability is zero.

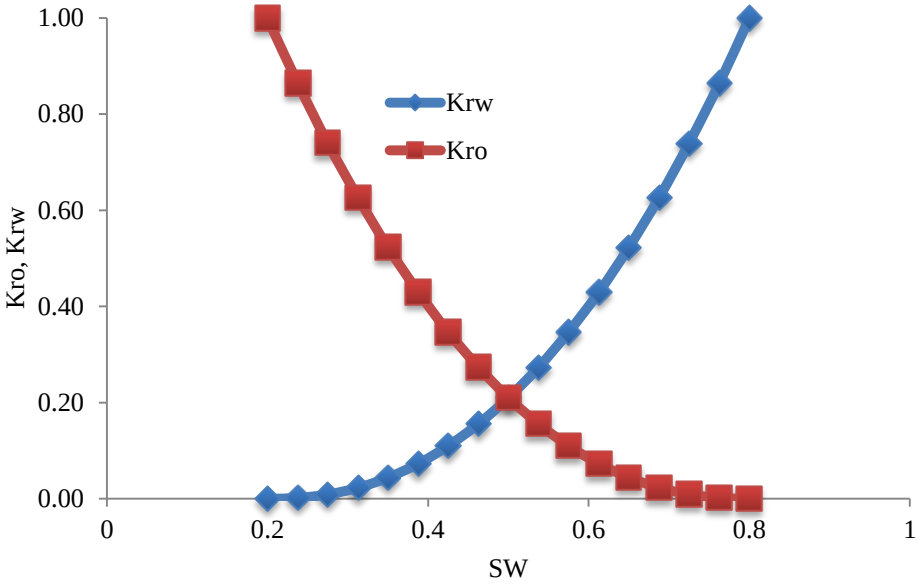

Figure 3.22—Water and oil relative permeability curves

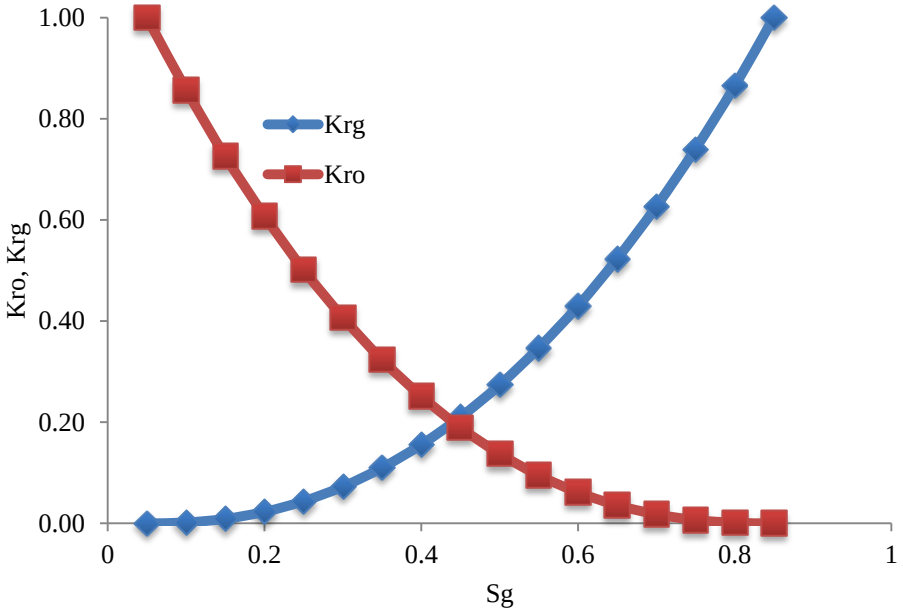

Figure 3.23—Liquid and gas relative permeability curves

3.2.3 Fluid PVT

Viscosity of oil sample at reservoir condition is 3 cp. **Figure 3.24** shows correlation between oil viscosity and pressure. **Figure 3.25** shows the correlation between mix parameter ω and pressure for samples. A maximum value ω is obtained when pressure is higher than 1,700 psi, which is the minimum miscible pressure for this sample. In this study, the highest injection pressure at injector was set to 2,100 psi, which means that miscible flooding is possible for this oil sample.

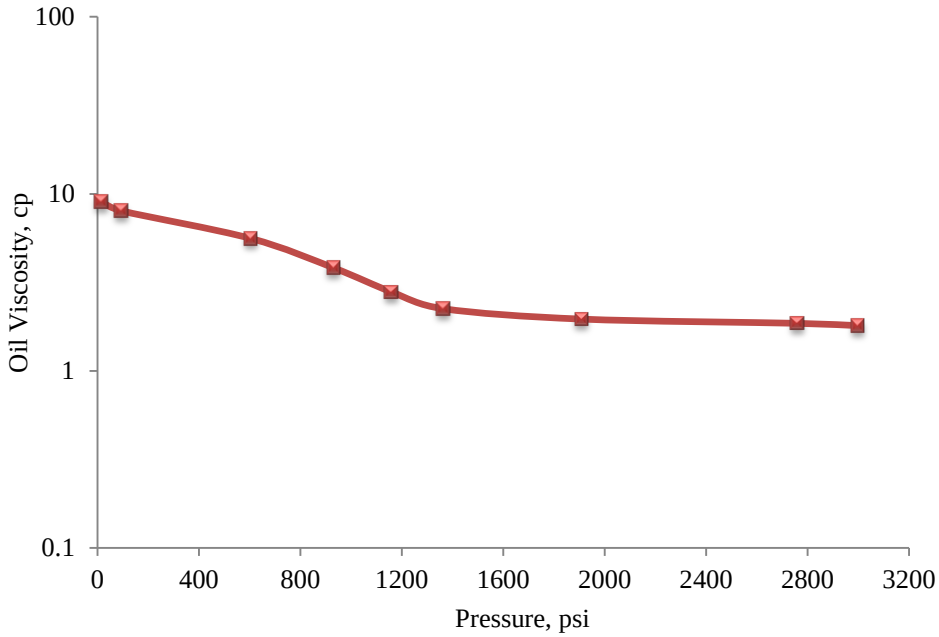

Figure 3.24—Correlation between oil viscosity and pressure

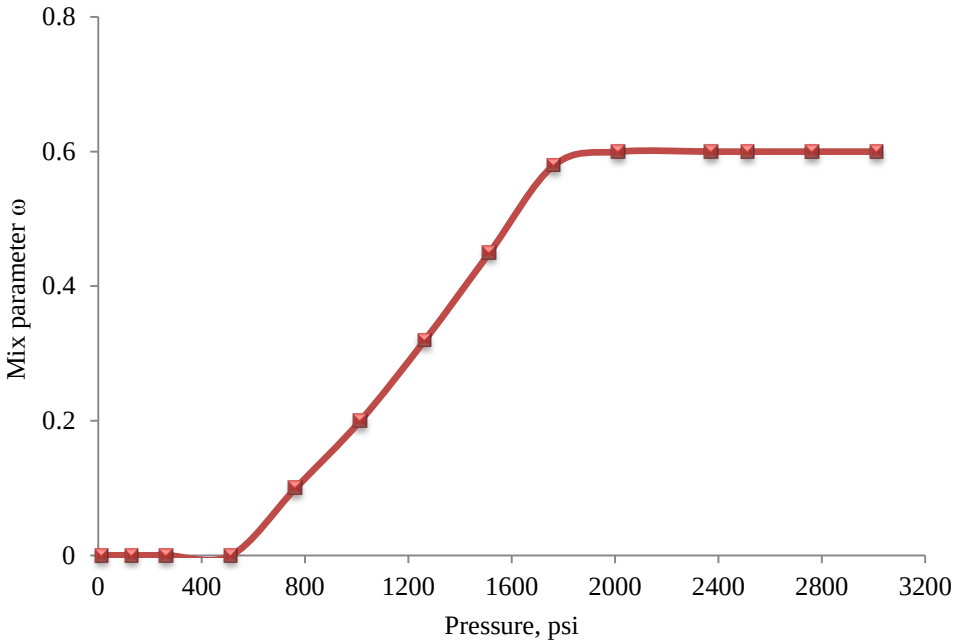

Figure 3.25—Correlation between mix parameter ω and pressure

3.2.4 Upscale SPE10b Model

The size of fine scale model SPE10 is 60 × 216 × 48 cells (622080 cells). Based on lab computer capability, it would take more 100 hours to model one case of polymer alternating gas. Here we used streamline methods to upscale the model. The model was coarsened to 30 × 108 × 8 cells (25920 cells). Histogram and mapping was used to validate permeability upscaling. **Figure 3.26** to **3.29** shows that model after upscaling has similar distribution as fine grid.

We also studied the water flooding performance for these two models. Four producers at corner and one injector at center were defined. In this study, we injected water for 30 years with an injection 2,000 bbl/day (0.1 pore volume/year) and kept the liquid produce rate the same as injection rate. **Figure 3.30** to **3.37** shows the water flooding results from fine grid model and upscale model. These figures indicate that upscale model could represent the main characteristic of fine grid model and we can use upscale model instead of fine grid model for further study.

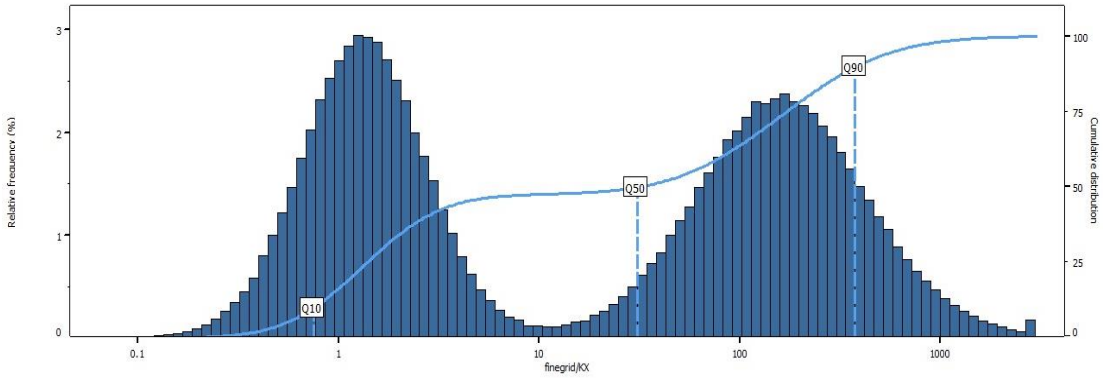

Figure 3.26—Histogram of X-permeability distribution from fine grid system

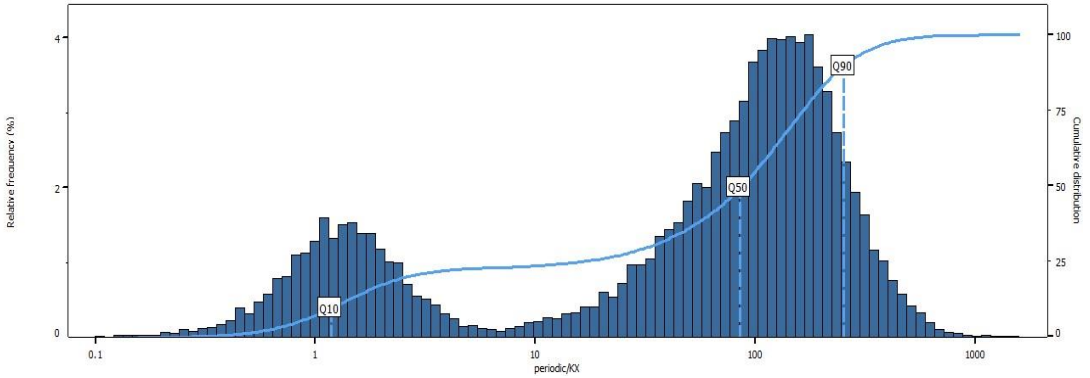

Figure 3.27—Histogram of X-permeability distribution from upscale system

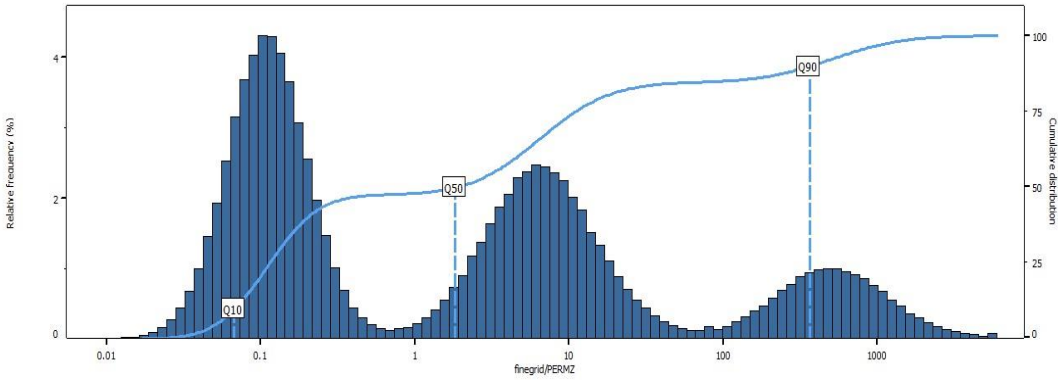

Figure 3.28—Histogram of Z-permeability distribution from fine grid system

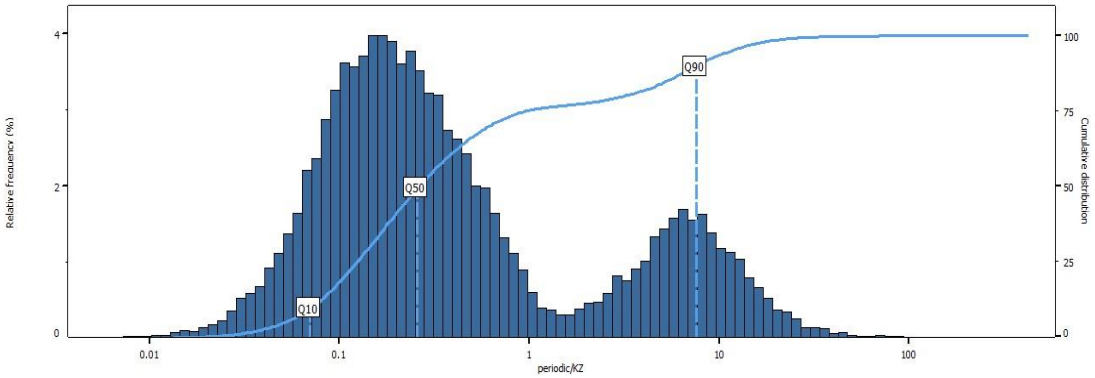

Figure 3.29—Histogram of Z-permeability distribution from upscale system

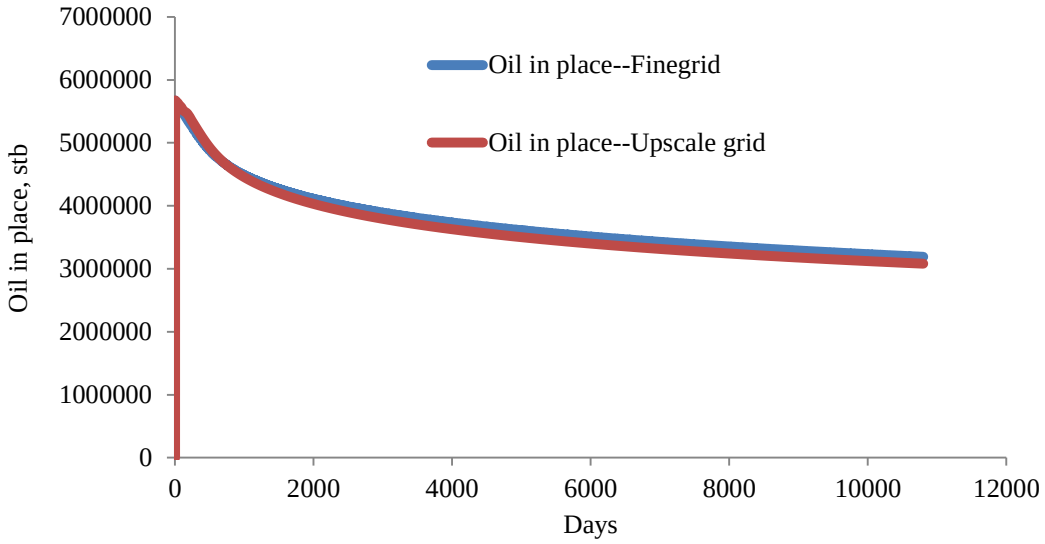

Figure 3.30—Oil in place for fine grid model and upscale model

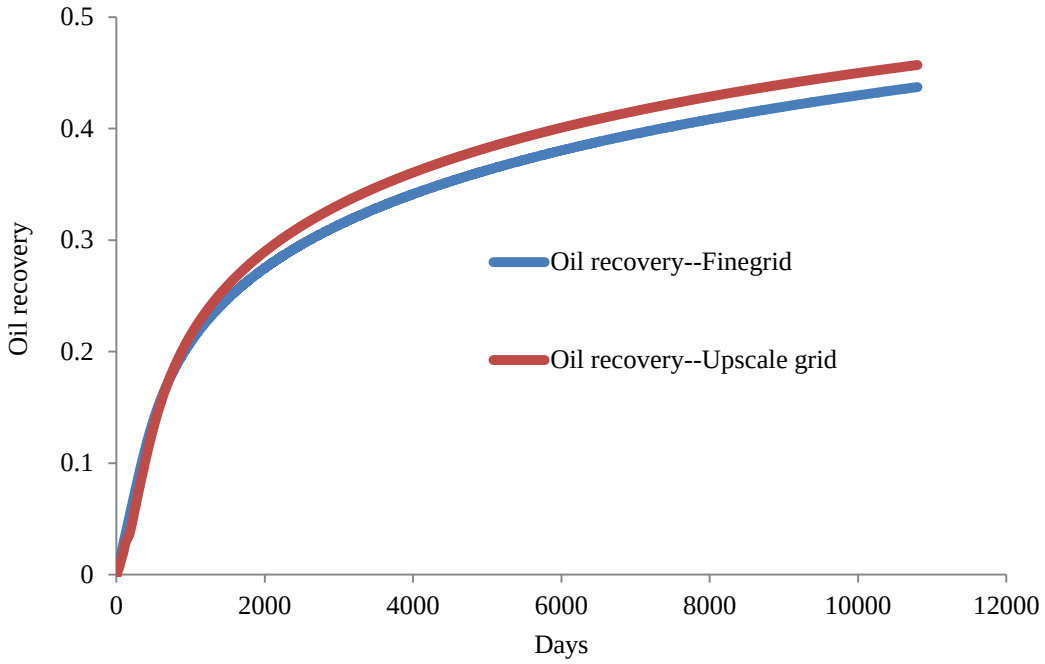

Figure 3.31—Oil recovery for fine grid model and upscale model

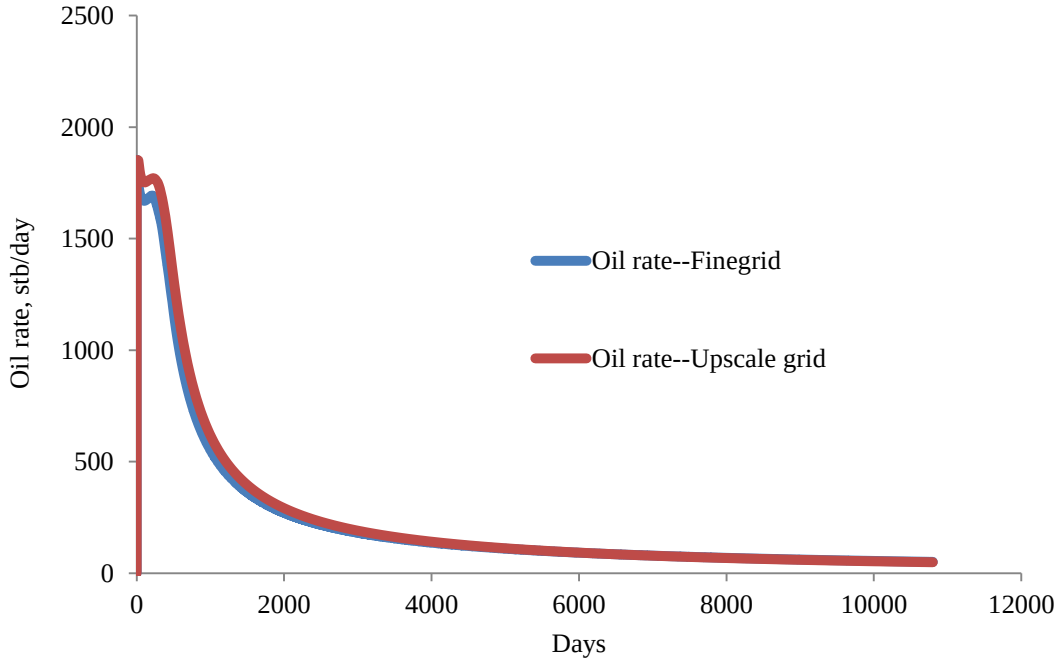

Figure 3.32—Oil rate for fine grid model and upscale model

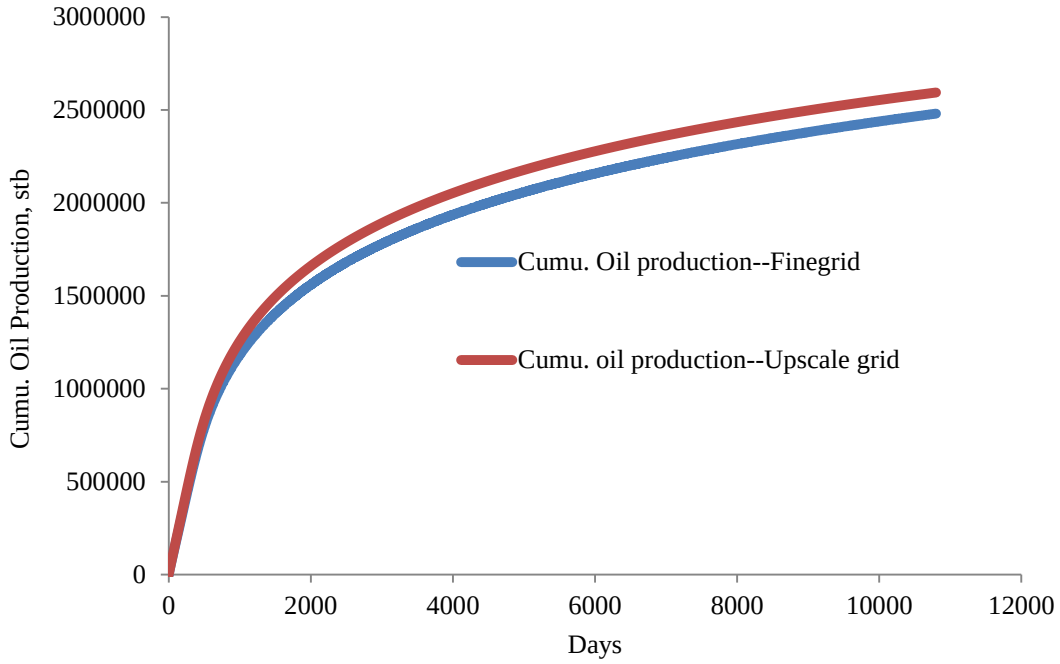

Figure 3.33—Cumulative oil production for fine grid model and upscale model

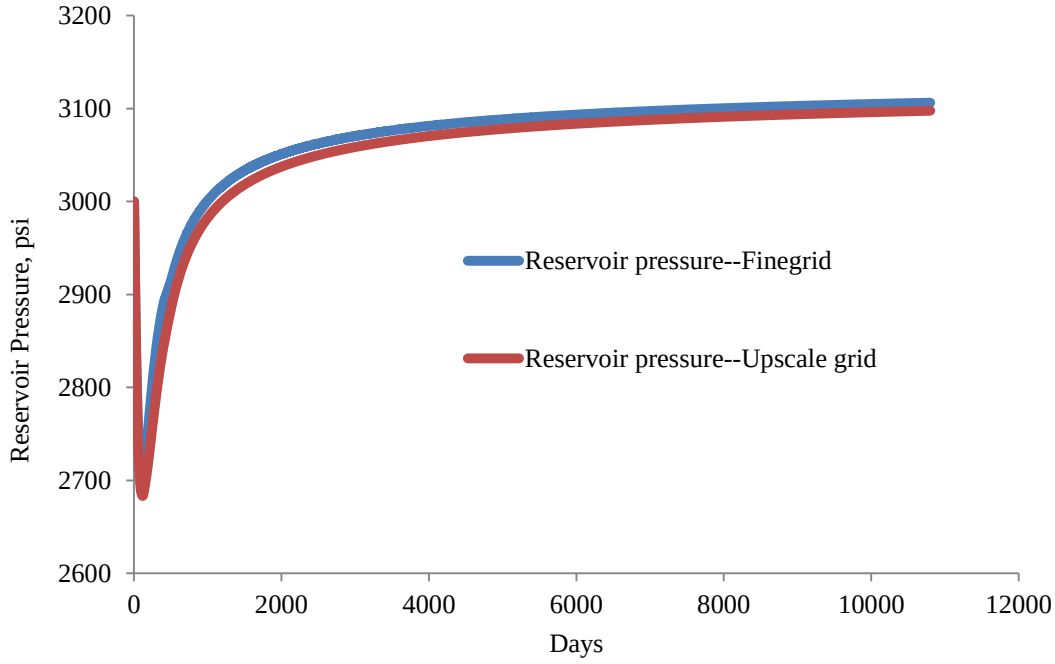

Figure 3.34—Reservoir pressure for fine grid model and upscale model

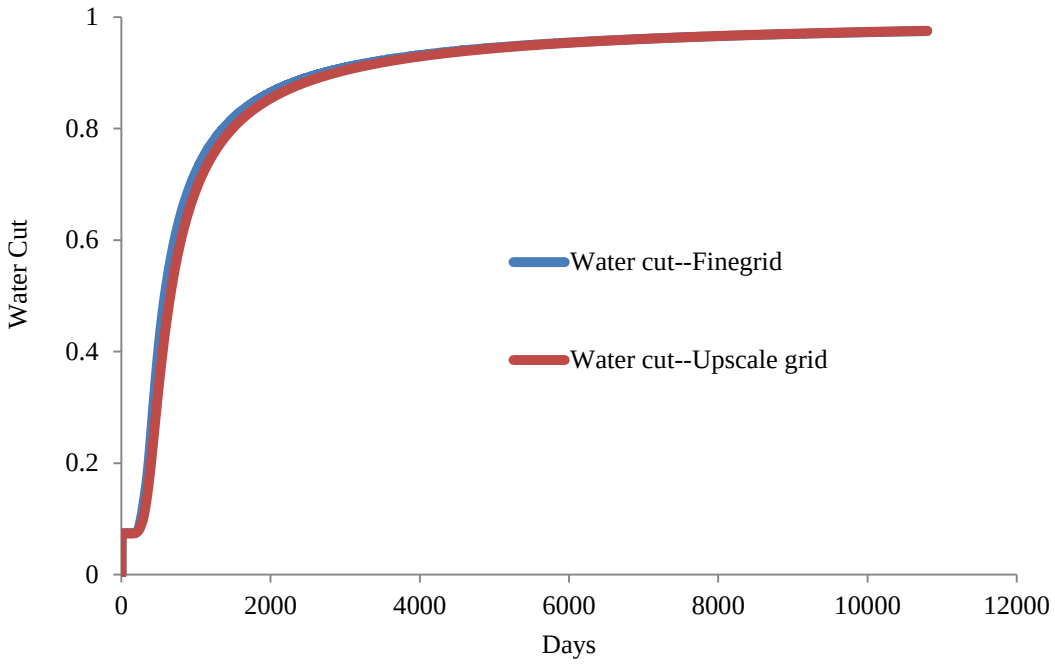

Figure 3.35—Water cut for fine grid model and upscale model

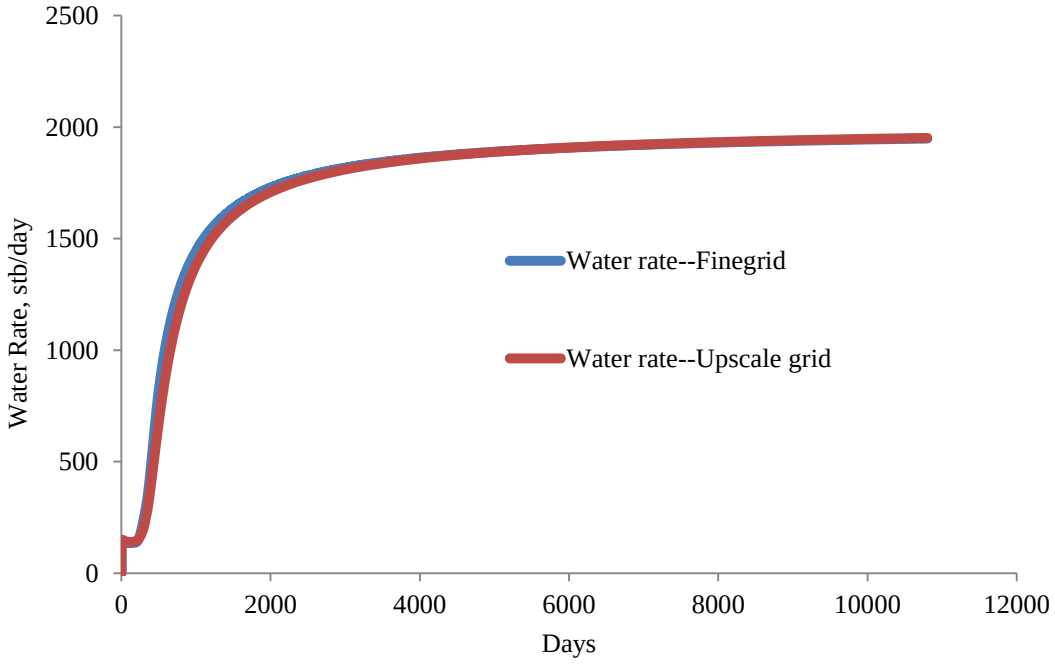

Figure 3.36—Water rate for fine grid model and upscale model

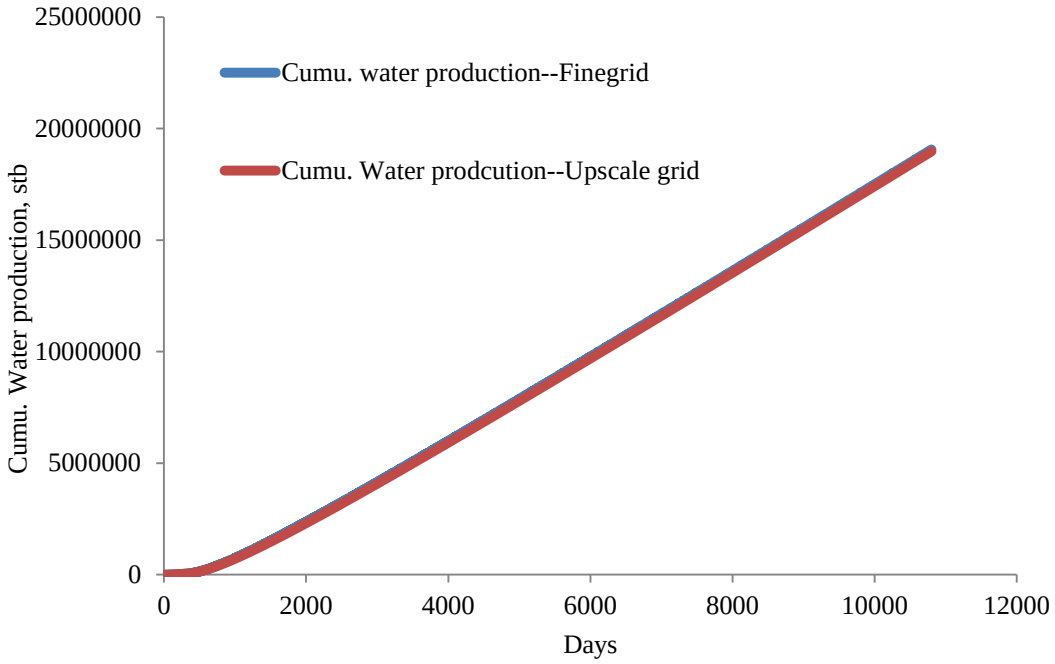

Figure 3.37—Cumulative water production for fine grid model and upscale model

3.2.5 Reservoir Simulation of PAG in SPE10 Model

In this reservoir model, four producers at corner and one injector at center were defined. In this study, we first injected water for 30 years with an injection of 2000 bbl/day (0.1 pore volume/year) and kept the liquid produce rate the same as injection rate. After 30 years production, the oil recovery is 45.74% and water cut 97.56%.

Optimize Polymer Concentration in Polymer Flooding Process. The relationship between polymer viscosity and polymer concentration is shown in Figure 3.6 and Function 2 in Figure 3.7 was used to describe the correlation between polymer adsorption and polymer concentration. The resistant residual factor is set to 1.8 when polymer concentration is equal to 0.55 lb/stb. We kept the same injection and production rate for polymer flooding while the polymer concentration varied from 0.1 to 0.4 lb/stb. **Figures 3.38-3.40** shows the simulation results. Increasing polymer concentration would increase total polymer volume, while when injection polymer with a concentration larger than 0.3 lb/stb would lower

water injection volume. As shown in Fig 3.38 and 3.39, injection of polymer with a concentration of 0.3 lb/stb would reach the same recovery and better polymer utilization compared with injection polymer of a concentration of 0.4 lb/stb.

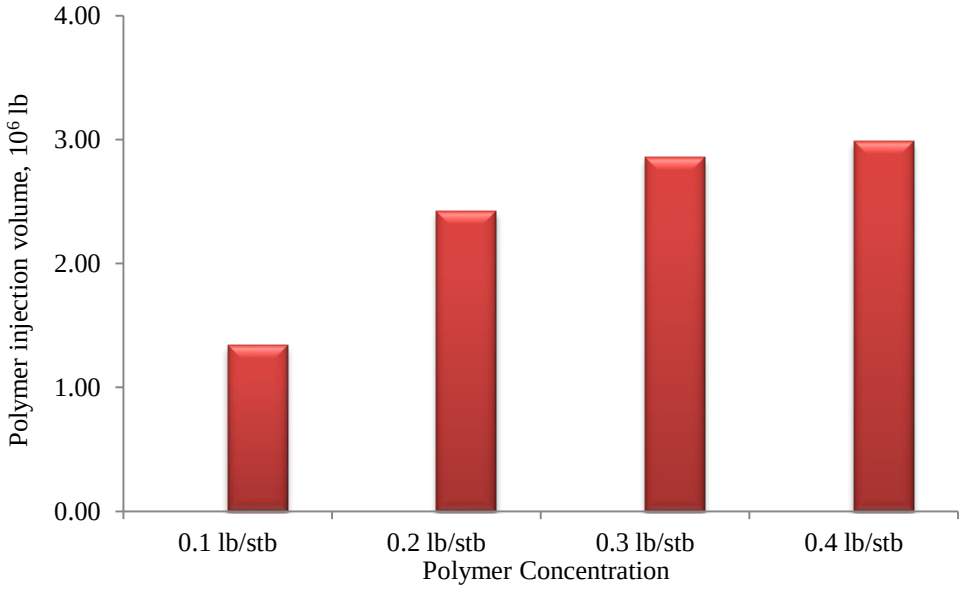

Figure 3.38—Polymer injection volume for different injection concentration

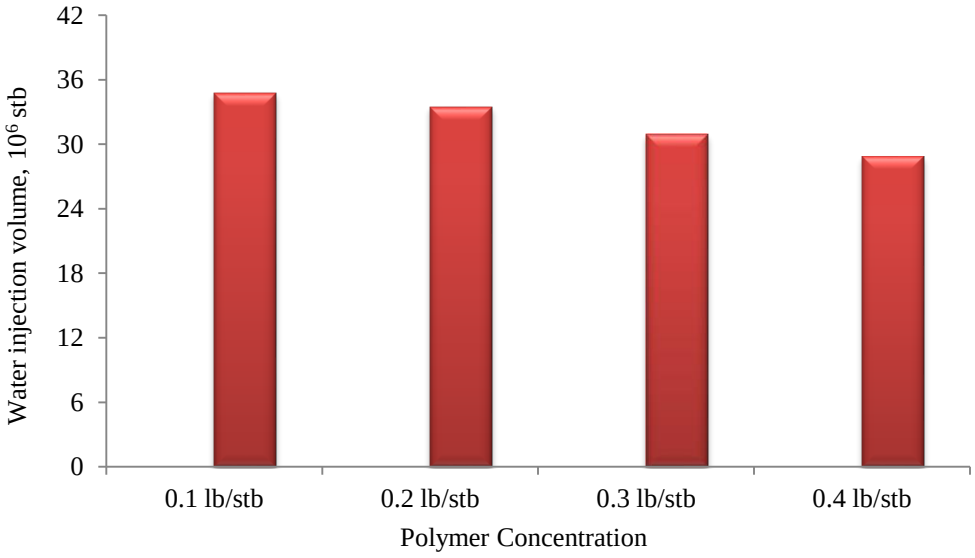

Figure 3.39—Water injection volume for different injection concentration

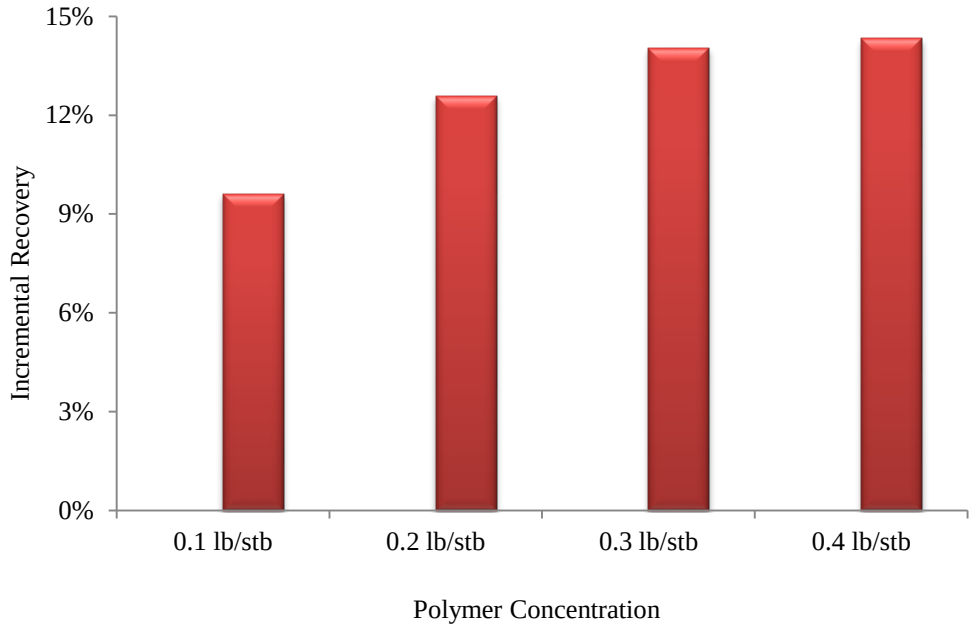

Figure 3.40—Incremental oil recovery for different injection concentration

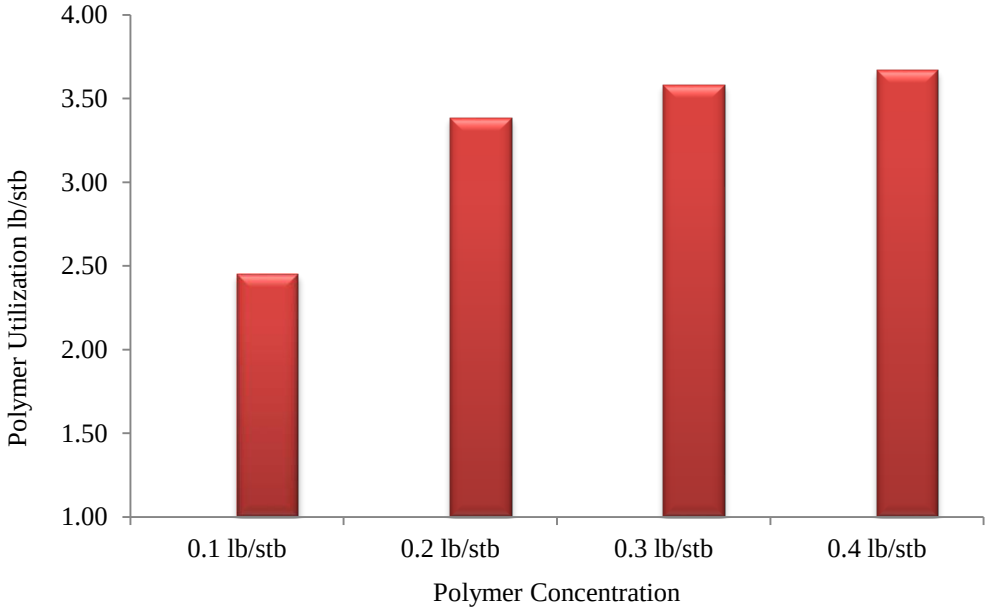

Figure 3.41—Polymer utilization for different injection concentration

Optimize Slug Ratio in WAG Process. In this study, three miscible CO_2-WAG injection tests with the same WAG slug size of 0.05 PV were conducted to study the effect of a different WAG slug ratio on the oil RF. The WAG slug ratio was defined as the ratio of the injected PV of brine to that of CO_2 in each WAG cycle at the actual reservoir conditions. Three different WAG slug ratios of 1:2, 1:1, and 2:1 were studied based on SPE10 model.

The oil recovery versus the WAG ratio in WAG process are plotted and compared in **Figure 3.42**. These three tests have quite high oil recovery. The ultimate oil recovery of slug ration 1:2 is the highest, followed by ratio 1:1 and 2:1. This is because slug ration 1:2 has the largest amount of CO_2 injected into the reservoir (**Figure 3.43**). Slug ratio 2:1 has the lowest oil recovery because the largest amount of water is injected. Among the three miscible CO2-WAG injection tests, slug ratio 1:1 shows the best performance as its oil recovery and oil production rate are rather high with a moderate consumption of CO_2. It can be concluded that the WAG slug ratio of 1:1 is particularly suitable for the miscible CO_2-WAG injection in this study.

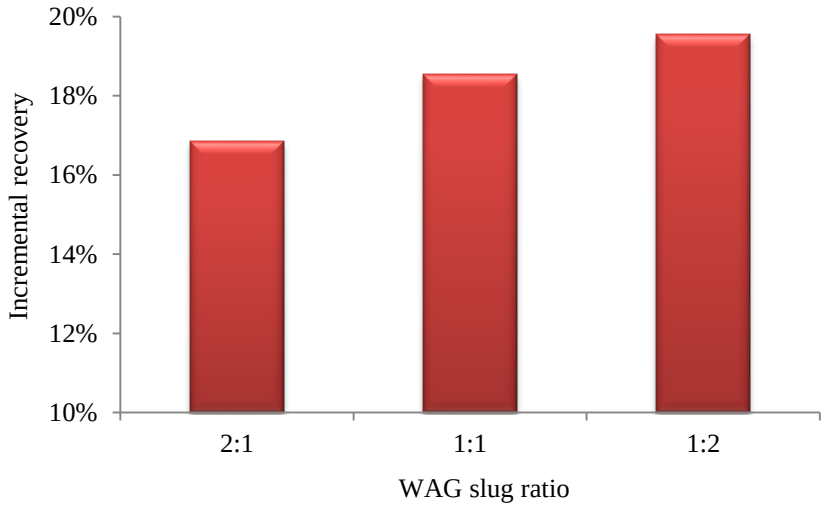

Figure 3.42—Incremental recovery from different WAG slug ratio

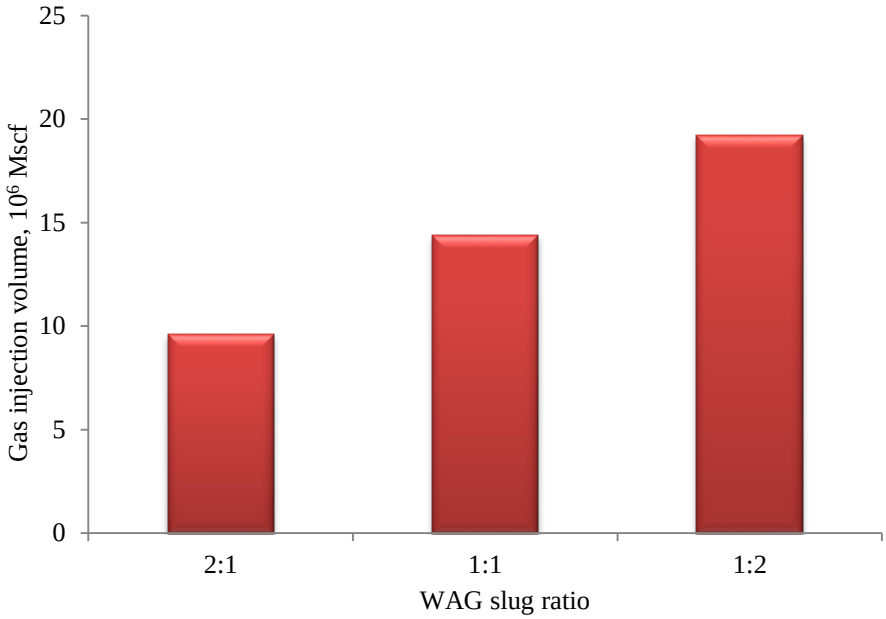

Figure 3.43—Injection gas volume for different WAG slug ratio

Optimize Polymer Concentration in PAG Process. A sensitivity analysis was performed on polymer concentration which affects the process significantly. We performed four simulation cases with different concentrations of polymer injected with water all the time, which are presented in **Table 3.3**. Different polymer concentration yields different injection fluid viscosity. In this study, bottom-hole pressure at injectors was set to 3,200 psi.

Table 3.3—Chemical concentrations for different cases in PAG process

Case Name	Polymer Concentration, lb/stb
PAG-1	0.10
PAG-2	0.15
PAG-3	0.20
PAG-4	0.25
PAG-5	0.30

Figure 3.44 to **3.45** indicates that increasing polymer concentration would significantly reduce water injectivity, especially, when polymer concentration is larger than 0.20 lb/stb. As polymer

concentration increases from 0.10 to 0.20 lb/stb, oil recovery increases from 22% to 24%. But concentration higher than 0.20 lb/stb would not recover significantly more oil (**Figure 3.46**). Considering the recovery and polymer consumption, a polymer concentration of 0.20 lb/stb was used for comparison with other methods.

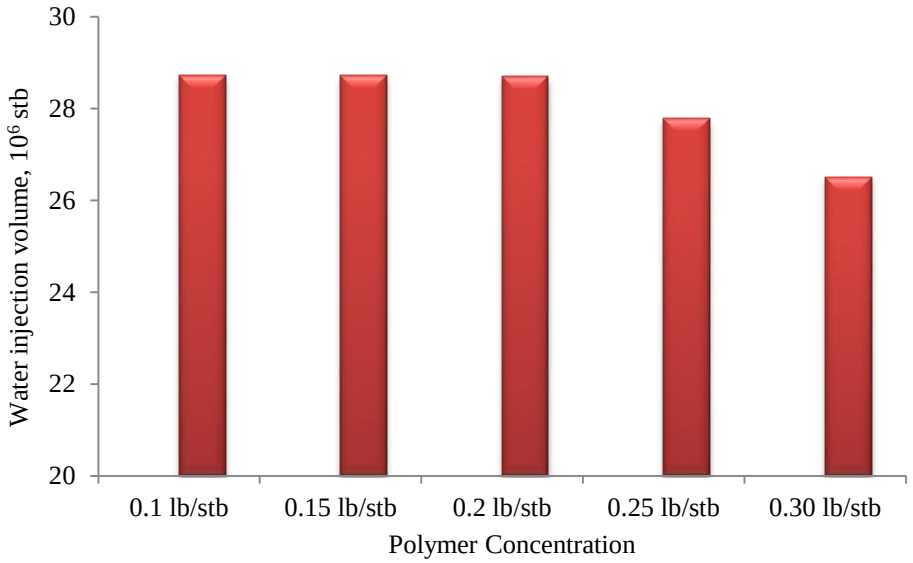

Figure 3.44—Water injectivity decreasing with polymer concentration

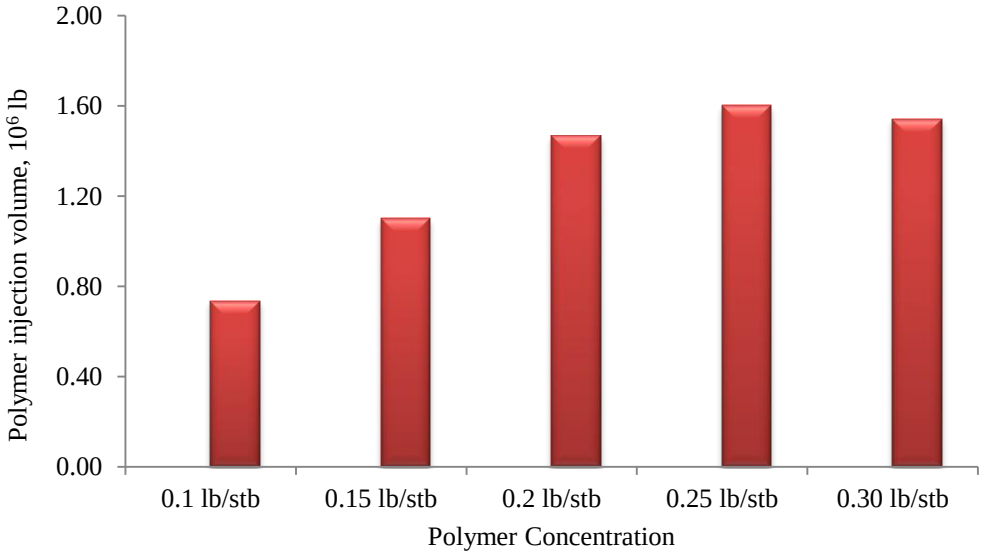

Figure 3.45—Polymer injection volume different polymer concentrations

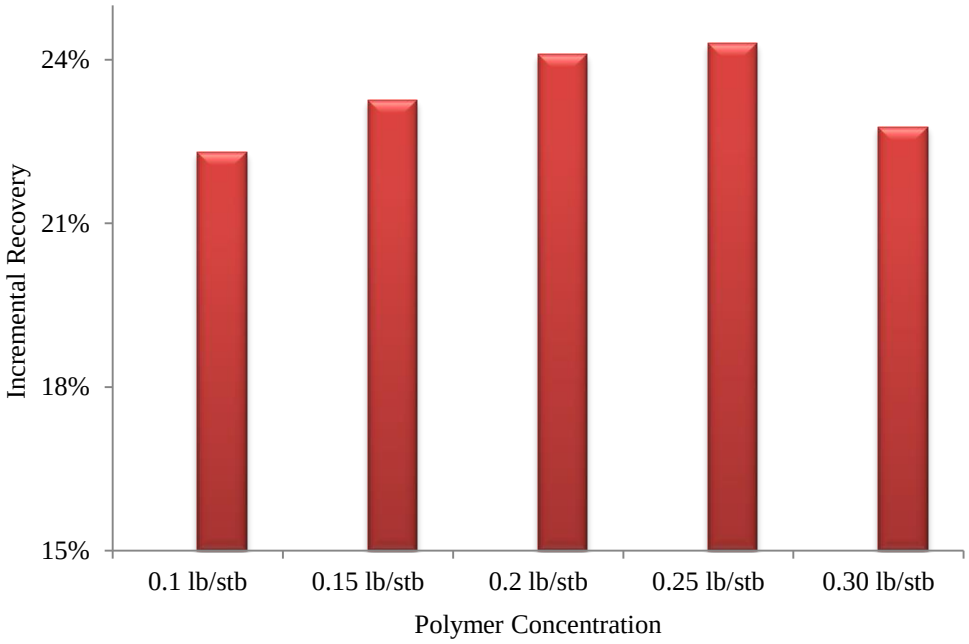

Figure 3.46—Recovery factor of different polymer concentrations

PAG Versus Polymer Flooding, WAG. Three cases (**Table 3.4**) were chosen for comparison. The reservoir performance during PAG was compared with polymer flooding and WAG. Simulation results show that oil recovery from PAG with a polymer concentration of 0.20 lb/stb is more than polymer flooding (with a polymer concentration of 0.30 lb/stb for twenty years) and WAG (**Figure 3.47**), which indicates that oil recovery increases with polymer injection. In **Figure 3.48** to **3.55**, the distribution of oil saturation in PAG process was compared with that of water flooding, WAG and polymer flooding process after 20 years injection.

It can be seen that the presence of gas (in PAG and WAG process) affects the oil saturation to a considerable extent. Residual oil saturation is much lower in PAG/WAG process than in water flooding and polymer flooding. In the polymer flooding, it is not possible for polymer solution to reach all of the reservoir zones, and some locations may undergo a low sweep with a given injection sequence, especially, for low permeability zone. Gas could reach the low permeability zone due to lower molecular volume for gas than for water (Figure 3.49 and 3.50).

The figures 3.48-3.55 reveal that the process of polymer alternating gas enhance the sweep efficiency compared to water alternating gas, and improve displace efficiency compared to polymer flooding.

We also compared the cost of each method based on following assumptions:

(1) Polymer cost: $ 3.0/lb

(2) Gas purchase cost: $ 2.0/Mscf

(3) Gas recycling cost: $ 0.5/Mscf

(4) No other fee was considered in this study.

As shown in **Table 3.5**, the costs of these three methods are about $9.9 -11.0 /bbl, which means all these three method would be economic favorable under current oil price (more than $80/stb). The method PAG has similar cost as WAG and polymer flooding and the recovery is about 6 to 10% higher than polymer flooding and WAG. PAG is good choice for this model.

Table 3.4—Chemical concentrations for different EOR methods

Case Name	Polymer Concentration, lb/stb	Slug ratio
Polymer flooding	0.3	--
WAG	0.0	1:1
PAG	0.20	1:1

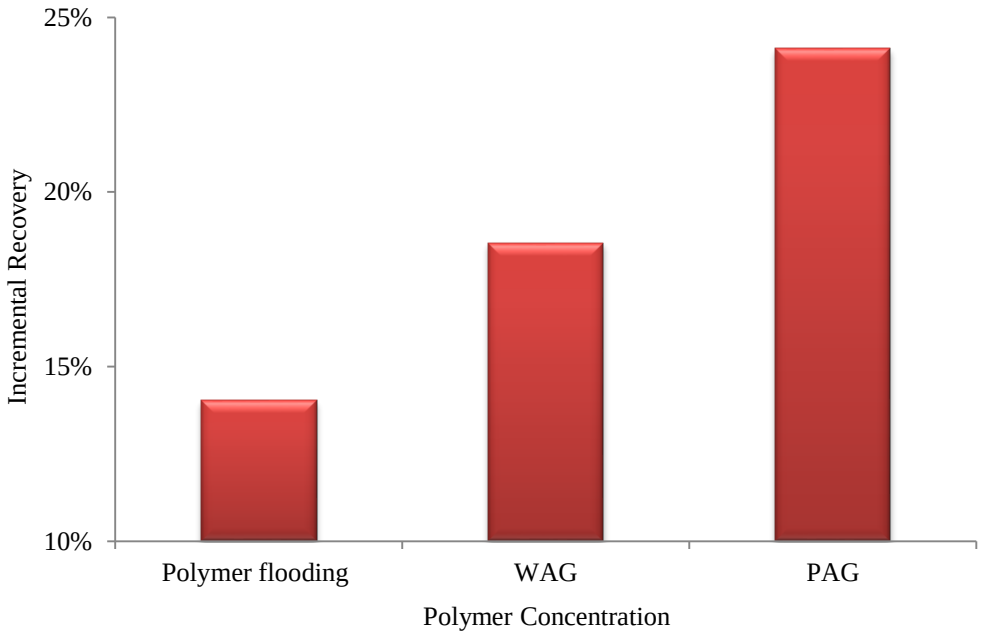

Figure 3.47—Recovery factor of different EOR methods in SPE 10 model

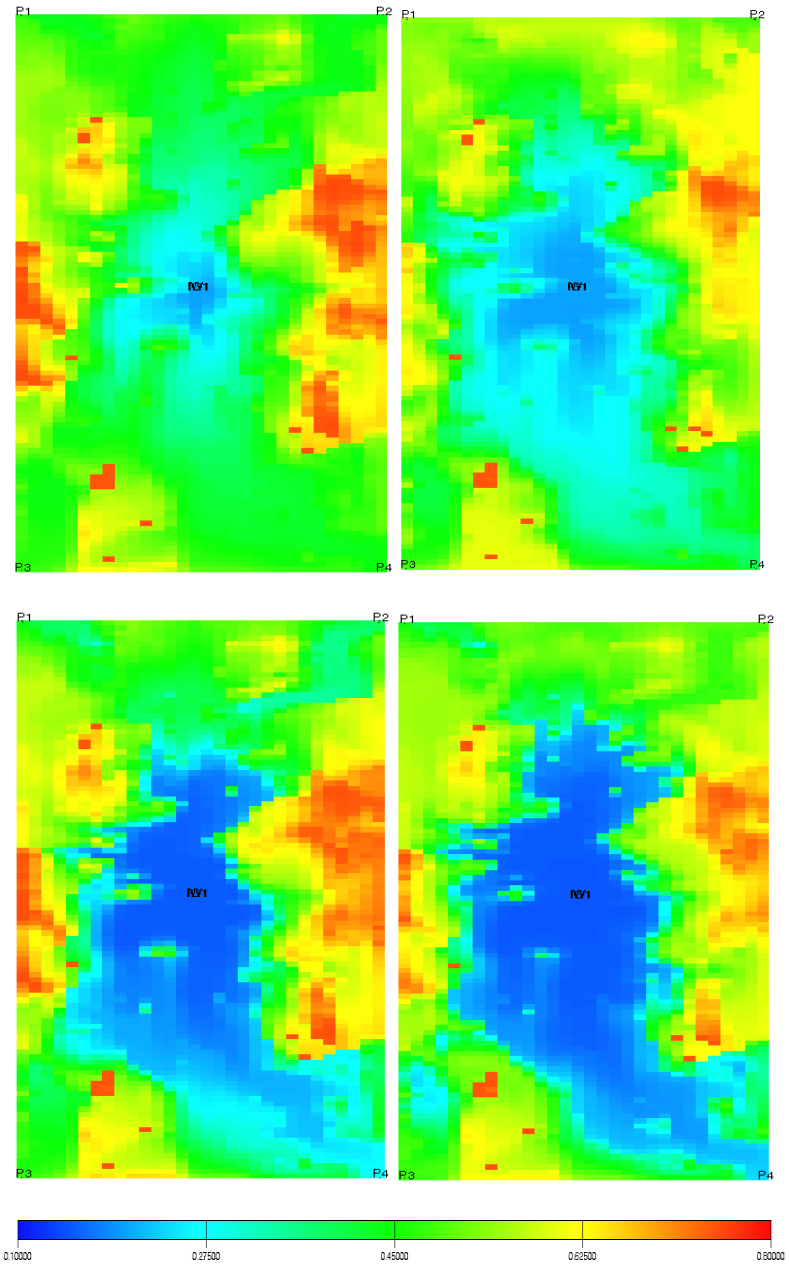

Figure 3.48—Oil saturation for different development methods in Layer 1

(from up-left to down-right: water flooding, polymer flooding, WAG and PAG)

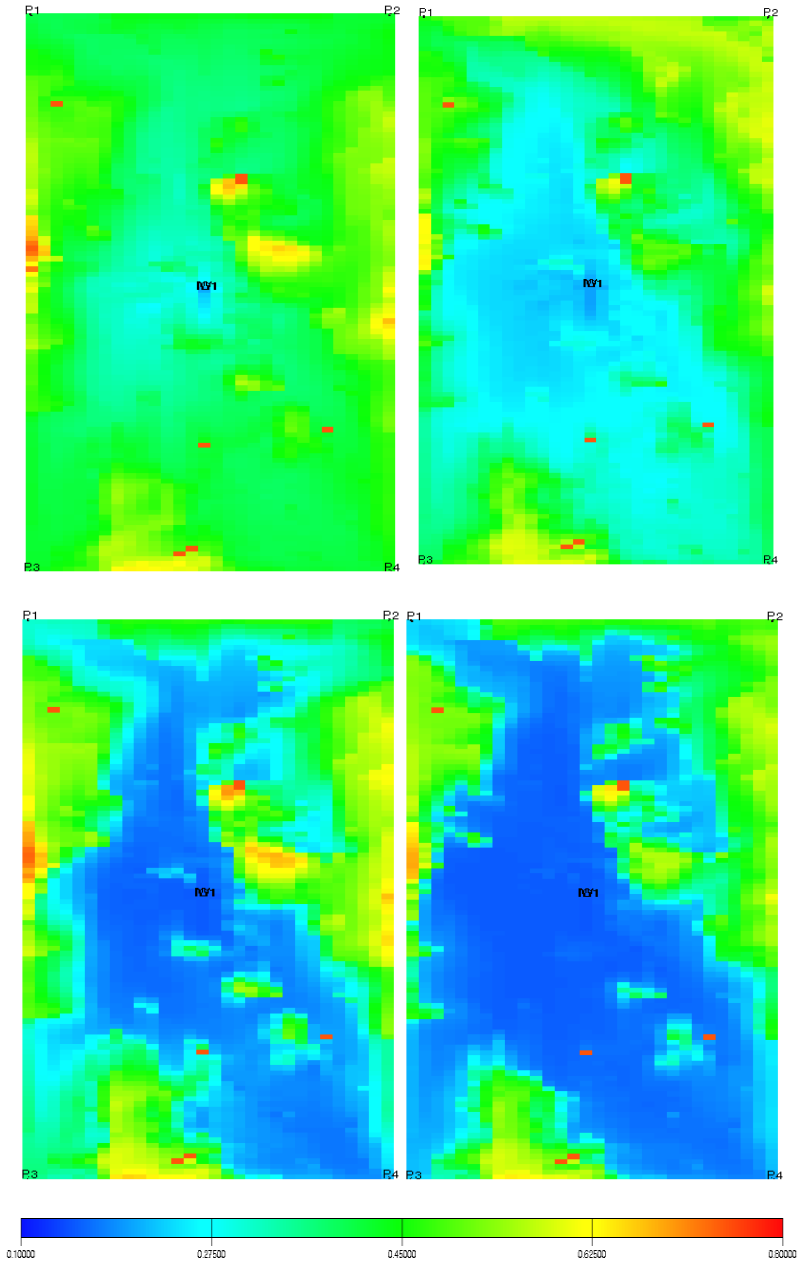

Figure 3.49—Oil saturation for different development methods in Layer 2

(from up-left to down-right: water flooding, polymer flooding, WAG and PAG)

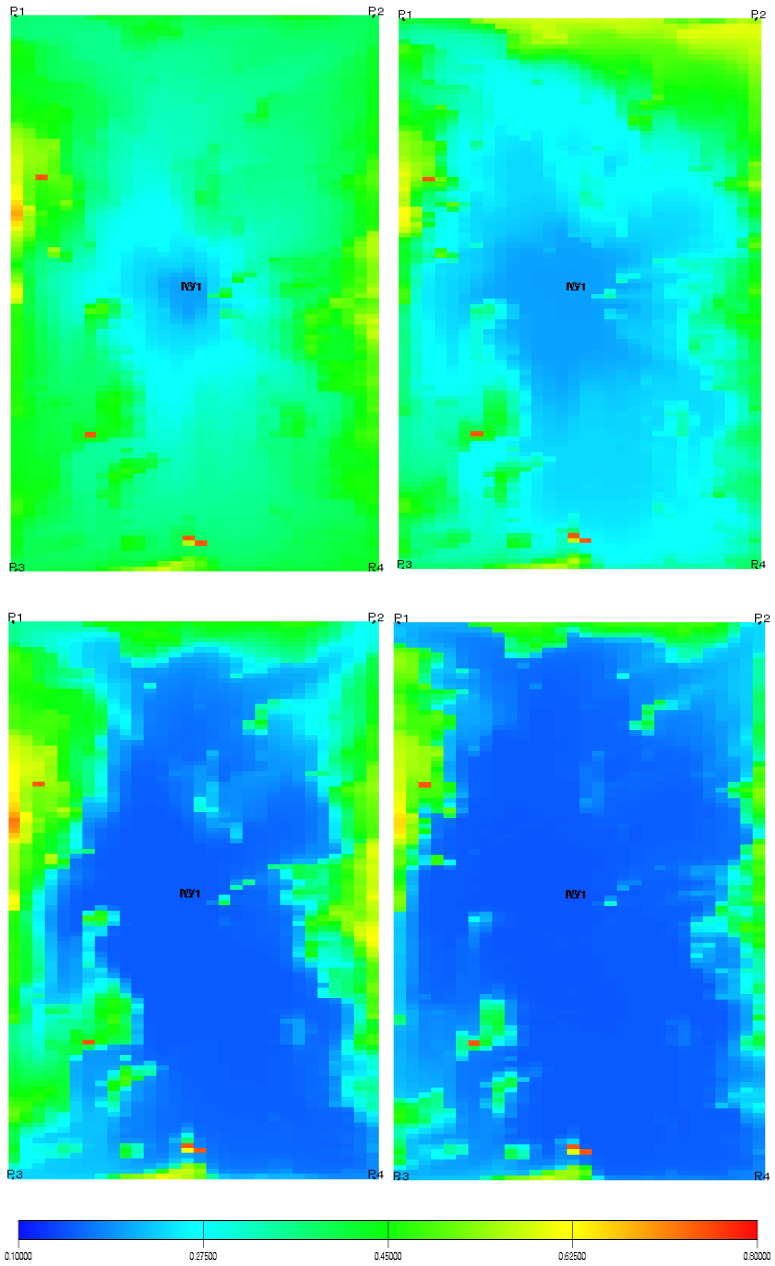

Figure 3.50—Oil saturation for different development methods in Layer 3

(from up-left to down-right: water flooding, polymer flooding, WAG and PAG)

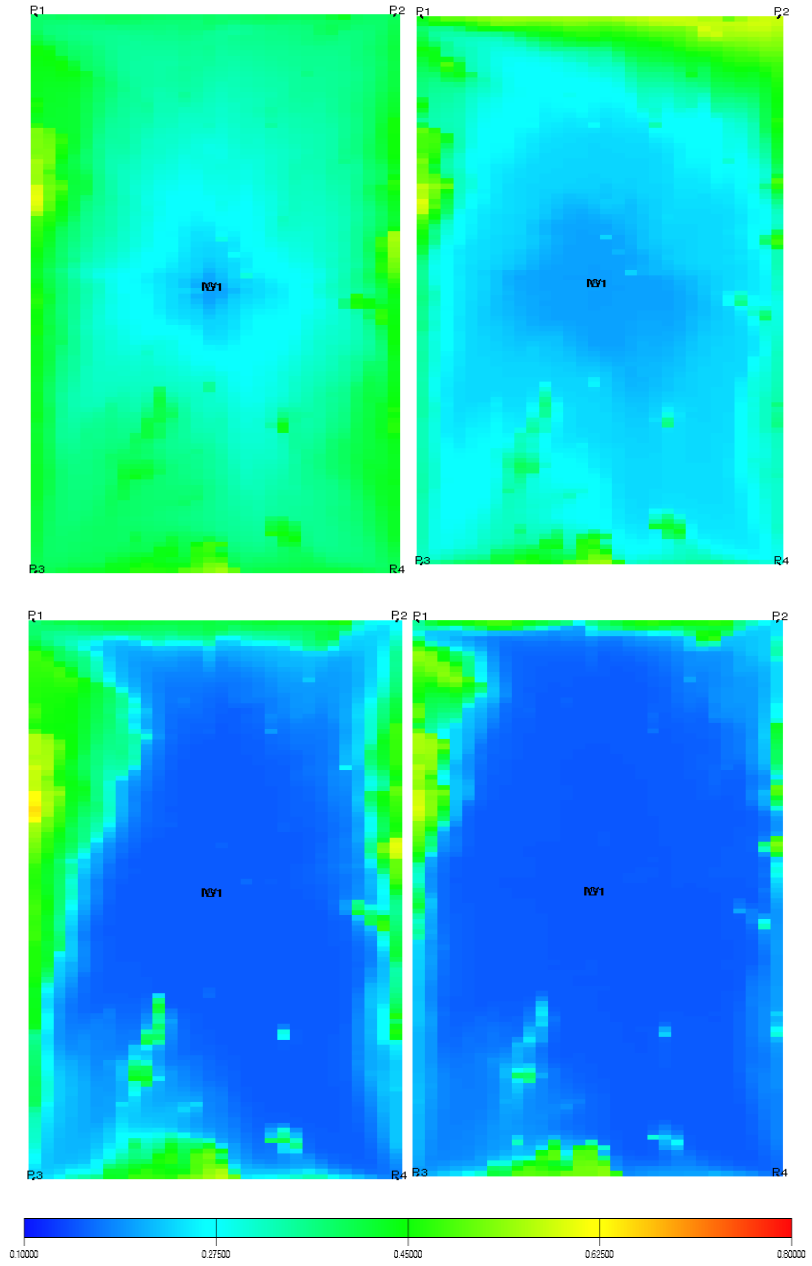

Figure 3.51—Oil saturation for different development methods in Layer 4

(from up-left to down-right: water flooding, polymer flooding, WAG and PAG)

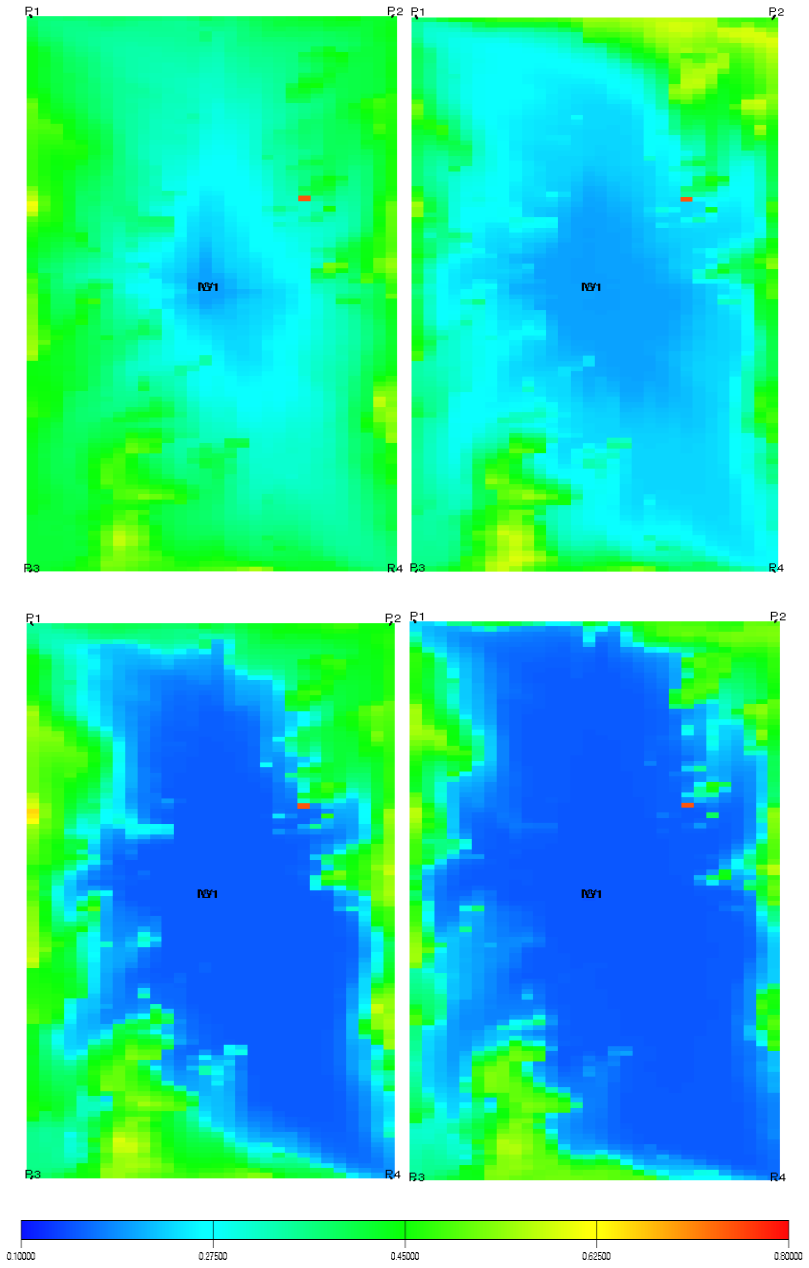

Figure 3.52—Oil saturation for different development methods in Layer 5

(from up-left to down-right: water flooding, polymer flooding, WAG and PAG)

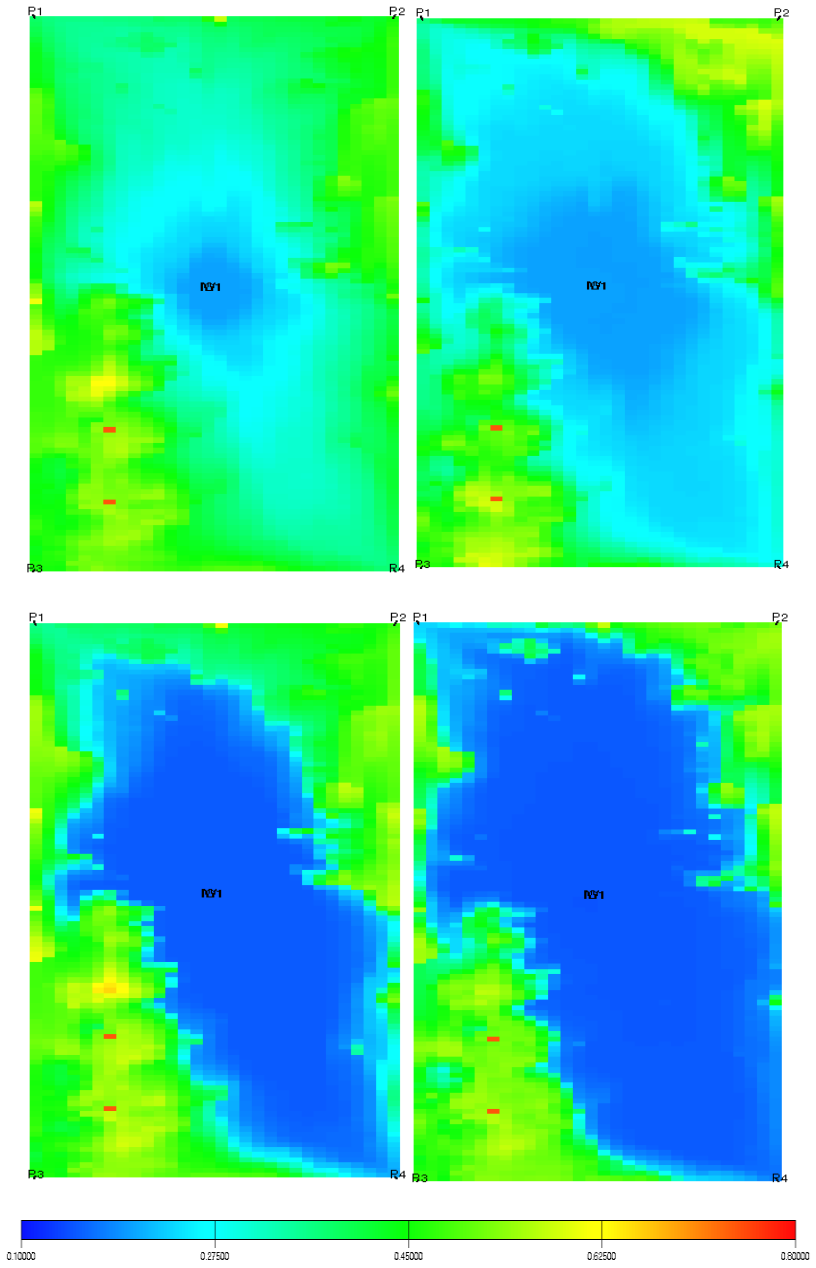

Figure 3.53—Oil saturation for different development methods in Layer 6

(from up-left to down-right: water flooding, polymer flooding, WAG and PAG)

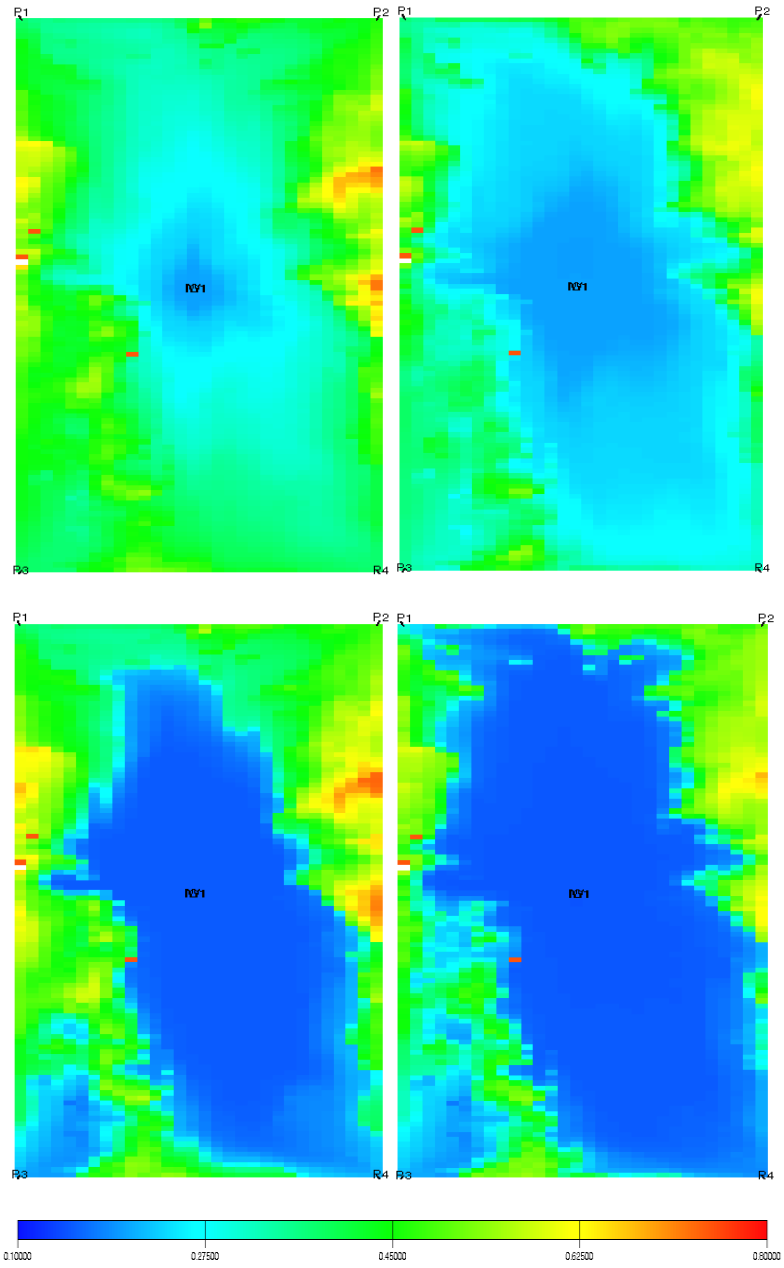

Figure 3.54—Oil saturation for different development methods in Layer 7

(from up-left to down-right: water flooding, polymer flooding, WAG and PAG)

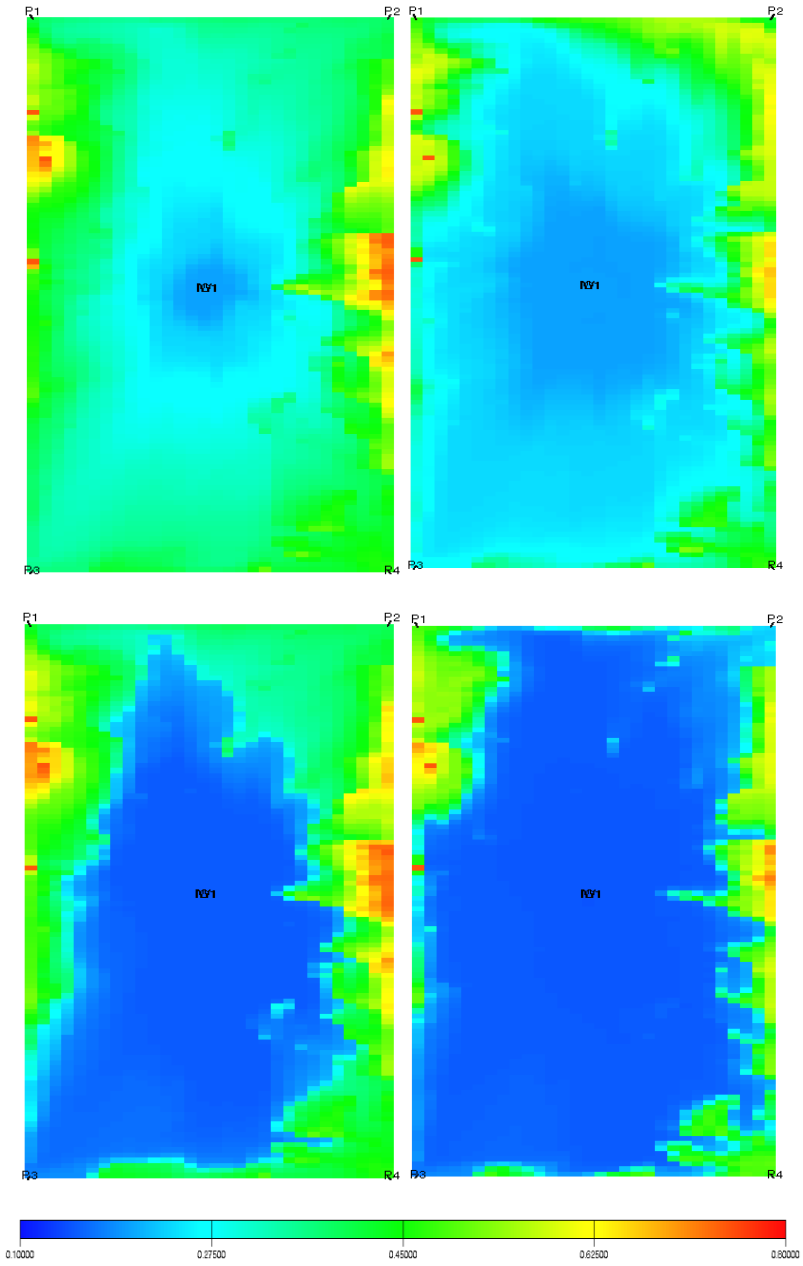

Figure 3.55—Oil saturation for different development methods in Layer 8

(from up-left to down-right: water flooding, polymer flooding, WAG and PAG)

Table 3.5—Comparison among PAG, WAG and polymer flooding

	Polymer injection volume 10^6 lb	Gas injection volume 10^6 Mscf	Gas production volume 10^6 Mscf	Incremental oil recovery 10^6 stb	Polymer cost \$ 10^6	Gas purchase price 10^6	Gas recycle gas 10^6	Cost \$/bbl
Polymer flooding	2.86	0.00	0.00	0.80	8.57	0.00	0.00	10.75
WAG	0.00	14.40	12.25	1.05	0.00	4.30	6.13	9.91
PAG	1.47	14.40	12.28	1.37	4.40	4.24	6.14	10.81

4. RESERVOIR SIMULATION OF PAG IN THE NORTH BURBANK UNIT

High heterogeneity and high permeability at the top layers of reservoir are the two main challenges for gas flooding in the North Burbank Unit. In this section, five typical sections were chosen for study. We optimized the CO_2 flooding injection and production, investigated the oil rate and gas rate performance in continue gas injection and WAG process. Then we optimized the polymer concentration and injection slug patterns in the PAG process in these five sections. We further compared the performance among PAG, WAG, CGI and polymer flooding. We also evaluated the economics of different EOR methods for each section.

4.1 Introduction of the North Burbank Unit

As mentioned by Johnson (1992), the North Burbank Unit is located on the northeastern Oklahoma Cherokee platform (**Figure 4.1**). The Burbank sandstone is the main reservoir of the field. The "Burbank sandstone" is the local informal name for the Red Fork sandstone. It is part of the Desmoinesian Cherokee Group, which includes sandstones, shales, and thin limestones. As shown in **Table 4.1**, the Cherokee sandstones include, in ascending order, the Bartlesville, Red Fork, Sonner, and Prue. The Burbank sandstone has produced more than 90% of the oil and minor gas from depths of 2800 to 3200 feet. Minor oil and gas has been produced from younger Pennsylvanian sandstones, Mississippian "Chat," and Ordovician sandstones. Johnson (1992) also described that Burbank sandstones were fluvial-deltaic and stratigraphic trap.

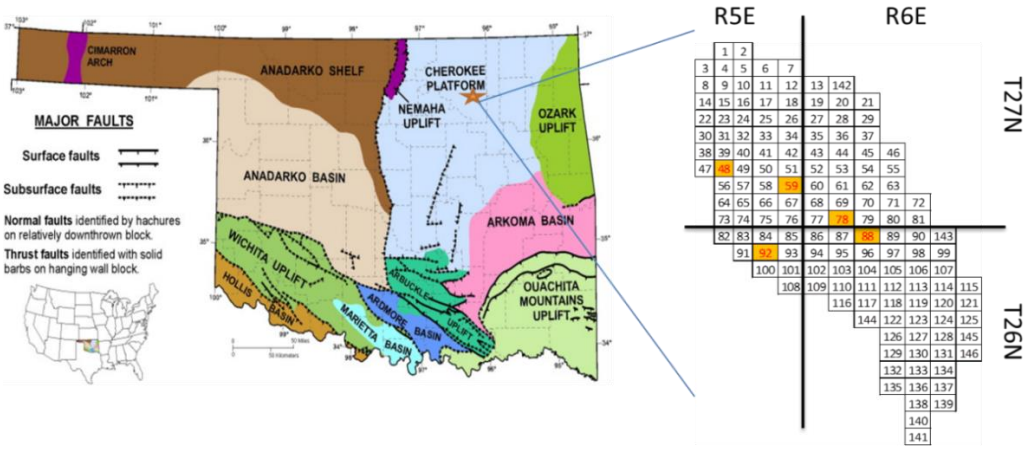

a) Location of the North Burbank Unit (Brain, 2012) b) Highlighted tracts

Figure 4.1—Geologic map of the North Burbank Unit

Table 4.1—General stratigraphic column of the Cherokee group and Burbank sandstone

EON	System	Series	Group		Subsurface Name
PALEOZOIC	Pennsylvanian	Desmoinesian	Marmaton		Big Lime
					Oswego Limestone
			Cherokee	Cabaniss	Prue Sandstone
					Verdigris Limestone
					Upper Sonner Sandstone
					Henryetta Coal
					Middle Sonner Sandstone
					Lower Sonner Sandstone
					Pink Limestone
				Krebs	Red Fork Sandstone(Burbank Sandstone)
					Inola Limestone
					Bartlesville Sandstone
					Brown Limestone

Sources: Overpressuring and Seal Structure of Pennsylvanian Red Fork Formation in the Anadarko Basin, Oklahoma

(edited after Virginie, 1995)

4.1.1 Development History of the North Burbank Unit

The North Burbank Pool, located in Kay and Osage Counties, Oklahoma, was discovered by the Marland Oil Company in May 1920. The discovery well (named the No.1 Tribal) was located in the east

Section. 36, T27N, R5E on the small Hay Creek anticline. In September of that year, the Carter Oil Company drilled two wells on another small anticline 2 miles to the southeast, in Section. 9, T26N, R6E (Hunter 1956).

Development drilling proceeded rapidly, and by 1924, 75% of the wells in the main part of the field had been drilled. The initial potential of wells in the Burbank sandstone varied from 10 to 12,000 BOPD. As shown in **Figure 4.2**, peak production was reached in July 1923, when the average daily production was 122,000 BOPD. Production declined rapidly as a result of the wide-open operation. The practice of pulling vacuum on wells was begun in 1924 in an effort to increase production. Produced gas injection began in 1926 by various operators in the field. Injection of purchased gas from outside began in 1935.

Approximately 150 million barrels had been produced under primary and gas injection by 1951 when what was then one of the world's largest waterflooding projects began operation. Between 40,000 and 50,000 barrels of water from the nearby Arkansas River were injected to the field (Riggs, 1954). Approximately 182 million barrels have been produced by the secondary recovery phase. Most of the current production now comes from waterflooding, with a high water cut of 99.5%.

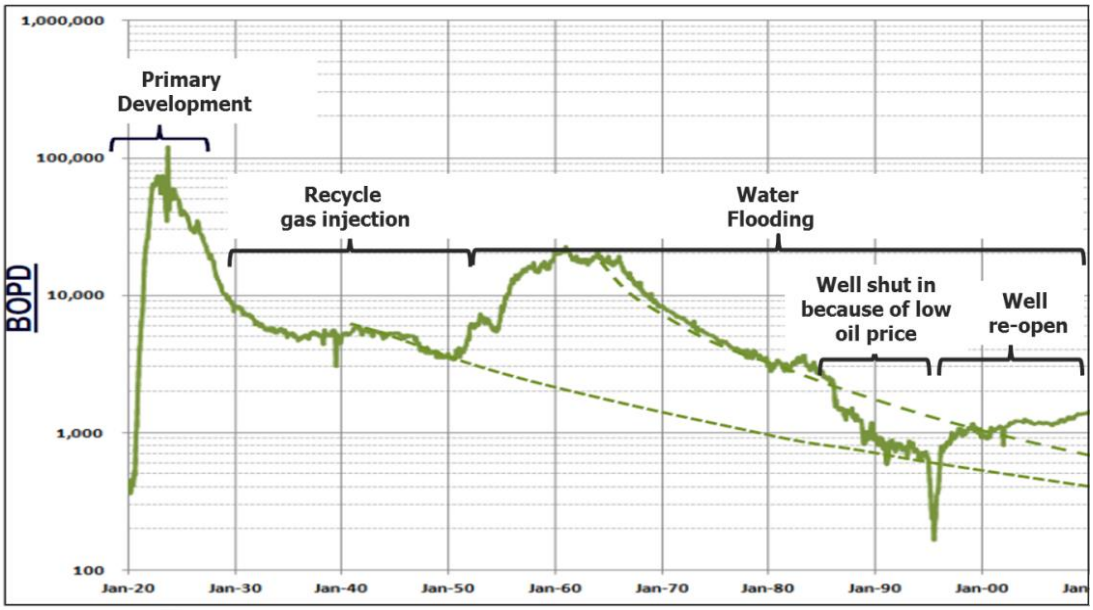

Figure 4.2—The North Burbank Unit production history.

4.1.2 Reservoir and Fluid Properties

The gross oil pay thickness of the North Burbank Unit varies from 30 to 100 feet, with an average of 47-50 feet (Johnson, et al. 1992; Hunter 1956). The subsea is about 2,850-3,100 feet, reservoir temperature is 118 °F, and the oil gravity is 35-40 API. The initial reservoir pressure is 1,600 psi, which is believed to be above the initial saturation pressure for oil. The initial solution gas-oil ratio was estimated to be 380 ft^3/bbl.

The average connate water saturation for the pool has been estimated to be 25-35%. An average microscopic residual oil saturation of 20% was used in our evaluation based on numerous special core analysis data. **Table 4.2** summarizes basic reservoir, field and fluid characteristics (Johnson, et al., 1992).

Table 4.2—Summary of reservoir, field and fluid characteristics

Reservoir	Formations	Red Fork sandstone
	Ages	Pennsylvanian, Desmoinesian
	Depths to Tops of Reservoirs	2900 feet
	Gross Thickness	2850-3100 feet
	Net Thickness--Average	50 feet
	Net Thickness--Maximum	100 feet
	Lithology	Fining-upward, very fine to medium-grained sandstone with some carbonate silica and clay cement
	Porosity Type	Intergranular and moldic due to dissolution of framework grains
	Average Porosity	0.2
	Permeability	Variable: 0-1200 md, Average permeability: 50-80 md
	Well Spacing	10 well/acre
Field	Primary Recovery	150 million bbl
	Secondary Recovery	182 million bbl
	In Place, Total Reserves	824 million bbl
Fluid	API Gravity	35-40°
	Initial GOR	380 $feet^3$/bbl
	Viscosity	0.8 cp
	Connate Water	25-35%
	Temperature	118 °F

Based on core data, two typical reservoir characteristics of the North Burbank Unit were found: high permeability in top layers and a Dykstra-Parsons coefficient of permeability variation (VDP) from 0.50 to 0.98 (**Figure 4.3** and **4.4**).

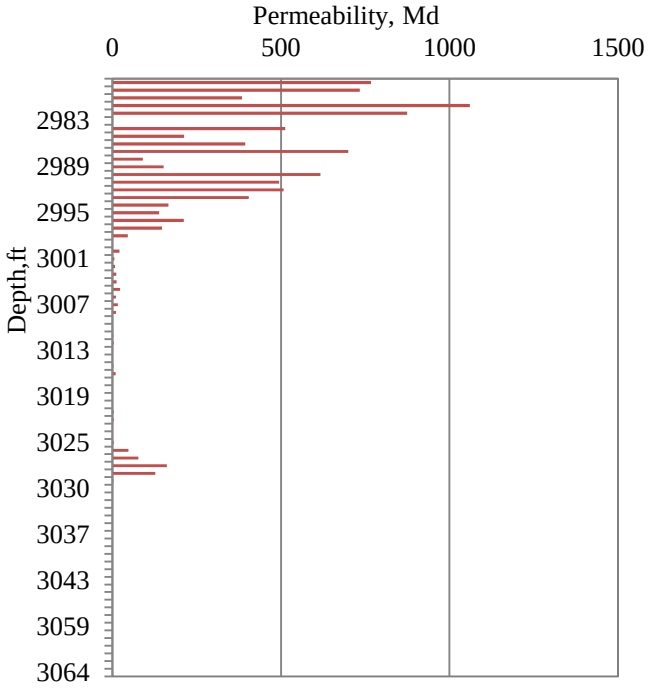

Figure 4.3—Permeability vs. depth at well NBU48-28 (Core data, 2006)

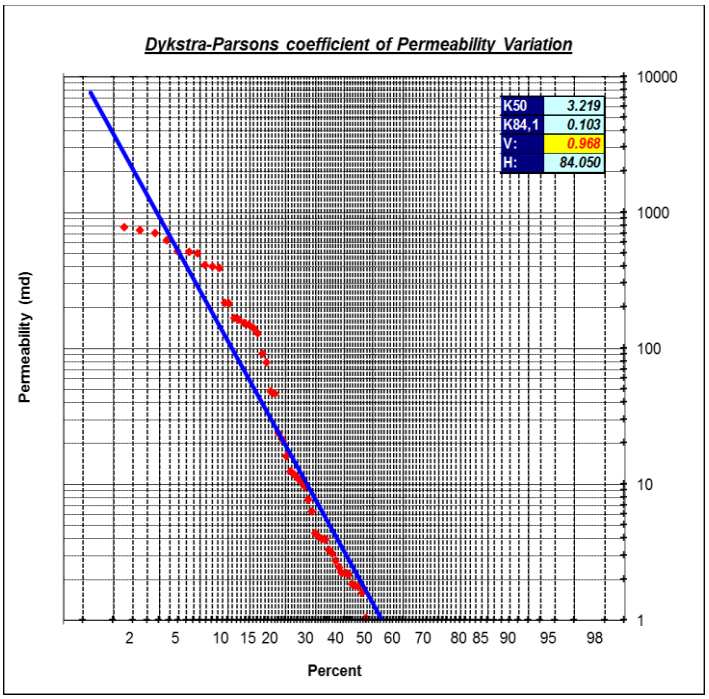

Figure 4.4—Dykstra-Parsons Coefficient of Permeability Variation (VDP) at well NBU48-28 (Core data, 2006)

4.2 Extensive EOR History in North Burbank Unit

4.2.1 Polymer Flooding Pilot in TR40/49

The project (Clampitt and Reid, 1975) contained four injection and 12 producing wells located on about 160 acres in the south part of Tract 40 and the north part of Tract 49 (Figure 4.5). The waterflood pattern was a modified staggered line drive with twice as many producers as injectors.

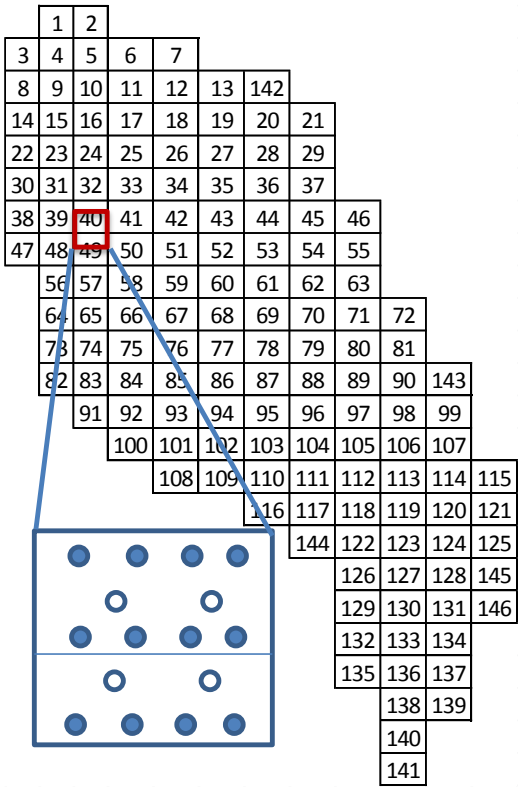

Figure 4.5—Polymerflood in the tracts 40 and 49, North Burbank Unit, Osage County, Oklahoma

The sand lies at a depth of approximately 3000 feet in the area of Tracts 40 and 49. The average thickness of the net pay with permeability more than 1 md varies from 37 feet in Tract 49 to approximately 50 feet in Tract 40. A type log, showing Gamma-Ray and Neutron curves along with permeability and porosity values typical of wells in the project area, was presented as **Figure 4.6**. Porosity

ranges from 32% in the very high permeability zones to 11% to 12% in zones with only 1 md of permeability.

A permeability profile across Tracts 40 and 49 showed the reservoir to be heterogeneous in the vertical direction with a VDP value of 0.87. The high permeability zone of more than 200 md in the upper part of the sand was present in 20 tracts.

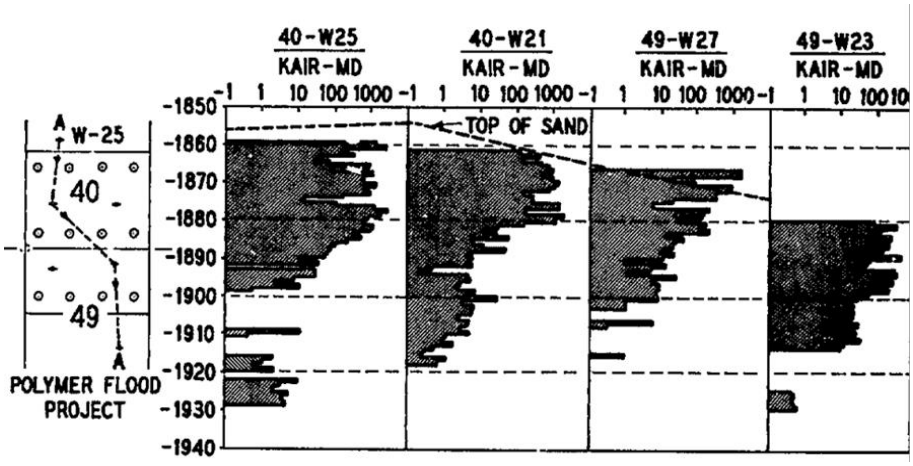

Figure 4.6—Permeability profile across tracts 40 and 49

The polyacrylamide (Pusher1000) was used in the field test at concentrations of 25 to 250 ppm. The oil-rate curve in **Figure 4.7** and **4.8** shows clearly a significant increase, which has been sustained or over 4 years. With the increase of oil rate, the average water-oil ratio decreased from the range of 80-90 to a lower level of 50-60. Tertiary oil recovery from center wells was about 53,000 bbl and tertiary oil recovery from this project was about 76,500 bbl. The cost of operation (excluding the polymer and polymer injection equipment) was the same as the conventional waterflooding. Gross channeling of injection water through fractures in the project area did not occur.

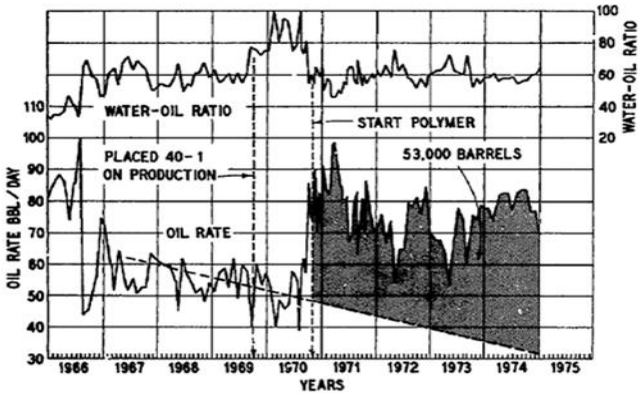

Figure 4.7—Production performance for center four wells

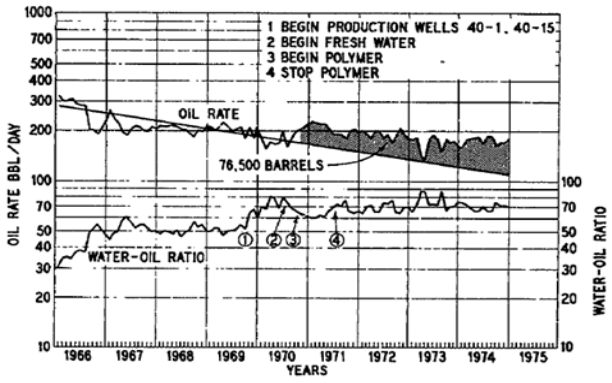

Figure 4.8—Production performance for all 12 project wells

4.2.2 Surfactant /Polymer Flooding in TR97

In 1975, Phillips Petroleum Company initiated a pilot project to demonstrate the feasibility of applying a surfactant polymer flood to an oil-wet sandstone reservoir that was nearing the end of its producing life. Phillips developed a 90-acre pilot project to test the feasibility of applying a surfactant polymer flood to the unit to extend the producing life and increase ultimate oil recovery (Trantham, Patterson and Boneau 1978, Trantham, 1983, Lorenz, Trantham, Zornes and Dodd, 1986).

Tract 97 was selected as surfactant polymer flood pilot. The well pattern consists of nine 10-acre inverted five spots with an injection well surrounded by four producing wells (**Figure 4.9**). In the waterflood operations in the NBU, the oil wells produce at an average water/oil ratio of 97.

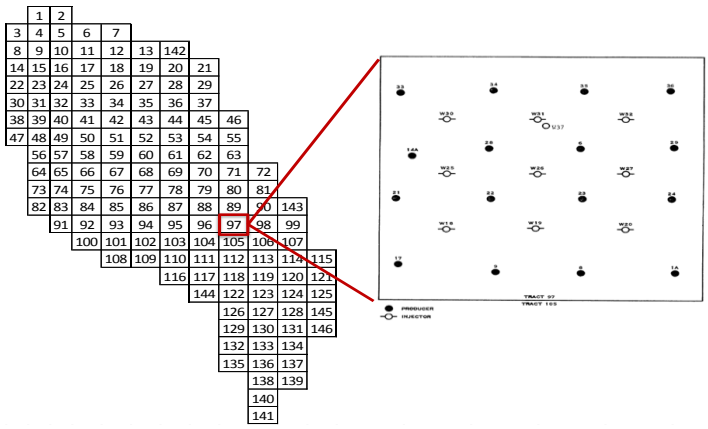

Figure 4.9—Well pattern for surfactant /polymer flooding

Table **4.3** and **4.4** shows the injection sequence for surfactant /polymer flooding. Before surfactant injection, more than 1,400,000 bbl of fresh water was mixed with 900,000 bbl of produced salt water and was injected into the Burbank sand. About 300,000 bbl surfactant solution was injected from Aug. 2nd to Sep 15th in 1976.

Polymer injection started on Sep 15th, 1976, and was completed on Jan. 16th, 1978. Total injection of polymer solution was 2,700,000 bbl. The polymer is a high-molecular-weight anionic polyacrylamide. The initial injection polymer concentration was 2,000 ppm and then decreased to 100 ppm at the end of injection.

Figure 4.10 shows that as early as middle November of 1976, these were indications of response to chemical injection. The WOR began steady decline as the oil rate increased. By the end of Jun 1977, the oil production rate reached 190 bbl/day with a WOR of 63. Analysis of production data before chemical injection began shows that without chemical injection the oil rate would be about 58 bbl/day with WOR of about 200. At the end of June, about 19,000 bbl of tertiary oil had been recovered. Ultimate tertiary oil recovery of this project was about 300,000 bbl, which was lower than expected (600,000 bbl). The commercializing surfactant/polymer pilot in Tract 97 was considered economic unfavorable particularly in areas of extreme high vertical heterogeneity

Table 4.3—Injection schedule

	Injection volume (bbl)		Concentration	Actual		
Fluid injected	Planned	Actual	Design	High	Avg.	Low
Fresh water	963,000	1,402,508				
Salt water	963,000	966,561	15 wt% Nacl	22.5	14.9	10.7
Surfactant	288,000	294,736	0.9 wt% Nacl	0.99	0.89	0.81
			3.0 wt% alcohol	3.35	2.92	2.55
			6.0 wt% sulfonate	6.35	6.01	5.75
Polymer	2,499,850	2,669,409	see table 4.4			

Table 4.4—Polymer injection schedule

		Concentration		
		Actual ppm		
Total Polymer %	Design ppm	High	Avg	low
3.30	2500	2680	2280	1060
5.10	2000	2050	1930	1760
8.00	1500	1820	1640	1500
9.10	1100	1340	1220	1160
11.00	800	980	870	520
15.60	600	600	630	580
15.40	460	500	470	280
12.20	250	280	240	210
20.30	100	100	100	100

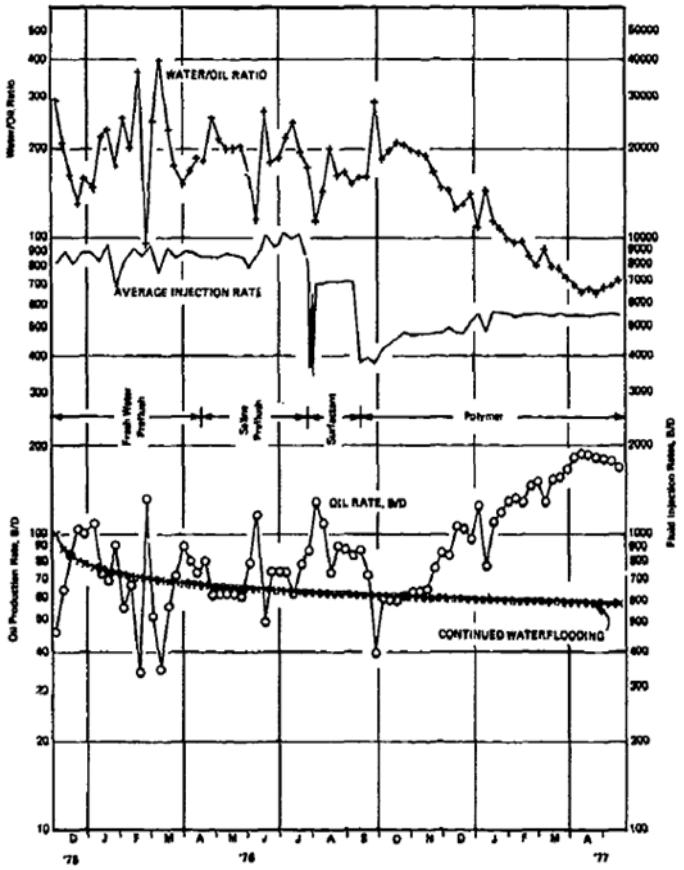

Figure 4.10—Total pilot performance, Tract 97

4.2.3 Polymer Flooding in Block A

Due to the success of the polymer flood pilot in the highly heterogeneous Tract 40-49 area, the northern portion of the North Burbank Unit was examined in selecting the 9 tract (named it Block A) commercial scale expansion area (Tracy and Dauben 1982, Joseph and Paul 1982, Zornes et al. 1986, Moffitt et al. 1993, Trantham and Moffitt 1982, Moffitt and Mitchell 1983, Zornes, Cornelius and Long, 1986). Each tract was screened on the basis of:

(1) total initial potential

(2) ratio of primary to secondary oil recovered

(3) total flow capacity of wells in the tract, and

(4) the cumulative producing WOR ratio during water flooding

A core profile (**Figure 4.11**) from the project area shows the heterogeneity primarily resulted from a few feet of upper zone having permeability of over a Darcy with less than a 100 md average in the lower portion of the core. **Table 4.5** shows the average thickness, flow capacity, permeability variation, porosity and permeability. In most of wells, the permeability variation was about 0.7-0.9.

Lab test showed that the average RRF to fresh water after polymer was near 8, while after the aluminum citrate process it was about 44. Based on laboratory test, reservoir simulation comparisons and pricing considerations, a liquid emulsion polymer product, Dow J-357 (Dowell 1000E) and aluminum citrate in the form of a 2.9 aluminum concentrate were used for this project.

The North Burbank Unit Block a polymer flood project was initiated in September 1980, with the injection of fresh water pre-flush into 36 wells within the 1,440-acre project area.

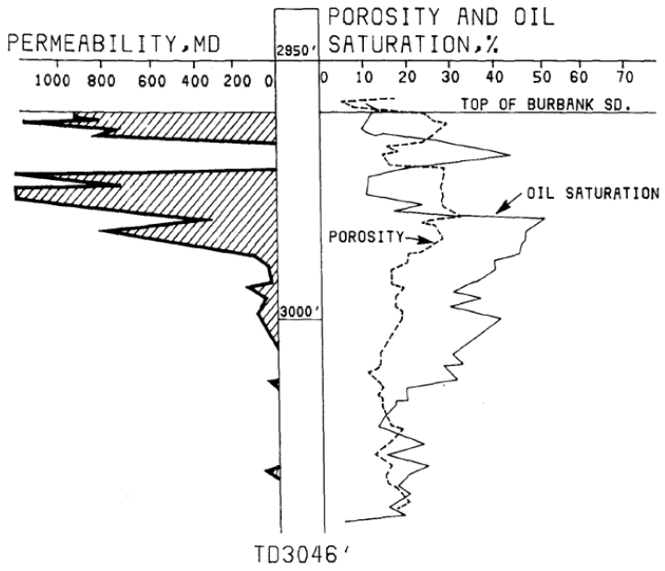

Figure 4.11—Core profile in well NBU 41-17

Table 4.5—Core data for wells in block A

Well	Thickness Ft.	Total flow Capacity, MD-Ft	Permeability Variation	Average Permeability MD	Average Porosity %
33-W21	31.0	25,406	0.9	820	24.7
34-4A	51.0	16,403	0.8	322	21.3
34-W23	28.8	807	0.6	28	18.2
35-W21	50.0	4,714	0.6	94	19.4
35-W23	40.6	1,054	0.6	26	16.5
41-17	50.0	20,412	0.9	408	21.1
41-W21	36.0	36,347	0.9	1010	25.2
41-W25	43.6	20,241	0.9	464	21.3
41-W318	46.7	5,383	0.5	115	18.2
42-W21	63.0	11,104	0.8	176	19.7
42-W25	51.0	24,145	0.7	473	25.2
43-14A	41.5	12,058	0.8	291	19.6
43-W25	46.7	9,073	0.8	194	20.3
50-W27	43.3	8,124	0.8	188	17.2
51-W23	42.4	1,183	0.5	28	14.7
51-W27	59.0	7,588	0.9	129	18.3
52-W27	48.0	3,050	0.7	64	14.6

The fluid injection sequence and quantities injected for the Tract 41 and Tract 43 mixing and injection system are detailed in **Table 4.6** and **4.7**, respectively. The chemical injection sequence had included 500 ppm active polymer augmented by 500 ppm aluminum citrate crosslinking agent, 250 ppm polymer, 50 ppm polymer, fresh water post-flush, and finally produced brine injection. A total of 4.17 MM pounds of polyacrylamide was injected into 36 wells. Fresh water and polymer production were monitored at 84 producing wells in an attempt to correlate with oil production response.

An economic production response occurred from the use of the Philips in-depth polymer-aluminum citrate-polymer process in this naturally fractured sandstone reservoir. As shown in **Figure 4.12**, oil production rate is over 30,000 BOPM (mid-1985) from a pre-project rate of less than 15,000 BOPM on average and the producing water-oil-ratio (WOR) was reduced from over 100 to less than 50. Total cumulative oil recovery was estimated at over 4.4MM STB, near 85% of the pre-project projection, assuming an economic limit of 2 BOPD per well.

Table 4.6—Sequence of fluid injection-Tract 43 injection system

Injection Fluid	Volume bbls	Avg. Rate BWPD	Pore Volume %
Fresh water preflush	2,570,800	17,850	8.63
Initial polymer, 500 ppm	1,231,800	17,850	4.13
Fresh water spacer	292,100	17,180	0.98
Aluminum citrate	133,700	7,865	0.45
Fresh water spacer	275,000	15,280	0.92
Primary polymer , 500 ppm	579,500	16,560	1.94
Fresh water	130,200	18,600	0.44
Primary polymer , 500 ppm	3,417,800	17,620	11.47
Primary polymer ,250 ppm	3,470,500	17,180	11.65
Primary polymer , 50 ppm	-	-	-

Table 4.7—Sequence of fluid injection-Tract 41 injection system

Injection Fluid	Duration days	Volume bbls	Net Active Chemical lbm	Pore Volume %
Fresh water preflush	211	9,127,000	-	13.46
Initial polymer, 500 ppm	69	2,984,800	480,000	4.4
Fresh water spacer	17	717,400	-	1.06
Aluminum citrate	16	544,900	92,810	0.8
Fresh water spacer	19	537,600	-	0.79
Primary polymer , 500 ppm	12	522,200	90,350	0.77
Fresh water	22	329,800	-	0.49
Primary polymer , 500 ppm	236	7,990,000	1,382,405	11.78
Primary polymer ,250 ppm	215	6,939,500	623,570	10.24
Primary polymer , 50 ppm	338	10,171,500	172,674	15
Fresh water postflush	555	17,134,367	-	25.27
Produced Brine	1756	47,294,500	-	69.76
Total polymer injected at Tract 41, lbm:2,748,999				

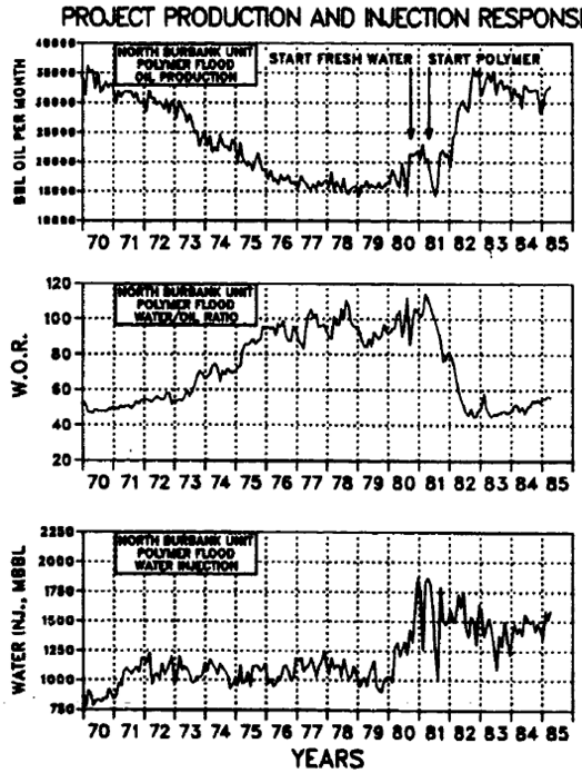

Figure 4.12—The North Burbank Unit Block A polymer flooding project performance

4.3 PVT Model

The Peng-Robinson equation of state (EOS) was used in this study for fluid modeling of the North Burbank Unit. After lumping 40 components into 11 pseudo-components, molecular weight, critical pressure, critical temperature, binary interaction coefficients, and Pedersen viscosity coefficients are regressed to match experimental data with simulated data. **Figures 4.13** to **4.17** show the matching results after regression, which increase our confidence in the PVT model that we set up and used in predictions by the reservoir simulator. It is worth mentioning that as CO_2 fraction increases from 0.0 to 0.75 with a constant temperature of 122 degF, the swelling factor for light oil increases to 1.58 (Figure 5). **Table 4.8** shows the 11-pseudo-component fluid system and the parameters used in both the compositional model and black oil model.

Based on the PVT model we obtained, we calculated fluid viscosity and MMP. As CO_2 mole fraction increases from 0.0 to 0.75, fluid viscosity declines from 3 to 1 cp (**Figure 4.18**). Calculated MMP for the North Burbank Unit oil is about 1,680 psi (**Figure 4.19**). Considering initial reservoir pressure is about 1,600 psi and the highest injection pressure is about 2,100 psi, CO_2 miscible flooding is possible for this light oil formation.

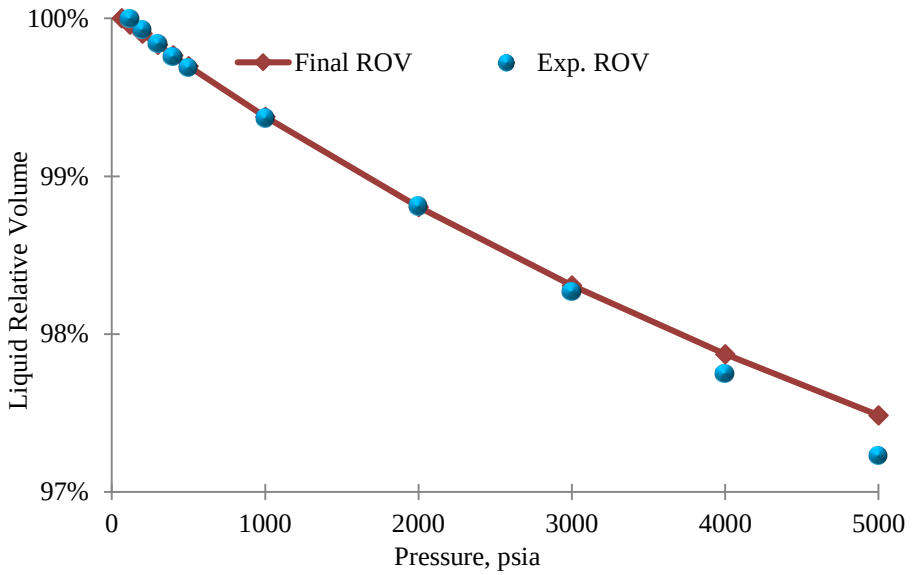

Figure 4.13—Constant composition expansion (CCE) liquid relative volume matching result

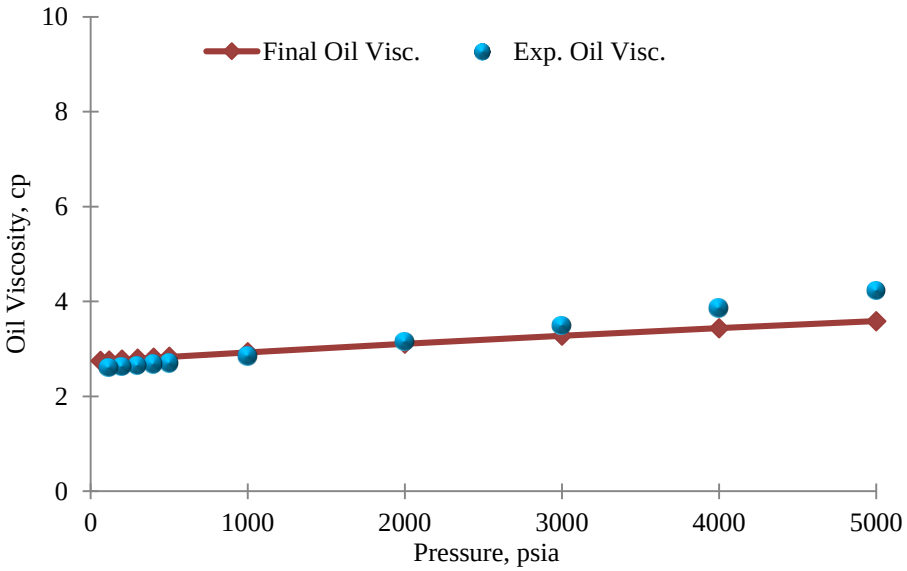

Figure 4.14—CCE oil viscosity matching result

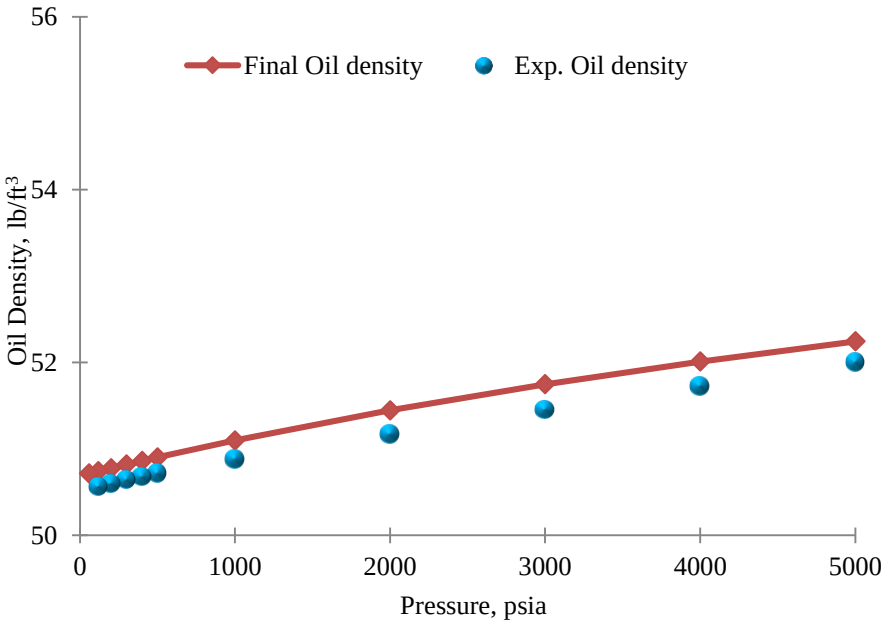

Figure 4.15—CCE oil density matching result

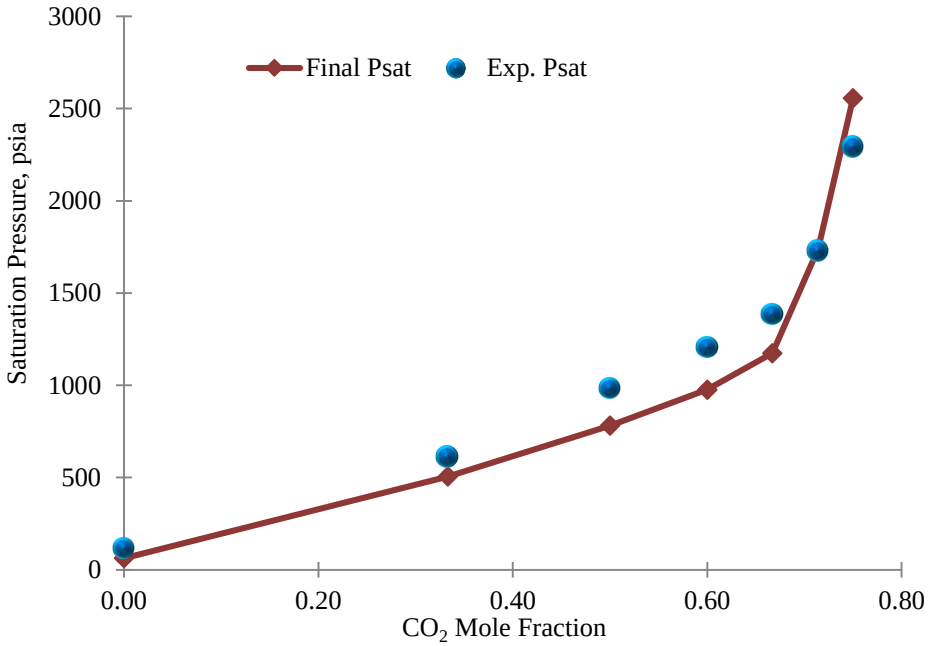

Figure 4.16—Saturation pressure matching result

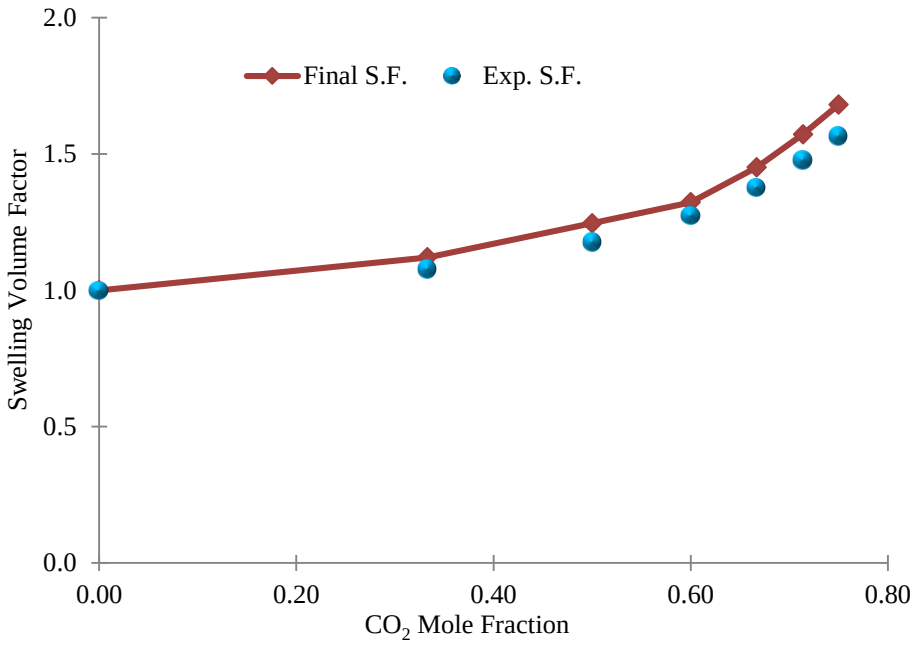

Figure 4.17—Swelling factor matching result

Table 4.8—Component parameters and fluid composition

Component	Specific Gravity	Mole Weight, g/mol	Pc, atm	Tc, K	Acentric Factor	Composition, % (in 2010)
N_2	0.81	28.01	33.5	126.2	0.04	0.17
CO_2	0.82	44.01	72.8	304.2	0.23	0.18
CH_4	0.3	16.04	45.4	190.6	0.01	1.61
C_2H_6	0.36	30.07	48.2	305.4	0.1	1.18
C_3H_8	0.51	44.1	41.9	369.8	0.15	1.77
IC_4 to NC_4	0.58	58.12	37.2	421.7	0.19	2.89
IC_5 to NC_5	0.63	72.15	33.3	466.14	0.24	3.64
FC_6	0.69	84	32.5	507.5	0.28	3.56
C_7 to C_{10}	0.75	113.99	30.1	583.94	0.37	30.53
C_{11} to C_{17}	0.82	183.39	23.7	691.94	0.58	29.04
C_{18} to C_{30}	0.91	431.2	14.3	826.85	0.94	25.43

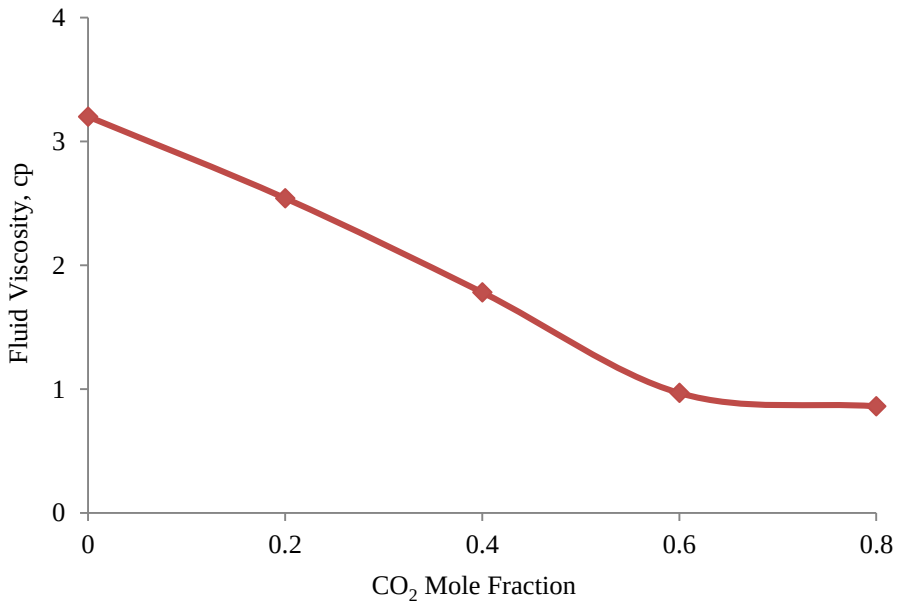

Figure 4.18—Correlation of fluid viscosity versus CO_2 mole fraction

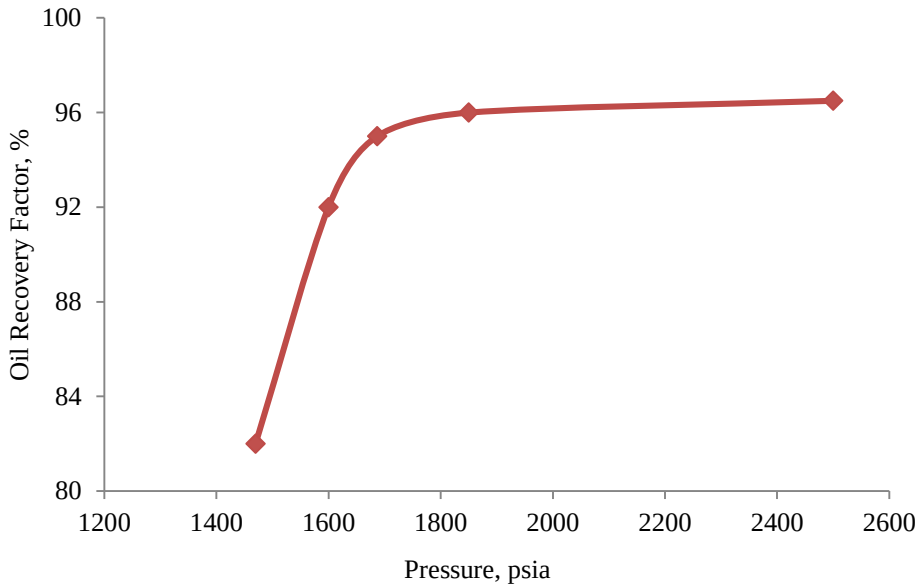

Figure 4.19—Calculated MMP from software

4.4 Parameters for Polymer Flooding

Rock adsorption and polymer viscosity are two important parameters for polymer flooding. The correlations of rock adsorption and polymer viscosity with polymer concentration shown in **Figure 4.20** and **4.21** were used for the polymer flooding simulation in this study. We also assumed a residual resistance factor (RRF) value of 1.8 at 0.55 lb/stb in this study.

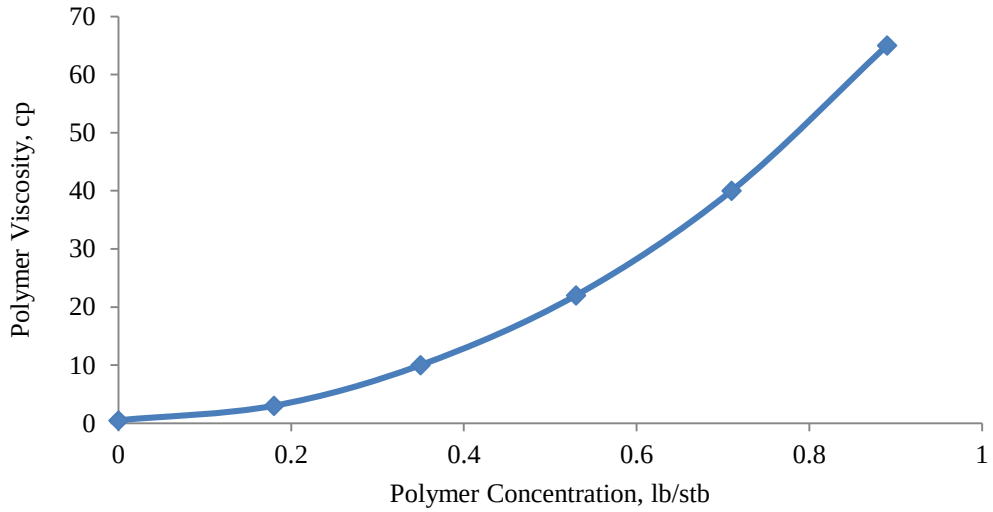

Figure 4.20—Correlation between polymer concentration and polymer viscosity

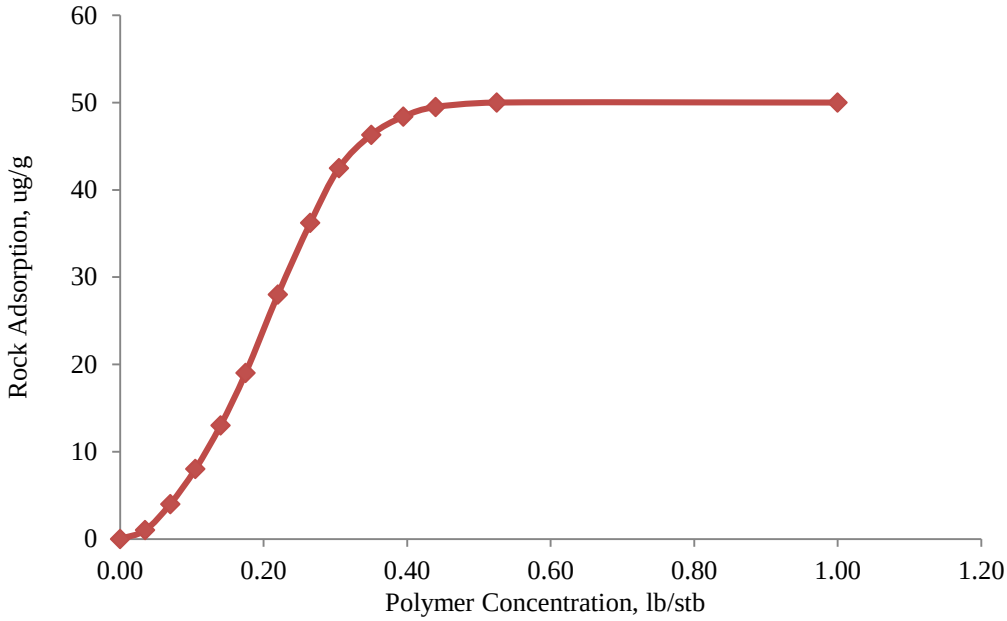

Figure 4.21—Correlation between polymer concentration and rock adsorption

4.5 PAG Simulation in Section 78

A black oil model using a detailed geologic characterization was built to optimize the PAG process in the section 78 of North Burbank Unit. Simulation layers represent actual flow units and resemble the large variation of reservoir properties. A 90-year history match was performed to validate the model. Production data predicted by the pseudo-miscible model was matched with the compositional model. Polymer injection concentration and injection slug were optimized using pseudo-miscible model. Oil rate, GOR and recovery performances were compared among different EOR methods.

4.5.1 Reservoir Model

TR78 in the North Burbank Unit, a typical section with high heterogeneity of the reservoir and high permeability at the top layers, was selected for the purpose of modeling. TR78 was characterized by a gridded network with permeability and porosity parameters specified for each block. For this model, a 0.5 × 0.5-mile reservoir section was divided into 60 grid blocks in the x-direction, 60 grid blocks in the y-direction, and 10 grid blocks in the z-direction. In the x- and y-directions, the grid blocks are 44 ft in

length. The grid blocks in the z-direction vary from 4 to 24 ft, which results in a pay zone of 90.7 ft. **Figure 4.22** shows x-horizontal permeability (kh) in the model. The vertical permeability (kv) is 0.01 times the x-horizontal permeability, while y-horizontal permeability is three times the x-horizontal permeability. **Table 4.9** presents the input reservoir rock and fluid properties used for the simulation.

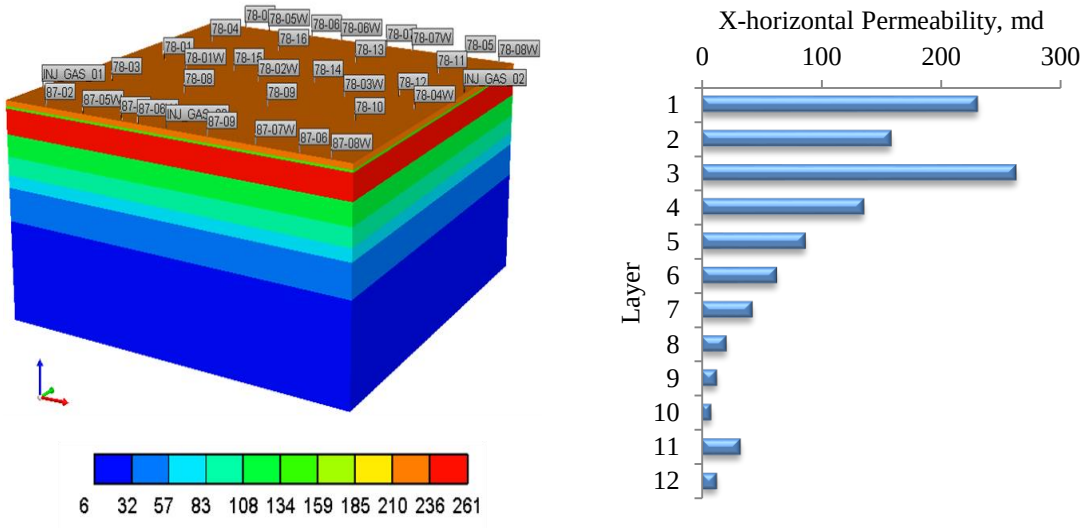

a) X-horizontal permeability distribution b) X-horizontal permeability value by layers

Figure 4.22—X-horizontal permeability model in 78

Table 4.9—Reservoir rock and fluid properties in TR78

Reservoir Rock		Reservoir Fluid	
Parameters	Values	Parameters	Values
Size of Model, ft	2,640×2,640×90.7	Water Density, lb/ft^3	62.97
Number of Grid	60×60×10	Water Viscosity, cp	0.5
VDP	0.85	Oil Density, lb/ft^3	50 to 52
kv/kh	0.01	Oil Viscosity, cp	2 to 4
Porosity	0.15 to 0.27	Initial Oil Saturation	0.61 to 0.80
Initial Pressure, psi	1350	Initial Water Saturation	0.20 to 0.39
Permeability, mD	6 to 230		

4.5.2 Reservoir Model Validation Before CO_2 Flooding

Using the reservoir model described above, we matched the pre-CO_2 flood oil and water production history during primary depletion and secondary development. Liquid production rate was used as the primary constraint in the simulation. A good match of oil rate and water cut was reached (**Figure 4.23**), which validates the reservoir model.

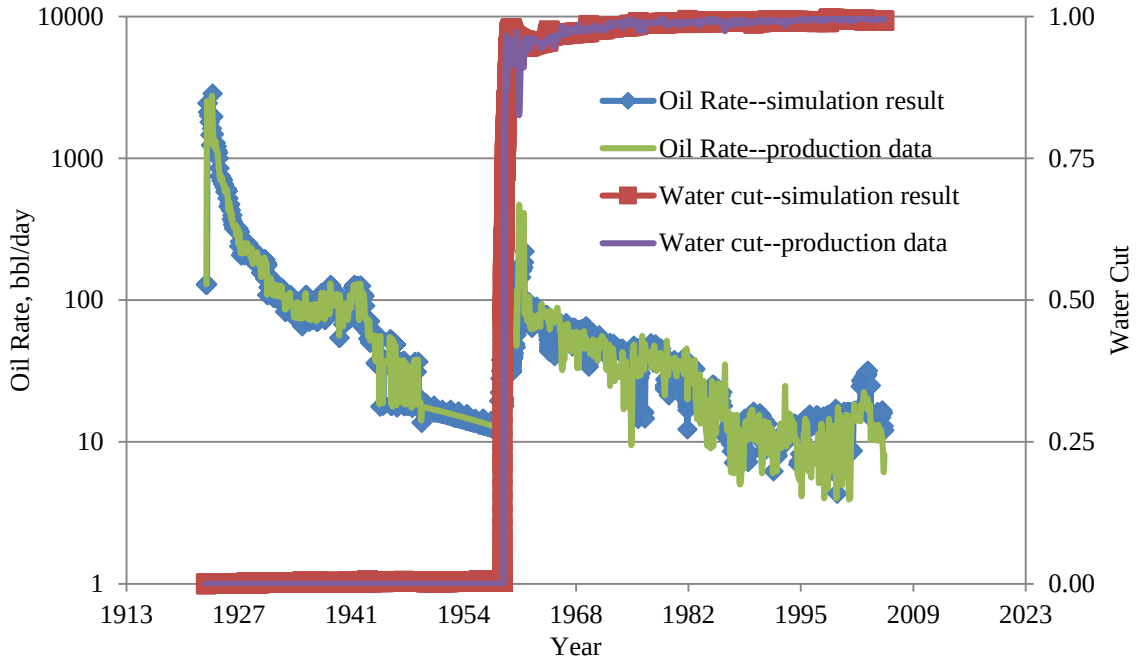

Figure 4.23—History matching result of oil rate and water cut inTR78

4.5.3 Pseudo-Miscible Model Validation

A pseudo-miscible model was used in E100 to model the miscible and solvent. E100 introduces a mixing parameter, ω, which determines the amount of mixing between the miscible fluids within a grid block. A value of zero corresponds to the case of a negligible dispersion rate, whereas a value of one corresponds to complete mixing. Because the fluid model is changed from a compositional model to a black oil model, it is necessary to test the fluid model consistency with existing data. In this study, the correlation of mixing parameter ω and pressure was obtained (**Figure 4.24**) by matching production data

predicted by the pseudo-miscible model with the compositional model (**Figure 4.25**). The highest ω value is 0.6, and the minimum miscible pressure is 1,700 psi (Figure 4.29), which is similar to the MMP value from the experiment and PVT calculation**.**

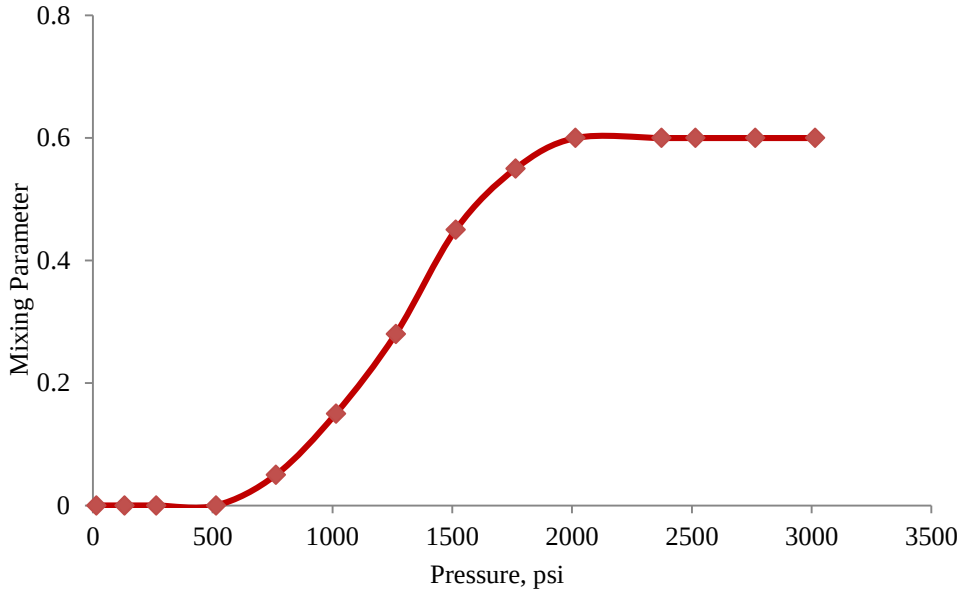

Figure 4.24—Correlation between mixing parameter and pressure

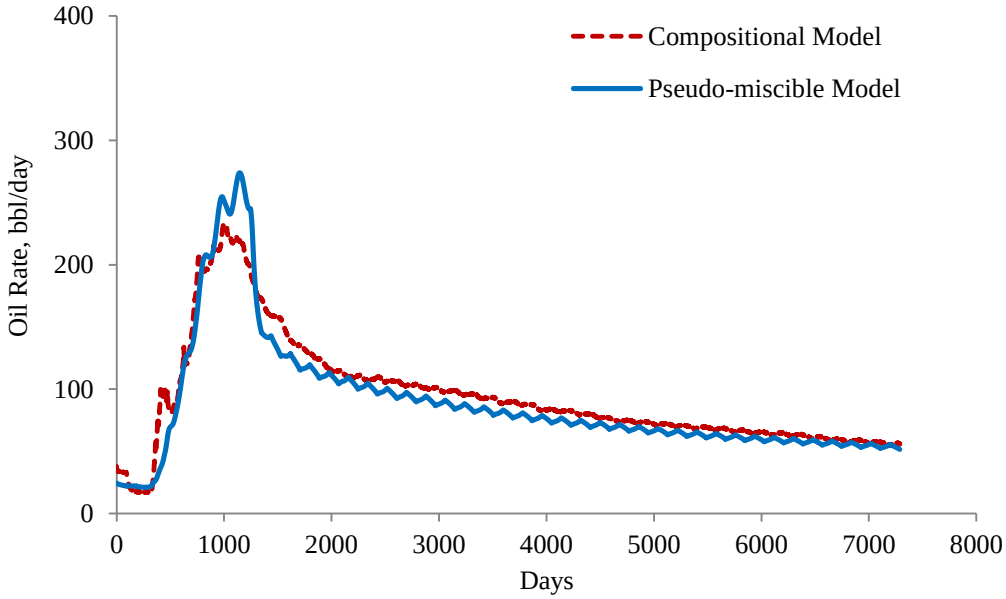

Figure 4.25—Production matching between pseudo-miscible model and composition model

4.5.4 Optimization Polymer Concentration in the PAG Process

A sensitivity analysis was performed on polymer concentration which affects the process significantly. We performed four simulation cases with different concentrations of polymer injected with water all the time, which are presented in **Table 4.10**. Different polymer concentration yielded different injection fluid viscosity. In this study, bottom-hole pressure at injectors was set to 2,100 psi which is fracturing pressure in this field.

Table 4.10—Chemical concentrations for different cases in TR78

Case Name	Polymer Concentration, lb/stb
PAG-1	0.10
PAG-2	0.15
PAG-3	0.20
PAG-4	0.25

Figure 4.26 indicates that increasing polymer concentration would significantly reduce water injectivity, especially, when polymer concentration is larger than 0.20 lb/stb. Polymer injection would not change gas injectivity. However, increasing polymer concentration would reduce the peak oil rate (Phase I), which is dominated by gas injection. After gas breakthrough (Phase II), increasing the concentration from 0.10 to 0.20 lb/stb would increase oil rate, while increasing the concentration from 0.20 to 0.25 lb/stb would reduce oil rate due to injectivity problems (**Figure 4.32**). Similarly, as polymer concentration increases from 0.10 to 0.20 lb/stb, oil recovery increases from 15 to 19%. But concentration higher than 0.20 lb/stb would not recover significantly more oil (**Figure 4.27**). Considering the recovery and polymer consumption, a polymer concentration of 0.20 lb/stb was used for the comparison.

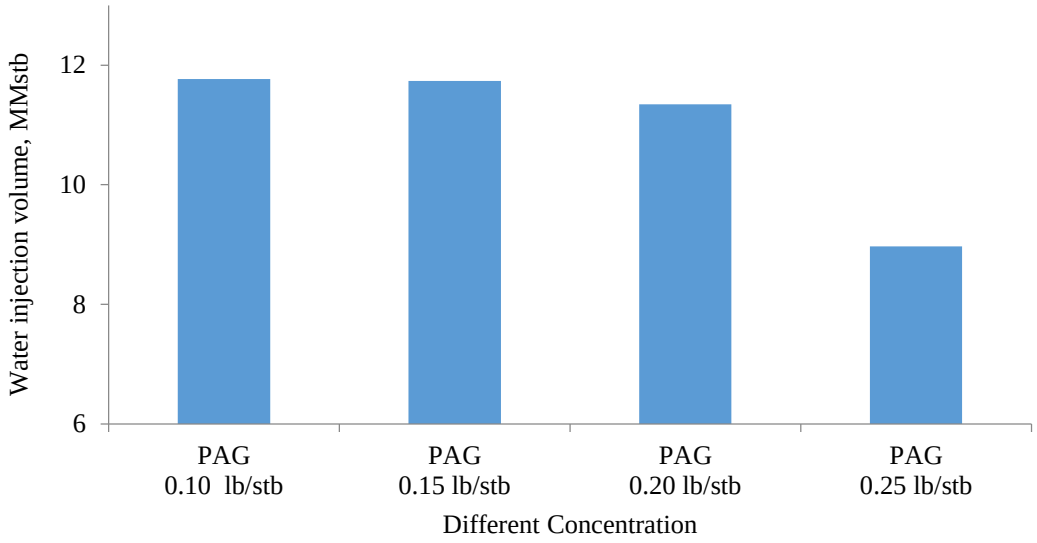

Figure 4.26—Water injectivity decreasing with polymer concentration in TR78

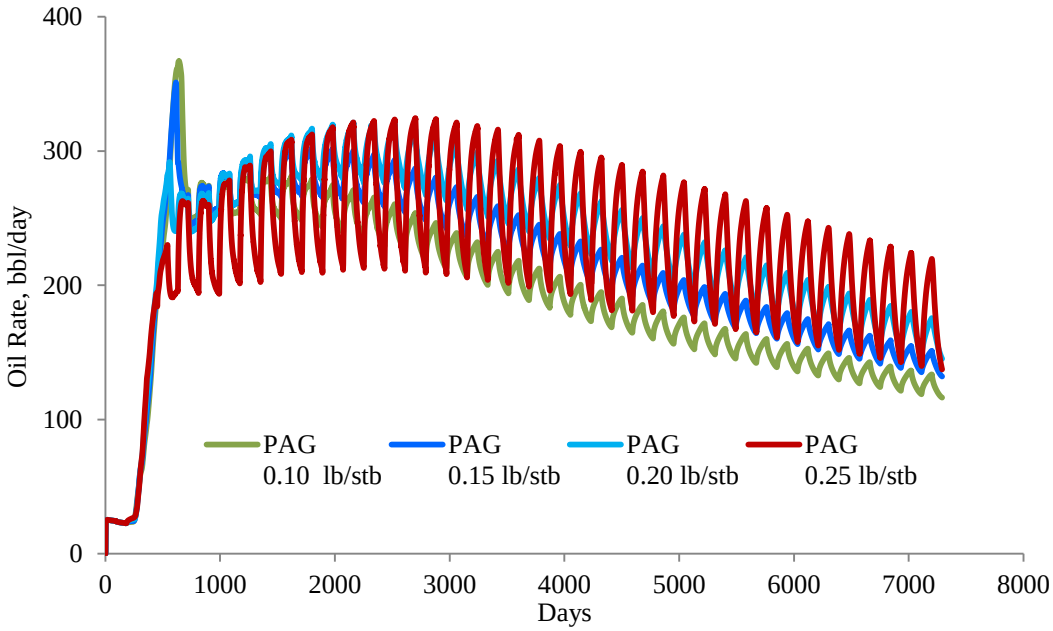

Figure 4.27—Oil rate of different polymer concentrations in TR78

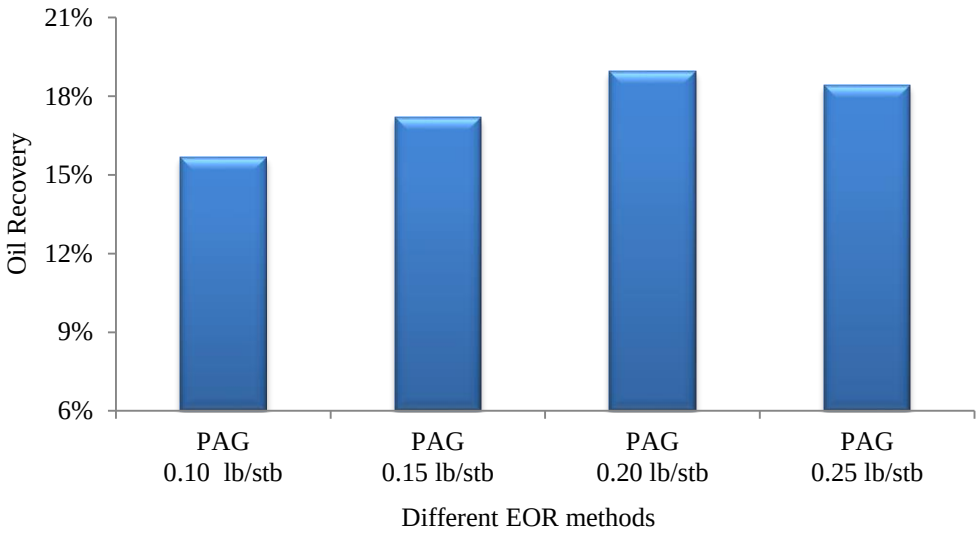

Figure 4.28—Recovery factor of different polymer concentrations in TR78

4.5.5 PAG Versus Polymer Flooding, WAG and CGI

The reservoir performance during PAG was compared with polymer flooding, WAG and CGI. After optimization, a concentration of 0.40 lb/stb is injected in polymer flooding process. In the CGI process, gas injection rate is 0.1 pore volume per year. While the same fluid injection rate and WAG ratio 1:1 are used in WAG process. Simulation results show that oil recovery from PAG with a polymer concentration of 0.20 lb/stb is more than polymer flooding, CGI and WAG (**Figure 4.29**), which indicates that oil recovery increases with polymer injection.

We forecasted oil production rate for the four different EOR process (**Figure 4.30**). The oil rate by CGI declines sharply due to gas breakthrough and gas override. The highest oil rate of CGI is reached after 18 months injection, while it takes 24 and 18 months for WAG and PAG to reach oil rate peak, respectively. It takes much longer time to reach the peak oil rate for polymer flooding, and the oil rate from polymer flooding declines slower than WAG and CGI. PAG has two oil rate peaks. One is due to gas injection (Phase I), and the other is a result of polymer injection and gas injection (Phase II).

Figure 4.31 shows the gas-oil ratio of these three processes. Gas production occurs after 7-month CO_2 injection for CGI, while it takes 8-9 months for WAG and PAG. Gas breakthrough (GOR larger than 5 Mscf/bbl) occurs after 17 months CO_2 injection for CGI, and it takes 27 months for WAG. We do not

find significantly gas breakthrough in PAG process. PAG does improve the gas breakthrough. The gas ratio of PAG is much lower than WAG, which means that PAG would reduce gas production and more CO_2 would be left in reservoir.

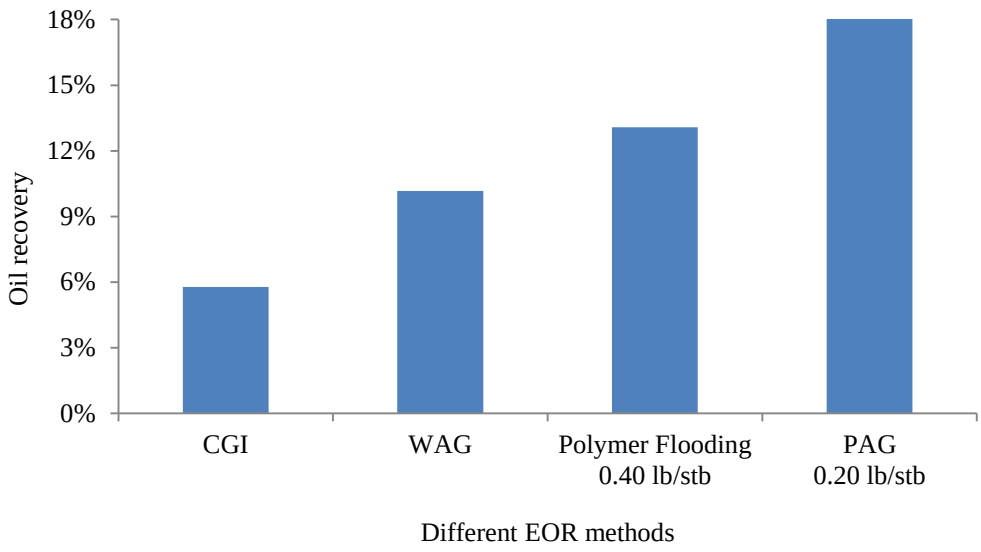

Figure 4.29—Recovery factor of different EOR processes in TR78

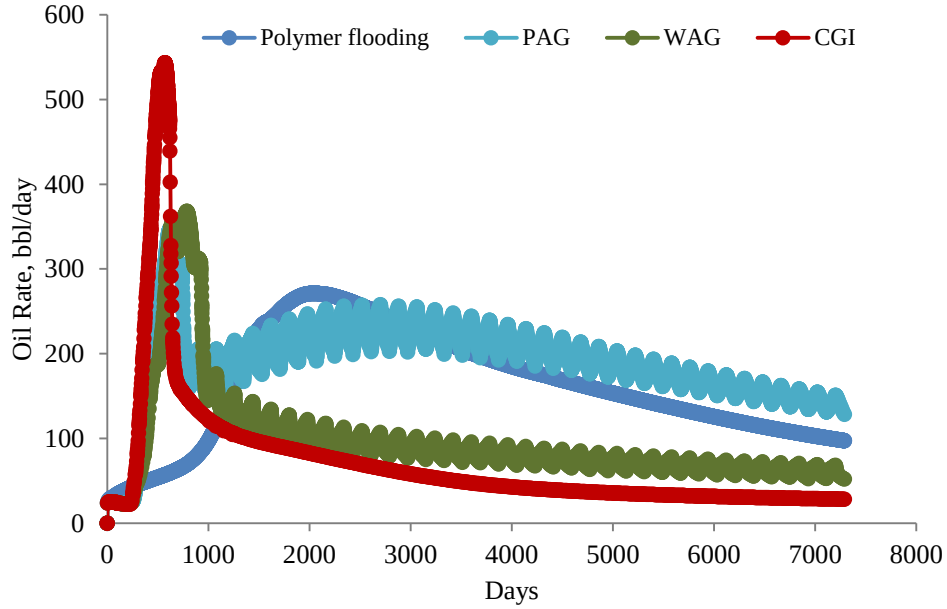

Figure 4.30—Production rate of different processes inTR78

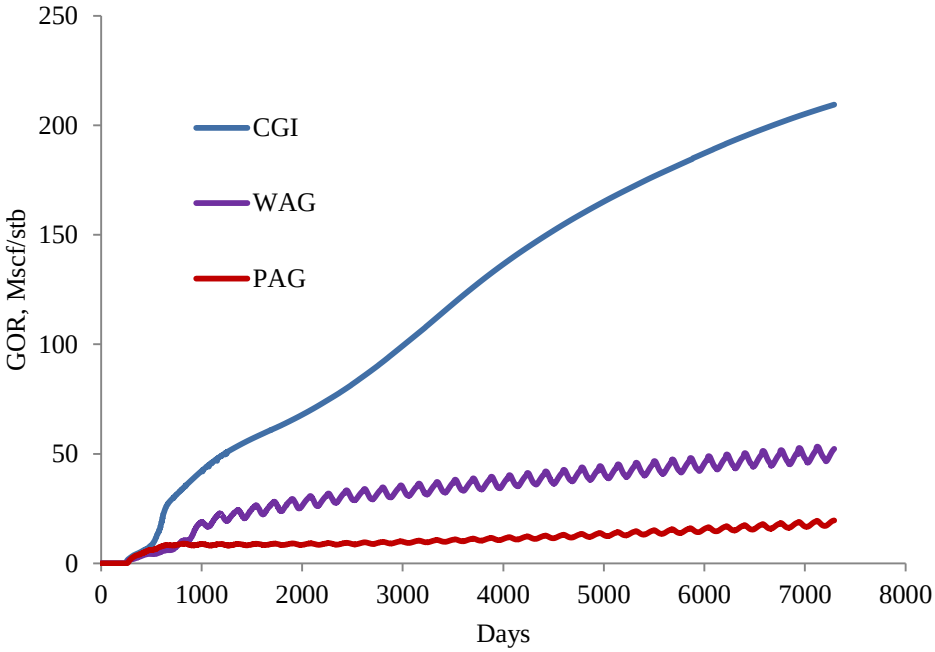

Figure 4.31—Gas-oil ratio of different processes in TR78

Figure 4.32 shows the water saturation distribution of the first layer for WAG and PAG, respectively. Water sweep efficiency of the PAG process is significantly increased compared with WAG. We compared the percentage of water injected into each zone for WAG and PAG (**Figure 4.33**). More water is injected into middle- and lower-permeability zones in PAG (40%) than in WAG (27%). The improvement of vertical and areal sweep efficiency is a consequence of improving water/oil mobility ratio. In addition, the polymer reduces the contrasts in permeability by preferentially plugging the high-permeability zones. This forces the water to flood the lower-permeability zones and increases the sweep efficiency.

As shown in **Figure 4.34**, WAG and PAG have much lower oil saturation than polymer flooding in layer-1, which is dominated by gas flooding. For lower layers, PAG and polymer flooding have larger blue area than WAG which means sweep efficiency improves in lower layers by polymer. Oil saturation in this area is much lowers for PAG process when compared with polymer flooding, which means displace efficiency improved by PAG. Figure 4.35 shows the gas saturation after 15 years injections. It indicates that less gas in top layers, and more gas in lower layers in PAG process when compared with WAG. That

figure hints gas vertical sweep efficiency is improved in PAG process. As shown Figure **4.36** and **4.37**, oil recovery increases significantly in top high permeability layers, while the most increment oil from both high permeability and medium permeability layers.

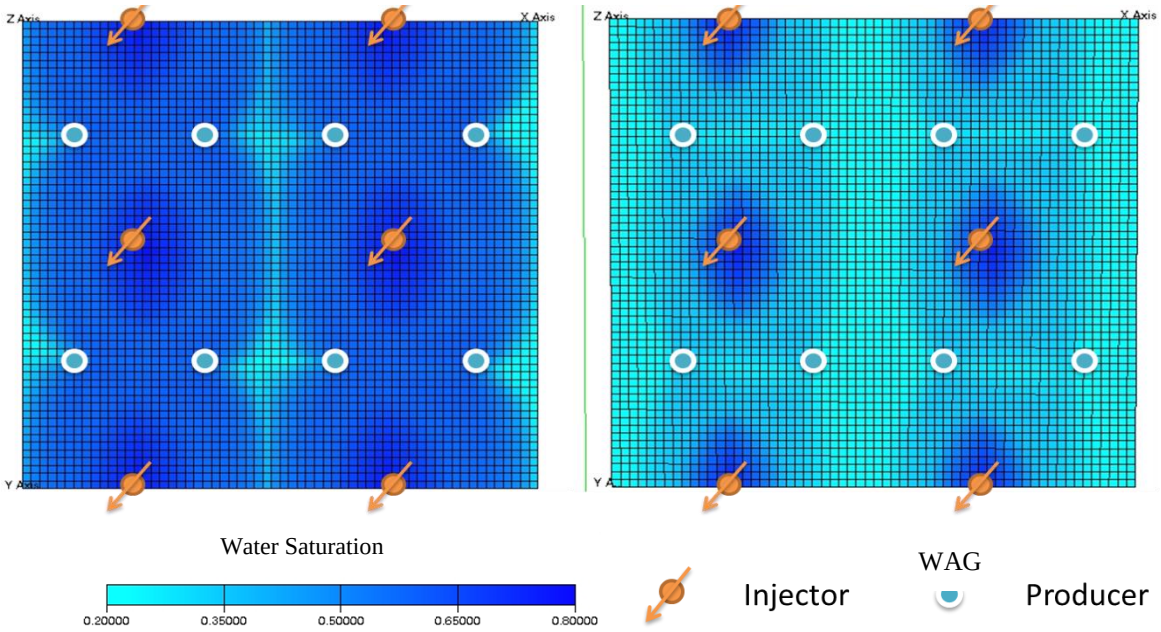

Figure 4.32—Layer-1 water saturation distribution after WAG/PAG flooding in TR78

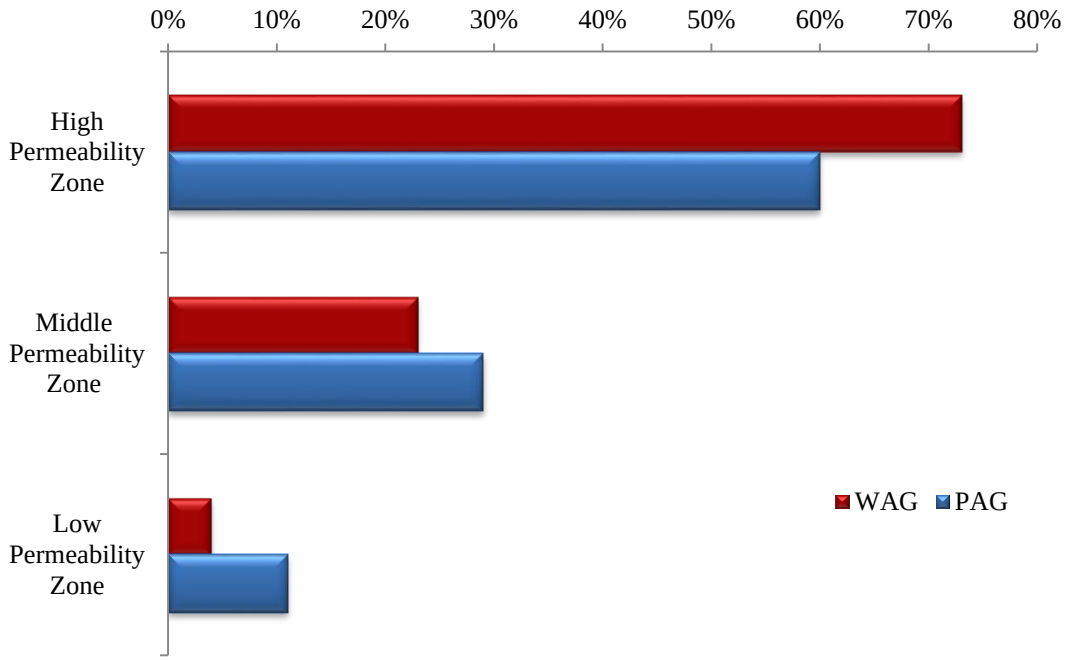

Figure 4.33—Percentage of water injected into different permeability zones for WAG and PAG

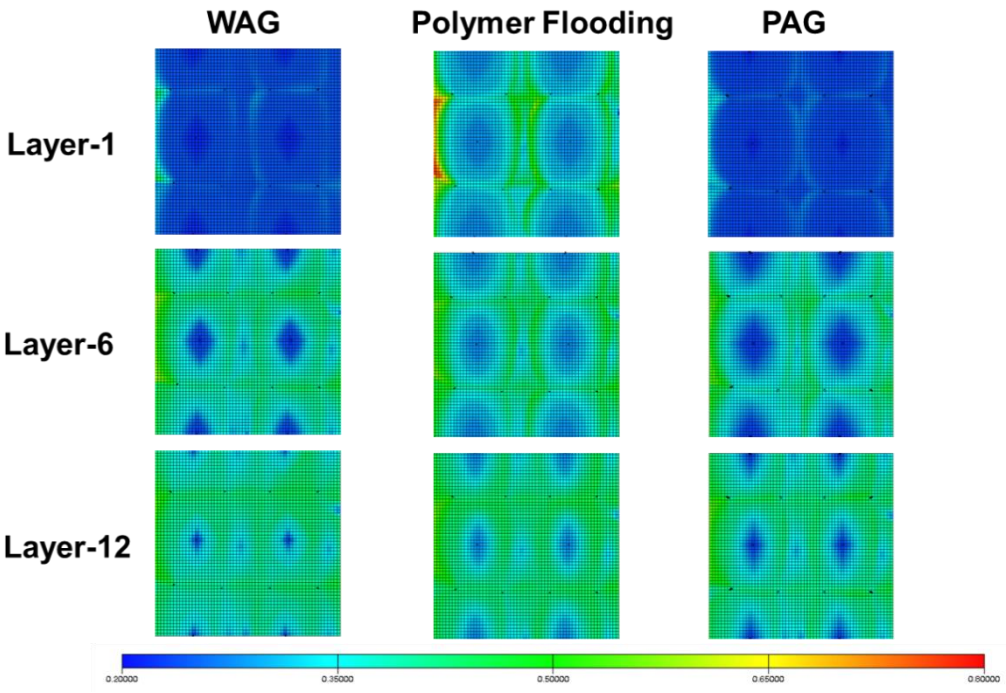

Figure 4.34—Oil saturation after 20 years injection in TR78

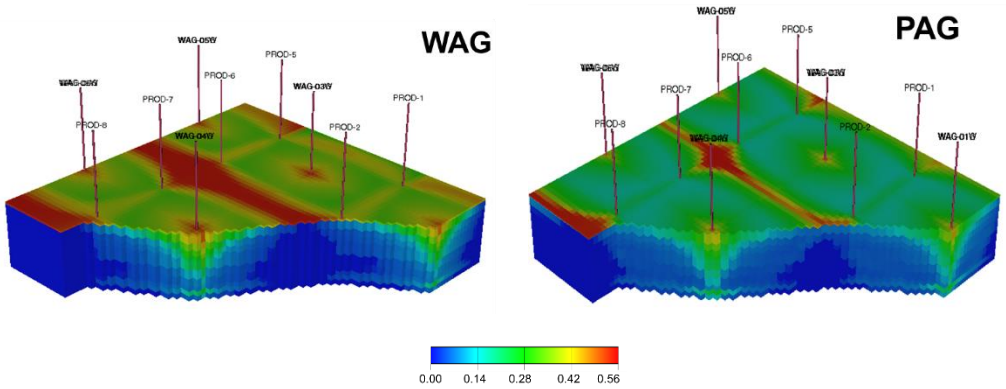

Figure 4.35—Gas saturation after 15 years injection in TR78

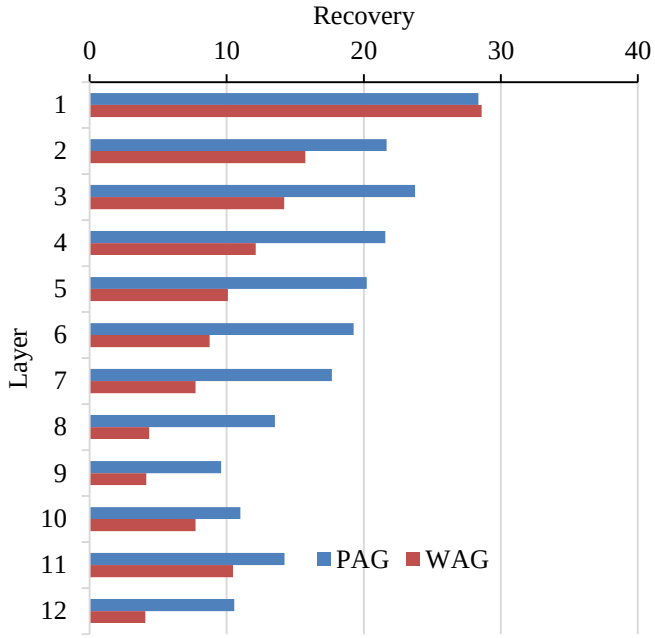

Figure 4.36—Enhanced recovery from each layer in TR78

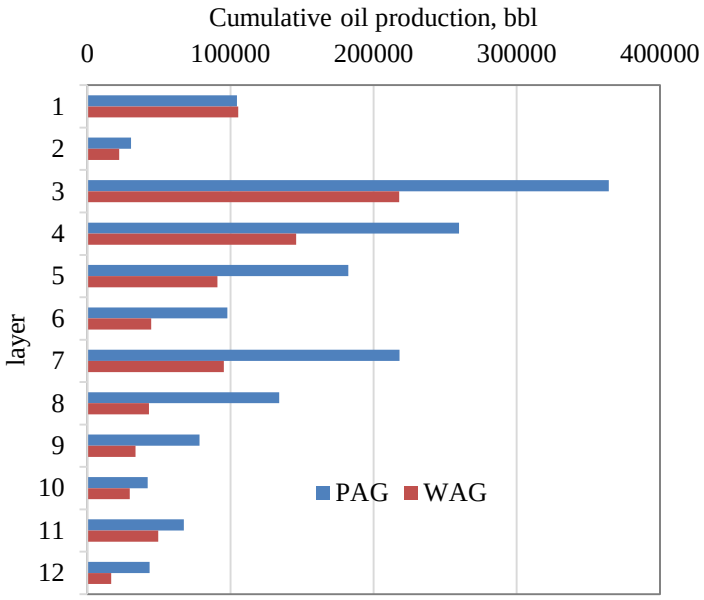

Figure 4.37—Incremental oil from each layer in TR78

4.5.6 Sensitivity Analysis—Slug Pattern

To identify which slug pattern yielded a better recovery, four different schemes were conducted (**Figure 4.38**). Pattern-1 always injects a polymer of 0.20 lb/stb with water. Pattern-2 adds a polymer of 0.20 lb/stb to water after gas breakthrough. Pattern-3 injects a polymer of 0.20 lb/stb with water only at the beginning. Pattern-4 injects a polymer of 0.20 lb/stb with water at the beginning and decreases polymer concentration to 0.10 lb/stb at the end of the WAG process.

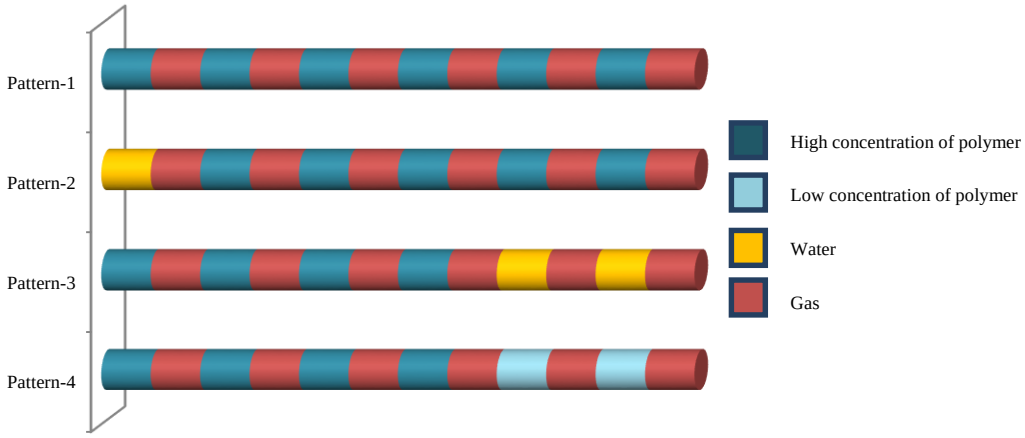

Figure 4.38—Slug patterns of four different schemes in TR78

Slug patterns affect the recovery factor of PAG (**Figure 4.39)**. Pattern-2, which adds a polymer of 0.20 lb/stb to water after gas breakthrough, has the lowest recovery. It indicates that earlier polymer injection is preferred. Recovery from Patterns-1, -3, and -4 are similar, which suggests that both polymer injection in the beginning and lower polymer concentrations (Patterns-3 and -4) are good choices to reduce polymer consumption. Polymer utilization is calculated as

$$Polymer\ utilization = \frac{Total\ polymer\ consumption}{Total\ oil\ from\ PAG - Total\ oil\ from\ WAG} \qquad \text{Equation 4.1}$$

Polymer utilization ranges from 2.20 to 2.84 lb/stb for these four patterns in the PAG process (**Figure 4.40**). Thus, the PAG process has high polymer utilization as successful polymer flooding. Pattern-3 has the best polymer utilization. The following process was used in TR78: injecting polymer with a concentration of 0.20 lb/stb for 15 years in the PAG process and then chasing with the WAG process for 5 years. Oil recovery increased by this pattern was forecasted to be 18.7%, which is 8.7% higher than conventional WAG.

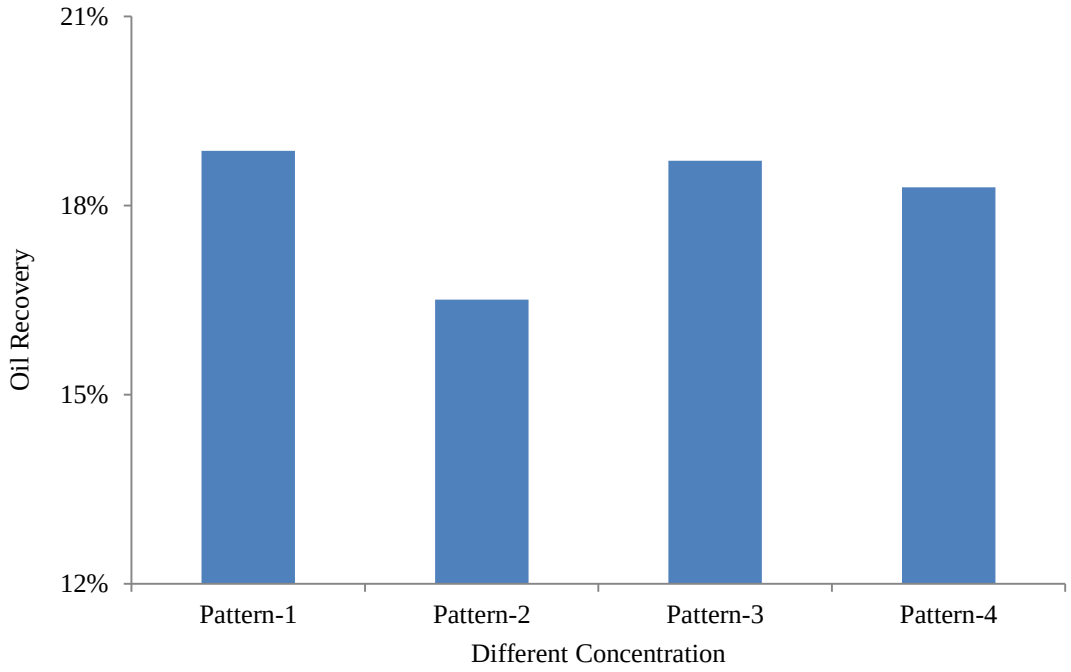

Figure 4.39—Recovery factor of different slug patterns in TR78

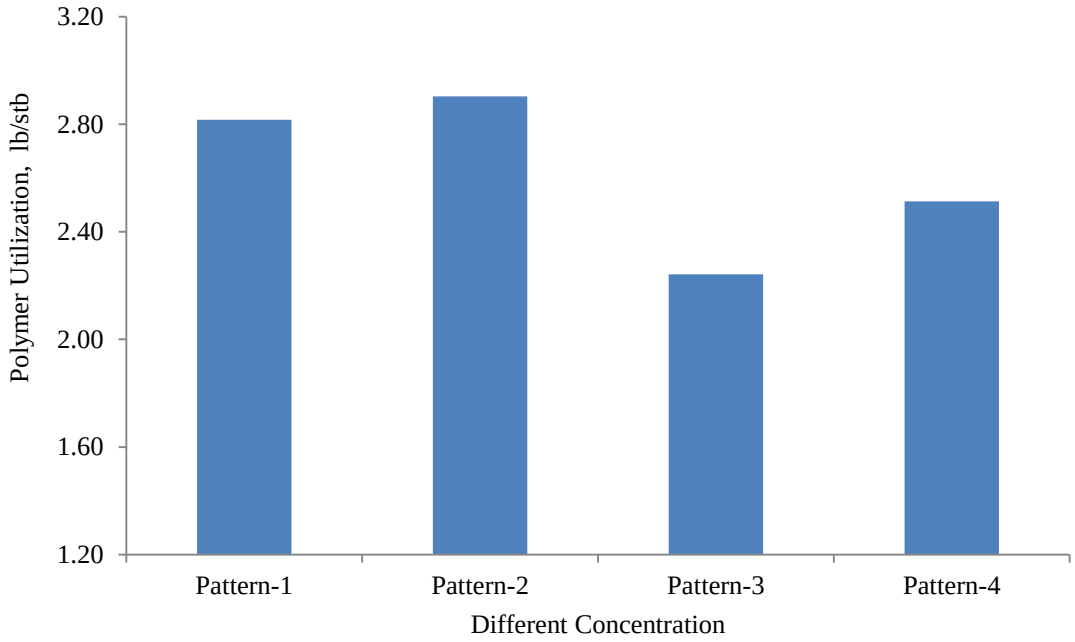

Figure 4.40—Polymer utilization of different slug patterns in TR78

4.6 PAG Simulation in Section 59

4.6.1 Reservoir Model

For the purpose of modeling, the ST59 was characterized by a gridded network with permeability and porosity parameters specified for each block. For this model, the 0.5 × 0.5-mile reservoir section was divided into 60 grid blocks in the x-direction, 60 grid blocks in the y-direction, and 6 grid blocks in the z-direction. In the x- and y-directions, the grid blocks are 44 ft in length. The grid blocks in the z-direction vary from 7 to 32 ft thick, which results in a pay zone of 89 ft. **Figure 4.41** shows x-horizontal permeability (kh) in the model. The vertical permeability (kv) is 0.01 times the x-horizontal permeability, while y-horizontal permeability is 3 times the x-horizontal permeability.

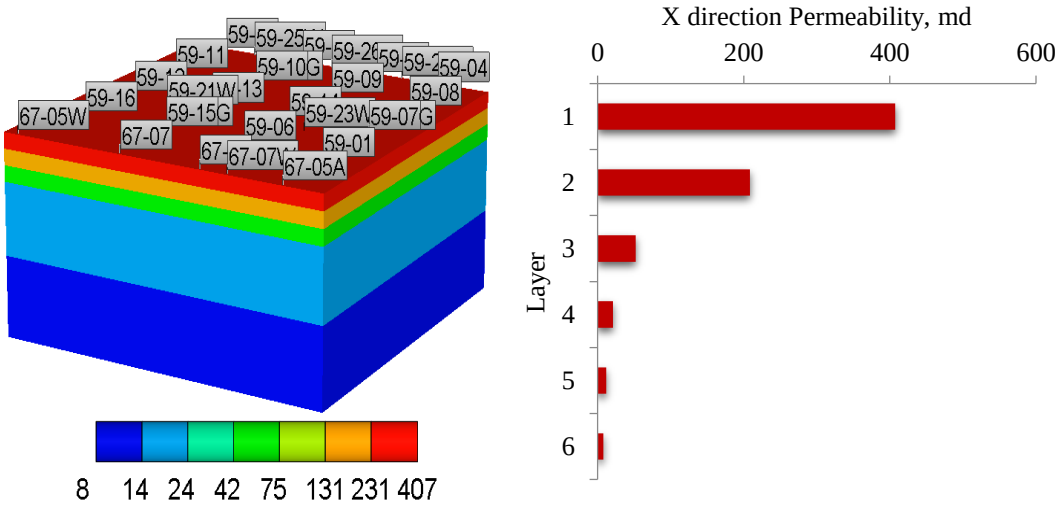

Figure 4.41—X-horizontal permeability of each layer in TR59

After optimizing the WAG, following parameters was used for PAG study. Well pattern is shown in **Figure 4.42**. Fluid injection rate is 0.1 pore volume per year (gas and water injection rate is the same 0.05 pore volume per year) and WAG ratio is 1:1 (90 days water injection alternating with 90 days gas injection) were used in study.

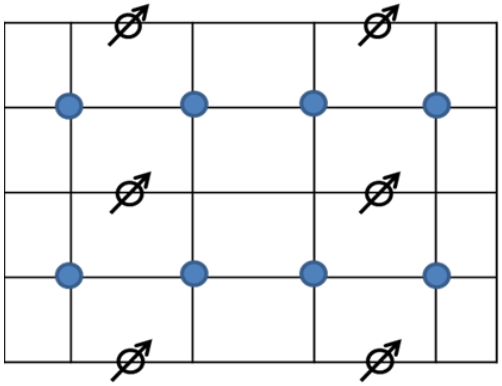

Figure 4.42—Well pattern in TR59

4.6.2 Optimization Polymer Concentration in the PAG Process

Four simulation cases with different polymer concentrations were performed (**Table 4.11)**. Different polymer concentration yields different injection fluid viscosity. In this study, bottom-hole pressure at injectors was set to 2,100 psi which is fracturing pressure in this field.

Table 4.11—Chemical concentrations for different cases in TR59

Case Name	Polymer Concentration, lb/stb
PAG-1	0.10
PAG-2	0.15
PAG-3	0.20
PAG-4	0.25

As shown in **Figure 4.43,** when increasing polymer concentration from 0.10 lb/stb to 0.25 lb/stb, water injection decreases about 40%, especially, when polymer concentration is larger than 0.20 lb/stb. Oil rate comparison among different injection concentration was made for each case in **Figure 4.44**. Note that the peak oil at Phase I (before 500 days) reduces when we increase polymer concentration. At Phase II (after 500 days), increasing the polymer concentration from 0.10 to 0.20 lb/stb would increase oil rate. However, increasing the concentration from 0.20 to 0.25 lb/stb would reduce oil rate due to water injectivity problem (**Figure 4.43**). Similarly, as polymer concentration increases from 0.10 to 0.20 lb/stb, oil recovery increases from 13 to 16%. But concentration higher than 0.20 lb/stb would not recover

significantly more oil (**Figure 4.45**). Considering the recovery and polymer consumption, a polymer concentration of 0.20 lb/stb was used for the TR59 in the PAG process.

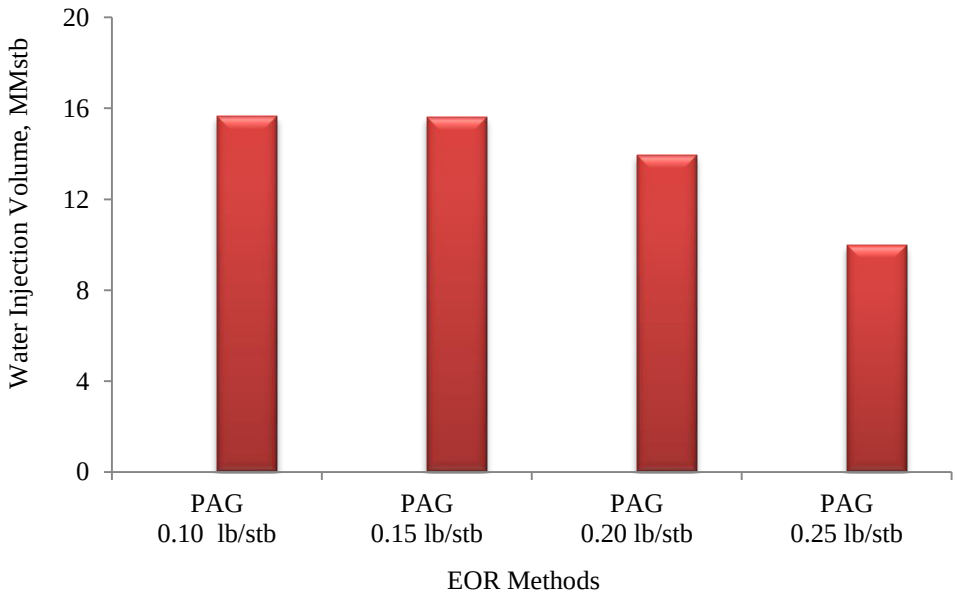

Figure 4.43—Water injectivity decreasing with polymer concentration in TR59

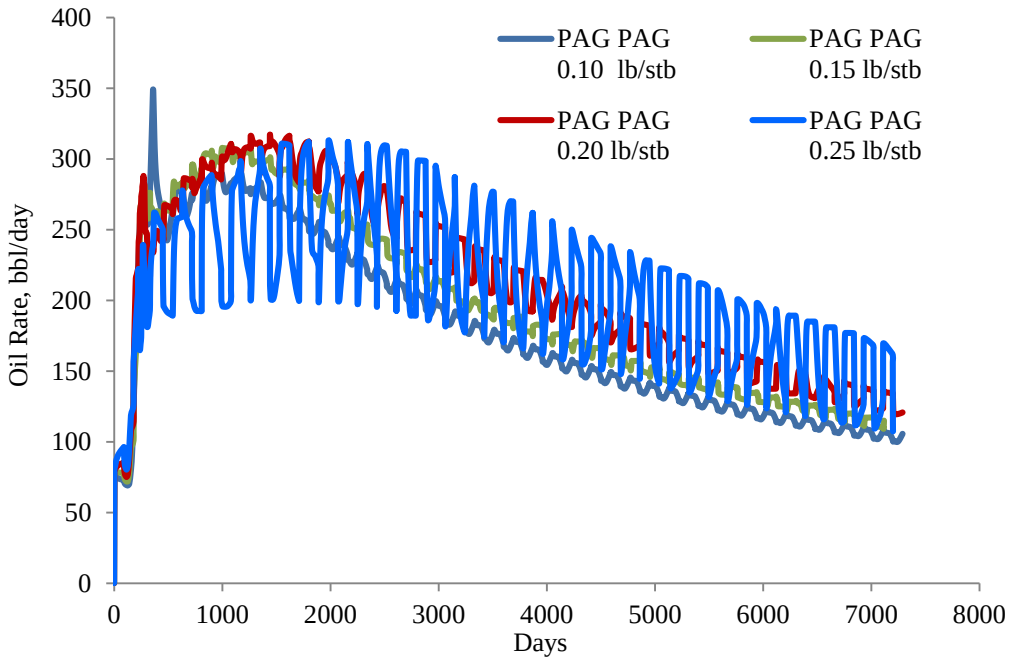

Figure 4.44—Oil rate of different polymer concentrations in TR59

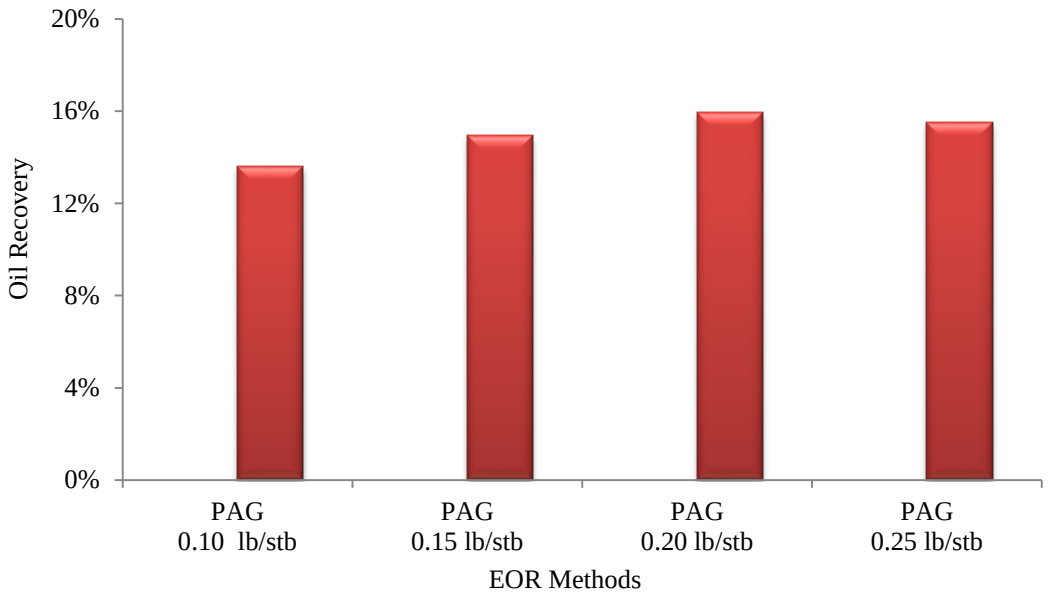

Figure 4.45—Recovery factor of different polymer concentrations in TR59

4.6.2 PAG Versus Polymer Flooding and WAG

To identify which injection method yielded a better recovery, four different schemes were conducted (**Figure 4.46**). Pattern-1 (polymer flooding) injects polymer of 0.15 lb/stb with water for twenty years. Pattern-2 (polymer-water flooding) injects polymer of 0.15 lb/stb with water for ten years then follow with water injection for ten years. Pattern-3 (WAG) uses WAG injection for twenty years. Pattern-4 (PAG) injects polymer of 0.20 lb/stb with water and alternative with gas for twenty years. Same volume of polymer was injected for pattern-2 and pattern-4.

We forecasted oil production rate for the four different EOR processes (**Figure 4.47**). Significant difference can be observed among different EOR methods in terms of oil production. In Figure 4.43 the oil rate for WAG reaches peak rate after 1 year gas injection and then decline sharply, while the oil rate in polymer flooding increases slowly and reaches peak rate after 3 years injection and then decline slowly. The polymer concentration is zero which contributes to the later oil rate decline in the polymer water flooding process. The oil rate from PAG process is much higher than other EOR methods after 15 months injection and declines slower than the other methods. For the recovery in **Figure 4.48** and **Table 4.12**,

polymer flooding could produce 9.03% OOIP after water flooding, while this value is 7.35% for polymer-water flooding. It shows that this reservoir also is a good candidate for polymer flooding. Recovery after PAG injection is 14.99%, which is 5-8% higher than other injection method. It indicates combining polymer and gas injection is better than other methods mentioned above.

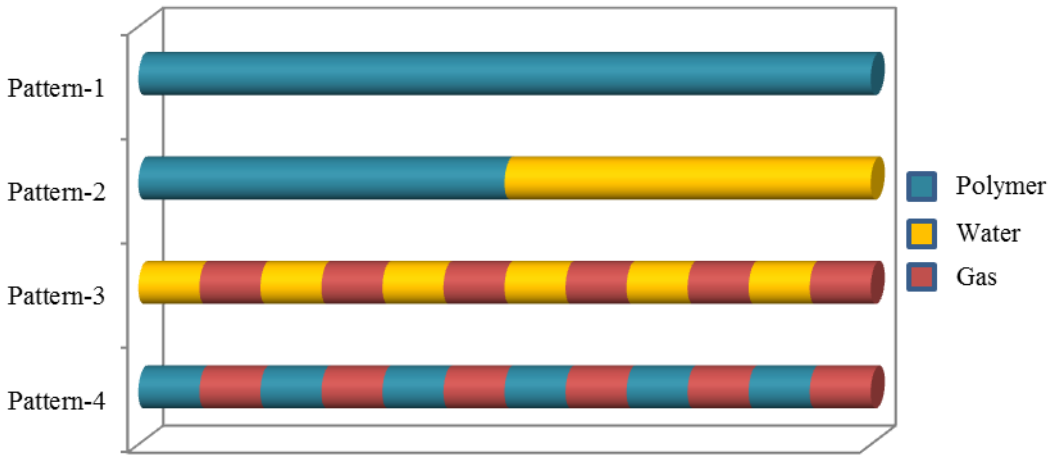

Figure 4.46—Slug patterns of four different schemes in TR59

Table 4.12—Summary of different methods in TR59

	Recovery %	Polymer Consumption 10^6 lb	Oil Increased 10^6 stb	Polymer Utilization lb/stb
Polymer Flooding	9.19	4.30	0.88	4.88
Polymer-Water Flooding	7.24	2.17	0.69	3.10
WAG	9.69	0.00	0.93	0.00
PAG	14.99	2.34	1.43	4.68*

*using Equation 4.1

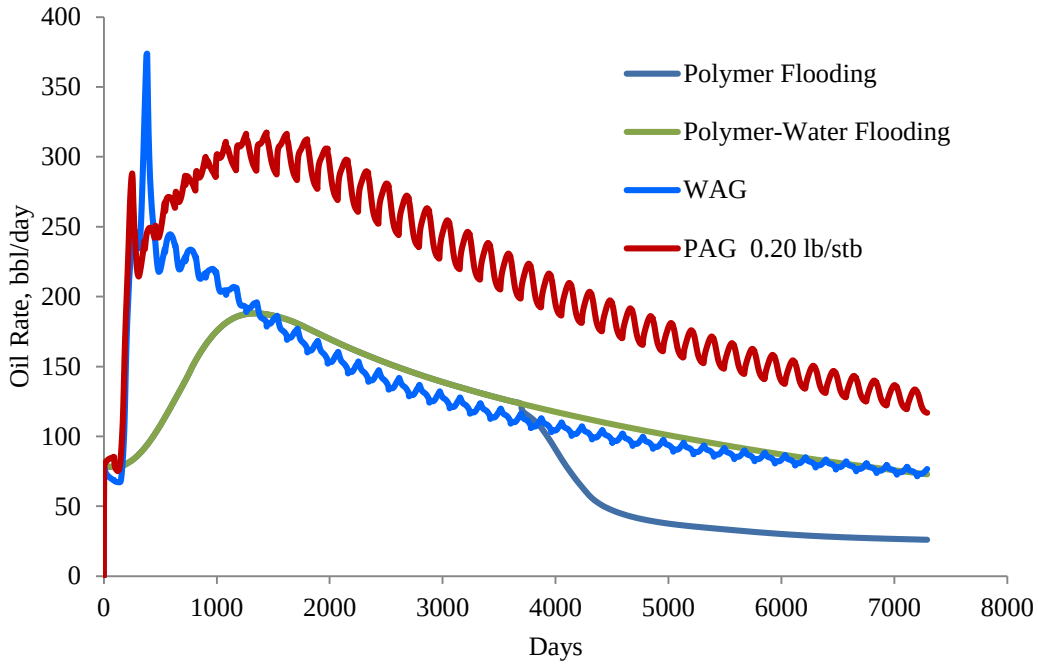

Figure 4.47—Oil production rate with different injection slugs in TR59

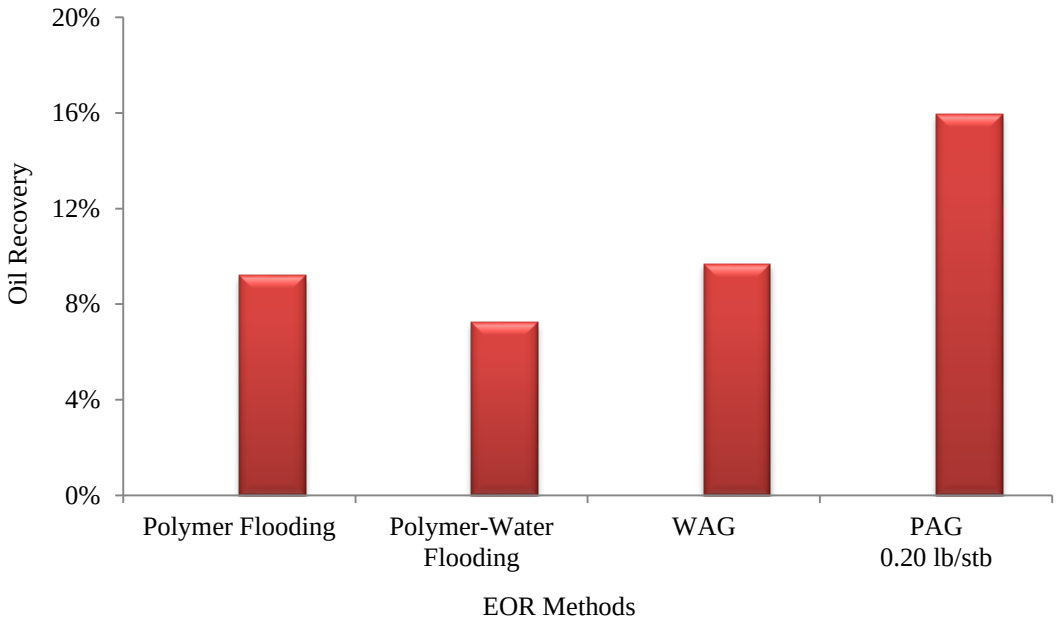

Figure 4.48—Oil recovery under different methods in TR59

4.7 PAG Simulation in Section 48

4.7.1 Reservoir Model

For this model TR48, the 0.5 × 0.5-mile reservoir section was divided into 60 grid blocks in the x-direction, 60 grid blocks in the y-direction, and 10 grid blocks in the z-direction. In the x- and y-directions, the grid blocks are 44 ft in length. The grid blocks in the z-direction vary from 4 to 24 ft thick, which results in a pay zone of 91 ft. **Figure 4.49** shows x-horizontal permeability (kh) in the model. The vertical permeability (kv) is 0.01 times the x-horizontal permeability, while y-horizontal permeability is 3 times the x-horizontal permeability. **Table 4.8** presents the input reservoir rock and fluid properties used for the simulation.

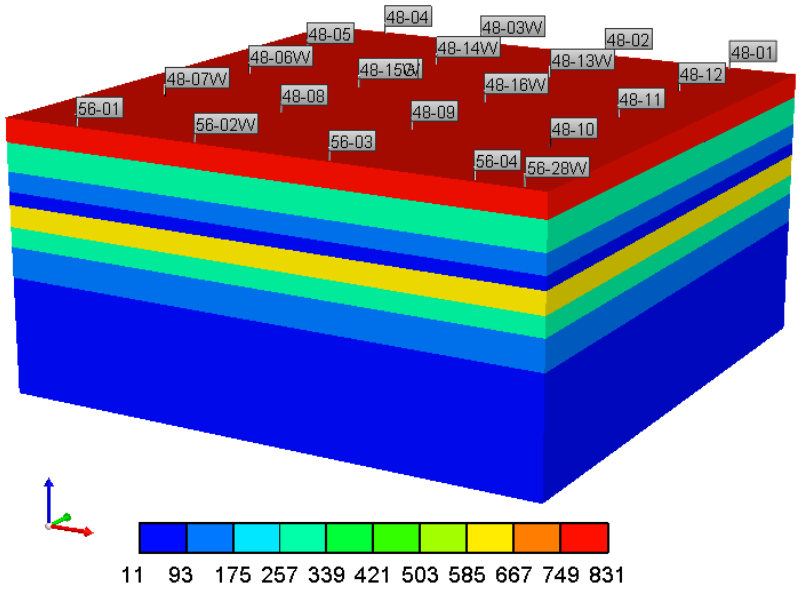

Figure 4.49—X-horizontal permeability (right) of each layer in TR48

4.7.2 Reservoir Model Validation Before CO_2 Flooding

With the reservoir model described above, simulation runs are made to history match the reservoir's pre-CO_2 flood oil and water production during primary depletion and secondary development. Liquid production rate is used as the primary constraint. A good match of oil rate and water cut was reached (**Figure 4.50**), which validates the reservoir model.

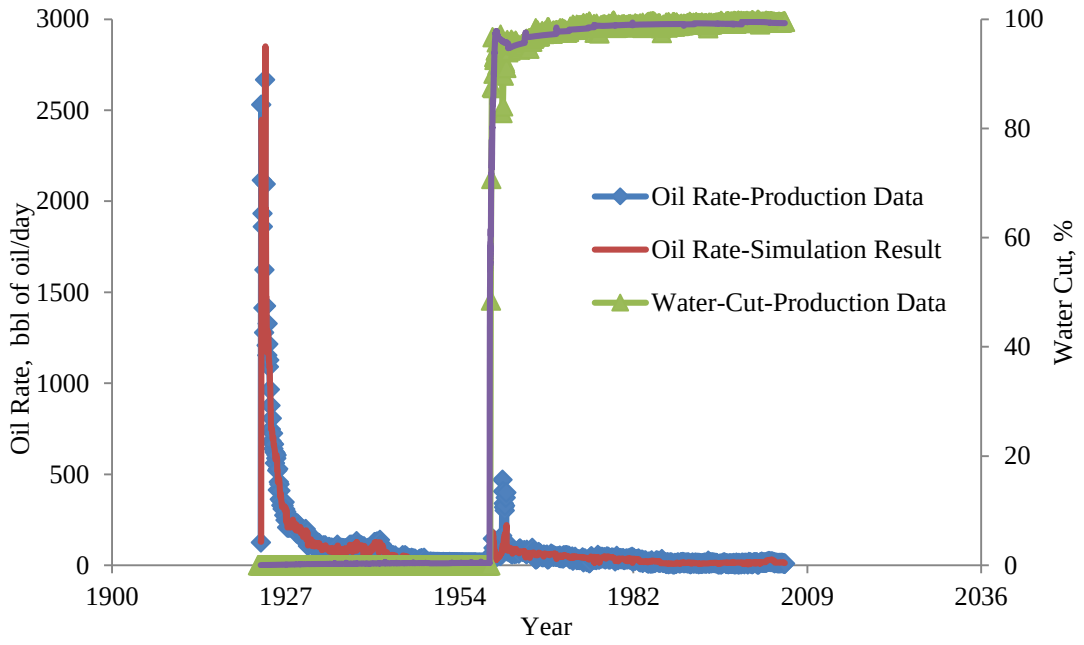

Figure 4.50—History matching result of oil rate and water cut in TR48

4.7.3 Sensitivity Analysis—Polymer Concentration

Four simulation cases with different polymer concentrations were performed (**Table 4.13)**. Different polymer concentration yields different injection fluid viscosity. In this study, bottom-hole pressure at injectors was set to 2,100 psi which is fracturing pressure in this field.

Table 4.13—Chemical concentrations for different cases in TR48

Case Name	Polymer Concentration, lb/stb
PAG-1	0.15
PAG-2	0.25
PAG-3	0.35
PAG-4	0.45

Figure 4.51 indicates that increasing polymer concentration would significantly reduce water injectivity, especially, when polymer concentration is larger than 0.35 lb/stb. As polymer concentration increases from 0.15 to 0.35 lb/stb, oil recovery increases from 9 to 13%. But when concentration is higher

than 0.35 lb/stb, recover reduces a little because less water is injected (**Figure 4.52**). Considering the recovery and polymer consumption, a polymer concentration of 0.35 lb/stb was used for the TR48 in the PAG process.

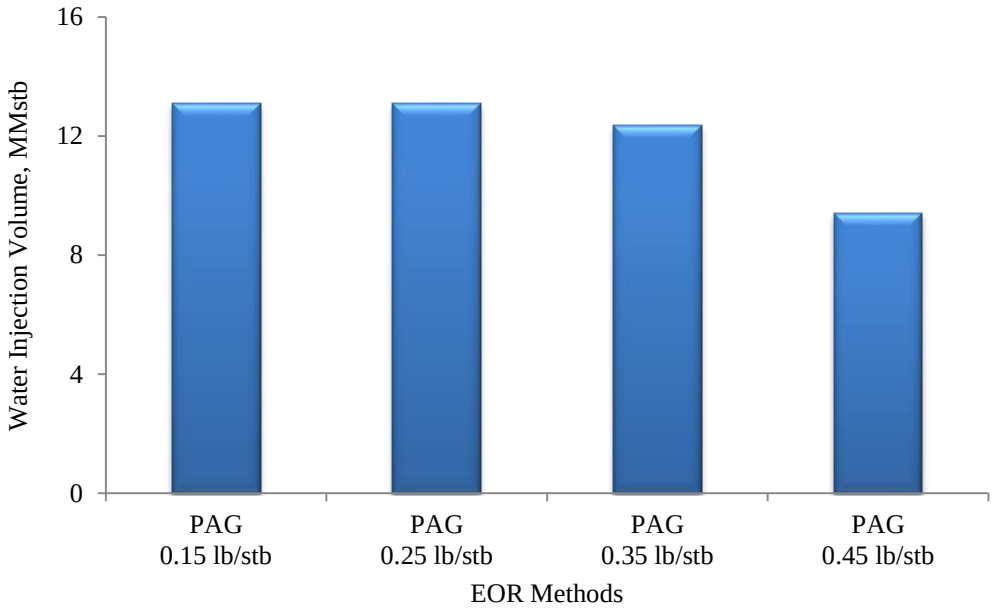

Figure 4.51—Water injectivity decreasing with polymer concentration in TR48

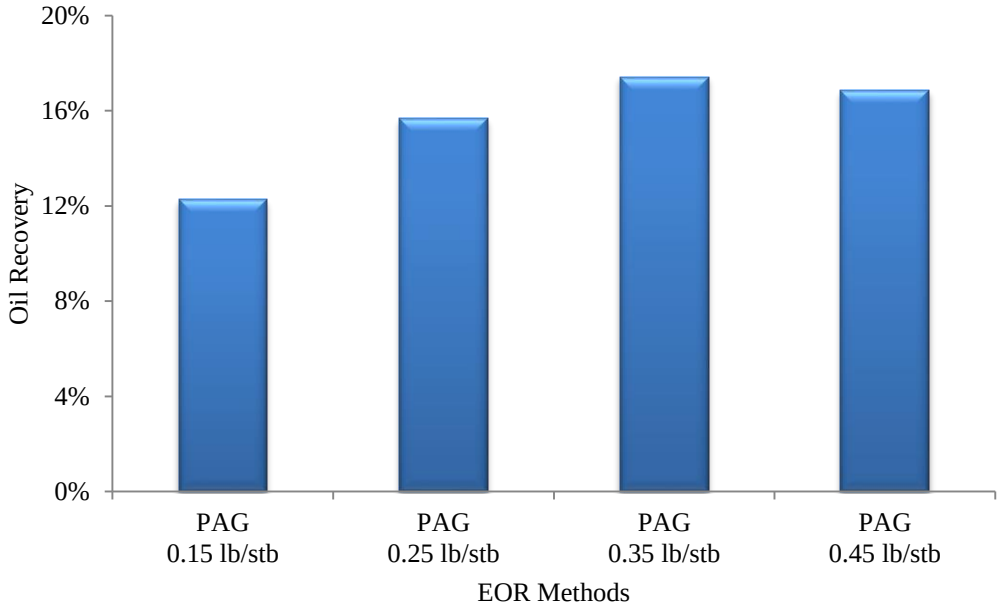

Figure 4.52—Recovery factor of different polymer concentrations in TR48

4.7.4 PAG Versus Polymer Flooding and WAG

The reservoir performance during PAG was compared with polymer flooding and WAG. Simulation results show that oil recovery from polymer with a polymer concentration of 0.70 lb/stb is higher than PAG (with a polymer concentration of 0.35 lb/stb for 20 years) and WAG (**Figure 4.53**), which indicates that this reservoir is a good candidate for polymer flooding. The simulation results also show that using PAG could get better performance than WAG in such a high heterogeneous reservoir.

We forecasted oil production rate for the three different EOR process (**Figure 4.54**). The peak oil rate is about 535, 280, 225 bbl/day for polymer flooding, PAG and WAG respectively. **Figure 4.55** shows the gas-oil ratio of these three processes. Gas production occurs after 7 months of CO_2 injection for WAG and PAG. CO_2 breakthroughs occur after 2 years injection for the WAG and PAG process, while GOR in PAG process is much lower than WAG.

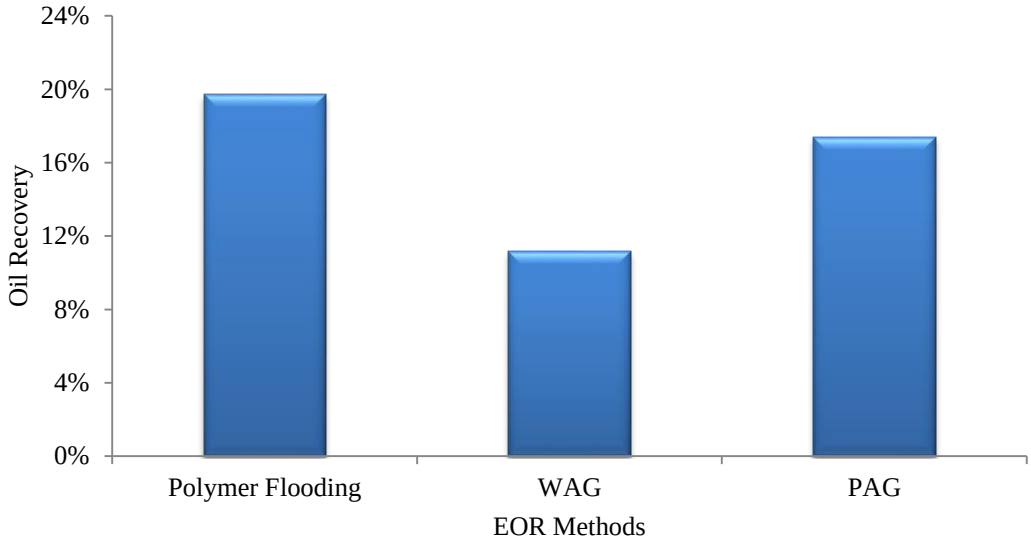

Figure 4.53—Recovery factor of different EOR processes in TR48

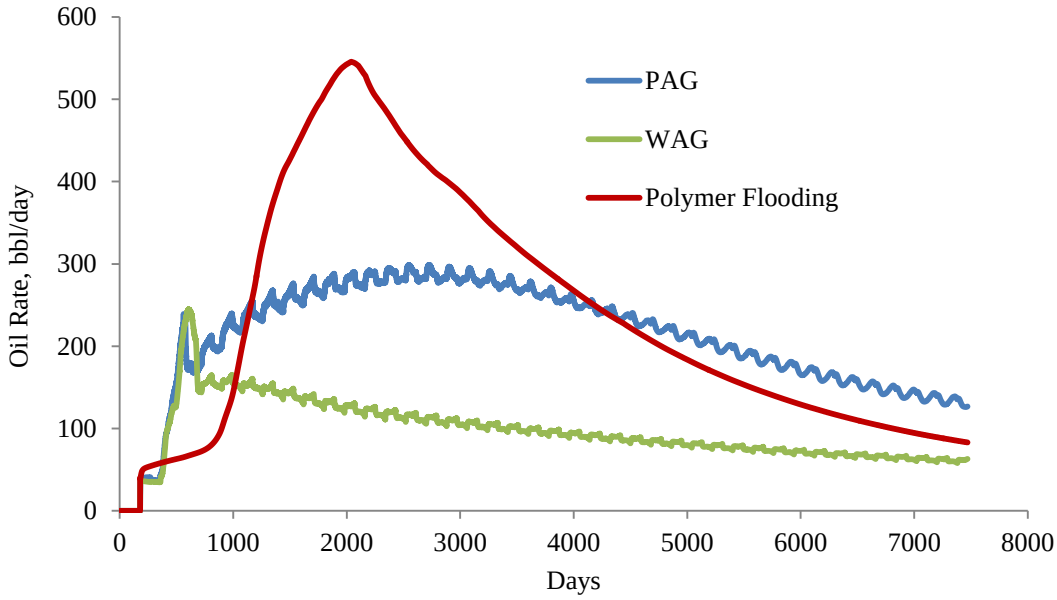

Figure 4.54—Production rate of different processes in TR48

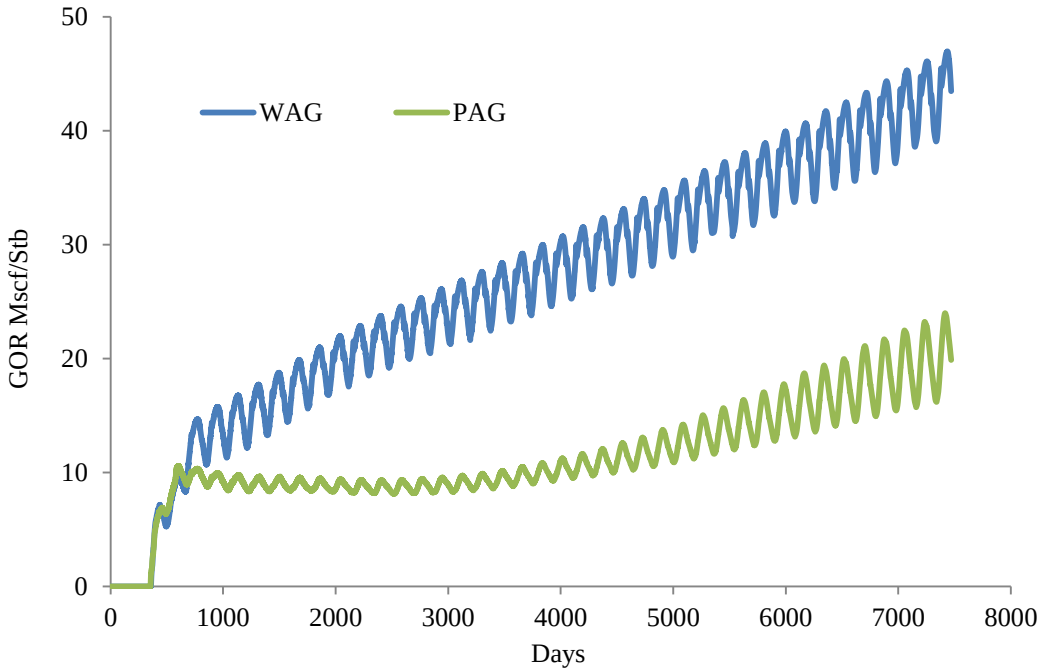

Figure 4.55—Gas-oil ratio of different processes in TR48

4.8 PAG Simulation in Section 92

4.8.1 Reservoir Model

For the purpose of modeling, ST92 was characterized by a gridded network with permeability and porosity parameters specified for each block. The 0.5 miles by 0.5 miles reservoir section was divided into 60 grid blocks in the x-direction, 60 grid blocks in the y-direction, and 10 grid blocks in the z-direction. In the x- and y- directions, the grid blocks are 44 feet in length. The grid blocks in the z-direction are varying from 2-16 feet thick, which results in a pay zone of 78.8 ft. **Figure 4.56** shows x- horizontal permeability (kh) in the model. The vertical permeability (kv) is 0.01 times of x-horizontal permeability, while y-horizontal permeability is 3 times of x-horizontal permeability.

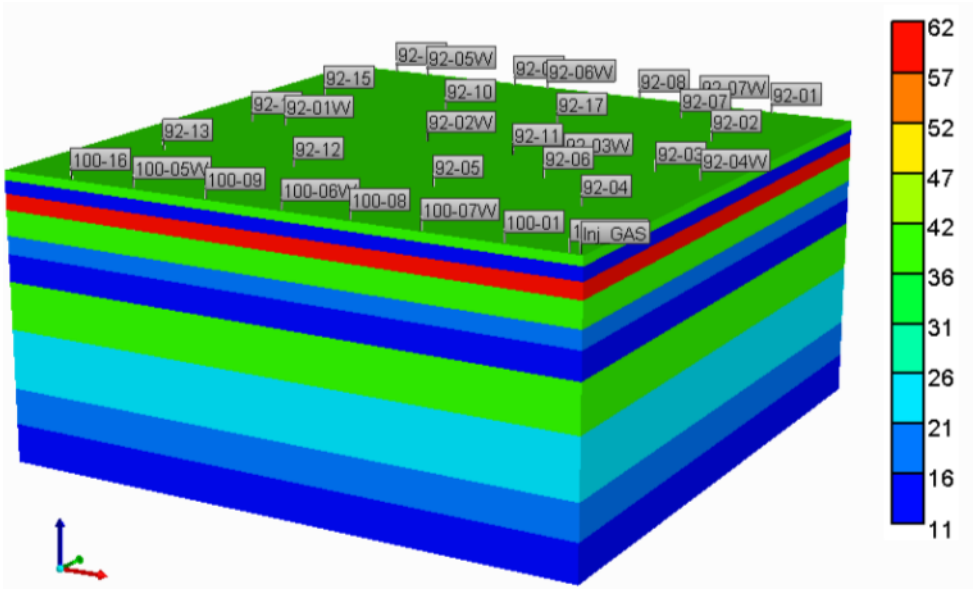

Figure 4.56—X- horizontal permeability model in TR92

4.8.2 Reservoir Model Validation Before CO_2 Flooding

With the reservoir model described above, simulation runs to history match the reservoir's pre-CO_2 flood oil and water production during primary depletion and secondary development. Liquid production rate was used as the primary constraints. As shown in **Figure 4.57**, good matching results are reached.

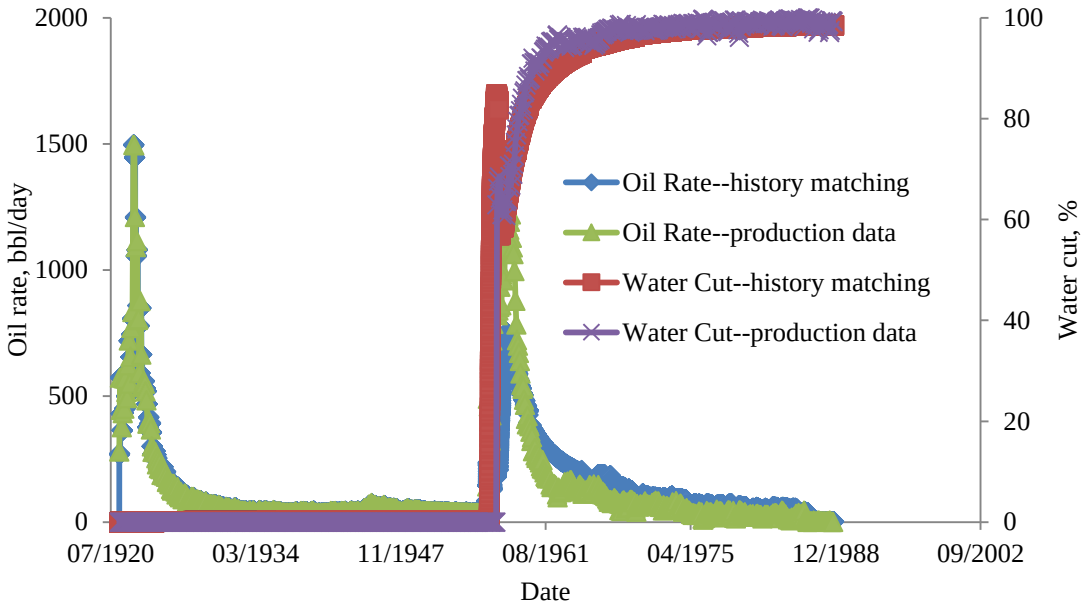

Figure 4.57—History matching result of oil rate and water cut in TR92

4.8.3 Sensitivity Analysis—Polymer Concentration

Four simulation cases with different polymer concentrations were performed (**Table 4.14)**. Different polymer concentration yields different injection fluid viscosity. In this study, bottom-hole pressure at injectors was set to 2,100 psi which is fracturing pressure in this field.

Table 4.14—Chemical concentrations for different cases in TR92

Case Name	Polymer Concentration, lb/stb
PAG-1	0.05
PAG-2	0.10
PAG-3	0.15
PAG-4	0.20

Figure 4.58 indicates that increasing polymer concentration would significantly reduce water injectivity, especially when polymer concentration is larger than 0.10 lb/stb. As polymer concentration increases from 0.05 to 0.10 lb/stb, oil recovery increases from 9 to 14% (**Figure 4.59**). But concentration that is higher than 0.10 lb/stb would not significantly recover more oil. Considering the recovery and polymer consumption, a polymer concentration of 0.10 lb/stb was used for the TR92 in the PAG process.

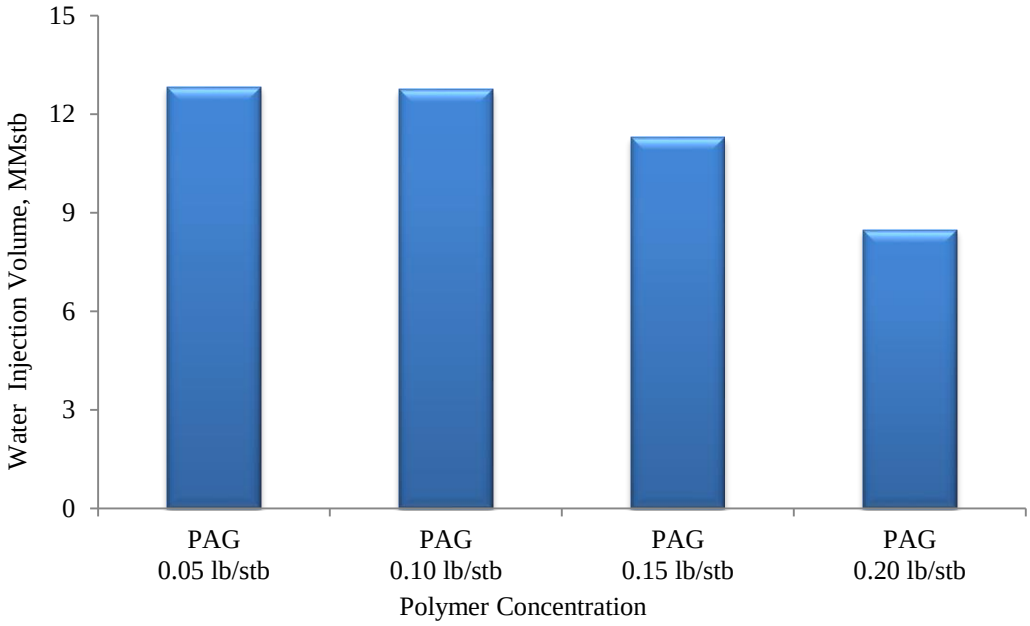

Figure 4.58—Water injectivity decreasing with polymer concentration in TR92

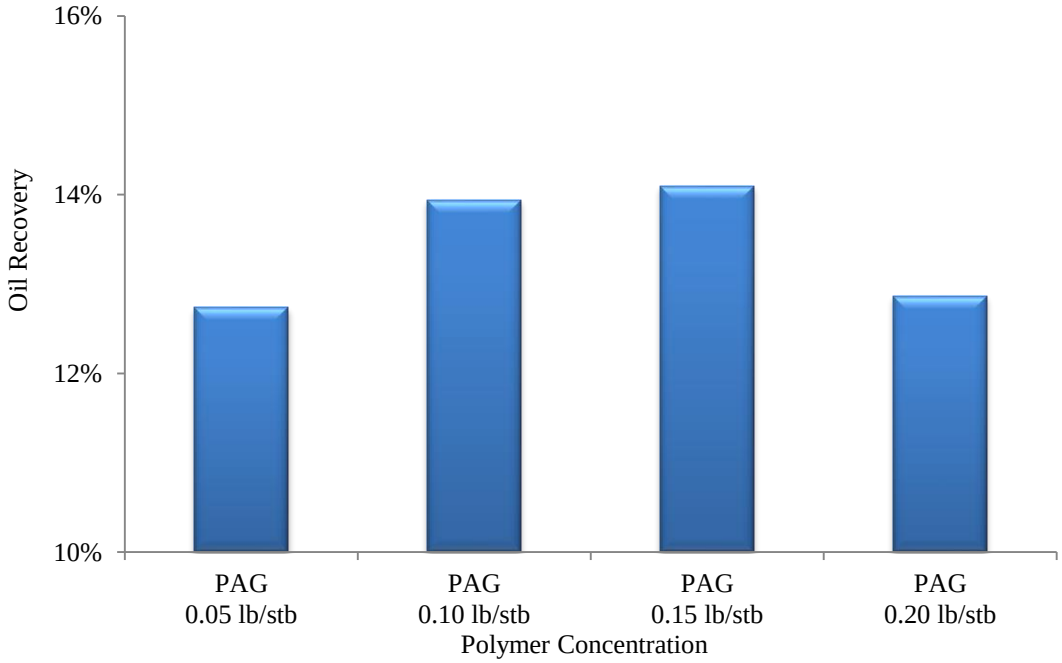

Figure 4.59—Recovery factor of different polymer concentrations in TR92

4.8.4 PAG Versus Polymer Flooding and WAG:

To identify which injection method yields a better recovery, three different schemes were conducted. Pattern-1 (polymer flooding) injects polymer of 0.15 lb/stb with water for twenty years. Pattern-2 (WAG) uses WAG injection for twenty years. Pattern-3 (PAG) injects polymer of 0.10 lb/stb with water and alternative with gas for twenty years.

We forecasted oil recovery for the three different EOR processes (**Figure 4.60**). Polymer flooding could produce 7.8% OOIP after water flooding. Recovery from pattern-2 is 10.1% higher than recovery from water flooding. Recovery after PAG injection is 13.9%, which is 3-6% higher than other injection methods. It indicates combining polymer and gas injection is better than other methods mentioned above.

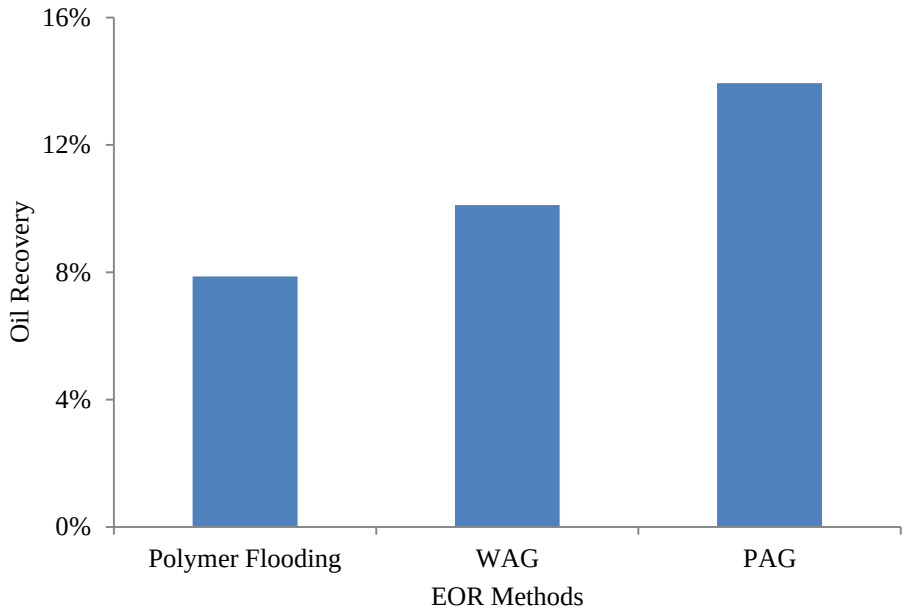

Figure 4.60—Recovery factor of different EOR processes in TR92

4.9 PAG Simulation in Section 88

4.9.1 Reservoir Model

The ST88 was characterized by a gridded network with permeability and porosity parameters specified for each block. For this model, the 0.5 miles by 0.5 miles reservoir section was divided into 60

grid blocks in the x-direction, 60 grid blocks in the y-direction, and 10 grid blocks in the z-direction. In the x- and y- directions, the grid blocks are 44 feet in length. The grid blocks in the z-direction vary from 1-15 feet thick, which results in a pay zone of 71.6 ft. **Figure 4.61** shows x- horizontal permeability (kh) in the model. The vertical permeability (kv) is 0.01 times of x-horizontal permeability, while y- horizontal permeability is 3 times of x-horizontal permeability.

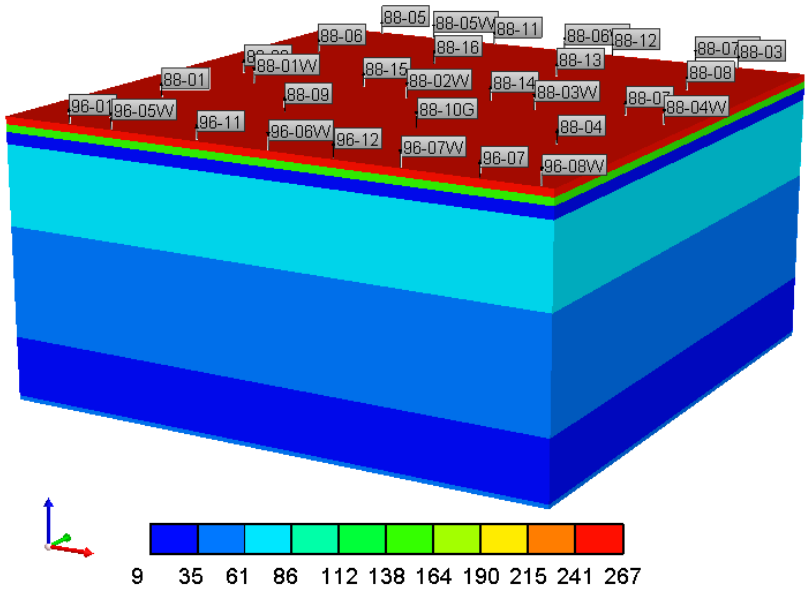

Figure 4.61—X- horizontal permeability model in TR88

4.9.2 Reservoir Model Validation Before CO_2 Flooding

With the reservoir model described above, simulation runs to history match the reservoir's pre-CO_2 flood oil and water production during primary depletion and secondary development. Liquid production rate was used as the primary constraints. Good matching results are reached (**Figure 4.62**). **Figure 4.63** indicates that average oil saturation is 0.37 after 50 years of waterflooding and layers 1, 6,7,8,9 have higher oil saturation than the other layers.

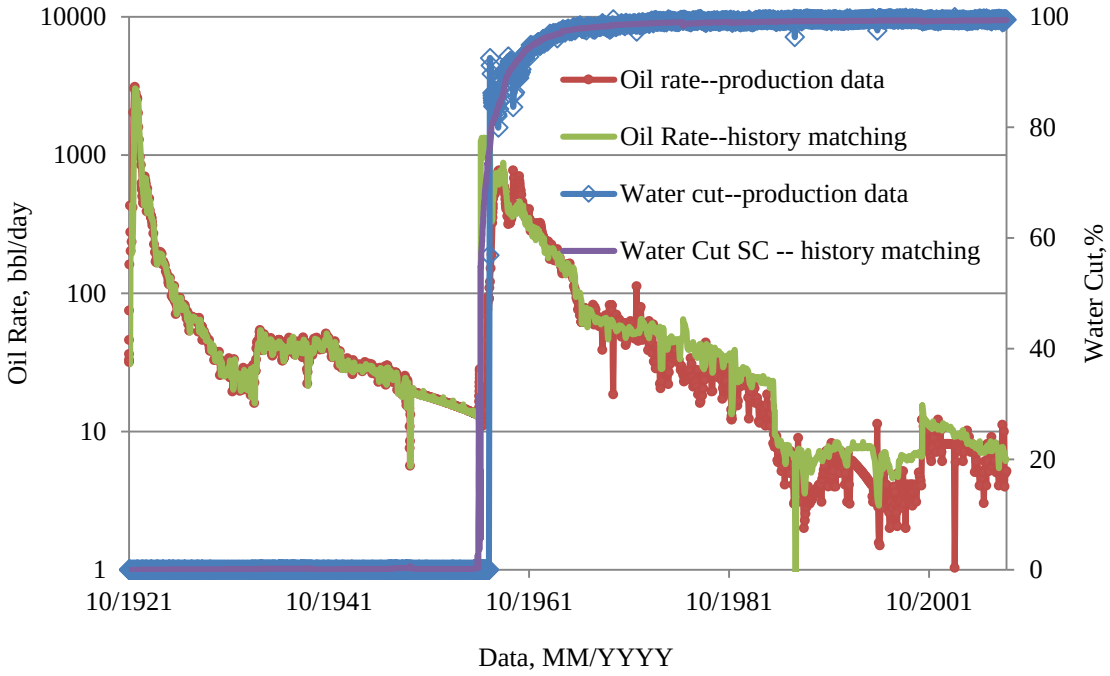

Figure 4.62—History matching result of oil rate and water cut in TR88

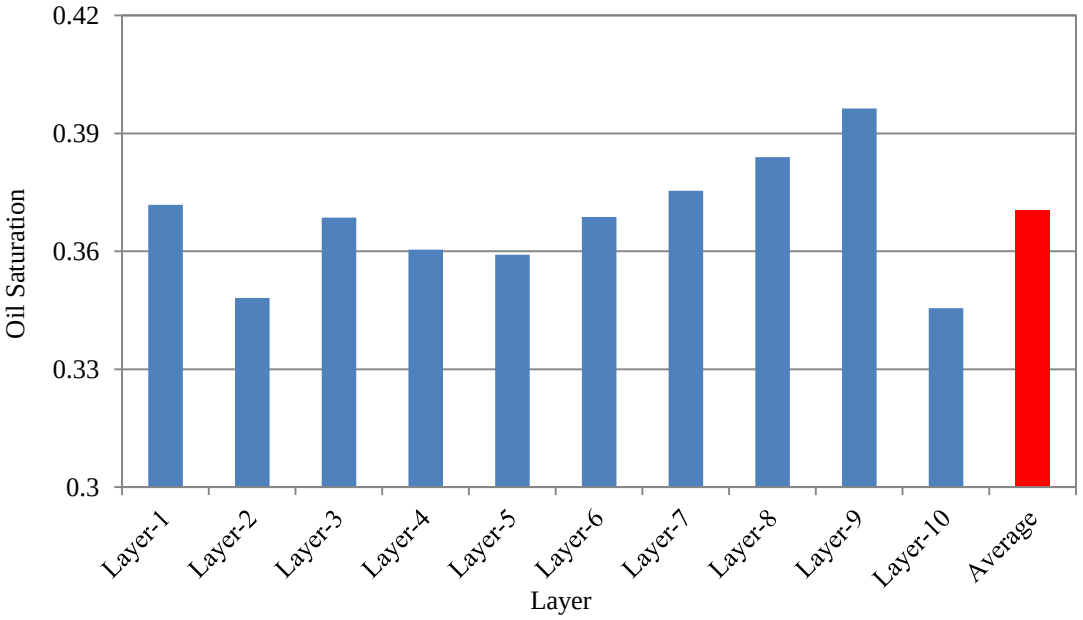

Figure 4.63—Oil saturation after waterflooding in TR88 (04/01/2009)

4.9.3 Sensitivity Analysis—Polymer Concentration

Four simulation cases with different polymer concentrations were performed (**Table 4.15)**. Different polymer concentration yielded different injection fluid viscosity. In this study, bottom-hole pressure at injectors was set to 2,100 psi which is fracturing pressure in this field.

Table 4.15—Chemical concentrations for different cases in TR88

Case Name	Polymer Concentration, lb/stb
PAG-1	0.05
PAG-2	0.10
PAG-3	0.15
PAG-4	0.20

Figure 4.64 indicates that increasing polymer concentration would significantly reduce water injectivity. As polymer concentration increases from 0.05 to 0.15 lb/stb, oil recovery increases from 16.6 to 18.4% (**Figure 4.65**). But concentration higher than 0.15 lb/stb would reduce oil recovery. Considering the recovery and polymer consumption, a polymer concentration of 0.15 lb/stb was used for the TR88 in the PAG process.

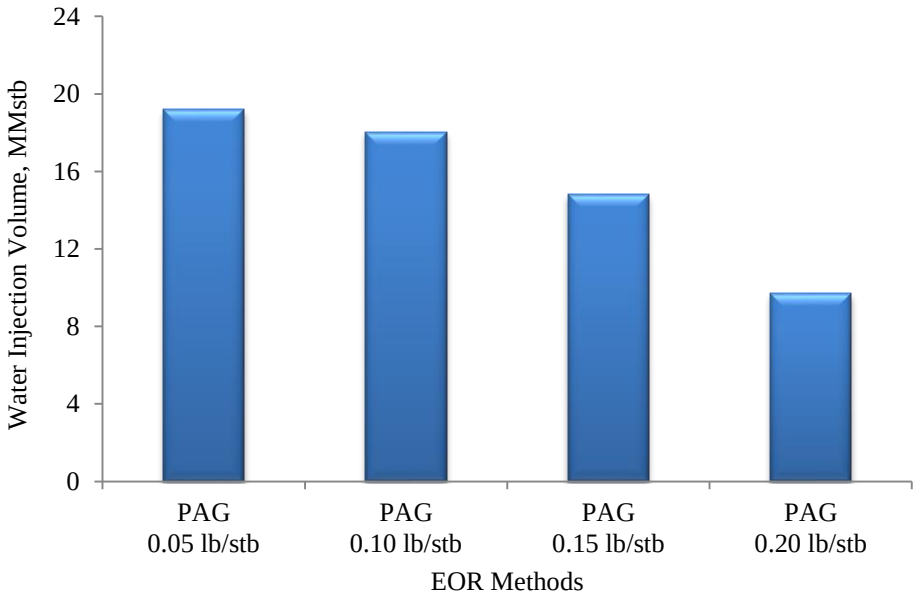

Figure 4.64—Water injectivity decreasing with polymer concentration in TR88

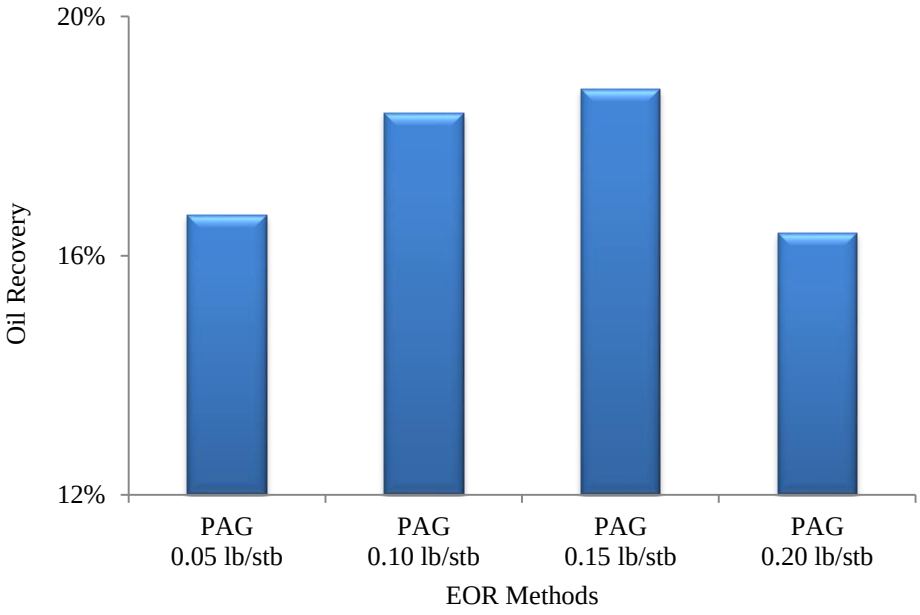

Figure 4.65—Recovery factor of different polymer concentrations in TR88

4.9.4 PAG Versus Polymer Flooding and WAG

Three different schemes were conducted to identify which injection method yielded a better recovery. Pattern-1 (polymer flooding) injected polymer of 0.30 lb/stb with water for twenty years. Pattern-2 (WAG) used WAG injection for twenty years. Pattern-3 (PAG) injected polymer of 0.15 lb/stb with water and alternative with gas for twenty years.

As shown in **Figure 4.66**, polymer flooding could produce 7.2% OOIP after water flooding. Recovery from pattern-2 is 13.7% higher than recovery from water flooding. Recovery after PAG injection is 18.5%, which is 5-11% higher than other injection method. It indicates combining polymer and gas injection is better than other methods mentioned above.

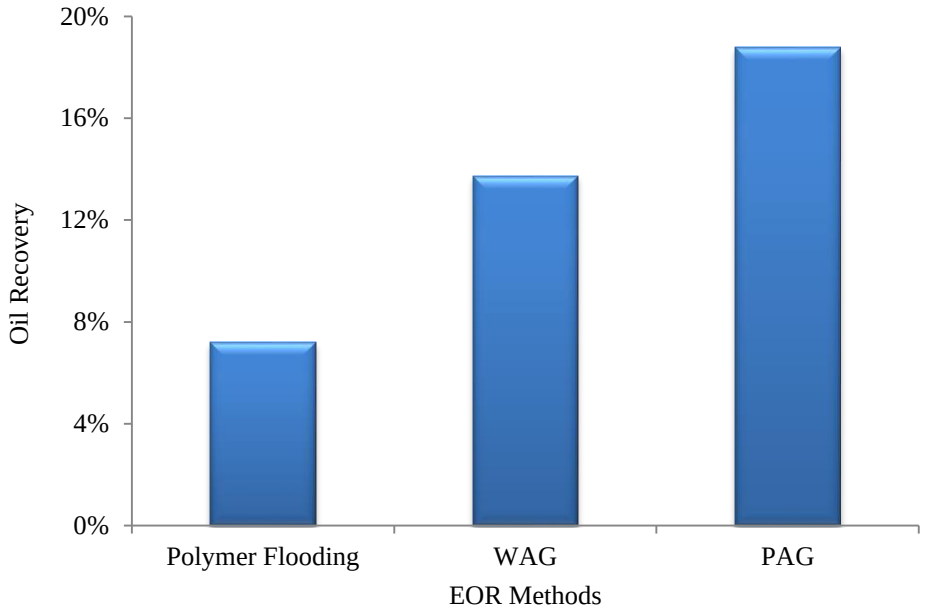

Figure 4.66—Recovery factor of different EOR processes in TR88

4.10 Economic Evaluation of PAG

4.10.1 Compare Oil Revenue and Net Present Value among Different EOR Methods for TR78

Profitability analysis of the project is a very important evaluation after the technical analysis is completed. This analysis is the basis for investment decision of the project. For this EOR project economic analysis and proper decisions have been done based on Net Present Value (NPV). NPV takes into consideration the value of cash earned in the future and converts the money to the present value. The equation below is used to calculate NPV.

$$NPV = \sum_{1}^{T} \frac{C_t}{(1+r)^t} - C_o \qquad \text{Equation 4.2}$$

C_t = net cash inflow during the period

C_o= initial investment

r = discount rate, and

t = number of time periods

In this simulation study of PAG method started from 2013 to 2033. A project is categorized as profitable when NPV is positive. And we are always encouraged to choose higher NPV when we have many alternatives with positive NPV. A high NPV indicates a high profitability from the project.

In our case, only revenue was gotten from selling of crude oil. It was assumed that expenses only included CO_2 cost, CO_2 recycling cost, operation cost, and polymer costs. For the estimation of income, annual total production data were taken from the Eclipse and exported to excel. The following prices (**Table 4.16**) for oil, gas and chemicals were used. **Table 4.17** shows the cases were used to economic evaluation.

Table 4.16—Economic parameters

Table 4.15	
CO_2 price	$2.0 /Mscf
Oil price	$80/bbl
CO_2 recycling cost	$ 0.50/Mscf
Discount factor	15%
Polymer price	$3.0/lb
Operation fee for WAG	$3.0/bbl
Operation fee for polymer	$3.0/bbl
Operation fee for PAG	$5.0/bbl
Up-front capital for WAG	$4,000,000
Up-front capital for Polymer flooding	$4,000,000
Up-front capital for PAG	$6,000,000

Table 4.17—Three EOR methods chosen for economic evaluation

WAG	Water alternating gas for 20 years
Polymer flooding	Injection polymer with a concentration 0.40 lb/stb for 20 years
PAG	Injection polymer (with a concentration 0.20 lb/stb) alternating gas for 20 years

Tables 4.18 to **23** represent the procedure about how to calculate NPV for WAG, polymer flooding and PAG. NPV for each year was calculated by cumulating annual present value. Oil revenue from PAG process is about $\$135\times10^6$, which is about $\$40\text{-}60\times10^6$ higher than WAG and polymer flooding (**Figure 4.67**). **Figure 4.68** indicates that cumulative incremental NPV is $\$15\times10^6$ for WAG process in the end of simulation life which is key element for decision making of investment. Obviously, it is positive in

this case and can make project being accepted. The polymer flooding has similar NPV value as WAG process, while it takes more than 4 years to get the investment back. WAG and PAG take 2-3 years get investment back. The NPV is $\$26\times10^6$ for PAG process in the end of simulation life which is higher than WAG process. As long as the expected net present value is positive, the project should be accepted. But considering many alternatives, the case with polymer alternating gas leads to much profit. And based on the profitability evaluation and from investment point of view injecting polymer alternating gas should be better than injecting water alternating gas for TR78.

Table 4.18—WAG injection and production data and cost in TR78

Year	Total gas injection (MSCF/year)	Total water injection (STB/year)	Total oil production (STB/year)	Total gas production (MSCF/year)	CO_2 purchase $	CO_2 recycle $	Operation fee $
0	0	0	0	0	0	0	0
1	1094400	590201	12149	12242	2164317	6121	36448
2	1094400	590599	87902	449762	1289276	224881	263706
3	1094400	595890	91289	861050	466700	430525	273866
4	1094400	584910	73231	911785	365230	455893	219693
5	1094400	590400	63561	973778	241245	486889	190683
6	1094400	604800	57149	1018823	151154	509412	171448
7	1094400	590400	51611	1027407	133987	513703	154833
8	1094400	576000	47252	1026218	136365	513109	141757
9	1094400	604800	45539	1060204	68392	530102	136618
10	1094400	604800	42932	1066120	56560	533060	128795
11	1094400	576000	39777	1045616	97568	522808	119330
12	1094400	604800	38762	1075165	38470	537583	116285
13	1094400	576000	36155	1052768	83264	526384	108466
14	1094400	604800	35459	1081551	25698	540776	106378
15	1094400	576000	33224	1058139	72522	529070	99673
16	1094400	604800	32710	1086374	16052	543187	98131
17	1094400	576000	30786	1062198	64404	531099	92359
18	1094400	604800	30435	1090056	8688	545028	91306
19	1120362	576000	29105	1078422	83880	539211	87315
20	1068438	576000	27595	1054092	28692	527046	82786

Table 4.19—NPV for water alternating gas in TR78 (oil price: $80/bbl)

Year	Oil Revenue $ ×10^3	Cash flow $ ×10^3	Discount factor	NPV $ ×10^3
0	0	-4000	1	-4000
1	972	-1235	0.8696	-5074
2	7032	5254	0.7561	-1101
3	7303	6132	0.6575	2931
4	5858	4818	0.5718	5686
5	5085	4166	0.4972	7757
6	4572	3740	0.4323	9374
7	4129	3326	0.3759	10624
8	3780	2989	0.3269	11601
9	3643	2908	0.2843	12428
10	3435	2716	0.2472	13099
11	3182	2442	0.2149	13624
12	3101	2409	0.1869	14075
13	2892	2174	0.1625	14428
14	2837	2164	0.1413	14734
15	2658	1957	0.1229	14974
16	2617	1959	0.1069	15184
17	2463	1775	0.0929	15349
18	2435	1790	0.0808	15493
19	2328	1618	0.0703	15607
20	2208	1569	0.0611	15703

Table 4.20—Polymer injection and production data and cost in TR78

Year	Total water injection (STB/year)	Total oil production (STB/year)	Total polymer injection (lb/year)	Polymer cost $	Operation fee $
0	0	0	0	0	0
1	602389	14101	240956	722867	42302
2	917051	20533	366821	1100462	61599
3	1035698	31295	414279	1242838	93885
4	1085080	62066	434032	1302096	186198
5	1086976	89002	434790	1304371	267005
6	1042130	98290	416852	1250556	294869
7	1001068	95934	400427	1201282	287803
8	967352	89561	386941	1160822	268684
9	939536	82545	375814	1127443	247636
10	915360	75652	366144	1098432	226955
11	894645	69866	357858	1073574	209599
12	877299	65168	350920	1052759	195504
13	861644	60896	344658	1033973	182688
14	847029	56805	338812	1016436	170416
15	834606	52924	333843	1001528	158771
16	824052	49215	329621	988863	147646
17	814977	45689	325991	977972	137067
18	807152	42405	322861	968582	127215
19	800328	39420	320132	960395	118259
20	774720	35847	309888	929664	107541

Table 4.21—NPV for polymer flooding in TR78 (oil price: $80/bbl)

Year	Oil Revenue $ ×10^3	Cash flow $ ×10^3	Discount factor	NPV $ ×10^3
0	0	-4000	1	-4000
1	1128	363	0.8696	-3684
2	1643	481	0.7561	-3321
3	2504	1167	0.6575	-2554
4	4965	3477	0.5718	-566
5	7120	5549	0.4972	2193
6	7863	6318	0.4323	4924
7	7675	6186	0.3759	7250
8	7165	5735	0.3269	9125
9	6604	5229	0.2843	10611
10	6052	4727	0.2472	11779
11	5589	4306	0.2149	12705
12	5213	3965	0.1869	13446
13	4872	3655	0.1625	14040
14	4544	3358	0.1413	14514
15	4234	3074	0.1229	14892
16	3937	2801	0.1069	15191
17	3655	2540	0.0929	15428
18	3392	2297	0.0808	15613
19	3154	2075	0.0703	15759
20	2868	1831	0.0611	15871

Table 4.22—PAG injection and production data and cost in TR78

Year	Total gas injection (MSCF/year)	Total polymer injection (lb/year)	Total oil production (STB/year)	Total gas production (MSCF/year)	CO_2 purchase $	CO_2 recycle $
0	0	0	0	0	0	0
1	1092540	13711	20856	43760	2143367	10428
2	1093834	86011	590681	110942	1006307	295340
3	1094267	95134	812072	118593	564390	406036
4	1094117	102733	873710	118215	440814	436855
5	1094057	107432	928144	118160	331825	464072
6	1094129	109434	957366	118063	273527	478683
7	1094066	109117	973612	116797	240909	486806
8	1093968	107293	996501	117239	194934	498250
9	1093965	103013	1008738	115665	170455	504369
10	1093895	99590	1030756	117279	126279	515378
11	1093828	92863	1015206	111156	157245	507603
12	1093787	90805	1048674	116106	90226	524337
13	1093700	84461	1031041	110204	125318	515521
14	1093683	82149	1062664	115226	62038	531332
15	1093616	76217	1042745	109483	101742	521373
16	1093589	74003	1072729	114546	41720	536365
17	1093558	68644	1051285	108925	84546	525643
18	1093514	66672	1080179	114023	26670	540090
19	1121500	62662	1071270	108491	100460	535635
20	1065528	58203	1046958	108309	37140	523479

Table 4.23—NPV for polymer alternating gas in TR78 (oil price: $80/bbl)

Year	Polymer cost $	Operation fee $	Oil Revenue $ ×10^3	Cash flow $ ×10^3	Discount factor	NPV $ ×10^3
0	0	0	0	-6000	1	-6000
1	131279	68555	1097	-1257	0.8696	-7093
2	332825	430056	6881	4816	0.7561	-3451
3	355780	475670	7611	5809	0.6575	368
4	354644	513663	8219	6473	0.5718	4069
5	354479	537161	8595	6907	0.4972	7503
6	354189	547168	8755	7101	0.4323	10573
7	350392	545583	8729	7106	0.3759	13245
8	351716	536464	8583	7002	0.3269	15533
9	346995	515066	8241	6704	0.2843	17439
10	351836	497948	7967	6476	0.2472	19040
11	333468	464316	7429	5966	0.2149	20322
12	348319	454025	7264	5847	0.1869	21415
13	330612	422303	6757	5363	0.1625	22287
14	345677	410743	6572	5222	0.1413	23025
15	328450	381087	6097	4765	0.1229	23611
16	343637	370016	5920	4629	0.1069	24105
17	326775	343222	5492	4211	0.0929	24497
18	342068	333359	5334	4092	0.0808	24827
19	325472	313309	5013	3738	0.0703	25090
20	324928	291013	4656	3480	0.0611	25302

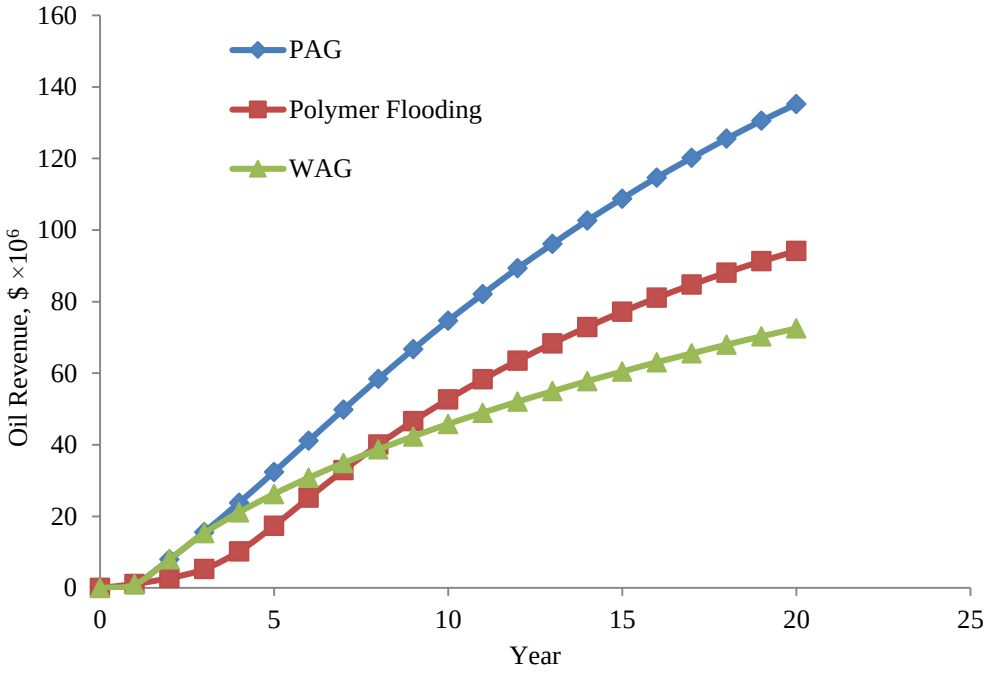

Figure 4.67—Oil revenue from different EOR methods in TR78

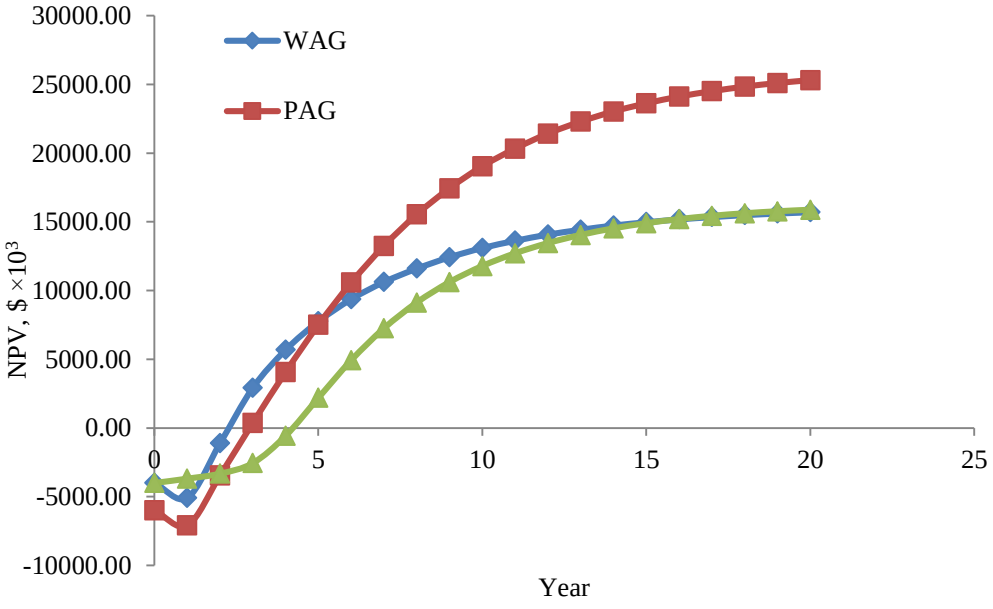

Figure 4.68—Net Present Value from different EOR methods in TR78

4.10.2 Sensitivity Analysis of Economic Evaluation for TR78

Sensitivity analysis was done to examine the effect of uncertainties in the predictions and assumptions on the profitability of the project. In our cases, six main parameters are uncertain and would be changed. These are oil price, CO_2 price, CO_2 recycling cost, operation cost, polymer price and discount rate. Each parameter was individually adjusted from the original base-case input data set. The analysis shows that how much the cumulative NPV is sensitive by changing each of these six variables. For this purpose, radar diagram was used. To do the sensitivity analysis, each single parameter (oil price, CO_2 price, CO_2 recycling cost, operation cost, and polymer price and discount rate.) was varied from low to high values while keeping all the other base case parameters constant. **Table 4.24** represents the range of assumed values for each parameter.

Table 4.24—Values for variables at low, base and high case in TR78

Variables	Low case	Base case	High case
Oil price, $/bbl	60	80	100
CO_2 price, $/mscf	1	2	3
CO_2 recycling price, $/mscf	0.25	0.5	0.75
Operation cost, $/bbl	3	5	7
Polymer price, $/lb	1.2	1.8	2.4
Discount rate	0.1	0.15	0.2

The graphs in figure were plotted based on change values (%) for each variable shown in **Fig 4.69**. (+25) % and (-25) % change in oil price causes (+59.55) % and (+59.55) % change respectively in NPV (**Table 4.25**). It means that change of oil price has a big effect on NPV value. Compared to polymer price effect, percentage change of discount rate has great effect on NPV where change of (-33.33) % and (+33.33) % in discount rate corresponds nearly 76.63) % and (+46.20) % change in NPV, respectively.

Polymer prices have much lower effect on NPV compared to oil price. Polymer price has the highest impact of (+5/-5) % on NPV when it is deviated by (-33/+33) % from base case surfactant price.

In conclusion, oil price has the highest impact on NPV in terms of percentage change. On the contrary, NPV is least sensitive to the polymer price.

Fig 4.70 shows that PAG still would obtain positive NPV at low oil price $40/bbl. And NPV may reach $\$29\times10^6$ when oil price is $100/bbl.

Table 4.25—Different variable changes and their impact on NPV in TR78

Variables	Low case	Base case	High case
Oil price change	-25.00%	0	25.00%
NPV change	-59.55%	0	59.55%
CO_2 price change	-50.00%	0	50.00%
NPV change	11.88%	0	-11.88%
CO_2 recycling price change	-50.00%	0	50.00%
NPV change	11.91%	0	-11.91%
Operation cost change	-40.00%	0	40.00%
NPV change	5.96%	0	-5.96%
Polymer price change	-33.00%	0	33.00%
NPV change	5.52%	0	-5.52%
Discount rate change	-33.00%	0	33.00%
NPV change	76.63%	0	-46.20%

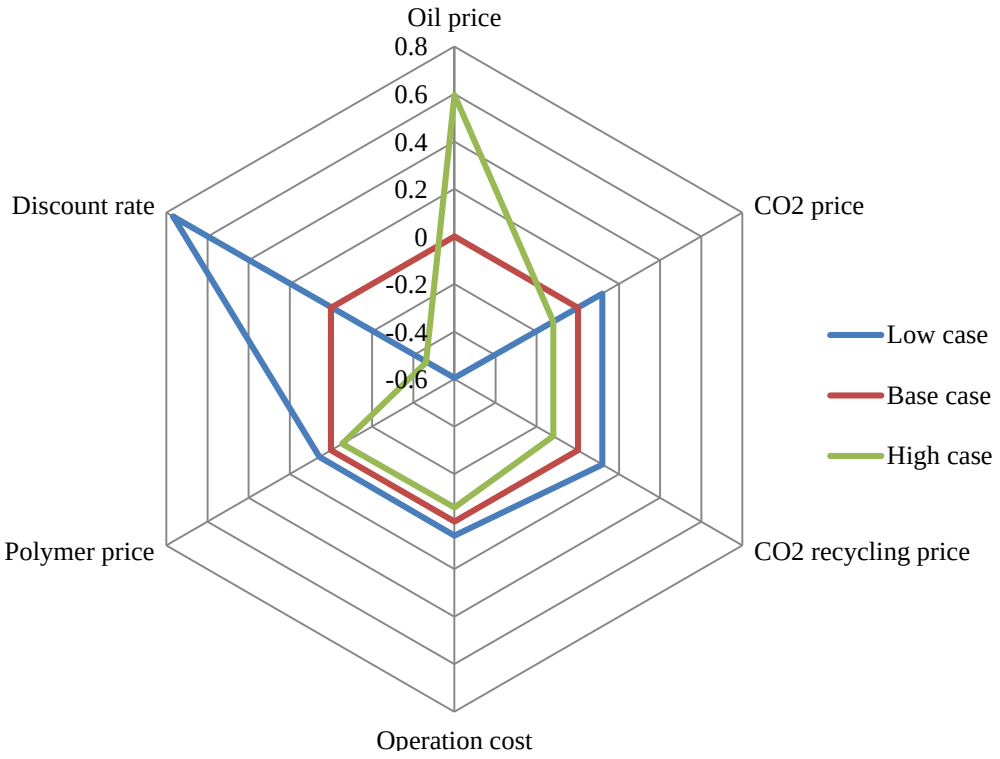

Figure 4.69—Radar diagram for polymer alternating gas flooding in TR78

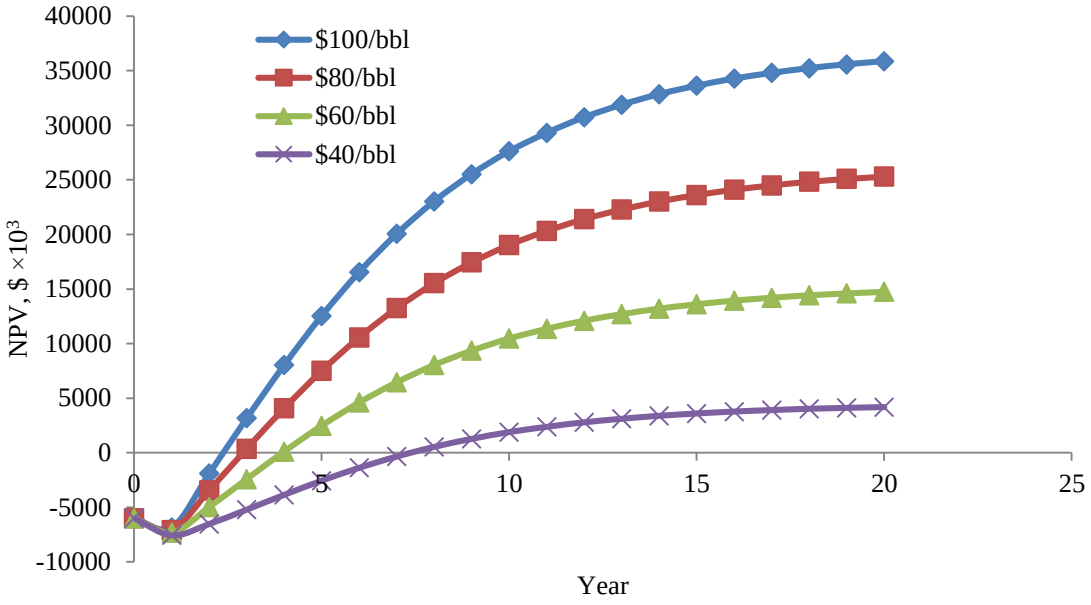

Figure 4.70—NPV VS. oil price for polymer alternating gas flooding in TR78

4.10.3 Summarize Economic Evaluation

We also studied oil revenues and net present values for other four sections. **Table 4.26** and **Figures 4.71** to **4.82** shows the oil revenue and NPV for each EOR method at oil price $80/bbl, and the relationship between NPV and oil price for polymer alternating gas flooding. From the table and figures, we can summarize that WAG process could get positive NPV at oil price $80/bbl in these five sections. And PAG could reach higher NPV in all these five sections. It means PAG could be economically successful in the North Burbank Unit. Compare to WAG, PAG would take longer to get investment back, due to the higher front investment and polymer cost. PAG could increase NPV from $\$15.70\times10^6$, $\$16.96\times10^6$, $\$13.69\times10^6$ to $\$25.30\times10^6$, $\$24.34\times10^6$, $\$20.77\times10^6$ in TR78, TR59 and TR48, respectively. While the improvement in TR92 and TR88 is less significant. It is necessary to mention that polymer flooding performance is less than PAG all sections except TR48, which has relative high permeability and high heterogeneity.

Table 4.26—Summarize of economic evaluation

		TR78	TR59	TR48	TR92	TR88
Oil Revenue	WAG, $ 10^6	72.53	73.50	57.04	51.10	87.40
	Polymer Flooding,$ 10^6	94.17	68.78	140.67	39.78	46.52
	PAG,$ 10^6	135.21	121.28	127.55	70.36	120.27
NPV	WAG, $ 10^6	15.70	16.96	13.69	7.91	15.92
	Polymer Flooding,$ 10^6	15.87	13.83	27.50	4.32	2.69
	PAG,$ 10^6	25.30	24.34	20.77	8.98	18.79
Oil Cost	WAG, $/bbl	16.69	16.13	16.55	17.60	15.89
	Polymer Flooding, $/bbl	18.27	15.14	22.32	15.50	36.87
	PAG, $/bbl	13.20	15.35	15.82	17.66	15.80

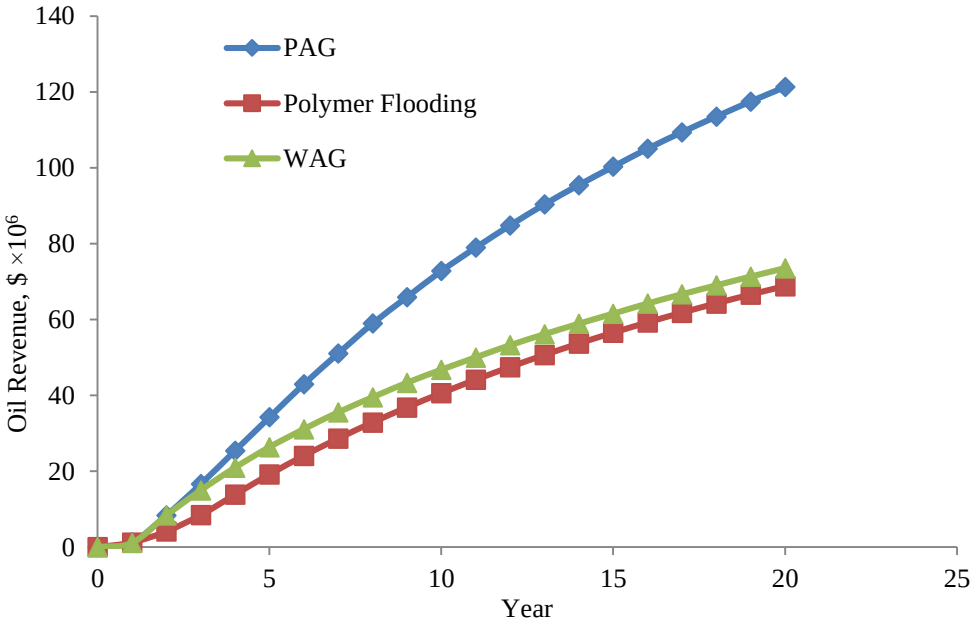

Figure 4.71—Oil revenue from different EOR methods (TR59)

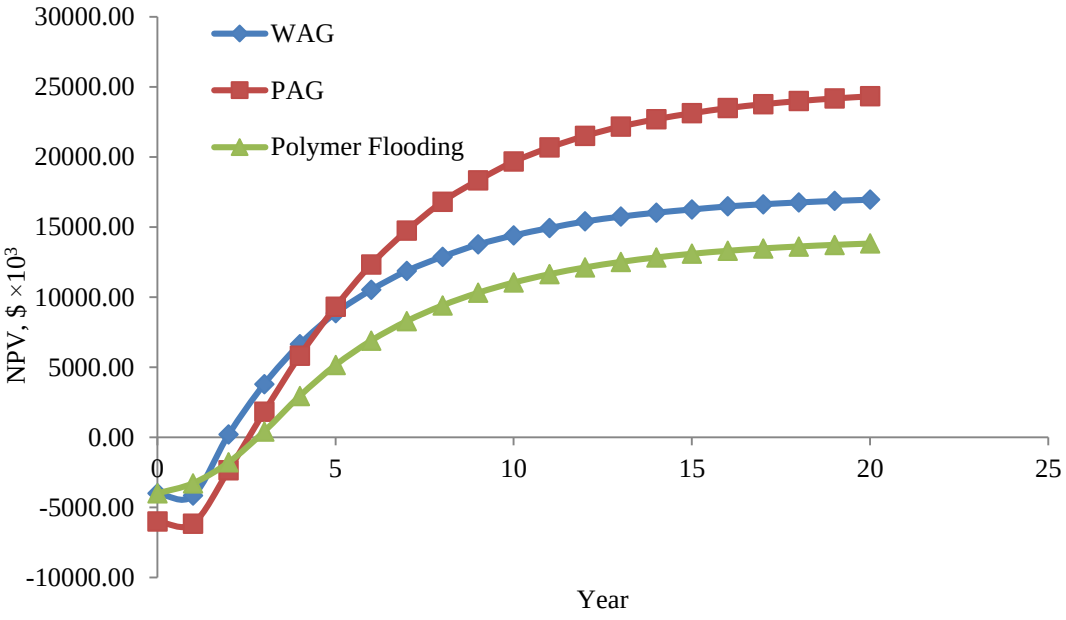

Figure 4.72—Net Present Value from different EOR methods (TR59)

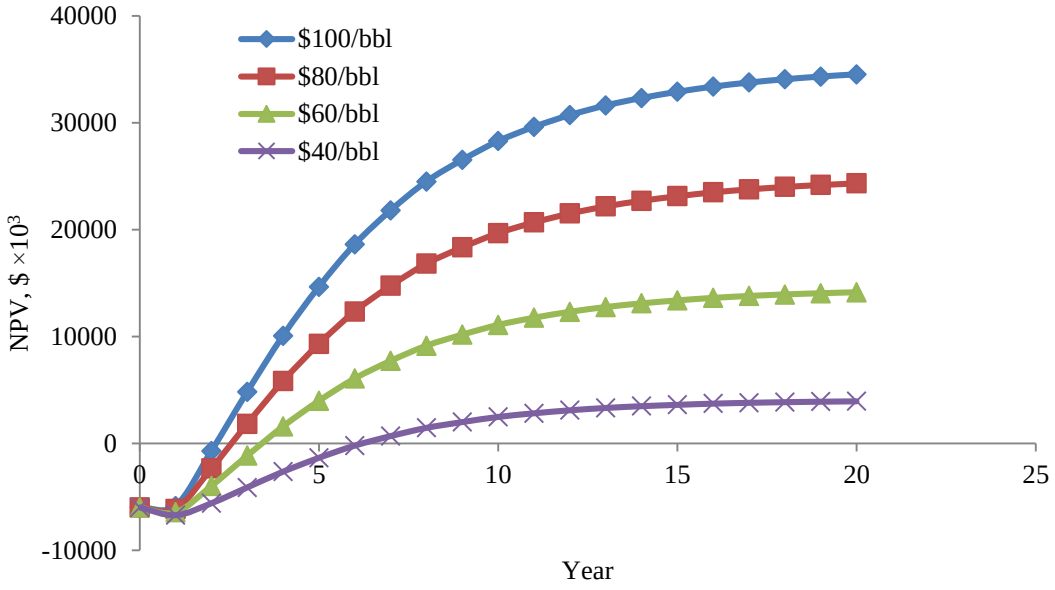

Figure 4.73—NPV VS. oil price for polymer alternating gas flooding (TR59)

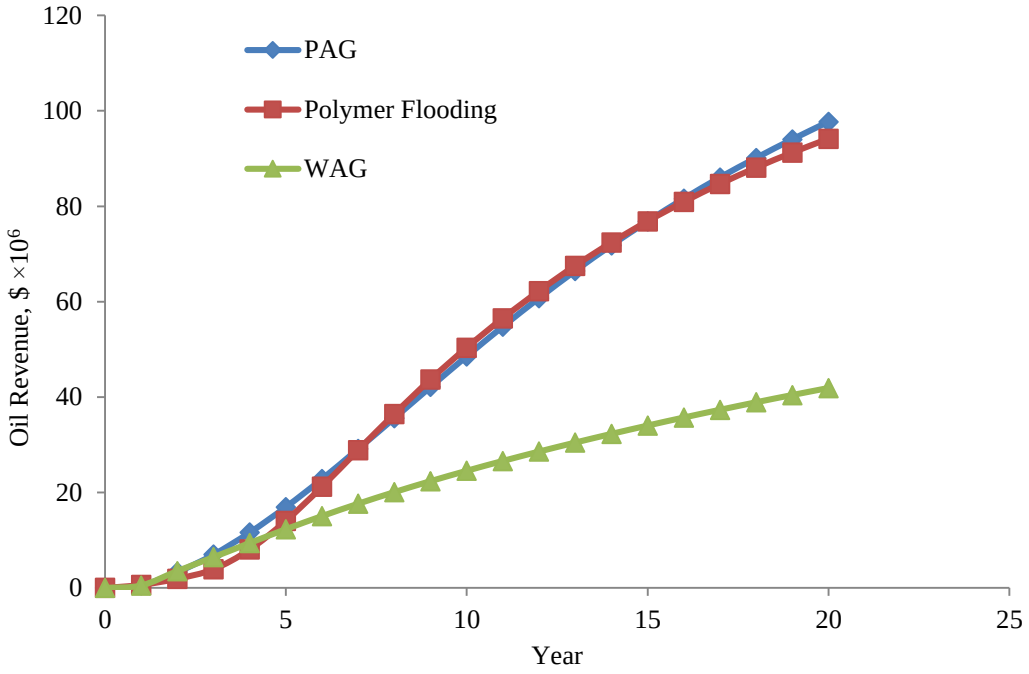

Figure 4.74—Oil revenue from different EOR methods (TR48)

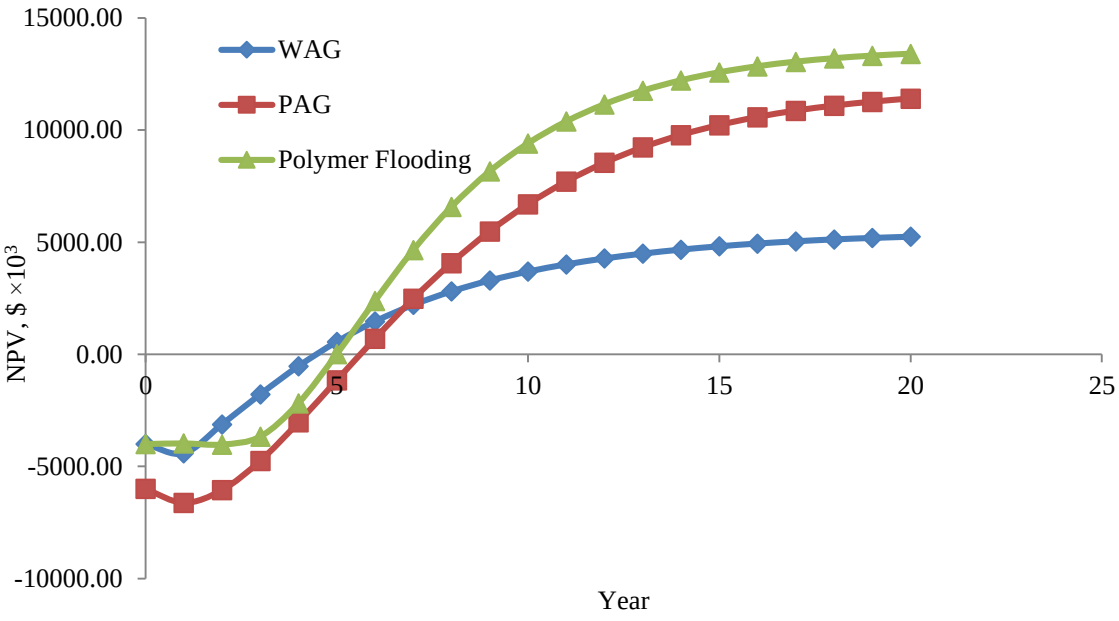

Figure 4.75—Net Present Value from different EOR methods (TR48)

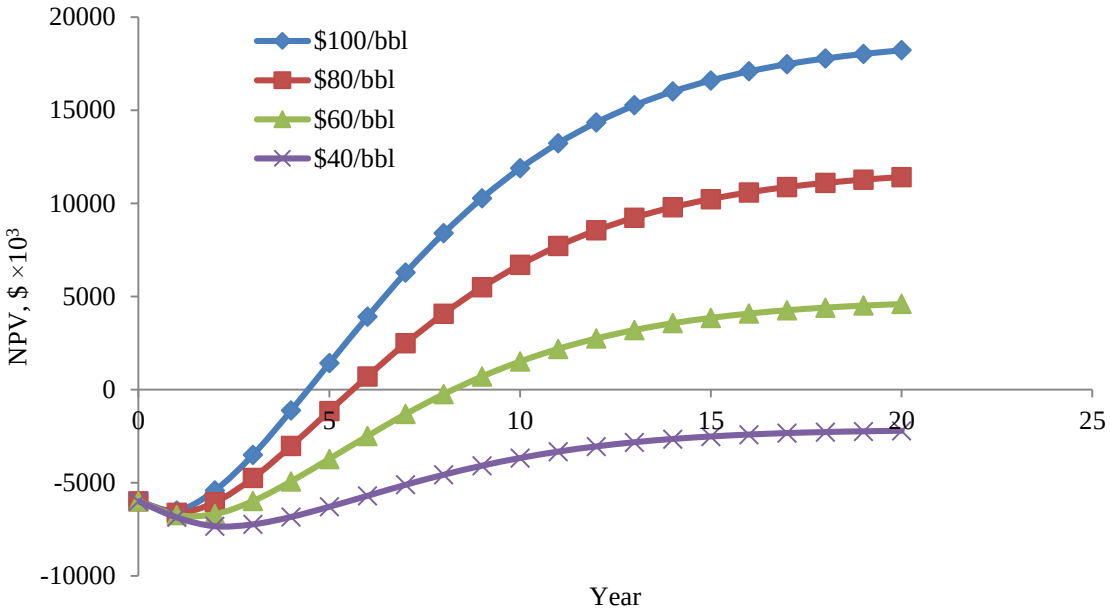

Figure 4.76—NPV VS. oil price for polymer alternating gas flooding (TR48)

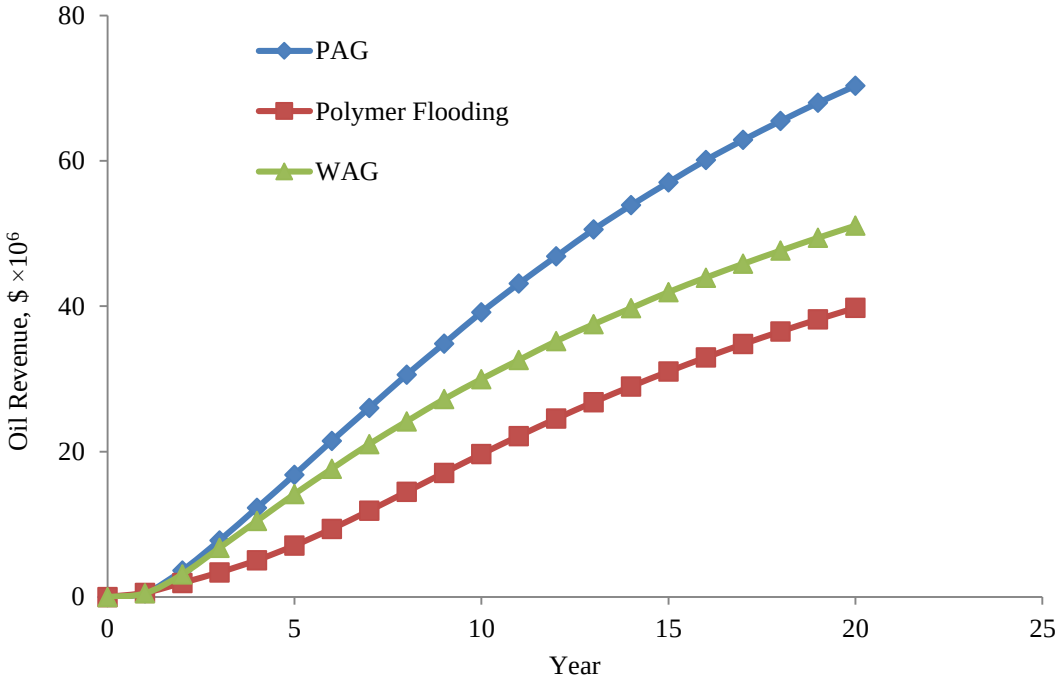

Figure 4.77—Oil revenue from different EOR methods (TR92)

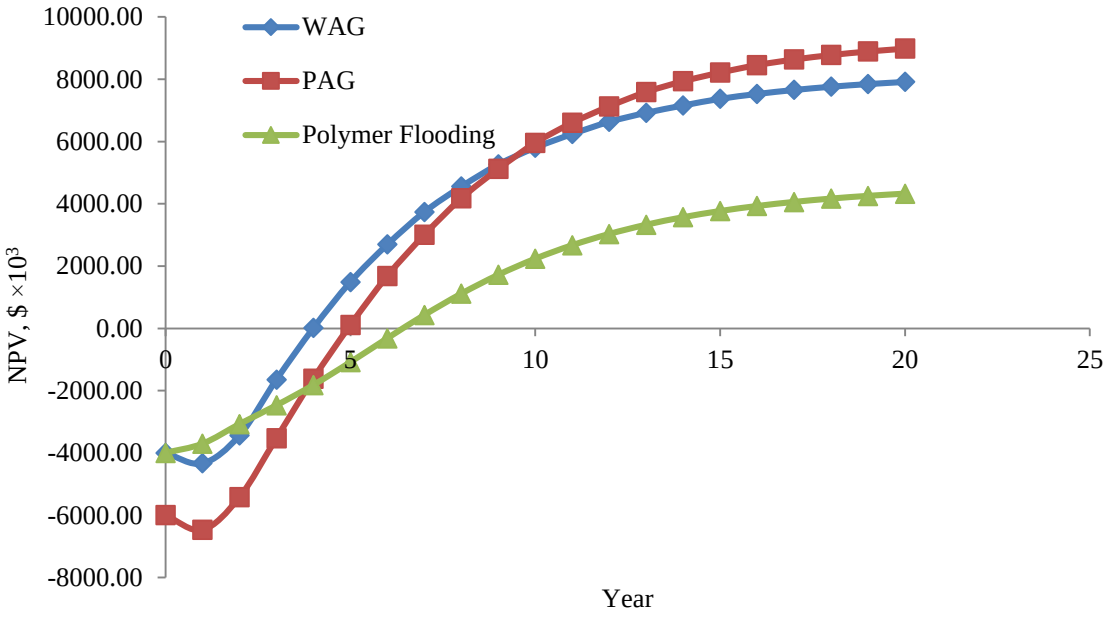

Figure 4.78—Net Present Value from different EOR methods (TR92)

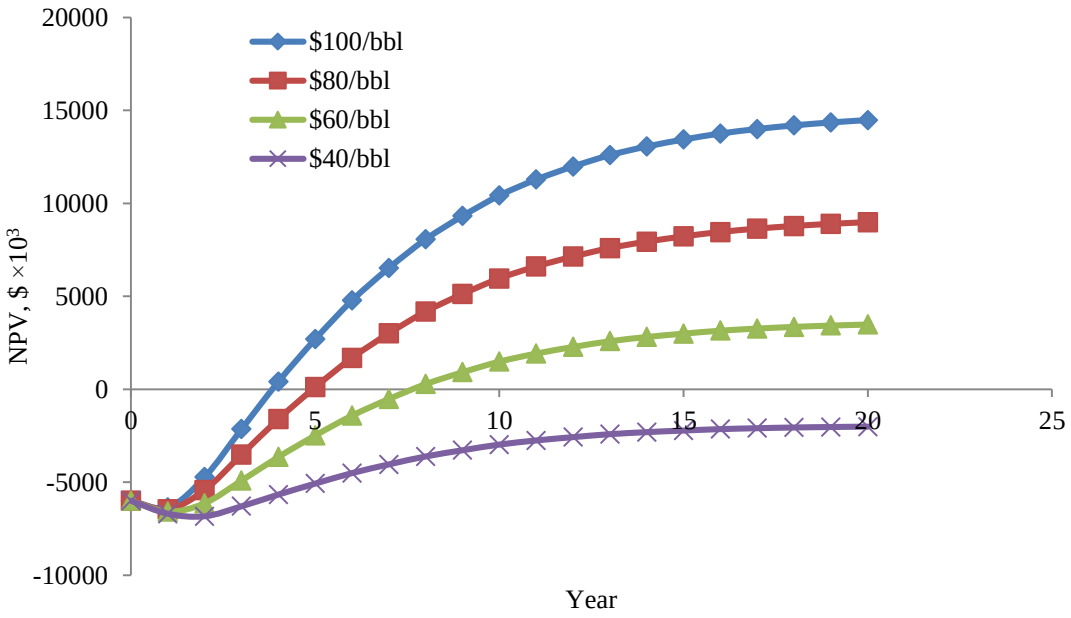

Figure 4.79—NPV VS. oil price for polymer alternating gas flooding (TR92)

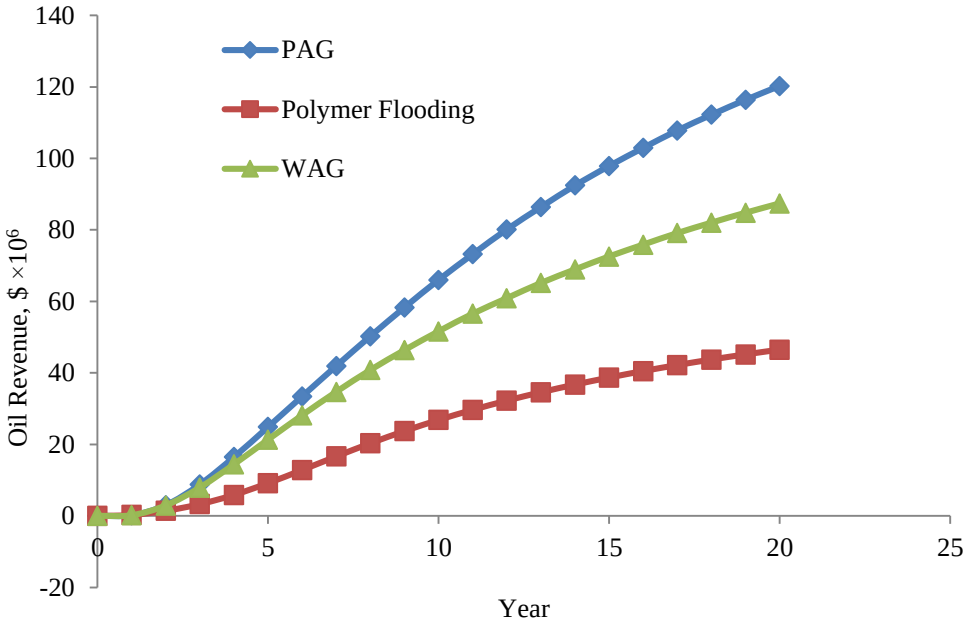

Figure 4.80—Oil revenue from different EOR methods (TR88)

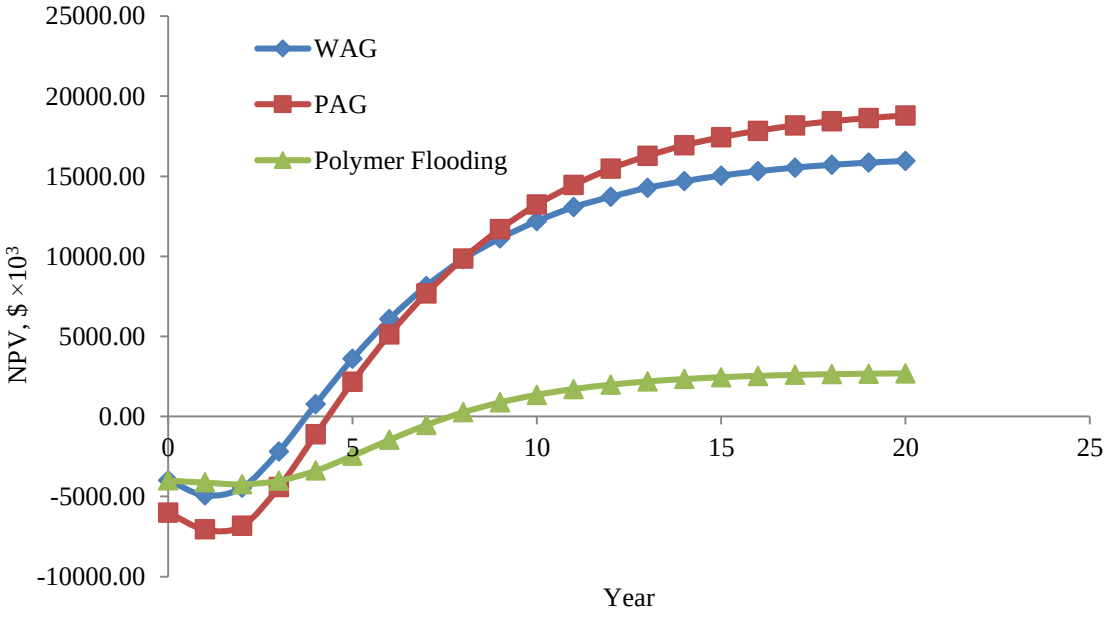

Figure 4.81—Net Present Value from different EOR methods (TR88)

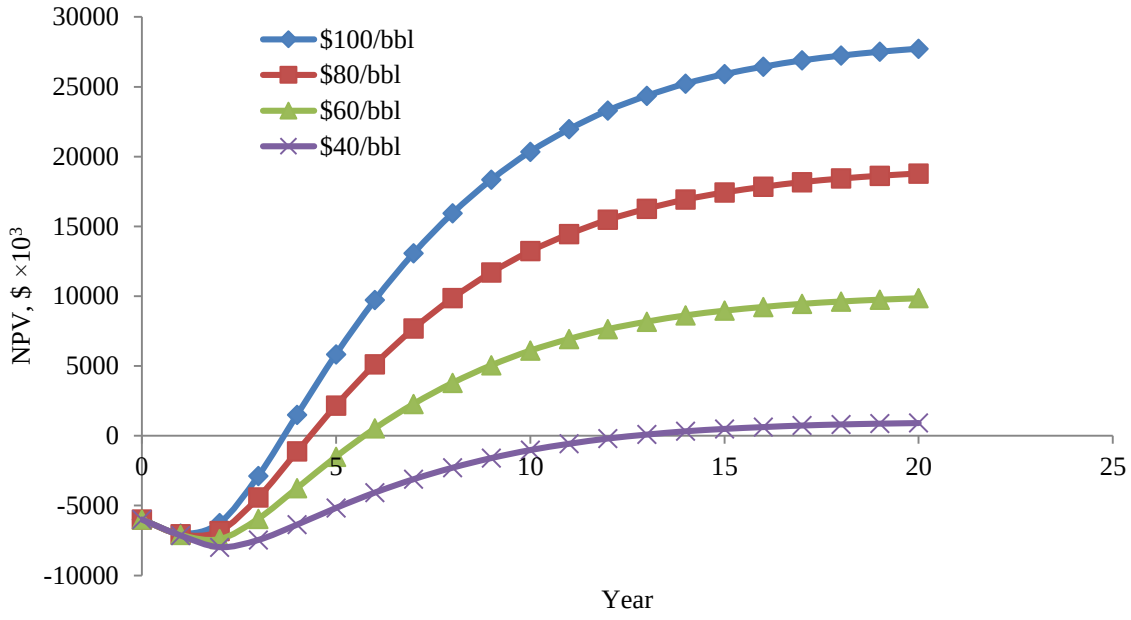

Figure 4.82—NPV VS. oil price for polymer alternating gas flooding (TR88)

4.11 Conclusions and Recommendations of PAG Simulation in the North Burbank Unit

A new EOR method named PAG was proposed to improve the efficiency of the conventional WAG process in the North Burbank Unit. The following conclusions and recommendations were made for this study:

(1) After optimizing polymer injection concentration and slug patterns, the following development strategy was suggested for TR78: inject polymer with a concentration of 0.20 lb/stb for 15 years in the PAG process and then chased with the WAG process for 5 years. Oil recovery increased by PAG in TR78 is forecasted to be 18.7%, which is 8.0% higher than WAG. The NPV for PAG process in TR78 is higher than WAG process based on assumptions.

(2) The simulation results show that recovery from WAG and PAG process after water flooding in five sections is about 9-12% and 14-18%, respectively. Compare to WAG, PAG could recovery other 4-7% oil.

(3) Based on assumptions, PAG could obtain higher NPV than WAG in all these five sections, PAG would take longer to get investment back, due to the higher front investment and polymer cost when compare with WAG, and NPV value is positive when oil price higher than $40/bbl, which indicates that PAG would be both technically and economically feasible in the North Burbank unit at current oil price (higher than $80/bbl).

(4) Compare with WAG, PAG could significantly increase recovery and NPV in TR78, TR59 and TR48, which have relative higher heterogeneous and higher permeability and the improvement in TR92 and TR88 is less significant due to the reservoirs are relative more homogeneity and lower permeability.

(5) Lab study on core flooding is required to analyze the feasibility of PAG in the North Burbank Unit.

(6) As mentioned in section 3, polymer adsorption has a significant impact on the polymer consumption and economic feasibility for polymer flooding and PAG. Measure polymer adsorption is required for PAG study.

(7) In this PAG simulation study, how gas relative permeability affect the recovery was not studied. Further research about it should be carried out.

5. USING CO_2 VISCOSIFIER TO IMPROVE CO_2 FLOODING PERFORMANCE

In this section, we carried out simulation research to evaluate the benefits of using viscosifier chemical in CO_2 EOR production. Eclipse E100, which could model pseudo-miscible process, was used for this study. Oil recovery and rate performances on different synthetic models which considered permeability heterogeneity were analyzed. The Upper Ness formation in lower part of SPE 10 model was used to study the CO_2 viscosifier performance in a reservoir with channels. At last, CO_2 viscosifier was used to improve gas mobility in TR78 in the North Burbank Unit.

5.1 CO_2 Viscosifier Simulation Based on Synthetic Reservoir

To illustrate the possible CO_2 viscosifier effects, the same reservoir and fluid model in the section 3.2 was used. We kept the same grid system as section 3.2 while reservoir average permeability and VDP value were changed.

CO_2 viscosity curves. To illustrate the possible CO_2 viscosifier effects, a series of curves, as shown in **Figure 5.1**, was used to represent the new viscosity-pressure relationship. We set the maximum viscosity increase as twenty-fold according to literature and then put in three other less significant viscosities between the neat CO_2 case and the twenty-fold viscosity. 2-, 5-, and 10- fold of CO_2 viscosity were used in this study according to literatures.

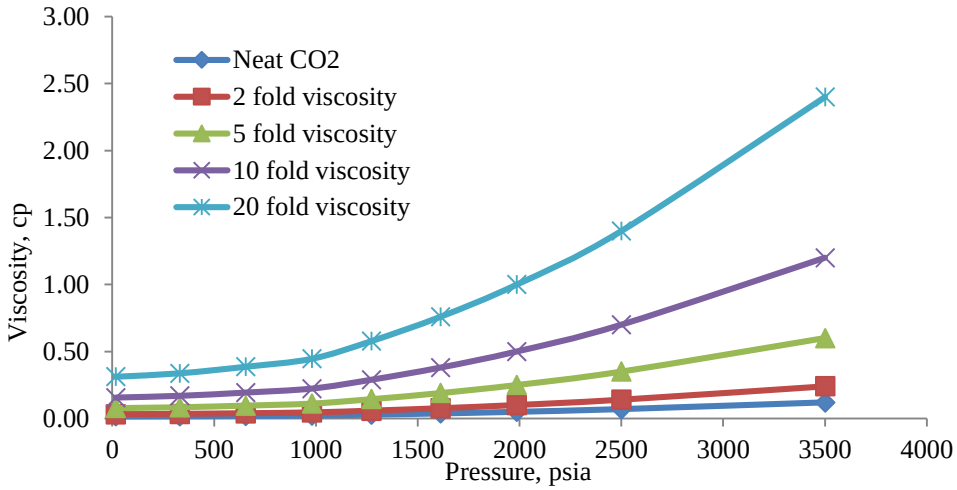

Figure 5.1—Different viscosity curves changing with pressure (edited from Cai 2010)

5.1.1 Reservoir Simulation of CO_2 viscosifier Based on Reservoir with permeability 500 md and VDP 0.53

The reservoir performance during CO_2 viscosifier flooding was compared with water flooding and neat CO_2 injection. Significant difference can be observed between neat CO_2 and 10-fold viscosified CO_2 in terms of oil production. In **Figure 5.2** the peak oil rate for neat CO_2 is 48 bbl/day and the peak oil rate for 10-fold viscosified CO_2 is 84 bbl/day. The more gas viscosity increases, the higher the peak rate obtains (Figure 5.2).

In **Figure 5.3**, neat CO_2 continue injection could increase recovery about 8% after water flooding. When increasing CO_2 viscosity about 10-fold, CO_2 flooding would increase recovery about 26% after water flooding, which is 17% higher than neat CO_2 injection. Figure 5.3 also points out that oil recovery from CO_2 viscosifier increases with CO_2 viscosity increasing.

The performance of CO_2 viscosifier during WAG was also studied. As shown in **Figure 5.4,** neat WAG would increase recovery about 8% after water flooding. When increasing CO_2 viscosity about 10-fold, WAG flooding could increase recovery about 20% after water flooding, which is 12% higher than neat CO_2 injection. Figure 5.4 also indicates that oil recovery from CO_2 viscosifier increases with CO_2 viscosity's increasing. We forecast oil production rates for the four different CO_2 viscosities. As shown in **Figure 5.5**, the more gas viscosity increases, the higher the peak rate reaches.

The simulation shows that continue gas injection obtains similar recovery result with WAG in this reservoir condition. It also illustrates that the improvement of recovery is more significant for CGI than for WAG when increase CO_2 viscosity.

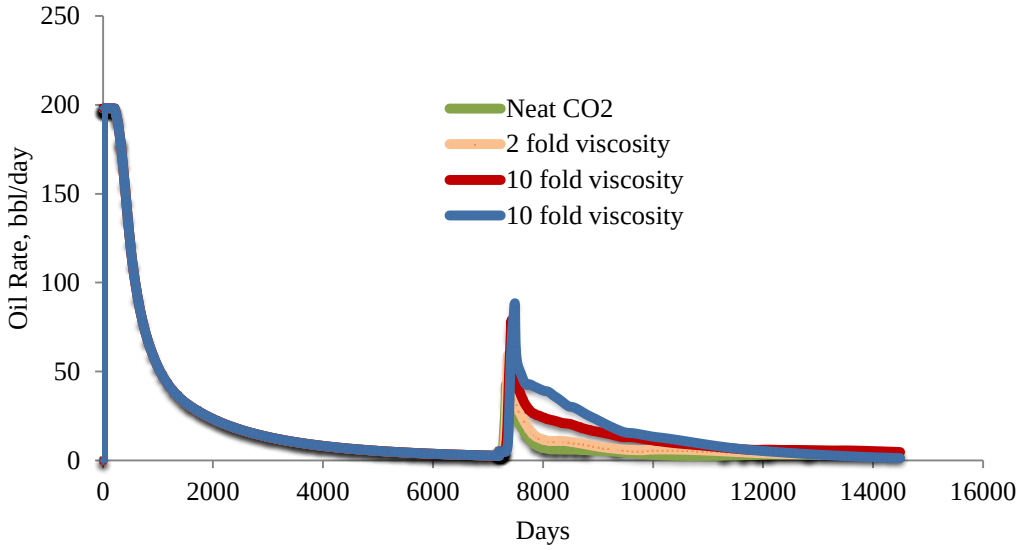

Figure 5.2—Production rate performance for different CO_2 viscosity in CGI process

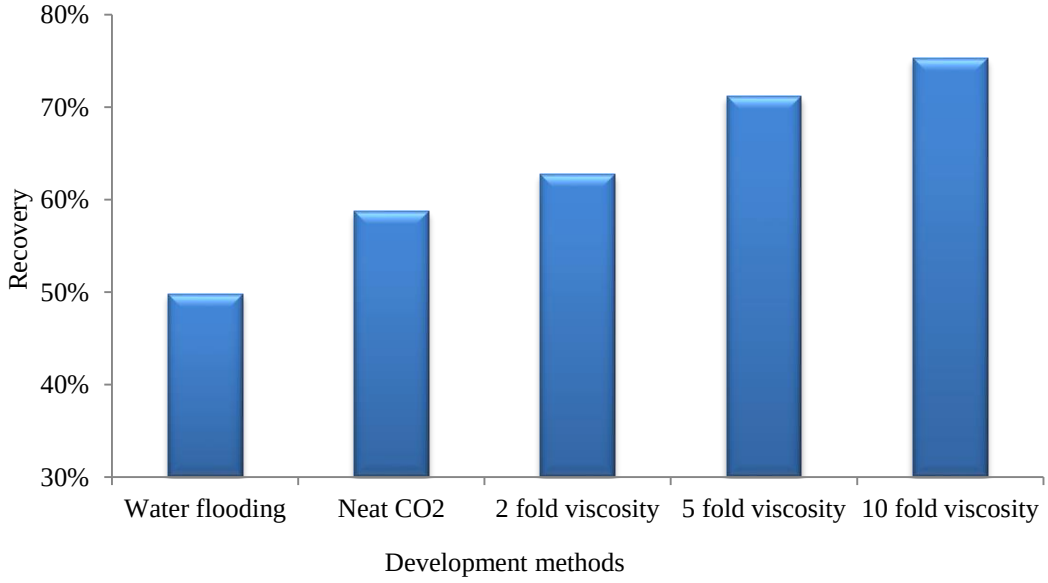

Figure 5.3—Oil recovery from different CO_2 viscosity in CGI process

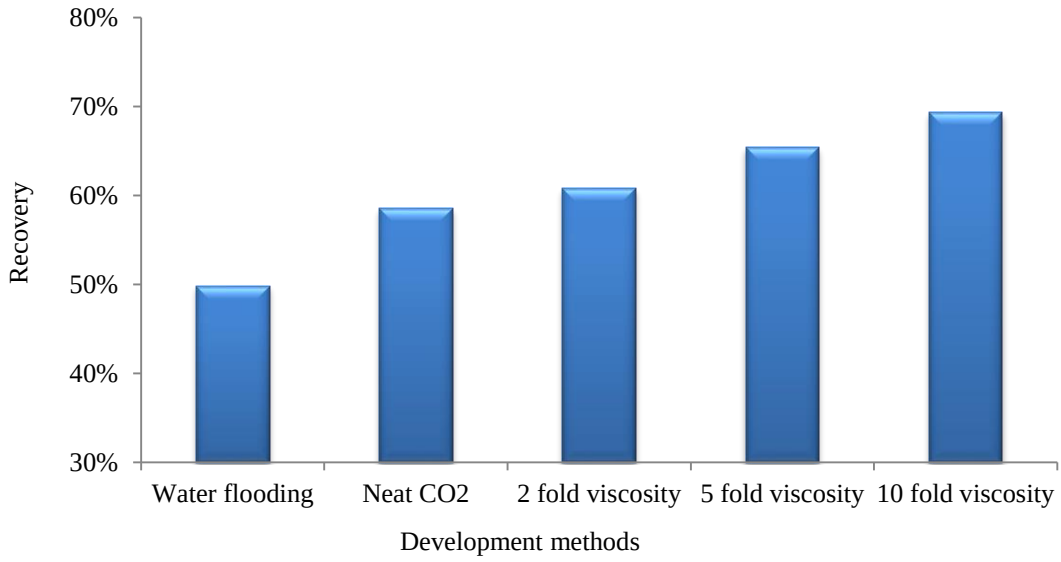

Figure 5.4—Oil recovery from different CO_2 viscosity in WAG process

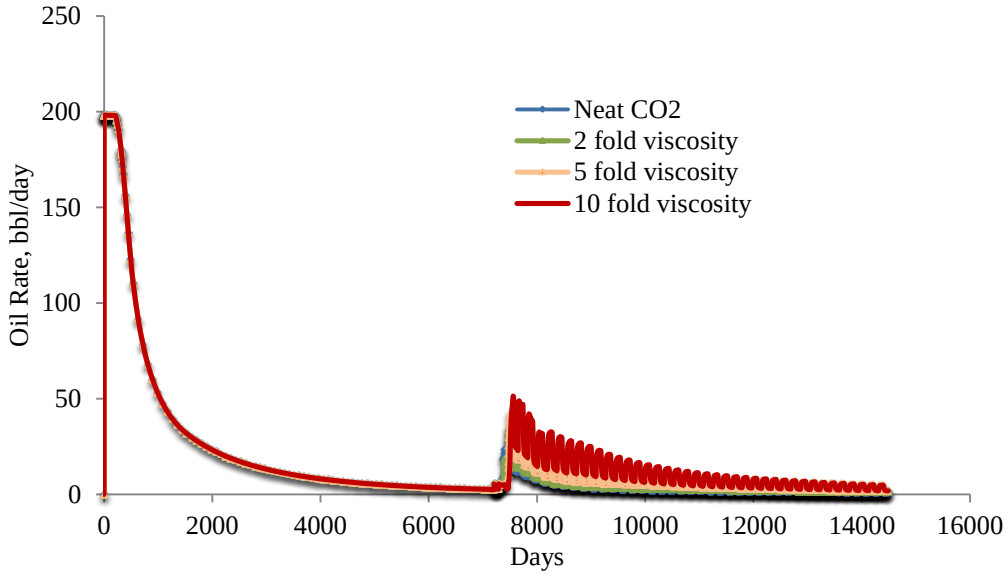

Figure 5.5—Production rate performance for different CO_2 viscosity in WAG process

5.1.2 Reservoir Simulation of CO_2 viscosifier Based on Reservoir with permeability 100 md and VDP 0.53

We studied CO_2 viscosifier performance in a low permeability reservoir with VDP 0.53. Neat CO_2 continue injection could increase recovery about 16% after water flooding (**Figure 5.6**). The improvement of neat CO_2 flooding in second model is more significant than first model. The reason is that conventional CGI could get higher recovery at low permeability and more homogeneous reservoir. In this model, increasing viscosity 5- and 10- fold obtain similar recovery in CGI process. It hints that the higher reservoir's permeability, the higher CO_2 viscosity should be used.

The performance of CO_2 viscosifier during WAG was studied. Neat WAG could increase recovery about 16% after water flooding (**Figure 5.7**). When increasing CO_2 viscosity about 10 fold, WAG flooding would increase recovery about 25% after water flooding, which is 9% higher than neat WAG injection. It also reveals that oil recovery from CO_2 viscosifier increases with CO_2 viscosity increasing. As the same as first model, the improvement of recovery is more significant for continue gas injection than for WAG when increase CO_2 viscosity.

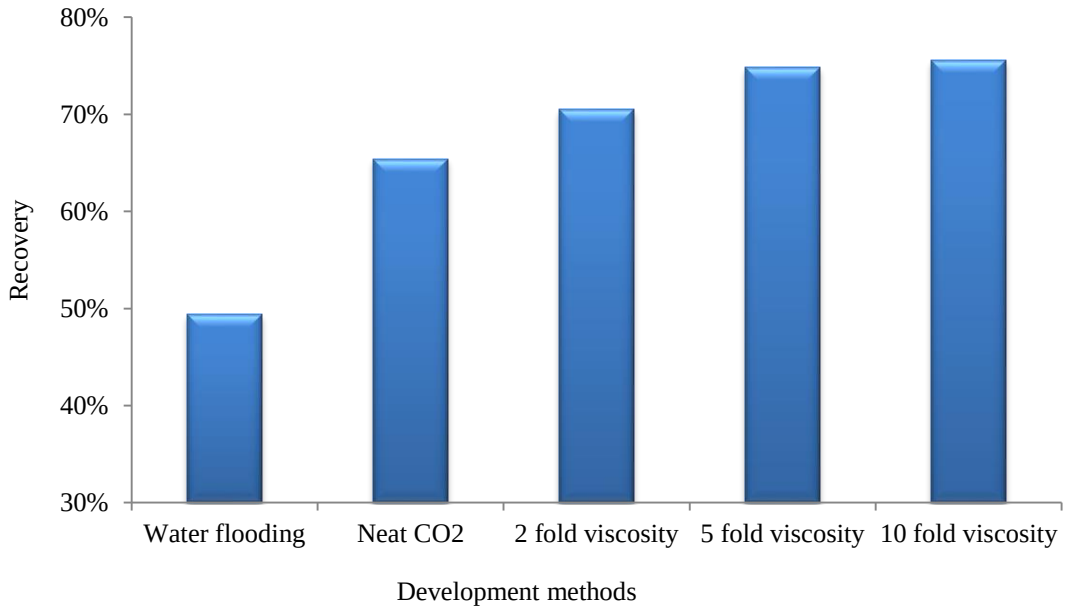

Figure 5.6—Oil recovery from CGI methods with permeability 100 md and VDP 0.53

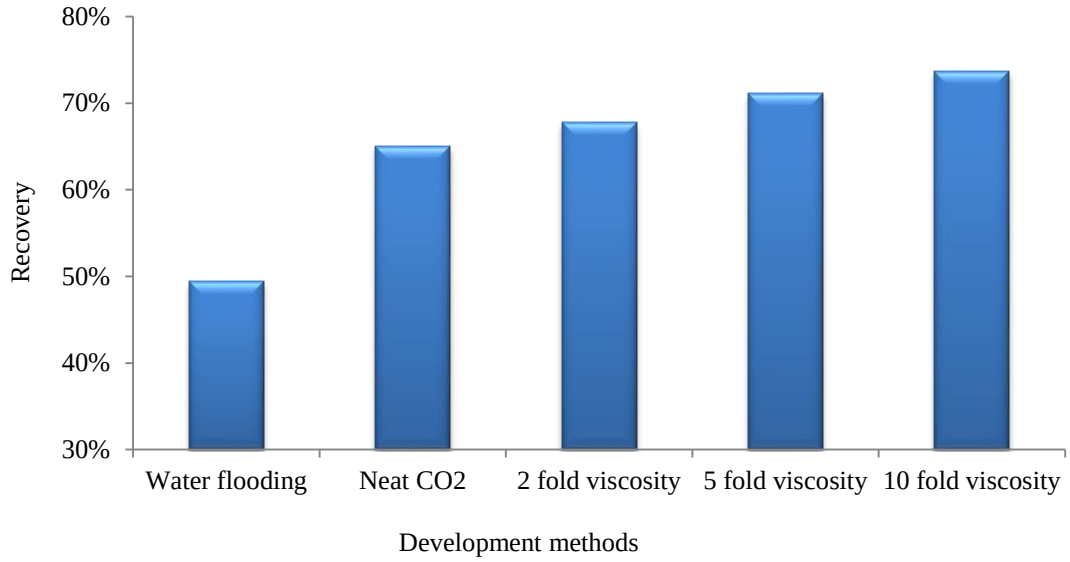

Figure 5.7—Oil recovery from WAG methods with permeability 100 md and VDP 0.53

5.1.3 Reservoir Simulation of CO_2 viscosifier Based on Reservoir with permeability 320 md and VDP 0.80

We also studied CO_2 viscosifier performance in high heterogeneity reservoir with a VDP value 0.80 and average permeability 320 md. Neat CO_2 continue injection could increase recovery about 8% after water flooding (**Figure 5.8**). The improvement of CO_2 flooding in the third model is not as significant as the second model. The reason is conventional CGI gets lower recovery at high permeability and heterogeneous reservoir. In this model, increasing viscosity 10-fold gets much higher recovery than 5-fold in the CGI process. Increasing viscosity 10-fold in CGI process could increase recovery about 17% compared with neat CO_2 injection.

Figure 5.9 shows the performance of CO_2 viscosifier during WAG process. Neat WAG could increase recovery about 8% after water flooding. When increasing CO_2 viscosity about 10 fold, WAG flooding could increase recovery about 16% after water flooding, which is 7% higher than neat WAG injection.

Figures 5.8 and 5.9 show that oil recovery from CO_2 viscosifier increases with CO_2 viscosity increasing. Figures also indicate that for low heterogeneous reservoir (the first and second model), increasing CO_2 viscosity 2-fold could increase recovery significantly, while for high heterogeneous reservoir (third model), higher fold viscosity increasing is required to markedly improve recovery.

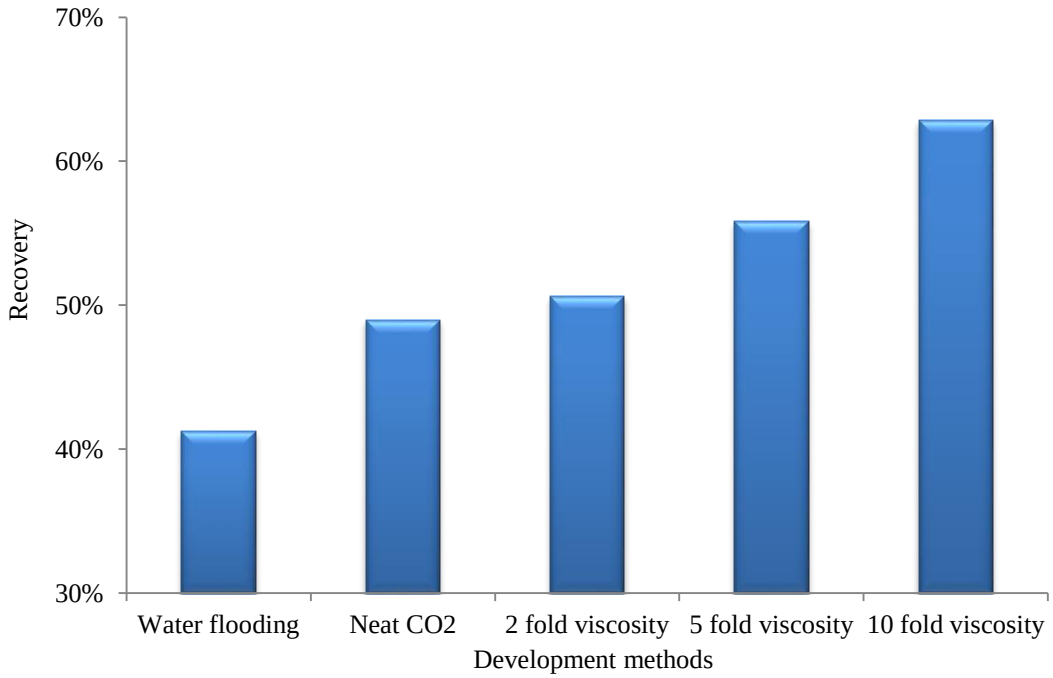

Figure 5.8—Oil recovery from CGI methods with permeability 320 md and VDP 0.8

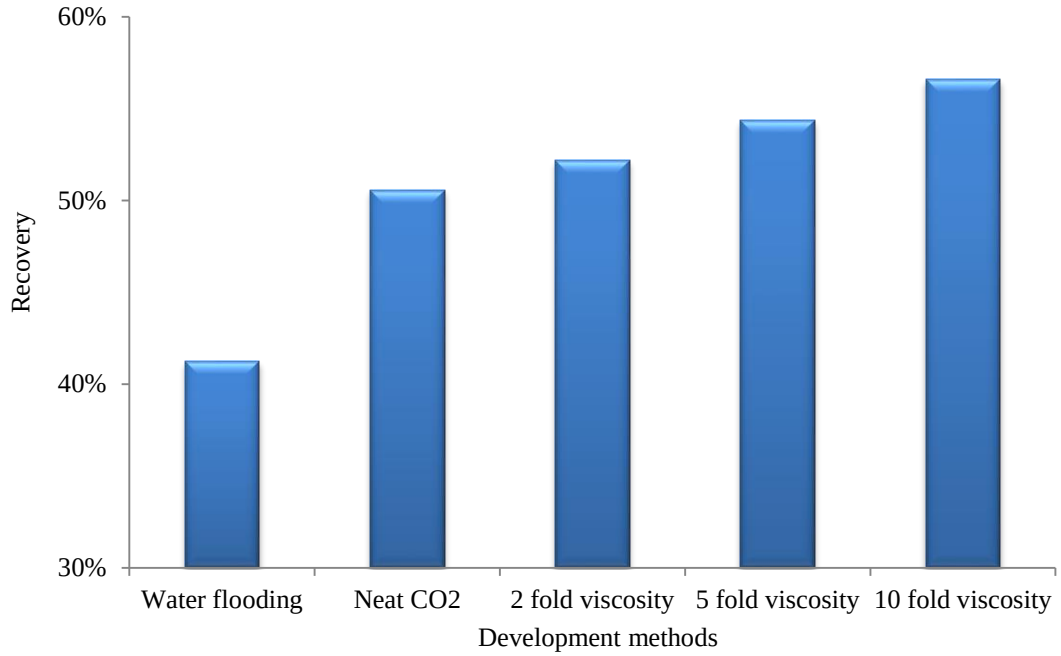

Figure 5.9—Oil recovery from WAG methods with permeability 320 md and VDP 0.8

5.2 Reservoir Simulation of CO_2 Viscosifier in SPE10 model

To illustrate the CO_2 viscosifier performance in a reservoir with channels, the same upscale reservoir and fluid model in the section 3.2 was used. Figure 5.1 is used to represent the new viscosity-pressure relationship. 2, 5-, 10-, and 20-fold of CO_2 viscosity are used in this study according to literature.

As shown in **Figure 5.10**, oil recovery is increased 23% when viscosity increases to 20-fold, which is 9% higher than neat WAG. Figure 5.17 also indicates that oil recovery from CO_2 viscosifier increases with CO_2 viscosity's increasing. We forecast oil production rates for the four different CO_2 viscosities. As shown in **Figure 5.11**, (1) the more gas viscosity increases, the later oil rate responds during gas injection, (2) the higher gas viscosity increases, the higher peak rate reaches.

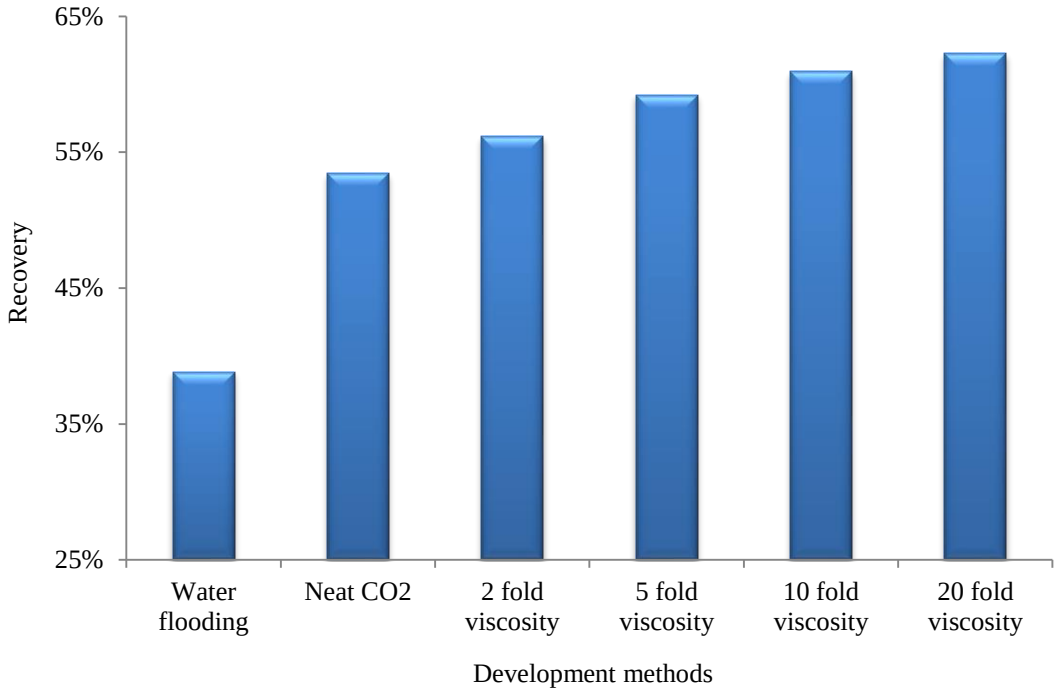

Figure 5.10—Oil recovery for different development methods in SPE 10 model

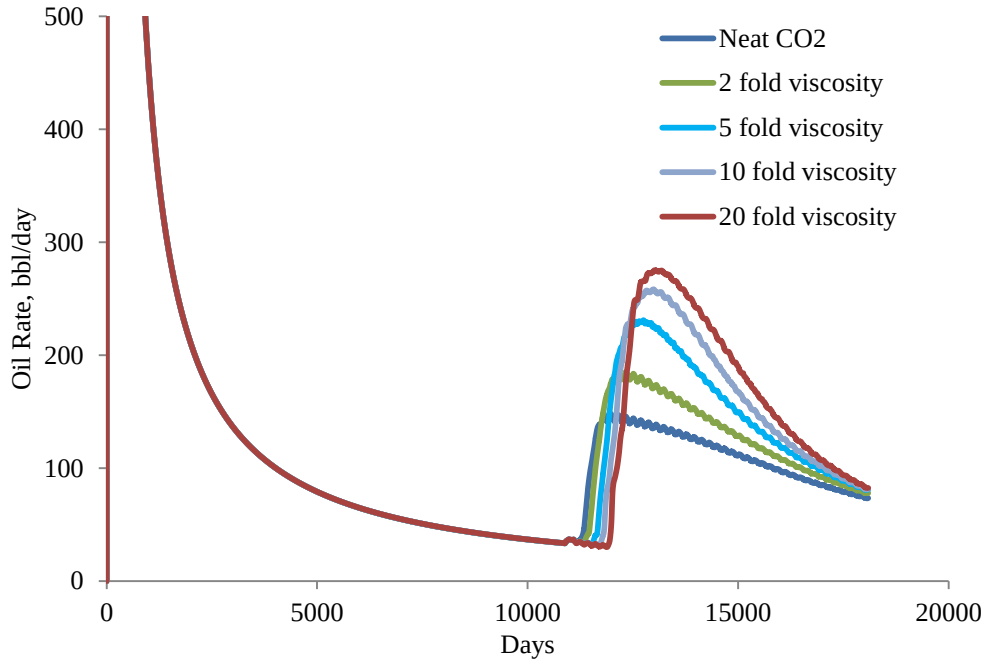

Figure 5.11—Production rate performance for different development methods in SPE 10 model

5.3 Reservoir Simulation of CO_2 Viscosifier in TR78 in North Burbank Unit

The reservoir model TR78 (described in section 4.5) was chosen for study. The oil recovery and oil production rate curves for the simulation are plotted for each case in **Figure 5.12** and **5.13**, respectively. The higher CO_2 viscosity, the higher oil recovery (Figure 5.12). Oil recovery doubles compared with neat CO_2 injection in CGI process when viscosity is increased 20-fold. For Case 1 with neat CO_2, oil peak rate is about 500 bbl/day after 650 days injection. For Case 3 with 10 fold viscosity increasing, oil peak rate is about 650 bbl/day after 800 days injection. The peak oil rate increases with CO_2 viscosity increasing (Figure 5.12). While it also shows that the more gas viscosity increases, the later oil rate responds during gas injection (Figure 5.12).

The gas-oil ratio curves are also plotted for each case in **Figure 5.14**. For Case 1 with neat CO_2, CO_2 breakthrough (here gas-oil ratio larger than 5 Mscf/bbl was considered as gas breakthrough) after 385 days gas injection. For Case 3 with 10 fold viscosity increasing, the CO_2 breakthrough occurs after 700 days gas injection. When no viscosifier is added for CO_2 flooding, the peak gas oil ration is about 156 Mscf/bbl at the end of injection. For Case 3 with 10 fold viscosity increasing, in the end of simulation the gas oil ratio is around 51 Mscf/bbl, which is much lower than Case 1. It indicates that the higher gas viscosity increases, the lower gas-oil ratio obtains.

The reservoir performance during CO_2 viscosifier flooding was also compared with neat WAG process. When viscosity increases 20-fold, the oil recovery is two times as WAG (**Figure 5.15**). Figure 5.12 expresses that oil recovery from CO_2 viscosifier increases with CO_2 viscosity increasing. For Case 1 with neat WAG, oil peak rate is about 330 bbl/day after 650 days injection (**Figure 5.16**). For Case 3 with 10 fold viscosity increase, oil peak rate is about 430 bbl/day after 1094 days injection. Compared with Figure 5.12 and 5.16, peak oil rate in WAG process is much lower CGI in this model.

The gas-oil ratio curves in WAG process are plotted for each case in **Figure 5.17**. For Case 1 with neat CO_2, CO_2 breakthrough after 586 days gas injection; for Case 3 with 10 fold viscosity increasing, the CO_2 breakthrough occurs after 1175 days gas injection; When no viscosifier is added for CO_2 flooding, the peak gas oil ration is about 40 Mscf/bbl at the end of injection. For Case 3 with 10 fold

viscosity increasing, at the end of simulation time the gas-oil ratio is around 25 Mscf/bbl, which is much lower than Case 1.

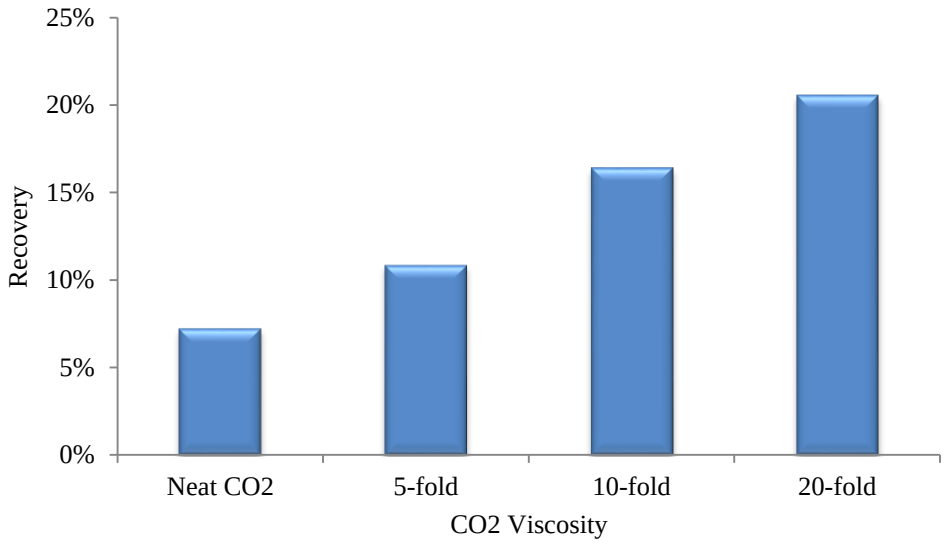

Figure 5.12—Recovery factor of different CO_2 viscosities in CGI process in TR78

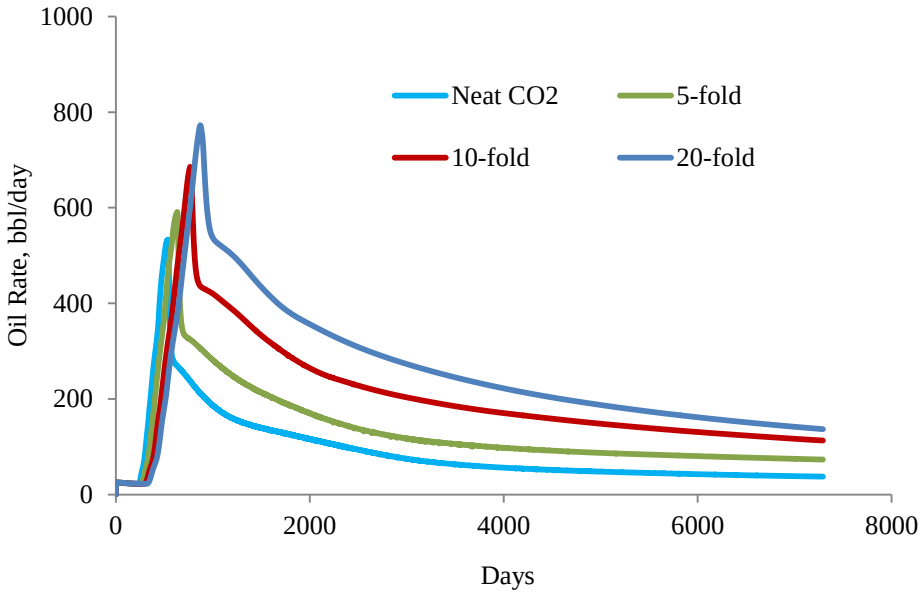

Figure 5.13—Production rate of different CO_2 viscosities in CGI process in TR78

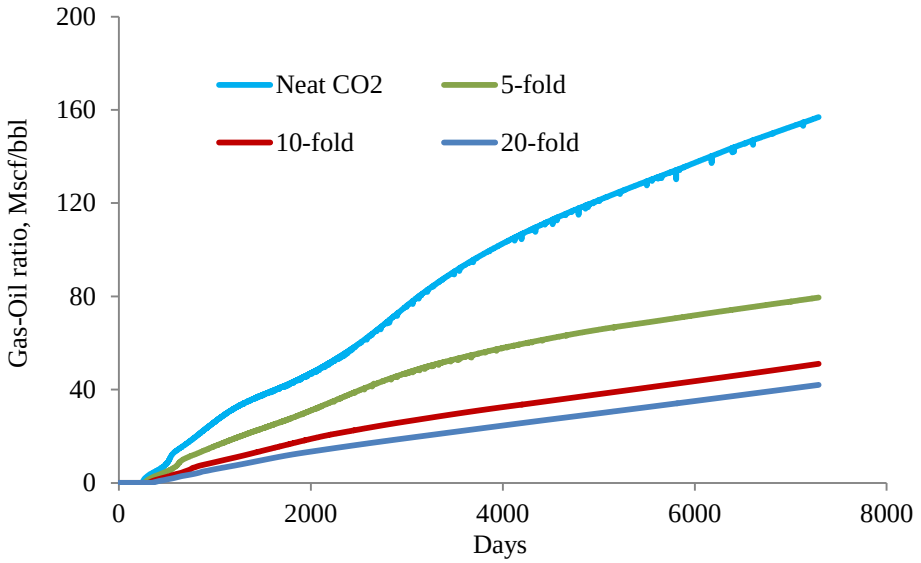

Figure 5.14—Gas-oil ratio of different CO_2 viscosities in CGI process in TR78

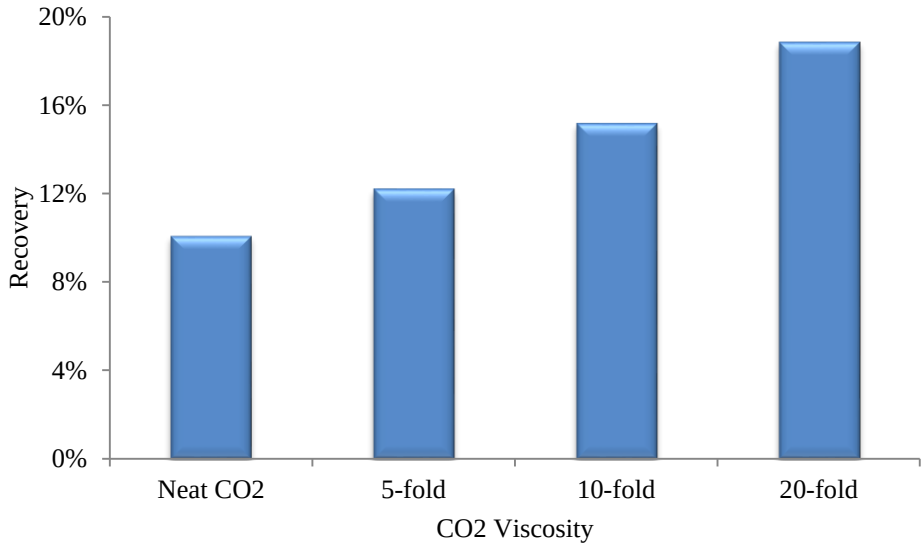

Figure 5.15—Recovery factor of different CO_2 viscosities in WAG process in TR78

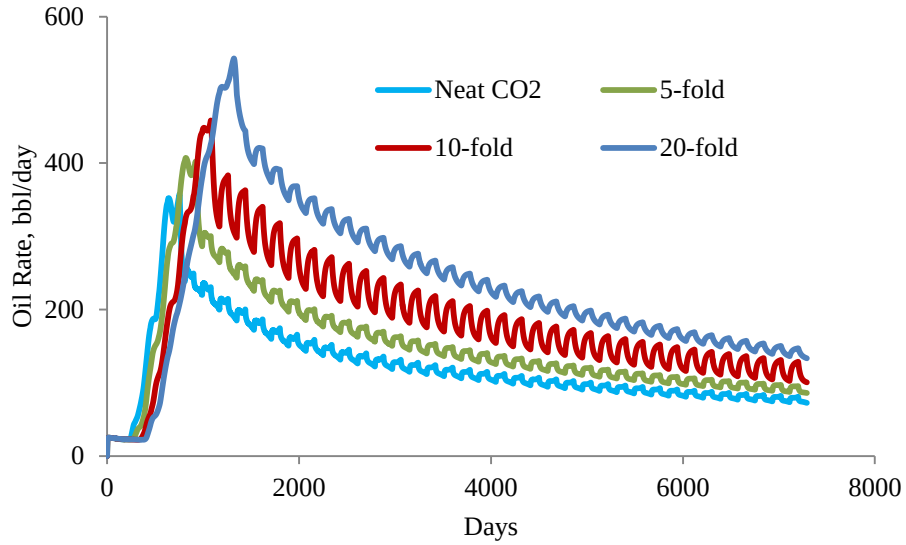

Figure 5.16—Production rate of different CO_2 viscosities in WAG process in TR78

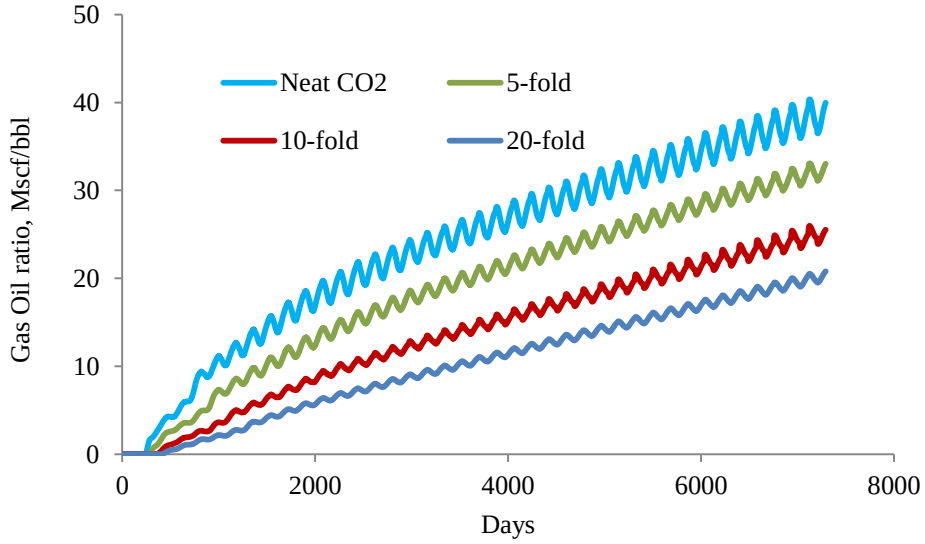

Figure 5.17—Gas-oil ratio of different CO_2 viscosities in WAG process in TR78

6. CONCLUSION AND FUTURE WORK

With the increasing importance of CO_2 flooding, they also pose very challenging questions for the reservoir engineers. The current techniques, like continue gas injection and water alternating gas, are quite mature and successful for enhance oil recovery. However, such techniques do not reach the excepted recovery factor, especially for reservoir with high-permeability zones or natural fractures. Cross-linked gel conformance control is most successful method to improve gas performance, while large volume gel polymer injection is required to reach successful treatment. Less than half of CO_2 foam is considered both technique and economic successful.

This work proposed some novel techniques for the improving the CO_2 performance in reservoir with high heterogeneous. Such techniques are proved to work efficiently in synthetic model, SPE 10 model and the North Burbank Unit, thus, provide good opportunities for recovery more oil from gas injection process.

However, each part of our research work also leave some open questions, that may require further investigations to improve the potential of the proposed techniques. Therefore, we also provide some suggestions for the future work in this section.

6.1 Conclusions

We first developed novel technique, named polymer alternating gas (PAG), for improving CO_2 sweep efficiency. The feature of this new method is that polymer is added to water during WAG process to improve mobility ratio, and polymer flooding and immiscible/ miscible CO_2 injection are combined. Based on this concept, three different type models are used to study the feasibility of polymer alternating gas.

In the end, we present CO_2 viscosifier, which can increase the viscosity of CO_2 directly and then improve the sweep efficiency. The CO_2 viscosifier performances in above three different type models are also analyzed in this dissertation.

The detailed conclusion and discussions can be summarized as below based on assumption and models used in this study:

(1) A new EOR method, polymer alternating gas, named PAG, was proposed to improve the efficiency of conventional WAG process.

(2) Synthetic simulation results indicate that PAG is very sensitive with polymer adsorption and concentration. Lower adsorption would lead to higher recovery and increase polymer concentration would increase oil recovery in PAG process when before injectivity problem occurs. The results also show that PAG could significantly increase recovery in both miscible and immiscible flooding. PAG could improve WAG perform in both high and low permeability heterogeneity reservoir with VDP vary from 0.5-0.9.

(3) Simulation results show that oil recovery from PAG with a polymer concentration of 0.20 lb/stb is more than polymer flooding and WAG in the lower part (Upper Ness) of SPE10 model. Recovery from PAG process is 10% higher than polymer flooding and 6% higher than WAG process.

(4) After optimizing polymer injection concentration and slug patterns, the following development strategy was suggested for TR78: inject polymer with a concentration of 0.20 lb/stb for 15 years in the PAG process and then chased with the WAG process for 5 years. Oil recovery increased by PAG in TR78 is forecasted to be 18.7%, which is 8.0% higher than WAG. Polymer utilization is about 2.20 lb/stb, which is economically feasible. The NPV for PAG process in the end of simulation life is higher than WAG process based on assumptions.

(5) The simulation results show that recovery from WAG and PAG process after water flooding in five sections is about 9-12% and 14-18%, respectively. Compare to WAG, PAG could recovery other 5-10% oil. Based on assumptions, PAG could obtain higher NPV than WAG in all these five sections, which indicates that PAG is both technically and economically feasible in the North Burbank unit.

(6) A black-oil pseudo-miscible model is used for study CO_2 viscosifier performance in synthetic model, SPE10 model and Section TR78 in the North Burbank Unit. Results show

that higher cumulative oil recovery and better sweep efficiency was observed for viscosified CO_2 case in homogeneous, heterogeneous and channels reservoir.

6.2 Future Work

To further improve the potential of our proposed techniques, some additional work may be required in the following areas:

(1) In the study, we only analyzed the sensitivity of VDP, fluid viscosity, channels in PAG process, while the end point of water, oil and gas usually have significant impact on recovery from polymer flooding, gas flooding and PAG. Further simulation to analyze the sensitivity of relative permeability curves in PAG process is required.

(2) When we studied the PAG performance in the Upper Ness formation in Spe10 model, we have not defined different relative permeability curves for channels and other matrix due to the data limited. Further studies on PAG performance in reservoir with channels are still required to address the problem.

(3) Current working used simple parameters for economic evaluation, future work can also take more realistic economic factors into considerations when analyze the PAG economic performance.

(4) The simulator E100-Eclipse, which could model polymer flooding and pseudo- miscible at the same time, is used for current working. Additional work about development simulator could model polymer flooding and compositional gas flooding at same time still required.

(5) Current work just focuses on simulation, further work to carry out core flooding experiment on PAG and CO_2 viscosifier is required.

REFERENCES

Aleidan, A.A and Mamora, D.D. 2010. SWACO_2 and WACO_2 Efficiency Improvement in Carbonate Cores by Lowering Water Salinity. Paper SPE 137548-MS presented at Canadian Unconventional Resources and International Petroleum Conference, Calgary, Alberta, Canada, 19-21 October.

Ali, H.A., Al-Ali and Schechter, S. David. 2013. Application of Polymer Gels as Conformance Control Agents for Carbon Dioxide EOR WAG Floods. Paper SPE 164096 presented at 2013 SPE International Symposium on Oilfield Chemistry. The Woodlands, TX, USA, 8-10 April.

Bae, J.H., and Irani, C.A. 1993. A Laboratory Investigation of Viscosified CO_2 Process. SPE Advanced Technology Series 1(1): 166-171. SPE-20467-PA.

Blaker, T., Aarra, M., Skauge, A., et al. 2002. Foam for Gas Mobility Control in the Snorre Field: The FAWAG Project. SPE Res Eval & Eng 5(4): 317-323. SPE-78824-PA.

Bond, D.C. and Holbrook, O.C. 1958. Gas Drive Oil Recovery Process. US Patent No. 2,866,507.

Borling, D.C. 1994. Injection Conformance Control Case Histories Using Gels at the Wertz Field CO_2 Tertiary Flood in Wyoming. Paper SPE 27825-MS presented at SPE Improved Oil Recovery Symposium. Tulsa, Oklahoma. 17-20 April.

Cain, M. 2010. Brookhaven Field: Conformance Challenges in an Active CO_2 Flood. Denbury Resources paper presented at the 16th Annual CO_2 Flooding Conference, Midland TX. 9–10, December.

Caudle, B.H. and Dyes, A.B. 1958. Improving Miscible Displacement by Gas-Water Injection. Paper SPE 911-G presented at 32nd Annual Fall Meeting of Society of Petroleum Engineers, Dallas, TX, October 6-9.

Christensen, J.R., Stenby, E.H. and Skauge, A. 1998. Review of WAG Field Experience. Paper SPE 39883-MS presented at International Petroleum Conference and Exhibition of Mexico, Villahermosa, Mexico, 3-5 March.

Christensen, J.R., Stenby, E.H. and Skauge, A. 2001. Review of WAG Field Experience. SPE Res Eval & Eng 4(2): 97-106. SPE-71203-PA.

Chou, S.I., Vasicek, S.L., Pisio, D.L. 1992. CO_2 Foam Field Trial at North Ward-Estes. SPE 24643, presented at the 67th SPE Annual Technical Conference and Exhibition, held in Washington, D.C., October 4–7.

Clampitt, R.L., Reid, T.B. 1975. An Economic Polymerflood in the North Burbank Unit, Osage County, Oklahoma. Paper SPE 5552-MS presented at the Fall Meeting of the Society of Petroleum Engineers of AIME, Dallas, Texas, 28 September-1 October.

Creel, P., Vavrek, G. 2001. Conformance Water-Management Team Developments and Solutions on Projects in the Permian Basin. SPE 70068-MS presented at the 2001 Permian Basin Oil and Gas Recovery Conference, Midland, TX, 14–16 May.

DeSimone, J.M., Guan, Z., and Elsbernd, C.S. 1992. Synthesis of Fluoropolymers in Supercritical Carbon Dioxide. Science, 14 August, 257:945-947.

DeSimone, J.M., Maury, E.E., Menceloglu, Y.Z., et al. 1994. Dispersion Polymerizations in Spercritical Carbon Dioxide, Science, 15 July, 1994, 265: 356-359.

Enick, R.M., Olsen, D.K., Ammer, J. R., et al. 2012. Mobility and Conformance Control for CO_2 EOR via Thickeners, Foams and Gels—A Literature Review of 40 years of Research and Pilot Tests. Paper SPE 154122-MS presented at SPE Improved Oil Recovery Symposium. Tulsa, Oklahoma. 14-18 April 2012.

Faisal, A., Bisdom, B., Zhumabek, B., et cl. 2009. Injectivity and Gravity Segregation in WAG and SWAG Enhanced Oil Recovery. Paper SPE 124197-MS presented at SPE Annual Technical Conference and Exhibition, New Orleans, Louisiana, 4-7 October.

Geiger, P. 2006. CO_2 EOR and Sequestration in Wyoming. Anadarko Petroleum, 4th Annual EOR Carbon Management Workshop, The Woodlands Waterway Marriott Hotel and Conference Center, Houston, Texas, 4-5 December.

Heller, J.P., Boone, D.A., Watts, R.J. 1985. Testing CO_2-Foam for Mobility Control at Rock Creek. SPE 14519, presented at the SPE Eastern Regional Meeting, held in Morgantown, WV, 6–8 November.

Heller, J.P., Dandge, D.K., Card, R.J., et al. 1985. Direct Thickeners for Mobility Control of CO_2 Floods. SPE Journal 25(5): 679-686. SPE-11789-PA.

Henry, Richard L., Fisher, D. Ramsey, Pennell, Stephen P., et al. 1996. Field Test of Foam to Reduce CO_2 Cycling. SPE 35402, presented at the SPE/DOE Improved Oil Recovery Symposium, Tulsa, OK, 21-24 April.

Hild, G.P. and Wackowski R.K. 1999. Reservoir Polymer Gel Treatments To Improve Miscible CO_2 Flood. SPE Res Eval & Eng 2(2):196-204. SPE-56008-PA.

Hoefner, M.L., Evans, E.M. 1995. CO_2 Foam: Results from Four Developmental Field Trials. SPE Reservoir Engineering, November, pp. 273–281.

Holm, L.W., Garrison, W.H. 1988. CO_2 Diversion with Foam in an Immiscible CO_2 Field Project. SPE 14963, SPE Reservoir Engineering, February, pp. 112–118.

Honnert, M., Creel, P., Tate, R., Everett, D. 2006. Five Years of Ongoing Conformance Work in the Central Mallet Unit CO_2 Flood in West Texas Yields Improved Economics for Operator. SPE

101701-MS presented at the First International Oil Conference and Exhibition. Cancun, Mexico, August 31–September 2.

Hunter, Z. Z. 1956. Progress Report, North Burbank Unit Water Flood-January 1, 1956: American Petroleum Institute, 1956, p.262-273.

Johnson, L. Christopher. 1992. Burbank Field—U.S.A. Anadarko Basin, Oklahoma. AAPG Special Volumes, TR: Stratigraphic Traps III, 333-345.

Jonas, T.M., Chou, S. I., Vasicek, S.L. 1990. Evaluation of a CO_2 Foam Field Trial: Rangley Weber Sand Unit. SPE 20468, presented at the SPE 65th Annual Technical Conference and Exhibition, held in New Orleans, LA, 23–26 September.

Karaoguz, O.K., Topguder, N.N.S., Lane, R.H., et al. 2007. Improved Sweep in Bati Raman Heavy-Oil CO_2 Flood: Bullhead Flowing Gel Treatments Plug Natural Fractures. SPE Res Eval & Eng 10(2):164-175. SPE-89400-PA.

Kendall, J.L., and DeSimone, J.M. 1997. Polymerizations in Liquid and Supercritical Carbon Dioxide. Proceedings of the 4th International Symposium on Supercritical Fluids, Sendai, Japan, May 11-14, 771-776.

Kulkarni, M.M. and Rao, D.N. 2005. Experimental investigation of miscible and immiscible Water-Alternating-Gas (WAG) process performance. Journal of Petroleum Science and Engineering 48(1–2): 1–20.

Lorenz, P.B., Trantham J.C., Zornes, D.R., et al. 1986. A Postflood Evaluation Test of the North Burbank Surfactant/Polymer Pilot. SPE Reservoir Engineering 1 (04). 341-353. SPE-12695-PA.

McClain, J.B., Betts, D.E., Canelas, D.A., et al. 1996. Characterization of Polymers and Amphiphiles in Supercritical CO_2 using Small Angle Neutron Scattering and Viscometry. Proceedings of the 1996 Spring Meeting of the ACS, Division of Polymeric Materials, Vol. 74, 234-235. New Orleans, LA.

Moffitt, P.D., Mitchell, J.F. 1983. North Burbank Unit Commercial Scale Polymerflood Project-Osage County, Oklahoma. Paper SPE 11560-MS presented at the SPE Production Operations Symposium, Oklahoma City, Oklahoma, 27 February-1 March.

Moffitt, P.D., Zornes, D.R., Moradi-Araghi, Ahmad, McGovern, J.M. 1993. Application of Fresh water and Brine Polymer Flooding in the North Burbank Unit, Osage County, Oklahoma. SPE Journal 8(02): 128-134. SPE-20466-PA.

Moritis, G. CO_2 and HC Injection Lead EOR Production Increase. Oil Gas J. 1990, 88, 49–82.

Moritis, G. EOR Production Report. Oil Gas J. 1992, 90, 60–65, 68–73, 76–78.

Moritis, G. EOR Production Report. Oil Gas J. 1994, vol. 92, 60–69, 72–78.

Moritis, G. 1996 EOR Worldwide Survey. Oil Gas J. 1996, vol. 94, 45–61.

Moritis, G. 1998 EOR Worldwide Survey. Oil Gas J. vol. 1998, vol. 96, 60–65, 68–71, 74–77.

Moritis, G. EOR weathers low oil prices. Oil Gas J. 2000, vol. vol. 98, 39–42, 44–53, 56–61.

Moritis, G. Special Report: Enhanced Oil Recovery. Oil Gas J. 2002, vol. 100, 72–83.

Moritis, G. EOR continues to unlock oil resources. Oil Gas J. 2004, vol. 102, 45, 48–50, 52–65.

Moritis, G. 2006 Worldwide EOR Survey. Oil Gas J. 2006, vol. 104, 46–57.

Moritis, G. 2008 Worldwide EOR Survey. Oil Gas J. 2008, vol. 106, 41–42, 44–59.

Moritis, G. 2010 Worldwide EOR Survey. Oil Gas J. 2010, vol. 108, 36-53.

Moritis, G. 2012 Worldwide EOR Survey. Oil Gas J. 2012, vol. 110, 41–59.

Moritis, G. 2014 Worldwide EOR Survey. Oil Gas J. 2014, vol. 112, 66-91.

Pipes, J.W. and Schoeling, L. G. 2014. Performance Review of Gel Polymer Treatments in a Miscible CO_2 Enhanced Recovery Project, SACROC Unit Kelly-Snyder Field. Paper SPE 169176-MS presented at SPE Improved Oil Recovery Symposium. Tulsa, Oklahoma. 12-16 April.

Sanders, A., Jones, R., Mann, T. 2010. Successful Implementation of CO_2-Foam for Conformance Control. presentation at the 2010 CO_2 Conference, Midland Texas, 9–10 December (a).

Sanders, A., Nguyen, Q., Nguyen, N. 2010. Twin-tailed Surfactants for Creating CO_2-in-Water Macroemulsions for Sweep Enhancement in CO_2 EOR. SPE 137689, presented at the Abu Dhabi International Petroleum Exhibition and Conference, held in Abu Dhabi, UAE, 1–4 November (b).

Smith, D. 1988. Injectivity and Surfactant-Based Mobility Control: Field Tests. Chapter 22 of Surfactant-Based Mobility Control – Progress in Miscible Flood Enhanced Oil Recovery, edited by Duane Smith, ACS Symposium Series 373, ACS, Washington DC, pp. 429–438.

Smith, D. D., Giraud, J.M., Kemp, C., et al. 2006. The Succesful Evolution of Anton Irish Conformance Efforts. SPE 103044, presented at the SPE Annual Technical Conference and Exhibition, San Antonio, TX, 24-27, September.

Sohrabi, M., Danesh, A., and Tehrani, D.H. 2005. Oil Recovery by Near-Miscible SWAG Injection. Paper SPE 94073-MS presented at the SPE EUROPEC/EAGE Annual Conference, Madrid, Spain, 13-16 June.

Stephenson, J. Derril. Graham G. Andrew, Luhning W. Richard, et al. 1993. Mobility Control Experience in the Joffre Viking Miscible CO_2 Flood. SPE Reservoir Engineering 8(03):183-188. SPE-23598-PA.

Stone, H.L. 2004. A Simultaneous Water and Gas Flood Design With Extraordinary Vertical Gas Sweep. Paper SPE 91724-MS presented at SPE International Petroleum Conference in Mexico, Puebla Pue., Mexico, 7-9 November.

Terry, R.E., Zaid, A., Angelos, C., et al. 1987. Polymerization in Supercritical CO2 to Improve CO_2/Oil Mobility Ratios. Paper SPE 16270-MS presented at the SPE International Symposium on Oilfield Chemistry, San Antonio, TX, 4-6 February.

Terry, R.E. 2001. "Enhanced Oil Recovery" in Encyclopedia of Physical Science and Technology 3rd Edition, vol. 18. Robert A. Meyers Ed., Academic Press (2001) pp 503-518.

Tracy, G.W., Dauben, D.L. 1982. An Evaluation of the North Burbank Unit Tertiary Recovery Pilot Test. Report No. DOE/BC/10033-2. Bartlesville, Oklahoma.

Topguder, N.N.S. 2010. A Review on Utilization of Crosslinked Polymer Gels for Improving Heavy Oil Recovery in Turkey. Paper SPE 131267 presented at SPE EUROPEC/EAGE Annual Conference and Exhibition, Barcelona, Spain, 14-17 June.

Trantham, J.C., Patterson, Jr. H.L., Boneau, D.F. 1978. The North Burbank Unit, Tract 97 Surfactant/Polymer Pilot Operation and Control. Journal of Petroleum Technology 30(07). 1,068-1,074. SPE-6746-PA.

Trantham, J.C., Moffitt, Paul. 1982. North Burbank Unit 1,440-Acre Polymer Flood Project Design. Paper SPE 10717-MS presented at the SPE Enhanced Oil Recovery Symposium, Tulsa, Oklahoma, 4-7 April.

Trantham, J.C. 1983. Prospects of Commercialization, Surfactant/Polymer Flooding, North Burbank Unit, Osage County, OK. Journal of Petroleum Technology 35(05). 872-880. SPE-9816-PA.

Tsau, Jyun-Syung, Heller, J.P. 1994. CO_2 Foam Field Verification Pilot Test at EVGSAU: Phase IIIA--Surfactant Performance Characterization and Quality Assurance. SPE 27785, presented at the SPE/DOE Improved Oil Recovery Symposium, Tulsa, OK, 17-20 April.

Virginie, T. D. 1995. Overpressuring and Seal Structure of Pennsylvanian Red Fork Formation in the Anadarko Basin; Oklahoma. Oklahoma State University.

Wagner, O.R., Weisrock, W.P., Patel, C. 1986. Field Application of Lignosulfonate Gels To Reduce Channeling, South Swan Hills Miscible Unit, Alberta, Canada. Paper SPE 15547-MS presented at SPE Annual Technical Conference and Exhibition. New Orleans, Louisiana. 5-8 October.

Woods, P., Schramko, K., Turner, D. et al. 1986. In-Situ Polymerization Controls CO_2/Water Channeling at Lick Creek. Paper SPE 14958-MS presented at the SPE Enhanced Oil Recovery Symposium, Tulsa, Oklahoma, 20-23 April.

Zhang, Y., Huang, S.S., and Luo, P. 2010. Coupling Immiscible CO_2 Technology and Polymer Injection to Maximize EOR Performance for Heavy Oils. Journal of Petroleum Technology **49**(5):252-33. SPE-137048-PA.

Zornes, D.R., Cornelius, A.J., and Long, H.Q. 1986. An Overview and Evaluation of the North Burbank Unit Block A Polymer Flood Project, Osage County, Oklahoma. Paper SPE 14113-MS presented at International Meeting on Petroleum Engineering, Beijing, China, 17-20 March.